KARST GEOMORPHOLOGY OF THE PUKETOI RANGE, NORTHERN WAIRARAPA, NEW ZEALAND.

A thesis presented in partial fulfilment of the requirements for the degree of Masters of Science in Geography at Massey University.

Stuart Lorris Halliday

December 1987

MAP LIBRARY
DEPARTMENT OF GEOGRAPHY
MASSEY UNIVERSITY,
PALMERSTON NORTH, NZ

Frontpiece Puketoi Range looking south from Trig 15. The Waewaepa Range is to the right. Note the changes in drainage texture with respect to geology.

"To sit on rocks; to muse o'er flood and fell;
To slowly trace the forest's shady scene;
Where things that own not man's dominion dwell;
And mortal foot hath ne'er or rarely been;
To climb the trackless mountain all unseen;
With the wild flock that never needs a fold;
Alone o'er steeps and foaming falls to lean;
This is not solitude; 'tis but to hold
Converse with Nature's charms; and view her stores unroll'd."

Colenso 1884.

ABSTRACT

The research described in this thesis is the first investigation of the karst geomorphology of Pliocene and Pleistocene limestones in the southern Hawke's Bay - northern Wairarapa area. The study area is the Puketoi Range, which is situated 30 km southeast of Dannevirke.

The geology of the range is examined and a new geological map of the area has been completed. The Te Aute Group (Pliocene in age) forms much of the range. This consists of two limestone beds, the Te Onepu and Awapapa Limestone Formations interbedded between two mudstone beds. This is overlain by younger Pleistocene material, the Kumeroa Formation, the upper portion of which is limestone underlain by mudstone.

Solutional processes and erosion within the range is investigated. Three distinctive types of water are identified: allogenic water derived from non-karst areas, autogenic water derived from the limestone, and mixed allogenic-autogenic water. Each of these water types has specific characteristics. The solutional erosion rate for a limestone basin within the range is approximately 58.2 $m^3/km^2/yr$.

Selected karst and non-karst landforms and features developed on the Puketoi Range are examined. Two of these features, case-hardened limestone and bogaz, have not previously been described in detail in New Zealand. Many of the features are the result of, or have been modified by, past periglacial climatic conditions. Other landforms are developing under present climatic conditions.

The characteristics of three drainage basins developed on limestone, mudstone and greywacke respectively, are investigated. The drainage density on mudstone is the highest of the three basins examined, and densities on limestone and greywacke are similar.

Sediment is examined from two caves in the area. Within Ramsay's Neck Cave ancient sediment was probably deposited during the Otira Glaciation. This sediment consists of ancient cave stream sediment, forming basal gravels overlain by fine-grained sediment and, in places, speleothems. This sediment contains allophane, a volcanically derived material, which was possibly deposited after a heavy volcanic ash fall within the cave's

drainage basin.

The sediment examined within PT17 Cave is contemporary gravel fluctuating in response to present hydrological conditions within the cave. Surface features indicate that in the past, gravel has completely infilled the cave, re-establishing surface drainage until the gravel was flushed from the cave.

The development of the Puketoi Range cuesta and its subsequent modification is examined. The two limestone beds on which the range has developed strongly control the shape and form of the range.

ACKNOWLEDGMENTS

I would like to thank the following people for their help and assistance in the course of my research:

I am particularly grateful to Dr Mike Shepherd for his supervision, encouragement and assistance in the field, and for his constructive criticism in the preparation of this thesis. Thanks to Dr John McArthur and Mr Richard Heerdegen, and other staff of the Geography Department, for their help. Thanks also to Dr R.D.Reeves, Chemistry Department, for help with the use of equipment in the analysis of water samples; Dr R.B.Stewart, Ms Jo Thomkins and other staff of the Soil Science Department for their help in the analysis of cave sediment. I am grateful to Dr Ashley Cody, NZGS Rotorua, for examination of the moonmilk sample.

I thank Mr Russell Burn, Coonoor, for accommodation, vehicles and assistance during fieldwork; Mr Richard Brown and other farmers along the Puketoi Range for allowing unlimited access to their properties. Thanks to Peter Entwistle, Sue Cade, Jeff Archer, and other cavers for the many hours spent looking for caves and help in their survey; Manawatu Speleological Group for the use of their aerial mosaic photos of the Puketoi Range, and the New Zealand Speleological Society for the grant to help with research expenses.

I am indebted to Mr Brian Solomon and Mr David Feek for technical assistance; Mrs Anne Stoddart for help with figures and Mrs Karen Puklowski for help with cartography.

Much thanks also to my Mum. I dedicate this thesis to my late Dad for all his encouragement. Also much thanks to Jacqui Aimers for the many days spent in the field, for proof-reading this thesis, help with drawing figures, painting the geology maps, and for all her tolerance and encouragement during the writting of this thesis.

TABLE OF CONTENTS

LIST OF APPENDICES

LIST OF FIGURES

LIST OF TABLES

LIST OF PHOTOGRAPHS

CHAPTER ONE
INTRODUCTION

The investigation of karst areas is a relatively new field of geomorphological and hydrological study in New Zealand. Karst is defined as: "terrain with distinctive landforms and drainage arising from greater rock solubility in natural waters than elsewhere" (Jennings 1985, p.1). The majority of research work into karst areas in New Zealand has been carried out from the late 1960's onwards, with only spasmodic investigations before this time. Thompson (1854, cited in Gunn 1978) produced the first written account of karst terrain in New Zealand and recorded the approximate position and appearance of caves in the Waitomo district. A review of New Zealand karst literature since this time is given in Gunn (1978).

Carbonate rocks are found throughout New Zealand (Morgan 1919; Willett 1965), ranging in age from Cambrian limestone in the Cobb Valley, north of Nelson, to semi-consolidated Holocene sands in Northland (Gunn 1978; Williams 1982a). Karst terrain does not develop on all carbonate rock. The prerequisites for karstification (relatively pure hard rock, high rainfall, and high local relief) must be met before karst features will develop. The most well known areas of karst in New Zealand are the King Country of the west central North Island (Oligocene limestone), the Punakaiki and Paturau districts on the northwest coast of the South Island (Oligocene limestone) and in the Owen and Arthur Ranges to the west of Nelson (Ordovician marble).

This thesis examines part of the Kahurangi karst, an area of karst developed on relatively young (Pliocene to Pleistocene) limestone on the East Coast of the North Island (Williams 1982a). The area of specific interest is the Puketoi Range. The limestone of this range forms part of a semi-continuous outcropping of thin alternating limestone beds along the East Coast, from northern Hawke's Bay to northern Wairarapa. No detailed geomorphological investigations of the karst in this area had previously been undertaken. Also, all previous investigations in karst geomorphology in New Zealand have been in areas of more massive limestone. For these reasons, the scope of this thesis has not been restricted to one particular area of study within karst geomorphology, but has attempted to give a broad coverage of many aspects of this and

associated research fields.

1.2 Aims and Approach

The specific aims of this research are:

(1) To map, in detail, the geology of the Puketoi Range, emphasising the extent, nature and distribution of limestone beds in the area.

(2) To describe the subaerial processes and landforms of karst, and non-karst areas along and near the Puketoi Range. Emphasis is placed on the solutional erosion of limestone compared with mechanical erosion of the area surrounding the range.

(3) To discuss subterranean processes and morphologies of the karst area of the Puketoi Range.

(4) To explain the evolution of the Puketoi Range: an area with thin alternating limestone beds.

In chapter 2, the tectonic history and palaeogeography of the East Coast and Puketoi Range are discussed. The chapter includes descriptions of the stratigraphy, lithology and petrology of the range and a discussion of the new geological map drawn for the area. Chapter 3 is a discussion of karst processes, in particular the spatial and temporal variation in solutional erosion, and the estimated solutional erosion rate of a limestone basin in the area. This is followed in chapter 4 by an examination of karst landforms of the range. In chapter 5, drainage characteristics on differing lithologies in the area surrounding the Puketoi Range are described. Chapter 6 includes a description and discussion of cave sediment and its significance in the geomorphological investigation of the range. Chapter 7 discusses cuesta development and the geomorphological evolution.

1.3 Study Area

There are numerous discontinuous outcrops of Pliocene and younger limestone along much of the East Coast of the North Island, from northern

Hawke's Bay to northern Wairarapa. The study area is confined to the Puketoi Range, and the eastern flanks of the Waewaepa Range, where beds of limestone are exposed. The Puketoi Range is situated approximately 20 km southsoutheast of Dannevirke and extends southward to approximately 16 km east of Eketahuna (see Fig. 1.1). The range is approximately 45 km long and varies in width from 2 km to 5 km (Fig. 1.2). The northern boundary of the study area is taken to be the Waitahora Valley Road (Grid Ref. U24/830916). (Note - Grid references, unless otherwise stated, are from the NZMS 260 map series. If not, the map series will be given before the grid reference.) The southern limit of the study area is where the limestone of the range thins out, that is, to the south of Pori (Grid Ref. T25/550595). The area is bounded on the eastern side by the steep scarp slope of the Puketoi Range, and on the west by the greywacke of the Waewaepa Range, and mudstones of Opoitian age.

1.4 Natural and Human History

At the time of the arrival of the first Europeans, the Puketoi and Waewaepa Ranges were covered by dense forest, fern, and swamp vegetation forming part of the much more extensive 'Forty Mile Bush'. The Bush extended from Mauriceville, in the south, to Woodville in the north (Carle 1980). Before forest clearance for farmland, there was a great diversity of forest tree species and forest birds. Giant totara, rimu and rata were common (Carle 1980). Gnarled rata and totara stumps of huge girth are still common in the area due to the wood of these trees being highly resistant to decay. Evidence of the historical diversity of bird-life is seen today in the wide variety of subfossil bird bones found within the caves of the region. Remains have also been found of frogs, snails, tuataras and the extinct moa (Halliday and Gudex 1984). Lists of historical botanical species, and subfossil remains identified in the area are included in Appendix One.

There was little Maori occupation of the area, probably due to its harshness and isolation. Evidence of their presence is therefore scant, apart from the existence of a route through the Makuri Gorge to the East Coast, which the present road now follows, and the discovery a number of years ago of a burial cave in the vicinity of Coonoor (S.MacIntyre pers. comm.).

Figure 1.1 Location map of study area and towns mentioned in the text.

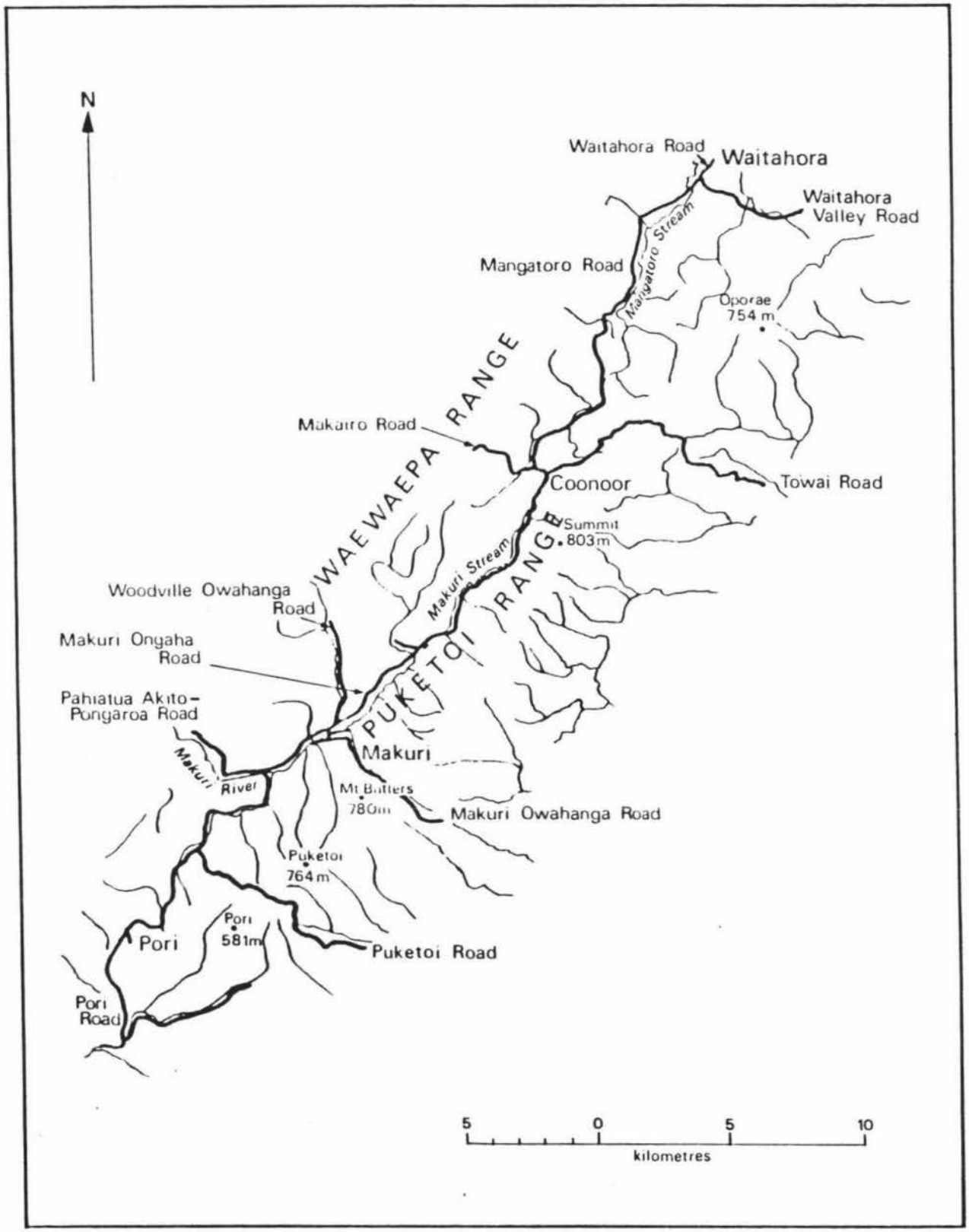

Figure 1.2 Place names mentioned in the text.

The first European settlement was in 1863 when Captain G.D.Hamilton began farming 12 600 ha of relatively clear country in the Mangatoro Valley (Wilson 1976; MAF Advisary Services Division, Dannevirke 1979).

In 1883 Parliament gave 10 000 pounds for the opening up of Crown Lands in the area (Carle 1980). This resulted in plans for the establishment of the township of Makuri in 1885 (opened in July 1887), with the first sections offered for sale in February 1892 (Bagnall 1976). The area is a natural break in the range and had once been a resting place for Maori parties travelling from coast to coast (Carle 1980).

The continuous demand for farm land resulted in the gazetting of the area for Special Settlement Association purposes from 1892 onwards. The land was divided into blocks averaging 200 acres (81 ha) with a maximum size of 320 acres (130 ha) (Carle 1980). By the summer of 1892 - 93 the first tracks had been cut into the district, these later being widened into dray roads. This resulted in the rapid influx of settlers, with the associated forest clearance, and early establishment of successful pastoral farming. By 1900 the present pattern of sheep and dairy farming was well established (MAF Advisory Services Division, Dannevirke 1979).

Today the western slope of the Puketoi Range, and the eastern flanks of the Waewaepa Range, are covered with introduced grasses (with small areas of regenerating forest) supporting sheep, cattle and goats. Farm properties range from 300 ha to 1000 ha, with a few large stations greater than 1000 ha. Stocking rates vary from 8 to 15 stock units per hectare, with Rommeys being the predominant sheep breed and cattle making up 10 to 30 percent of total stock units on most sheep and beef farms (MAF Advisory Service Division, Dannevirke 1979).

The development of shafts and other karst features has caused serious problems to farmers. Stock losses down shafts have been estimated as high as 15 percent (pers. comm., Waewaepa Station). This has resulted in many farmers using explosives and bulldozers in attempts to eliminate such hazards to stock.

The eastern scarp slope of the Puketoi Range has little agricultural potential due to the steepness of the land and is covered predominantly in regenerating forest.

1.5 Regional Climate

The Puketoi Range has mild summers and autumns but is cool in winter and spring. Rainfall is high and reasonably evenly spread, but its effectiveness is reduced by strong westerly winds in spring and late autumn.

Local wind patterns in the southern Hawke's Bay - northern Wairarapa region are strongly influenced by the shape of the land. Cook Strait, and to a lesser extent the Manawatu Gorge, funnel low-level air-streams from the Tasman Sea around the Tararua and Ruahine Ranges and into the region (Coulter 1969). The winds tend to be either westnorthwesterlies through the Manawatu Gorge, southwesterlies east of the Tararua and Ruahine Ranges, or northwesterlies near Cook Strait (Coulter 1969). The Puketoi Range forms a barrier to southerlies and easterlies, sheltering inland districts to the west (MAF Advisory Services Division, Dannevirke 1979) but the range funnels westerly winds, which may reach gale force (up to 150 km/h) during the equinoxes (Noble 1985). These winds have been termed the 'Puketoi gale' and may last several days. The northwesterly facing dip-slope exposed to these westerly winds experiences wide seasonal variations in soil moisture, while the southeasterly scarp is subjected to far less moisture variation due to its sheltered position (Noble 1985).

The rainfall and climatological data given below is based on information from the New Zealand Meteorological Service rainfall and climatological stations: D06501 Tataramoa, Makuri (Grid Ref. T25/644700) - record 1943 - 84; D06322 Waitohora (Grid Ref. U24/830917) - record 1959 - 84; and D06212 Dannevirke (Grid Ref. U23/746062) - record 1953 - 80. The rainfall record for Coonoor (Grid Ref. U24/738808) is based on Mr. Stuart MacIntyre's daily rainfall record, 1956 - 86, read at approximately 8.00 am each day.

The average yearly rainfall varies over the Puketoi Range, from a maximum of 2010 mm at Coonoor (480 m a.s.l.), to 1600 mm at Makuri (274 m a.s.l.) and 1278 mm at Waitahora (250 m a.s.l.) (see Fig. 1.3). There is, on average, 224 days of rainfall greater than 1.0 mm per day at Coonoor (61 percent of days per year), varying from a maximum average of 23 days of

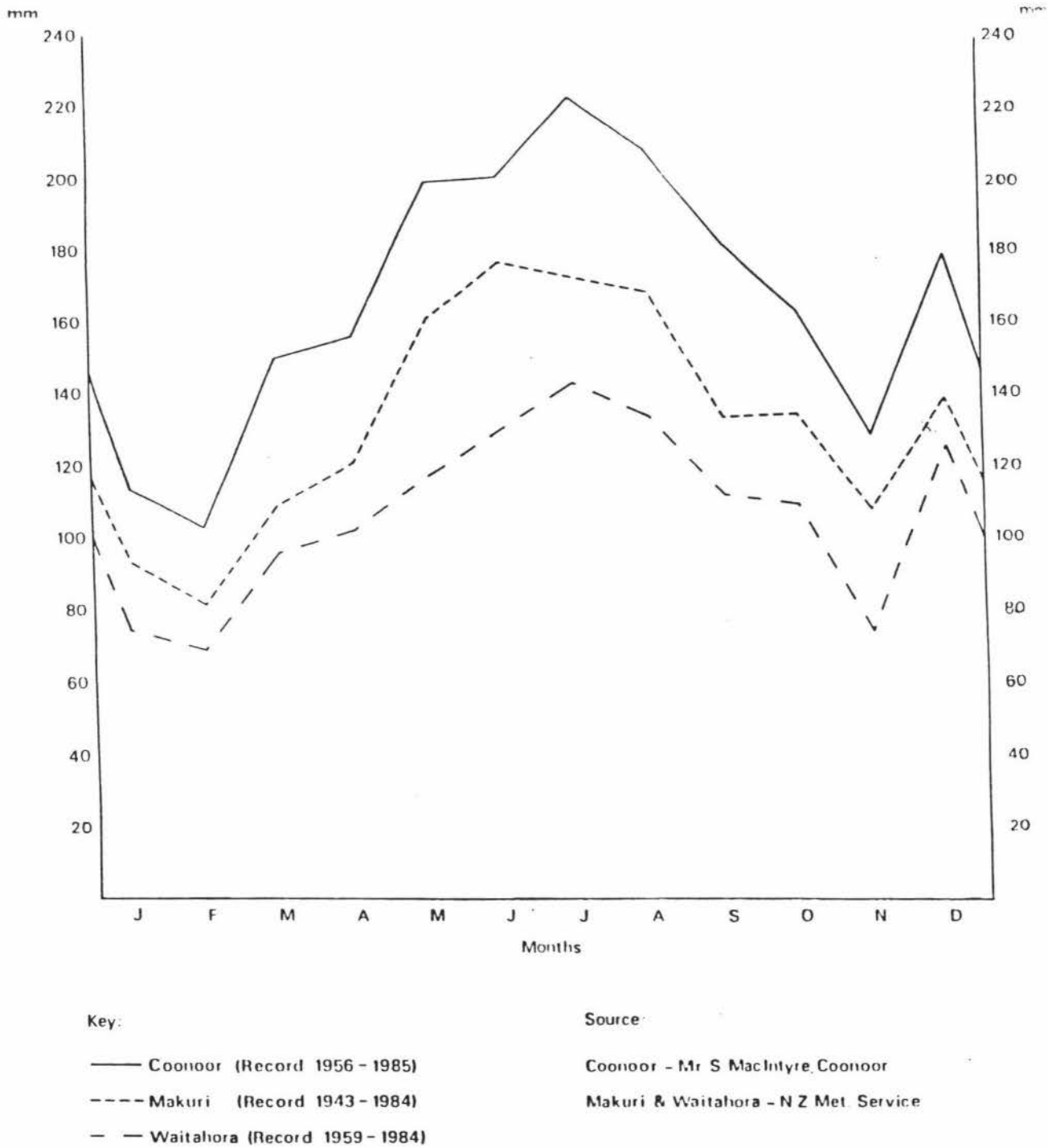

Figure 1.3 Graph of variation in rainfall distribution over the Puketoi Range.

rain in July (average of 223 mm) to a minimum of 13 days in February (average of 103 mm). About a third of the annual rainfall is in winter (June, July and August).

The climatological station at Dannevirke (207 m a.s.l.), the closest station to the study area, records an average yearly rainfall of 1093 mm. The mean annual temperature is 12.3 degrees Celsius, with an average daily maximum of 16.8 degrees Celsius, and an average daily minimum of 7.8 degrees Celsius. The Dannevirke climatological station averages approximately 59 days of ground frost per year and receives an average of 1754 hours of sunshine annually. The Puketoi Range, and hill country down to an altitude of 450 m, are covered by snow three to four times a year, but snow cover usually lasts only two to three days.

1.6 Soils

Soils developed in the Puketoi range in many situations reflect the parent material on which they have developed. This has resulted in much of the Puketoi Range, and eastern flanks of the Waewaepa Range, being covered by Pukeokahu steepland soils (New Zealand Land Inventory Worksheets N150, N152, N154), rendzina soils formed from calcareous rocks with either limestone, or calcareous sandstone and mudstone as the parent material. Gibbs (1980) describes rendzina soils in New Zealand as having either a black, or very dark, greyish-brown A horizon, with a strongly developed granular or nutty structure. Sometimes there may be a brown B horizon between the A horizon and disintegrating limestone rock.

Soils developed on non-calcareous parent material in the vicinity of the Puketoi Range generally reflect the nature of the underlying rock, with different soils developed on the greywacke, sandstone and mudstone surrounding the calcareous rocks of the Puketoi Range.

1.7 Periglacial Climate

Variations in climatic conditions during the Quaternary have influenced the morphology of many New Zealand regions. Some areas have been heavily glaciated in the past. In the North Island, evidence of previous glacial

advances can be seen on the central volcanic area and there is evidence of minor glaciation in the Tararua Range (Willett 1950). Within the Puketoi Range, the effects of past colder conditions have not been as dramatic as witnessed in the glaciated areas, but the present landscape of the range does show evidence of a past periglacial environment. A periglacial environment is primarily influenced by freeze-thaw oscillations in landform development (Tricart 1968).

The Otira Glaciation started 70 000 years B.P., and continued through to approximately 13 000 years B.P. (Salinger 1984). During this period there were four major glacial advances and three interstadials. The largest glacial advances in the Late Otiran were between 27 000 and 19 000 years B.P.. Palaeo-snow-line and pollen evidence indicate a temperature depression of 4 to 5 degrees Celsius below present-day values during this period (Chinn 1983; McGlone 1983). This period of cooler climatic conditions was followed by a period of warming. The beginning of the Aranuian (c. 13 000 B.P. to present) saw rapid glacial retreat, and ice diminishing to volumes close to that of present-day, by 12 000 B.P. (Chinn 1983).

Minor glaciation of the lower North Island was first noted by Adkin (1912) from evidence in the Tararua Range, particularly Park Valley (Grid Ref S25/140475). Willett (1950) estimated a 6 degree Celsius lowering in temperature during the Pleistocene to allow for nevé ice accumulation on the Tararua Range. He estimated the composite snow-line to be 1198 m lower than present. This estimate puts the snowline 200 m to 400 m lower than most modern workers' estimates (Chinn 1983; McGlone 1983).

The present highest point of the Puketoi Range is 803 m, 398 m below Willett's (1950) estimate of the Pleistocene snowline, and 600 m to 800 m below more modern workers' estimates (Chinn 1983; McGlone 1983). This would nevertheless have resulted in periglacial and near-periglacial climatic conditions over much of the Puketoi Range. Willett (1950) believes that the type of forest presently covering the Tararua Range would have survived only on the present coastal flats of the west coast during the Otira Glaciation. On the Puketoi Range, during the same period, the vegetation cover would therefore have been montane to alpine.

Neef (1967, 1984) was the first to find evidence within the Puketoi Range

of previous cooler phases during the Pleistocene. He observed solifluction deposits (resulting from soil and regolith saturated with water from summer thaw moving downhill as a soggy mass over the frozen ground beneath (Bloom 1978)) in the hill country near Pori. Here tongues of solifluction material were deposited up to 6 m thick and flowed for as much as 1.5 km down Kaitawa Creek and Hirinakitu Stream, on the western side of the range. These solifluction deposits contain blocks of limestone up to 1.5 m in length. Streams have subsequently entrenched their courses, through the solifluction material, to the approximate level of the original stream courses (Neef 1967).

Further evidence for the effects of a periglacial climate in the study area will be given in Chapter Four.

CHAPTER TWO
GEOLOGY

2.1 Introduction

In an area such as the Puketoi Range, the relationship between geomorphological processes and landform development cannot be fully understood without a knowledge of the geological structure and lithology. However, possibly owing to the isolated and exposed nature of the Puketoi Range, and its position on the boundary of the provinces of Hawke's Bay and Wairarapa, there is a lack of comprehensive geological investigations covering the range as a whole. Many of the previous geological studies of the area (see below for more detailed references) have been restricted to the individual provinces, resulting in a lack of continuity in the classification and nomenclature of geological beds within range.

After a careful study of all published geological literature of the area, it was recognised that confusion and inaccuracy could only be avoided by the production of a new geological map, incorporating the entire range, which would enable the data of previous workers to be assessed and correlated. For this reason, the production of a geological map became one of the major objectives of this thesis.

The following chapter has been divided into two sections. The first describes the structure and tectonic setting of the East Coast. This is followed by a discussion of the palaeogeography of the area. The second section, which is largely based on field studies, examines the structure, lithology and petrology of the geological beds comprising the Puketoi Range. This section concludes with a description of the stratigraphy and a new geological map of the range (see back pocket).

2.2 Previous Geological Work

The earliest reference to geological investigation of the southern Hawke's Bay - Wairarapa area appears in Hochstetter (1864, cited in Lillie 1953). Later Hochstetter, in his "New Zealand" (1867), gave a "synoptical view of geological formations and strata" and described the "Hawke's Bay series", as "...a group of limestones, sandstones and clay marls, replete with fossils belonging to the latest Tertiary Formations"

(p.61).Some of the fossils described are from the Te Aute Group fauna (Lillie 1953).

Crawford (1870) investigated the area when it was still in thick virgin forest and made the first geological description of the Puketoi Range. He states: "I found the blue clay, (which he had found throughout the district) and on the ridges above, Tertiary sandstone beds, with the usual fossil shells" (Crawford 1870, p.349).

In 1877 Hector described the geology of the eastern district of the lower North Island, inland from Castlepoint, and including the Puketoi Range. He noted a succession of clay marls and limestones forming the range. McKay traversed the country between Cape Kidnappers and Cape Turnagain. He produced the first geological sketch map, on a scale of 1:50 000, and proposed the first stratigraphic classification of eighteen different beds comprising the Cretaceous and Tertiary strata (McKay 1877a, 1877b). Of the eighteen beds he proposed, the original classification of several formations has been retained to the present day.

Henderson in 1915 drew attention to the prominent Mangatuna Fault, which is located at the contact between the greywacke of the Waewaepa Range and the limestone of the Puketoi Range.

Ongley (1935) mapped the 4400 square kilometre Eketahuna Subdivision, publishing a geological map on the scale of 1:253 440. He outlined the approximate distribution of the post Opotian strata of which the Puketoi Range forms a part. Neef (1967, 1984) considers this as particularly accurate where Ongley found well defined lithological changes.

Lillie (1953) mapped strata in the Dannevirke Subdivision, describing the Mangatoro, Te Aute and Kumeroa Formations on which the Puketoi Range has developed. This work, and that of Kingma (1971) on the Te Aute Subdivision, is incorporated in the 1:250 000 Dannevirke sheet (Kingma 1962). Laing (1963) described and mapped the Waipatiki area (NZMS 3 N150/5). This encompasses the northern end of the Puketoi Range, that is, the area around Oporae (Grid Ref. U24/824875) identifying three formations: Oporae (Opoitian to Mangapanian in age), Totara Road Limestone (Mangapanian), and Kumeroa (Nukumaruan).

Neef (1967, 1974, 1984) described and mapped the Eketahuna District. This includes the southern end of the Puketoi Range, from approximately Makuri south, where he describes the Makuri group. This consists of sandstones, siltstones and limestones, Waipipian to Nukumaruan in age.

Beu et al. (1980) mapped the distribution of Cenozoic limestones, from northern Hawke's Bay to northern Wairarapa, and correlated limestone facies within a biostratigraphic framework. Harmsen (1984a, 1984b) described Pliocene temperate shallow marine sediments in southern Hawke's Bay, dividing the Te Aute Group into six formations, four of which outcrop in the Puketoi Range. More detailed reference will be made to the work of Lillie (1953), Neef (1967, 1974, 1984), Beu et al. (1980), and Harmsen (1984a, 1984b), later in this chapter. The stratigraphy which the above authors have used within the Hawke's Bay - northern Wairarapa region, is listed in Table 2.1. Absolute ages for the New Zealand series and stages, referred to in Table 2.1, and their relationship to international subdivisions of geological time, are provided in Table 2.2.

Numerous other authors have made passing reference to the southern Hawke's Bay - northern Wairarapa region, in the vicinity of the Puketoi Range, many in relation to potential reservoir rocks for hydrocarbon accumulations and the limestone resources for agricultural lime.

No modern studies have covered in detail the geology of the Puketoi Range as a whole. The lack of detailed geological maps and stratigraphic sections, and the non-uniform nomenclature may have deterred geomorphological studies.

2.3 Economic Geology

The analysis and distribution of limestone for sutiable agricultural use, in the southern Hawke's Bay - northern Wairarapa region, have been described (for example Aston 1915a, 1915b, 1918; Morgan 1919; Lillie 1953; Kitt 1962; and Moore and Belliss 1979). Pliocene limestones are presently quarried for agricultural lime in four major quarries in the central and southern Hawke's Bay, with a total production of 230 000 tonnes in 1977 (Moore and Belliss 1979). Limestone is also quarried for

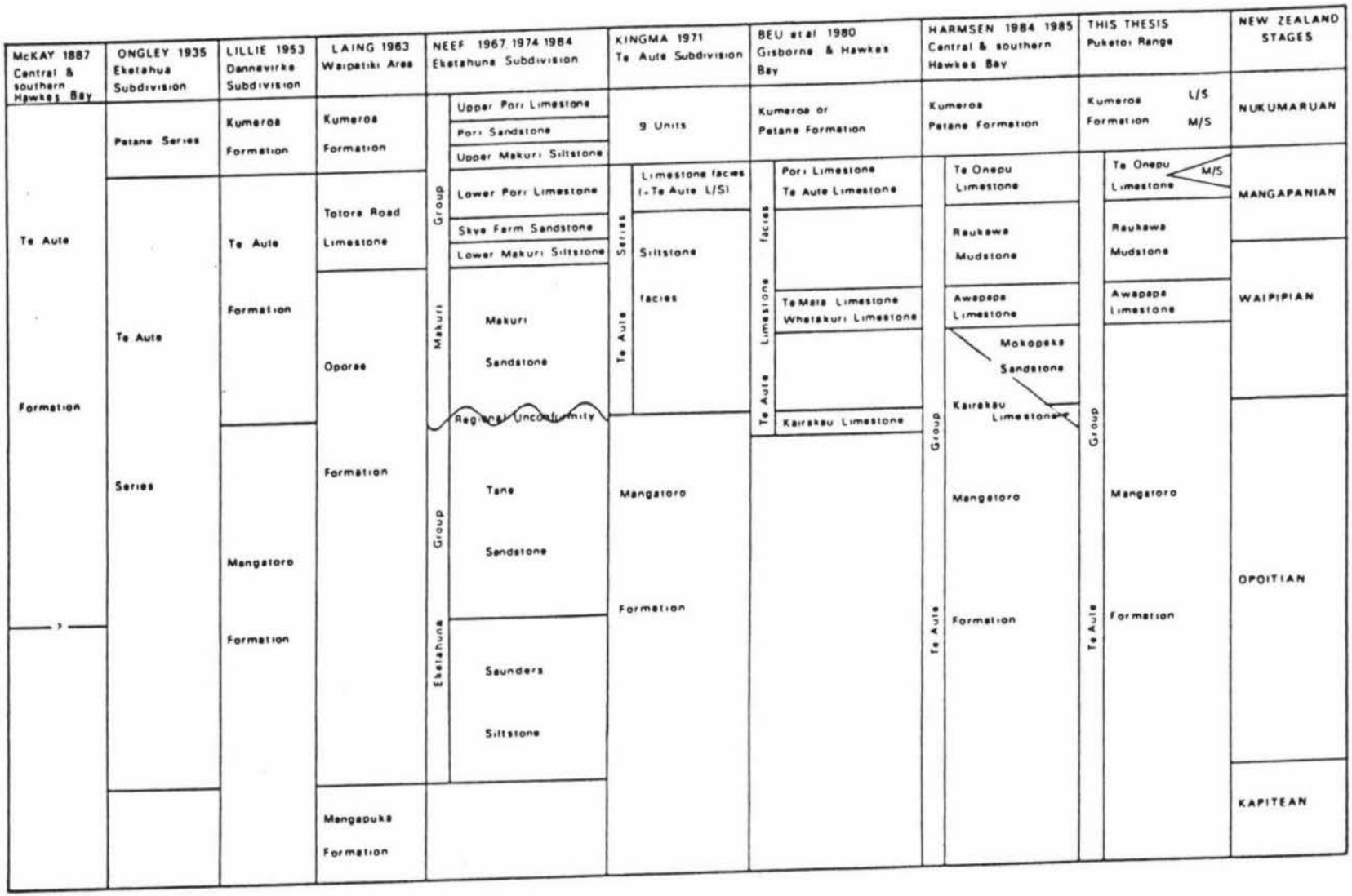

Table 2.1 Tabulation of stratigraphic nomenclature used by previous authors in Hawke's Bay and northern Wairarapa.

Series	Stage	Age of boundary (Ma)	International Divisions
HAWERA			HOLOCENE
		0 35	PLEISTOCENE
WANGANUI	CASTLECLIFFIAN	0 5	
		1 1	
	NUKUMARUAN	c 1 85	
		c 2 0	
	MANGAPANIAN	c 2 3	PLIOCENE
	WAIPIPIAN		
	OPOITIAN	3 2	
TARANAKI	KAPITEAN	5 0	
	TONGAPORUTUAN	c 6 0	MIOCENE

Table 2.2 Late Cenozoic chronostratigraphic divisions. Time in millions of years (Ma) and correlative international divisions. (From Neef 1984)

roading, for use in concrete products, and for building purposes, while large blocks are used for river bank and foreshore protection work. Some of the particularly pure limestone is used in glass manufacture (Kingma 1971).

The largest quarry in the Puketoi Range is the Makuri Gorge Quarry (Grid Ref. T25/609689). Analysis of this limestone gave purities between 88.8 percent and 96.0 percent (Moore and Belliss 1979). Aston's (1915b) analysis of elements in the limestone gave the following results: $CaCO_3$ 93.3 percent, insolubles 4.6 percent, Al/Fe oxides 1.3 percent, and $MgCO_3$ 0.8 percent. Average yearly production from the quarry for agricultural use, between 1973 and 1977, was 2876 tonnes (Moore and Belliss 1979).

Since the 1940's much of the East Coast of the North Island has been prospected for oil. The Pliocene limestones are potential reservoir

rocks for hydrocarbon accumulations. As well as having high porosity and permeability values, the limestones are transgressive and diachronous. This increases their hydrocarbon potential due to possible entrapment of oil, and/or gas, beneath an upper unconformity (Forder 1975).

Small oil and gas seeps have been known since late last century throughout the East Coast, particularly in the Gisborne area, but no economic accumulations of oil have been found (Leslie and Hollingsworth 1972). A review of the hydrocarbon potential of the area was made by the Petroleum Corporation of New Zealand (Exploration) Ltd, in 1978 (cited in Harmsen 1984a). The Pliocene limestone was found to be freshwater saturated from the examination of wells drilled in the southern part of the East Coast Basin. This indicates that these potential reservoirs have been extensively flushed and can no longer be considered to have significant petroleum potential.

2.4 Structural and Tectonic Framework of the East Coast, North Island

The boundary between the Pacific and Indian plates passes along the eastern margin of the North Island (Walcott 1978; Cole and Lewis 1981; Davey et al. 1986) forming a 500 km elongated depression known as the Hikurangi Trough. The oceanic crust of the Pacific Plate is subducted obliquely beneath continential crust of the Indian Plate, to form the Taupo-Hikurangi arc-trench system, (Fig. 2.1). This extends from the Hikurangi Trough, on the eastern side, to the Taupo Volcanic Zone on the western side. The relative motion between the two plates varies from almost normal to the plate boundary, in the northern part of the North Island, to almost transcurrent in the south of the North Island (Davey et el. 1986).

For approximately 200 km west of the Hikurangi Trough, the Benioff Zone dips beneath the accretionary prism. The prism is up to 150 km wide and characterized by a series of imbricate thrust faults, along which movement becomes progressively more oblique (dextral) towards the west. On the outer eastern edge of the prism is the accretionary slope, comprised of a series of ridges and basins 5 km to 30 km wide and 10 km to 60 km long (Lewis 1980). Sediments on the accretionary slope are progressively older westwards, away from the Hikurangi Trough, with the

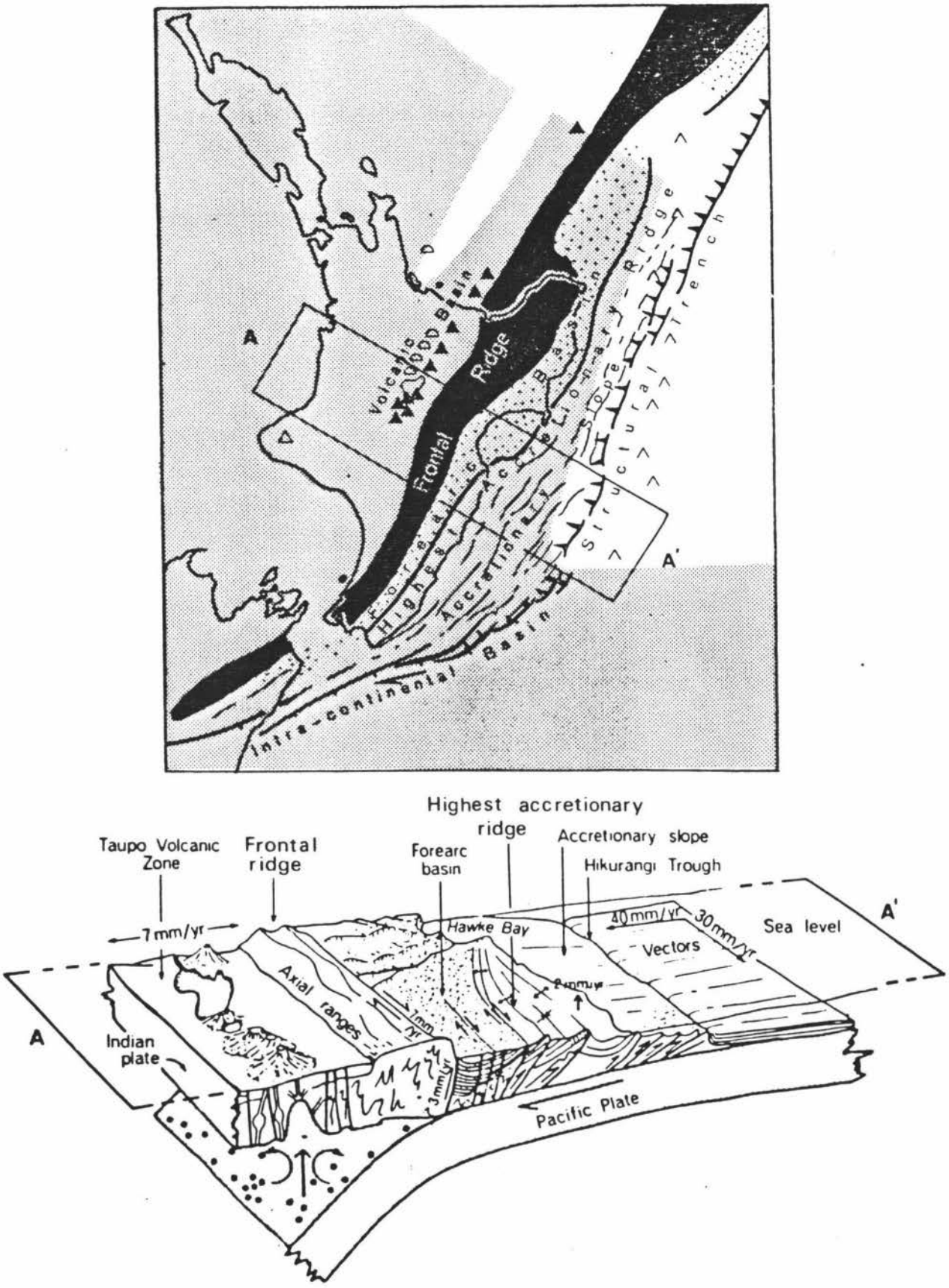

Figure 2.1 A map and block diagram illustrating a plate tectonic interpretation of the structure and landforms of Hawke's Bay. Fine stipple represents continental crust. Lines represent faults, mostly thrust faults. Solid diamonds represent andesite-dacite arc. Open domes represent rhyolite and pantellerite volcanoes. Open diamond represents Egmont high-K andesite volcano. Inverted V indicates possible volcanic knolls. The map is from Cole and Lewis (1981) and the cross-section from Kamp (1982).

older sediments forming the higher accretionary ridges, for example, the Puketoi Range.

The inner part of the prism is structurally a forearc basin (also termed the highest accretionary basin) filled by thick Plio-Pleistocene sediments. The sediments are crossed by strike-slip faults which increase in number and displacement westward (Cole 1984).

The prism is bound on the west by a frontal ridge composed of upper Palaeozoic-Mesozoic greywackes and argillites, as seen in the Ruahine Range. This ridge is undergoing rapid uplift. Present uplift rates are estimated to vary from 2 m to 7 m per 1000 years along the axis of the ranges (Wellman 1967). Studies of marine terrace surfaces at the southern end of the North Island, give uplift rates of 3.0 m to 4.5 m per 1000 years (Ghani 1978).

The volcanic component of the Taupo-Hikurangi arc-trench system is the Taupo Volcanic Zone (Healy 1962) which extends northnortheast from Ohakune to White Island, and comprises a main andesitic arc.

In the remainder of this section the accretionary prism, and in particular, the highest accretionary ridge and the accretionary slope will be considered in more detail. Uplift of the ridge and offshore slope has resulted in the exposure, at the surface, of a semi-continuous outcrop of limestone along the East Coast of the North Island, part of which forms the Puketoi Range.

Along the East Coast of the North Island three clearly separate topographical landform units are recognised in relation to the accretionary prism system:

(1) The North Island axial range; including the Tararua, Ruahine, and Kaweka Ranges; in the west representing the frontal ridge. These ranges are composed of strongly deformed and uplifted Mesozoic greywacke.

(2) The East Coast Inland Depression which represents the highest accretionary basin, extending from Cook Strait to Hawke Bay, which is interrupted only by a basement high area in the vicinity of Mt. Bruce, northern Wairarapa (Bruce Hill No. 2 Grid Ref. T25/329479). The depression is made up of sunken late Pliocene to Pleistocene sediments.

(3) The East Coast Uplands, which represent the higher accretionary

ridges (together termed the "highest accretionary ridge" by Walcott 1978). This is a 30 km to 40 km wide belt of hilly country which separates the inland depression from the Pacific Ocean, and includes several minor ranges such as the Puketoi Range. The area is composed of highly deformed Cretaceous and Tertiary mudstones and limestones. This then extends down the accretionary slope to the Hikurangi Trough.

The accretionary prism, with its basin and ridge system, is the result of landward-thinning wedges of sediment being scraped from the surface of the subducting plate, as it is forced underneath the feather edge of the over-riding plate (Lewis 1980) (Fig. 2.1). As each new ridge is accreted, older wedges, with active thrust-faults between them, are pushed upwards, and landwards, and rotated towards the vertical. This forms the accretionary slope, with each wedge forming a topographic ridge that dams sediment to landward in an accretionary slope basin. The imbricate stack of wedges, particularly the highest accretionary ridge, form a major trench-flank ridge which creates the eastern margin of a relatively large highest accretionary basin.

The highest accretionary ridge from Hawke's Bay south to Uruti Point, southern Wairarapa, has a progression of seaward-faulted, or sharply dipping, anticlinal ridges (Lewis 1973; Katz 1974) and flat-floored, sediment filled synclinal basins, aligned more or less parallel to the slope (Pantin 1963; Lewis 1976). This extends seaward down the accretionary slope to the Hikurangi Trough. The basins range from 5 km to 30 km wide (ridge to ridge crest), and 10 km to 60 km long (Lewis 1980). Strata in the basins are thickest at their landward limit, varying from 200 m to 2000 m thick (Lewis 1980), and then wedge out towards the seaward anticline ridge tops. The oldest beds in any basin dip most steeply landward, and it is inferred from this that they have been tilted from the original, near-horizontal inclination, of the younger overlying beds (Lewis 1980).

Sedimentation changes, related to interglacial sea level highs, and glacial sea level lows, are thought to have produced unconformities within the Quaternary strata deposited on the accretionary slope (Lewis 1971, 1973). Lewis (1980) believes these unconformities can be tentatively correlated with dated maximum glacial extensions. On the basis of these correlations Lewis (1971) estimates the rate of uplift on

the coastal hills to range up to 1.7 m per 1000 years. He estimates the rates of subsidence in the shelf basins to range up to 1.5 m per 1000 years, with rates of tilting reaching a maximum of about 0.03 degrees per 1000 years. Analysis of deep water foraminiferal faunas, from sediment cores of some upper slope anticlines, show uplift of at least 1000 m since Pliocene times (Lewis 1974).

Present uplift rates along the Hawke's Bay coastline have been estimated by Berryman (cited in Kamp 1982) at 2 m per 1000 years. Uplift along the southern Wairarapa coastline is estimated at 1.7 m to 2.2 m per 1000 years at Oterei (Singh 1971). Uplift rates at the White Rocks vary from 0.75 m to 4.0 m per 1000 years, for the growing anticlines, and subsidence rates at 0.5 m to 2.2 m per 1000 years, for the growing synclines (Ghani 1978).

There is substantial sediment supply to the accretionary slope owing to the proximity of the eroding frontal ridge mountain system, the rising coastal hills, and showers of ash from volcanic activity. This continuous supply of material has filled the basins, and in some places draped over growing anticlinal ridges (Lewis 1980). The area of maximum sedimentation varies in relation to the sea level at the time of deposition, with the most rapid zone of deposition migrating back and forth as sea level varies in response to the waxing and waning of ice sheets. As sediment is deposited most rapidly in a coast-parallel prism (Lewis 1973), this prism will move in response to sea level changes. The prism is at present formed on the accretionary slope, ranging from 4 km to 10 km from the coastline, where water depth ranges from 30 m to 100 m. Sedimentation rates are estimated to range from 1.5 m to 3.0 m per 1000 years (Lewis 1980) with present sedimentation being rapid and muddy (Lewis 1980).

2.5 Palaeogeography and Depositional History of the East Coast of the North Island

During the late Miocene and early Pliocene the sea covered an extensive planed surface of Mesozoic greywacke basement rocks over the East Coast area. In Kapitian time, the Wanganui - Hawke's Bay seaway extended as far south as Eketuhuna depositing mud in that area and shallow water

sediments further north (Beu et al. 1980).

Deposition of the Te Aute Group strata began during the early Pliocene with the formation of the northeast-southwest trending fault-controlled depression, along the boundary between the Indian and Pacific plates. The depression was deepest around Hawke Bay; the greatest depth was approximately 500 m before the early Pliocene, with water depth never more than 100 m after this time (Harmsen 1984a). This depression extended westward across the area now occupied by the Ruahine Range and Wanganui Basin. This is based on Opoitian sediments on top of the Ruahine Range (Beu et al. 1980). The axis of the basin continued to subside, accumulating thick, monotonous mudstone (Mangatoro Formation) deposits through most of the Pliocene, along the basin axis adjacent to the Ruahine high.

The eastern side formed an extensive shallow platform on which alternating shallow water carbonates and deeper water terrigenous sediments were deposited (Harmsen 1984a). This Harmsen believed was the result of large-scale alternations in relative sea level positions. This is accounted for by the tectonic setting of the area, and glacio-eustatic changes in sea level, as first suggested by Vella (1965). These changes in sea level have had a major control in the lithology of the sediments, with widespread simultaneous cyclic variations inferred from changing water depth (Harmsen 1984a). This area was the first to be uplifted, forming the East Coast Uplands. Land was exposed in the early Pliocene to the north of Castlepoint, and by the late Pliocene, this area had extended northwards into Hawke's Bay (Fig. 2.2a).

Subsidence in the depression kept pace with sedimentation (3.5 cm per 1000 years) with local variations in the thickness, assumed by Harmsen (1984a) to result from contemporaneous tectonic deformation. During late Opoitian time, marked shoaling is evident in northern and central Hawke's Bay, with the deposition of the Kairakau Limestone and Mokopeka Sandstone Formations.

The early Waipipian was a time of widespread carbonate deposition, with extensive barnacle banks formed along the shallow western margin of the depression (Beu et al. 1980). This is attributed to a glacio-eustatic lowering of the sea level (Beu et al. 1980; Harmsen 1984a). Waipipian

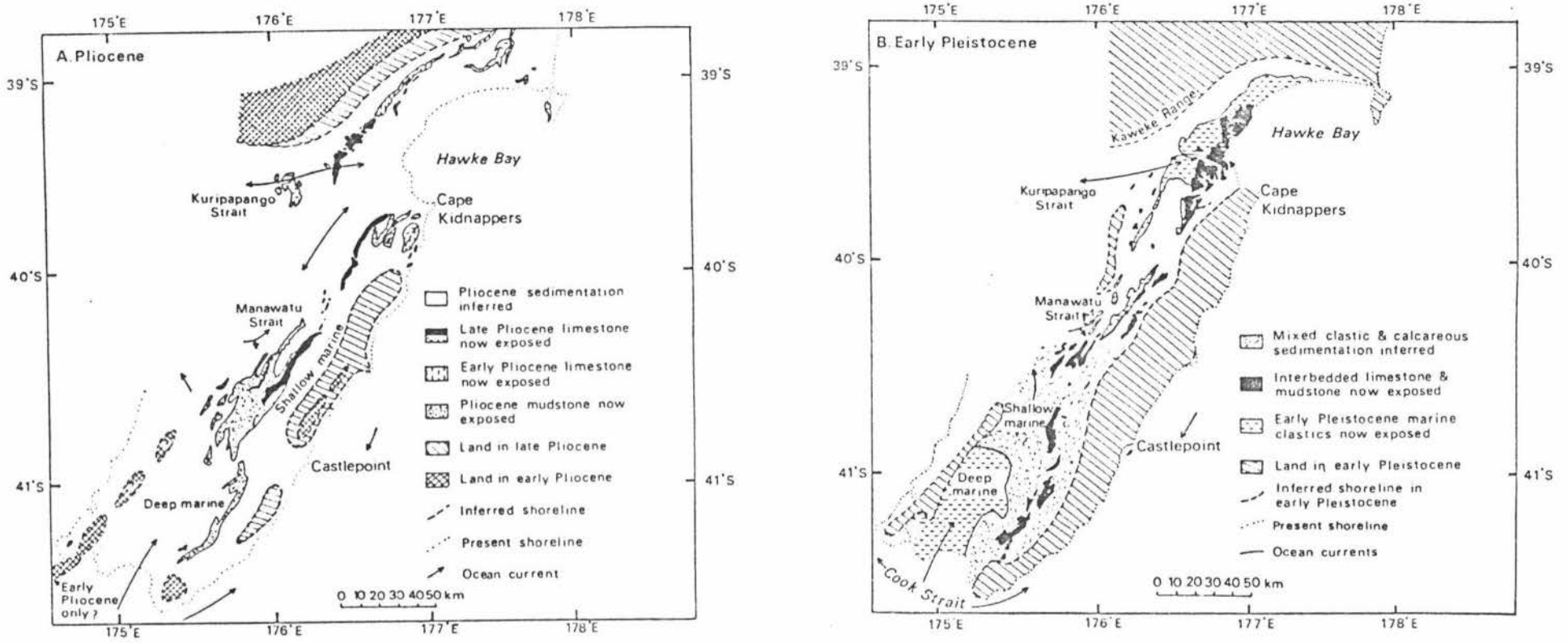

Figure 2.2 Palaeogeographic maps showing development of Hawke's Bay and Wairarapa. (a) Pliocene, (b) Early Pleistocene. (Redrawn from Kamp 1982, and Kamp and Vucetich 1982).

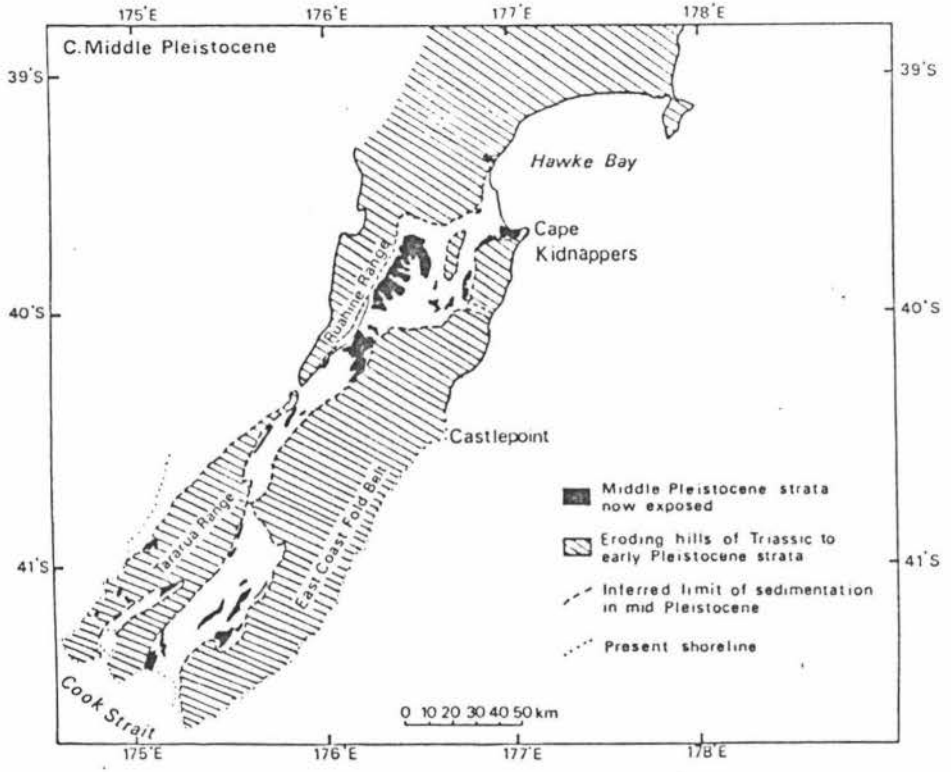

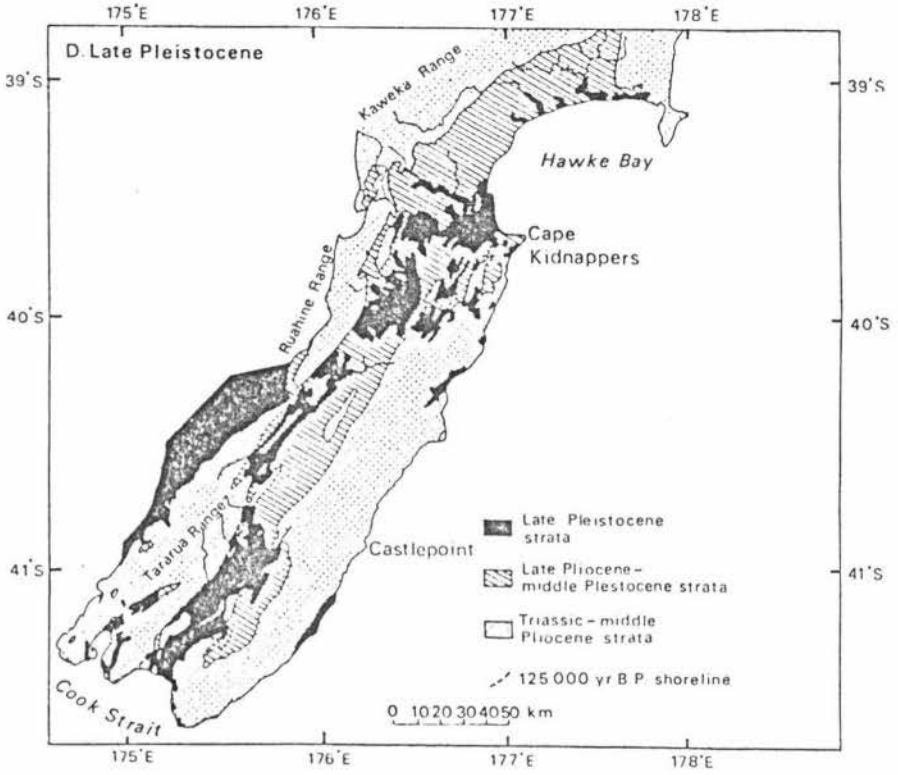

Figure 2.2 Palaeogeographic maps showing development of Hawke's Bay and Wairarapa. (c) Middle Pleistocene, (d) Late Pleistocene. (Redrawn from Kamp 1982, and Kamp and Vucetich 1982).

limestone and calcareous sandstone (Awapapa Formation) were deposited from Cape Kidnappers south to Eketahuna. These were deposited in very shallow depths, the limestone being an intertidal and shallow subtidal carbonate deposit. Their high terrigenous content also suggests proximity to the shoreline (Harmsen 1984a). The Wanganui - Hawke's Bay seaway still existed, with Waipipian limestone cropping out along the Ruahine Range (Browne 1978). Along the present Waewaepa Range, and elsewhere along the East Coast, where greywacke highs were uplifted, Waipipian limestones contain large subangular greywacke clasts at their base. This suggests sedimentation adjacent to an emerging greywacke fault block.

Coastal hills, from Cape Kidnappers to Cape Palliser, were above sea level by this time, with a major seaway still existing from Hawke's Bay southwards into the Wairarapa, and westward over the emerging Ruahine Range into the Wanganui Basin (Kamp 1982). This constriction and shallowing of the depression, to a depth of 30 m, throughout the Waipipian time, resulted in large-scale cross-bedding of the shallow bioclastic limestone. The coarse nature of sediment suggests strong tidal current activity (Harmsen 1984a). With the earthquake activity recorded in local mass-emplaced deposits and slump units, and the rapid variation in limestone thickness, Harmsen (1984a) believes tectonic deformation was the major external control on sedimentation during this time. In the late Waipipian, carbonate sedimentation was followed by renewed deposition of terrigenous sand and mud (Raukawa Mudstone), considered by Harmsen (1984a) to have resulted from increased water depth in response to a reduction in global ice volume.

Greywacke clasts within Mangapanian (late Pliocene) strata, along the margin of the depression, suggest emergent land to the east (Waewaepa Range) and west (Ruahine Range) of the depression (Harmsen 1984a). The Wanganui - Hawke's Bay seaway was still present. Sedimentation during this period was initially mud-dominated throughout the area, but shoaling to the north, possibly resulting from tectonic uplift (Beu et al. 1980; Harmsen 1984a), resulted in the deposition of Argyll Sandstone (Harmsen 1984a). This was followed by widespread, mainly mid-shelf (30 m to 60 m), carbonate deposition (Te Onepu Formation), with the formation of large sand waves and sand ridges, under the influence of strong tidal currents (Harmsen 1984a). This is believed by Harmsen (1984a) to have

resulted from a relative sea level rise through glacio-eustatic change.

The Wanganui - Hawke's Bay seaway still existed in early Nukumaruan time (Beu et al. 1980). The Ruahine Range had been uplifted by this time to form islands in its central part (Fig. 2.2b).

Increased tectonic activity caused the middle of the East Coast Depression to sink and the sides to rise (Beu et al. 1980). Uplift of the Mount Bruce Block (Grid Ref. T25/329479) closed the seaway to the south of Hawke's bay after early Nukumaruan time (Vella 1962).

Deposition of numerous thin, muddy, shelly limestone beds in central Hawke's Bay probably resulted from glacio-eustatic oscillations in sea level during the Nukumaruan time (Beu et al. 1980). This also occurred to a lesser extent in southern Hawke's Bay, as seen in the lithological changes in the Kumeroa Formation.

By the end of the early Pleistocene subsidence of the inland depression had ceased and the whole area was uplifted above sea level. The initial open folding in the Pliocene, changed to more widespread and tighter folding early in the Pleistocene, giving way to reverse and transcurrent faulting later (Kamp 1982). By the middle Pleistocene erosion of the surface was well established, with rivers transporting and depositing sediment, lakes accumulating sediment, and large gravel fans forming along the eastern margin of the Ruahine Range (Kamp 1982) (Fig. 2.2c).

Much of the landscape seen today developed during the late Pleistocene and Holocene periods (Fig. 2.2d). The uplift initiated in the middle Pleistocene continues through to the present, with volcanic activity periodically covering the area with airfall deposits (Kamp 1982). Chapter Seven covers in detail the geomorphological development of the cuesta, and karstic development of the Puketoi Range.

2.6 Tectonic and Depositional History of the Puketoi Range

The structural and tectonic framework, and the palaeogeography of the East Coast have been discussed above. This section will concentrate specifically on the Puketoi Range.

The Puketoi Range is the highest wedge of Tertiary sediment, forming part of the accretionary ridge system, uplifted by the subduction of the Pacific Plate beneath the Indian Plate. This wedge of sediment has been pushed upwards, and landwards, by the movements of the plates (Lewis 1980). Basement greywacke on the feather edge of the Indian Plate has been deformed in the process of subduction of the Pacific Plate. This has resulted in the basement high of greywacke, the Waewaepa Range (west of the Puketoi Range) being uplifted between the accretionary ridge system in the east, and the forearc basin in the west. Tertiary sediments have been eroded off the Waewaepa Range to expose the underlying greywacke. The rapid uplift of this range has influenced the pattern of sedimentation in the basin formed between this range and the Puketoi Range.

The proto-Puketoi Range developed as a sharply dipping anticlinal ridge which has subsequently been eroded to leave the limestone-capped dip slope on the western flank of the anticline. The original anticlinal form of the Puketoi Range is seen today in the many sharply dipping anticlinal ridges formed on the accretionary slope (Lewis 1973; Katz 1974). Calcareous material from current-swept and sediment-free anticlinal ridges was deposited in adjacent basins and on the flanks of the anticlines (Kamp 1982). Deposition tended to be thicker in the centre of the basins, thinning towards the top of the anticline ridge. This pattern of limestone deposition has strongly influenced the shape of the Puketoi Range.

The evolution of the range began with the deposition of sediment from late Miocene time onwards. The main stratigraphic group, the Te Aute Group, began forming in the early Pliocene and continued through to the late Pliocene. By early Waipipian time, the area which became the Puketoi Range was near sea level, with limestones and calcareous sandstones deposited. The Waewaepa Range had been uplifted above sea level, with erosion of the range supplying sediment to the basin.

By mid Waipipian time the area to the east of the Puketoi Range had also been uplifted and was beginning to erode. This resulted in the constriction and shallowing of a seaway between this eastern uplifted land and the Ruahine Range, with the Waewaepa Range forming an island between the two. Sedimentation in the area which formed the Puketoi

Range continued, with the deposition of alternating calcareous and non-calcareous deposits related to changes in sea level caused by either glacio-eustatic changes or tectonic uplift.

Sedimentation continued through to Nukumaruan time, when uplift of the Mount Bruce basement high closed the seaway. The area of the Puketoi Range rose above sea level in the early Pleistocene. Subsequent uplift and subaerial erosion has resulted in the landscape of the range seen today.

2.7 Geology of the Puketoi Range

In the following section, the geology of the Puketoi Range will be discussed. This is based on previously published work (Lillie 1953; Neef 1967, 1974, 1984; Harmsen 1984a, 1984b, 1985) and field work carried out by the author.

2.7.1 Structure

Structurally, the Puketoi Range may be termed a cuesta, consisting of a gently dipping west-facing slope, covered predominantly by the Te Onepu Limestone Formation, and an eastern steeply dipping scarp slope, formed on a succession of geological beds, particularly the Mangatoro Formation. Folding and faulting of these geological beds has occurred. The Alfredton-Makuri-Mangatuna fault runs the length of the Puketoi Range. In the northern section the fault forms a distinctive boundary separating the greywacke of the Waewaepa Range, from the Te Aute Group and Kumeroa Formation deposits of the Puketoi Range and eastern flank of the Waewaepa Range. Neef (1967, 1974, 1984) also identified many minor faults at the southern end of the range.

Large-scale and small-scale synclinal and anticlinal folding has occurred in the geological beds of the Puketoi Range. The range originally developed with the formation of a large asymmetrical anticline, on which a series of smaller synclines and anticlines have developed. This is clearly seen in the northern section of the Puketoi Range where a series of anticlinal and synclinal folds have formed (see cross-section A-A', back pocket).

The basin formed between the Puketoi and Waewaepa Range has been infilled with younger marine sediments, accumulating the Kumeroa Formation sediment during the Pleistocene. These sediments have formed adjacent to the Waewaepa Range as it was being uplifted. Eroded greywacke pebbles are found in the beds. The deposit has also been faulted and folded.

2.7.2 Lithology

Late Miocene to Pleistocene sediments were deposited in the location of the present Puketoi Range, and on the flanks of the emerging Waewaepa Range. These sediments are characterised by thin, 20 m to 70 m thick, alternating beds of barnacle-rich coquina limestone and calcareous sandstone. These are interbedded between 60 m to 240 m thick, terrigenous deposits of siltstone and mudstone, which are occasionally sandy or carbonaceous (Harmsen 1984a, 1984b, 1985).

Rapid vertical and lateral facies changes are also characteristic of the geological beds of the range. This results in a great variation of thickness and continuity of the beds. For example, the Raukawa Formation varies in thickness from 60 m, at Coonoor (Grid Ref. U24/784827 - 773833), to 40 m at Makuri (Grid Ref. T25/690671 - 680682).

The lithology of individual formations is given, in detail, in Appendix Two. The description of the Te Aute Group is based on the work of Harmsen (1984a, 1984b, 1985), while that of the Kumeroa Formation is from Lillie (1953).

2.7.3 Petrology of Te Aute Group Limestone, Puketoi Range

Sweeting (1978) examined the petrology of the limestone of the Puketoi Range. At this time, the published geological map of the area showed the whole of the range to be Te Aute Group deposits. From the map drawn by the author, Kumeroa Formation is identified in the area Sweeting examined. Therefore, some of her samples may have been Kumeroa Formation limestone and not Te Aute Group limestone as shown on Kingma's (1962) map.

From the eight to ten limestone specimens she examined, Sweeting made the following comments:

> "This is a very fossiliferous rock, all organisms closely packed together and although fragmental their margins are generally smooth and rounded and appear to have been transported over a prolonged period of deposition. The matrix in which these fossils are embedded is very fine and like them appears to have been laid down under very quiet conditions.
>
> Scattered through the rock are clean bright quartz fragments, some showing distinct prismatic outlines. The rock is clean and fresh and there are no evidences of any alteration products." (Sweeting 1978, p.254)

Sweeting estimated the effective porosity of the limestone as between 5 and 12 percent, with insoluble residue determined at 5 to 10 percent. All of the insoluble residue was quartz.

Sweeting also made the following general observation of the New Zealand Tertiary limestones, to which the Te Aute Group belongs. The limestone showed no recrystallisation, in the specimens she examined, though they were quite hard and lithified. She found calcite occuring as cloudy or smudgy patchs full of inclusions and fragments, and rarely occurring in rhombic or platey forms. She found no true micrites or sparites, the limestones mainly consisting of biomicrites and biosparites, with a fairly high porosity. The texture was fine to medium.

The quartz grains were large fractured grains and stout prismatic crystals and there were a few pyramidal sections, which occurred chiefly in clear allotrimorphic forms with no inclusive material (Sweeting 1978).

2.8 Geological Map of the Puketoi Range

Geological mapping of the Puketoi Range has, in the past, been restricted to either generalized coverage of the area, for example Kingma's (1962) work, or detailed geological investigation of only a small portion of the range, for example Neef's (1974) investigation. This lack of detailed geological information for the range as a whole restricts any geomorphological investigation of structure/landform relationships and it was for this reason detailed mapping of the range was undertaken by the author.

2.8.1 Method of geological investigation

Geological information used in the drawing of the map was obtained

primarily from fieldwork and aerial photograph interpretation, with additional information from previously published material. This information was placed onto aerial mosaic maps (N.Z.M.S. 3 Sheets N.150/5, 7, 8; N.153/6; and N.154/1, 4) at a scale of 1:15 840. The information was then transferred and reduced to a scale of 1:63 360, and finally to a scale of 1:50 000. The area mapped is covered by the metric maps N.Z.M.S. 260 U24, U25, T24, and T25.

Approximately four weeks was spent in the field investigating the geology of the range, with the area north of Coonoor receiving the greatest attention, owing to its geological complexity. The southern part of the range mapped by Neef (1967, 1974, 1984), was given a reconnaissance check to correlate his stratigraphic nomenclature with that of Harmsen (1984a, 1984b, 1985), and to confirm the position of beds described by Neef (1974). Much of the central part of the range was not field checked, either because of its isolated nature, or the simplicity of the geology as indicated by aerial photograph interpretation.

Aerial photographs at a scale of approximately 1:25 000 were used in conjunction with a stereoscope, to give a three dimensional image of the area. The photograph runs used were: SN 5139 G/26-30; SN 5139 H/31-35; SN 5139 I/30-33; SN 5310 A/10-15; SN 5310 B/7-13; SN 5310 C/5-9; SN 5408 G/16-18; and SN 5408 F/18. The photographic coverage included most of the range, and enabled the identification of geological beds.

The nomenclature used for the identification of the geological beds is based on the work of Harmsen (1984a, 1984b, 1985). The three stratigraphic columns described by Harmsen (1984b) are used as the basis for stratigraphic positioning of the geological beds along the range (Appendix Three). Neef's work on the southern end of the range was also used (Neef 1967, 1974, 1984). Faults and folds identified by Neef were transferred directly on to the map. Geological boundaries were correlated with the work of Harmsen, or adjusted when found to be incorrectly placed. The position of the greywacke of the Waewaepa Range is based on Lillie (1953) and Kingma (1962).

Position and naming of all the faults, anticlines and synclines are based on previous work. The Mangatuna fault was first recognised by Henderson

(1915). Other faults shown are described by Neef (1967, 1974, 1984). The synclines and anticlines shown are from the work of Laing (1963), Ridd (1964), and de Caen and Darley (1969), for the area north of Makuri, and from Neef (1967, 1974, 1984) for the area south of this. The Oporae anticline may possibly be more correctly termed a monocline, with the east facing beds dipping very gently. Dips are based on the author's fieldwork, Neef (1974), and Lillie (1953), with each indicated differently on the map.

The geological cross-sections shown at the bottom of the map are based on the results of the author's fieldwork and Neef (1974) (cross-section C-C'). They illustrate the close relationship between structure, lithology and landforms which will be examined later in chapters Four and Seven of this thesis.

Geological boundaries shown on the map indicate lithological changes identified by fieldwork or interpreted from aerial photographs; for example, the pronounced lithological change from the Te Onepu Limestone Formation to the underlying Raukawa Mudstone Formation. Further refinement of the map may be possible with detailed palaeontological studies. For instance, the boundary between the Te Onepu Formation and the overlying Kumeroa Formation cannot, in places, be accurately identified on the basis of lithology alone.

An accurate geological map of the Puketoi Range was required by the author before geomorphological investigations could be made. Other than the work of Neef (1967, 1974, 1984) on the southern end of the Puketoi Range, there was no detailed geological information available before the drawing of this geological map. Much of the previously published geological information about the Puketoi Range is very generalized or contains considerable inaccuracy. Kingma (1962, 1967), for example mapped the Puketoi Range on the basis of the age of the geological beds and not on lithological variation within the beds. This resulted in the majority of the range being mapped as Waitotaran and Opoitian in age, with only generalized lithological variation within each stage given.

Inaccuracy in the interpretation of the structure of the range has also occurred. This is seen in the work of Beu et al (1980) who estimated the thickness of the limestone within the range to be 200 m from a traverse

from Coonoor to the top of the range (Grid Ref. U24/797825-778918). This is considerably greater than the thickness which Harmsen (1984a, 1984b, 1985) estimated to be 20 m (for the Te Onepu Limestone Formation) and 40 m (for the Awapapa Limestone Formation) in the same area (Grid Ref. U24/784827-773833). Harmsen's estimates are considered by the author to be far more accurate.

CHAPTER THREE
SOLUTIONAL PROCESSES AND EROSION

3.1 Introduction

The solubility of limestone in natural waters results in the solutional development of karst landforms. The understanding of the solutional processes has greatly increased the understanding of the development of karst landforms.

Shaler (1890) was one of the first to propose ideas on the solubility of limestone, suggesting that the amount of CO_2 dissolved in soil water greatly influenced solution. Grund (1903) and Cumings (1906) recognised that carbonic acid was produced by water and CO_2.

The influence that air and water temperature have on the solution of limestone was also recognised at this time (Sawicki 1909). By the 1930's the importance of CO_2 in the solution of limestone was more fully understood (Adams and Swinnerton 1937), and the influence of climate on karst morphogenetic processes and resultant landform assemblages was also appreciated. For example, O.Lehmann in 1927 recognised altitudinal zonation in karst features and in 1936 H.Lehmann, from his work in the tropics, proposed that climate played a dominant role in karst morphogenetic processes.

In the early 1950's the influence of biological activity in the production of CO_2 was once again stressed (Schoeller 1950; Trombe 1952; Roques 1956). The influence that the relationship between temperature and CO_2 has on solutional processes was also observed (Birot 1954). Water at a lower temperature can contain more dissolved CO_2 than water at higher temperatures. Corbel (1959) concluded that colder climatic conditions result in more rapid solution than tropical climates. A year later Bögli (1960) argued to the contrary. He proposed that increased temperature resulted in the higher production of organic matter and, as a result, higher CO_2 concentrations in soil water. As a consequence, he argued that greater amounts of carbonic acid are produced in the humid tropics and subhumid regions.

Corbel's work received more attention because of its quantitative nature and also because of the boom in quantitative geomorphology at that time.

It was not until later in the 1960's that the effect of variation in temperature on CO_2 production was seen as being less important than CO_2 produced by vegetation. Also during this time, solutional rates and carbonate concentrations within karst areas were found to vary both horizontally and vertically. Williams (1968, p.1) proposed that solution is irregular in time and place resulting in variations in the spatial and temporal distribution of solution.

The importance of partial pressure of CO_2 is now clearly understood, as is the effect of temperature on solution. Geological variations in lithology and structure also influence solution (Sweeting and Sweeting 1969; Jennings 1971) but their effects are still not fully understood. The combined effects of climate, geology, relief, vegetation, soils, and drainage are now seen as being influentual in the solutional processes in individual drainage basins, and the resultant landform development.

Over the past 20 to 30 years, many estimates of karst solutional erosion rates have been made. Smith and Atkinson (1976) summarised 134 estimates of the rate of solutional erosion and 231 reports of the hardness of springs and river waters. Within New Zealand, Dowling (1974) and Williams and Dowling (1979) studied solution of Ordovician marble in northwest Nelson, and more recently Gunn (1978, 1981) estimated solutional erosion of Oligocene limestone in the Waitomo district.

This chapter discusses solutional processes and erosion within the Puketoi Range. This is the first investigation in New Zealand of solutional processes on Pliocene/Pleistocene limestones. The chapter begins with a discussion on the chemistry of solution. This is followed by a description of the method of investigation, and a list of water sampling sites within the Puketoi Range. The characteristics of the water sampled are discussed and an estimation is made of solutional erosion from a small drainage basin at Coonoor.

3.1.1 The Chemistry of Solution

The chemistry of limestone solution has been discussed by many researchers. In this section, only a brief discussion is given. For a more detailed account, see for example, Pickett, Bray and Stenner (1976).

Many processes operate in the development of karst landscapes, the most important possibly being solution of the limestone by water. The maximum solution of calcite in pure water is 13 mg l^{-1} at 16 degrees Celsius and 15 mg l^{-1} at 25 degrees Celsius (Jennings 1985). This is well below the concentration of calcium and magnesium found in the natural water systems of karst areas, where values commonly range from 200 mg l^{1} to 250 mg l^{-1} (Trudgill 1985).

The higher concentrations of $CaCO_3$ and $MgCO_3$, measured from water samples, are due to the increased aggressiveness of the water with the addition of acids, predominantly carbonic acid from dissolved CO_2. The main source of the CO_2 is plant root respiration and the bacterial decay of organic matter (Pitty 1966). Other acids, such as humic and sulphuric acids are of importance, but only locally.

The solution of $CaCO_3$ occurs through a complex series of ionic dissociations and reversible reactions, governed by activity constants and saturation equilibria. The following simplified discussion is taken from Jennings (1985). For a more detailed account, see Picknett (1976).

Hydrogen (H^+) and hydroxyl (OH^-) ions are found in solution, as some water molecules are always in a state of dissociation. These ions react with CO_2 to form carbonate acid:

$$\underset{(air)}{CO_2} \rightleftharpoons \underset{(aq)}{CO_2}$$

$$\underset{(aq)}{CO_2} + H_2O \rightleftharpoons H_2CO_3$$

Both of these reactions proceed slowly. The carbonic acid can also dissociate into its constituent ions.

The physical solution of $CaCO_3$ also proceeds slowly:

$$\underset{(solid)}{CaCO_3} \rightleftharpoons Ca^{2+} + CO_3^{2-}$$

The following two reactions occur extremely quickly:

$$CO_3^{2-} + H^+ \rightleftharpoons HCO_3^-$$

$$HCO_3^- + H^+ \rightleftharpoons H_2CO_3$$

The amount of limestone dissolved is therefore dependent on the hydrogen ion concentrations, and this in turn is usually dependent on the CO_2 in solution.

The quantity of CO_2 held in the water is governed by the water temperature and partial pressure of the carbon dioxide (pCO_2) in the air with which the water is in contact (Henry's Law). The temperature effect is an inverse one, with lower temperatures allowing more CO_2 into solution. The more CO_2 there is in the air, the more that can go into solution until an equlibrium is reached. The pCO_2 ranges from 0.03 percent by volume in open air, near sea level; to values of 0.5 to 2 percent in soil and cave air, with extreme values a magnitude higher (Jennings 1985).

Solution by acidic water continues until saturation equilibrium is reached between the air, water, and rock. In the open system this may vary from a few hours to a number of days, due to the slow progress of some of the reactions discussed above. In the closed system, which happens when soil water passes down into joints and fissures in the limestone, saturation is reached much sooner but at lower concentrations of $CaCO_3$.

3.2 Method of Investigation

In order to investigate the spatial and temporal variation of solution in the karst area of the Puketoi Range, and to estimate solutional erosion of a karst drainage basin within the area (see section 3.3), 15 water sampling sites were chosen from within the range. The water examined at these sites was derived from karst areas only, non-karst areas only, and water of mixed origin.

Three of these sites (3, 12, and 13) are from a drainage basin at Coonoor where solutional erosion of the range was estimated. This will be discussed later in the chapter.

Weekly sampling was carried out from 7.3.86 to 19.8.86, with additional samples collected from sites 3, 12, and 13 on 14.9.86.. The information about the measurements were recorded each time a water sample was collected, and is given in Appendix Four. The date and time was noted. The dry bulb and wet bulb air temperatures and relative humidity were recorded using a whirling hygrometer. This was spun continuously for approximately two minutes before the readings were taken. The temperature was read to the nearest 0.5 of a degree Fahrenheit. These measurements were converted to the equivalent in degrees Celsius. The relative humidity of the air at the time of the reading was estimated from the chart supplied with the whirling hygrometer.

The water temperature was also measured using a thermometer reading to 0.1 degrees Celsius. The thermometer was placed in the water for approximately two minutes before the reading was taken.

Water samples were collected in 100 ml polythene bottles from the surface layers of water from each site. Each bottle was labelled with a site number, and used in the collection of water from only that site. Before the collection of a sample, the bottle was washed three times in the water at the site. The sample was then brought back to Massey University, where it was analysed using a Varian techtron AA-100 spectrophotometer to measure calcium and magnesium content. The pH was also measured. The analysis of the samples was usually within two to three days of collection, with the period never exceeding six days.

3.2.1 Description of Water Sample Sites

A brief description of each sampling site is given below. This details the grid reference, physical features, and the lithology of the rock at each sampling site. These sites, and the rainfall data collection point are shown on Figure 3.1.

SITE 1 Mangatoro Stream (Grid Ref. U24/799927)

This site is situated at the northern end of the Puketoi Range, near the approximate northern limit of limestone beds in the range. The samples were collected from beside the bridge, where the Mangatoro Road crosses the Mangatoro Stream. Water at this site is derived from the greywacke

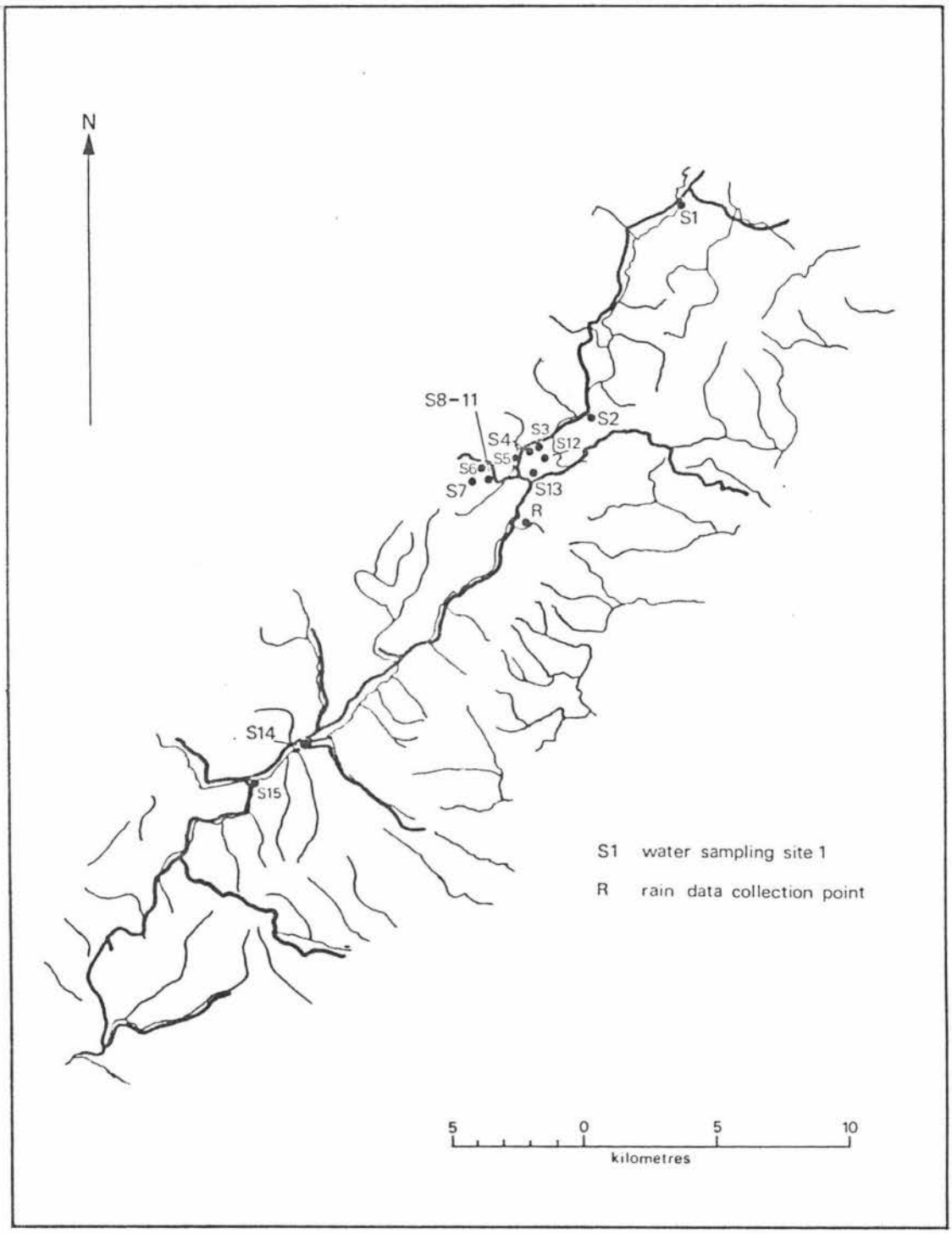

Figure 3.1 Water sampling sites and rainfall collection point in the Puketoi Range.

of the Waewaepa Range, and the limestones and mudstones of the Puketoi Range.

SITE 2 Mangatoro Stream (Grid Ref. U24/762842)

Site 2 is upstream from site 1, approximately midway between the headwaters of the stream and site 1. Samples were collected from beside the bridge, where the Mangatoro Road crosses the Mangatoro Stream. At this site water is also derived from the Waewaepa and Puketoi Ranges.

SITE 3 Towai Drainage Basin Resurgence, Mangatoro Stream
(Grid Ref. U24/737827)

Water collected from this site is derived from the caves and surface streams which flow from the crest of the Puketoi Range, down through the Famous Five Cave system to resurge at this site (Fig. 3.2). Samples were collected from the drain passing under the Mangatoro Road. Water samples from this site were used to estimate solutional erosion of limestone within the Puketoi Range.

SITE 4 Spring, Mangatoro Stream (Grid Ref. U24/737824)

Site 4 is a small spring on the western side of the Mangatoro Stream. Water examined here is from limestone. Each water sample was collected from the centre of the spring.

SITE 5 PT17 Cave Resurgence, Mangatoro Stream
(Grid Ref. U24/731820)

The true resurgence to the PT17 Cave system is approximately 100 m downstream and 20 m lower than the site sampled. Access to this resurgence is difficult, therefore a higher level overflow resurgence was sampled. Here water flows from two sites between the limestone boulders collapsed over the cave entrance. The water flowing through the cave is derived from the Waewaepa Range and water percolating through the limestone overlying the cave. Water samples were collected from the small stream flowing from this resurgence.

SITE 6 Stream from the Waewaepa Range (Grid Ref. U24/724817)

Site 6 and Site 7 are streams originating on the greywacke of the Waewaepa Range. Site 6 is the stream which flows directly into PT17 Cave. The samples were collected from the approximate boundary between the limestone of the Puketoi Range and the greywacke of the Waewaepa Range. The sampling site was slightly downstream of the gravel pit.

SITE 7 Stream from the Waewaepa Range (Grid Ref. U24/719812)

Samples were collected from the true left stream above the junction with the stream flowing along the boundary of the limestone and greywacke. This site was on the greywacke of the Waewaepa Range.

SITE 8 PT17 Cave, Coonoor (Grid Ref. U24/725814)

This, and sites 9, 10, and 11 are from within PT17 Cave (Fig. 6.4). Water sampled at these sites is derived from the greywacke of the Waewaepa Range and water percolating through the limestone above the cave. Site 8 is at the appearance of a small stream within the cave (marked as site 8 on Fig. 6.4. Sites 9, 10, and 11 are also marked on this figure).

SITE 9 PT17 Cave, Coonoor (Grid Ref. U24/725814)

Samples were collected from the bottom of the waterfall within the cave. This stream is the same as that sampled at site six on the surface.

SITE 10 PT17 Cave, Coonoor (Grid Ref. U24/725814)

This site is situated approximately 5 m downstream from the junction of the two streams ("Record Junction", Fig. 6.4) flowing through the cave, that is, the combined streamflow of water sampled from sites 8 and 9.

SITE 11 PT17 Cave, Coonoor (Grid Ref. U24/725814)

This site is situated at the downstream end of the cave ("Bottle Neck Squeeze", Fig. 6.4), where the water passes through a narrowing of the passage walls, then travels approximately 20 m downstream before

disappearing into a gravel sump.

SITE 12 Famous Five Cave Submergence (Grid Ref. U24/741817)

This site is situated within the Towai drainage basin. Samples were collected from the stream as it submerges into the Famous Five Cave system (Fig. 3.2). The water sampled here is derived from limestone areas only.

SITE 13 Famous Five Cave Resurgence (Grid Ref. U24/740822)

This site is also situated within the Towai drainage basin. Samples were collected from the pool at the resurgence of the Famous Five Cave system. This water is also derived from limestone areas only.

SITE 14 Makuri River (Grid Ref. T24/654704)

This site is situated at the bridge below the Makuri village, where the Makuri Owahanga Road crosses the Makuri River. The water sampled at this site is from the Waewaepa and Puketoi Ranges.

SITE FIFTEEN Makuri River (Grid Ref. T25/627688)

This site is situated below the bridge, where the Pori Road crosses the Makuri River. This site is the most southern collection site along the Puketoi Range. River height measurements were also taken from the staff positioned on the bridge. The water sampled here is derived from the Waewaepa and Puketoi Ranges.

3.2.2 Results

A total of 306 water samples were analysed from the 15 sites within the Puketoi Range. The information obtained from the analysis of the samples is given in Appendices Four, Five, and Six. Three distinctive types of water were identified within the springs, surface streams, and cave streams examined. The three water types are: allogenic water derived from non-karst areas, autogenic water derived from karst areas, and mixed allogenic-autogenic water derived from karst and non-karst areas. The characteristics used in distinguishing of each of these water types will

be described below. Table 3.1 indicates the type of water sampled at each site.

Table 3.1 Type of water sampled at each site.

	Allogenic	Autogenic	Mixed
Site Number	6, 7	3, 4, 12, 13	1, 2, 5, 8, 9, 10, 11, 14, 15

3.2.2.1 Allogenic Water

Allogenic water was identified at sites 6 and 7. This water is derived from the greywacke of the Waewaepa Range, and has had little or no contact with limestone. The water therefore has a low $CaCO_3$ content, and the $MgCO_3$ content is close to the $CaCO_3$ content.

The mean $CaCO_3$ values for these two sites was 9.02 mg l^{-1} at site 6 and 8.24 mg l^{-1} at site 7. These were the lowest mean $CaCO_3$ values recorded for the 15 sites investigated.

Mean $MgCO_3$ content of the water samples at both sites (8.36 mg l^{-1} at site 6 and 7.21 at site 7) were very close to the mean $CaCO_3$ content. On occasions the $MgCO_3$ content exceeded that of $CaCO_3$. For example, on 5.5.86 and again on 11.5.86 the $MgCO_3$ content was greater than $CaCO_3$ at site 6.

Allogenic water is aggressive to limestone with all samples analysed well below carbonate saturation (Appendix Five). This again reflects the lack of contact with limestone. At most other sampling sites, water samples were found to be saturated for some part of the year in which sampling was carried out.

A strong correlation was found between the total hardness and $CaCO_3$ at both sites. There was a negative correlation between water temperature and $CaCo_3$.

Fluctuations in the total hardness of the water samples were not very large except in late July when a period of heavy rain was followed by a dry period, then rain again. This caused the largest fluctuations in $CaCO_3$ and $MgCO_3$ content at both sites during the sampling period.

The existence of $CaCO_3$ and $MgCO_3$ within these water samples may indicate small quantities of limestone within the greywacke of the Waewaepa Range, as noted by Lillie (1953) in his lithological description of the greywacke. Other sources of calcium and magnesium could be rainwater (see section 3.3.3 from rainwater analysis of the area), although values of calcium and magnesium within rainfall samples measured by the author were very low. Artificial inputs from aerial topdressing of fertiliser may also be contributing to these low values at sites 6 and 7.

Magnesium carbonate values from the Waewaepa Range were similar to all other sites examined within the Puketoi Range. The reason for this consistency in values is unknown.

3.2.2.2 Autogenic Water

Water sampled at sites 3, 4, 12, and 13 was identified as autogenic water. This water is derived from limestone areas only. Contact with the limestone has resulted in generally high $CaCO_3$ values being recorded at these sites. The highest value, for all the samples examined, was recorded at site 3 (194.7 mg l^{-1}).

These high values result from extended periods of contact time with the limestone. Saturation of the water with $CaCO_3$ is frequently reached. This is particularly so during the summer when reduced rainfall decreases the flow-through time of the water percolating through the limestone, resulting in increased water hardness values. The high values are also maintained because there is no dilution with water from non-karst areas.

The period of contact with the limestone is reflected in the amount of carbonate the water carries. At site 4 the mean total hardness is 93.57 mg l^{-1}, well below values found at sites 3, 12, and 13 (for example, 143.41 mg l^{-1} at site 3). This indicates that water at site 4 has been in contact with limestone for a shorter period of time compared with other autogenic sites.

Fluctuations in total hardness values, which are related to storm events, are also less extreme than those at sites where mixed allogenic-autogenic water was sampled. This results from the infiltration of water into limestone, reducing direct runoff. This leads to a more constant supply of water to streams, reducing the sharp water-flow peak associated with storms events recorded in non-karst areas.

A very high correlation between $CaCO_3$ and total hardness was found at all autogenic sampling sites. This reflects the small contribution $MgCO_3$ has to the total hardness at these sites.

3.2.2.3 Mixed Allogenic-autogenic Water

Mixed allogenic-autogenic water was identified at sites 1, 2, 5, 8, 9, 10, 11, 14, and 15. Four of the sites were in surface streams (sites 1, 2, 14, and 15), while the remainder were within PT17 Cave.

The surface stream sampling sites revealed the greatest fluctuation in the total hardness, reflecting the strong influence storm events have on the water at these sites. The volume of water from non-karst areas during a storm event will dilute the carbonate within the stream, reducing the saturation of the water. During the summer period, when runoff is low, stream samples were found to be saturated because of the reduced input from rainfall. This was not evident during the winter when dilution occurs.

Five sampling sites were from the PT17 Cave system. This cave is fed by water from the greywacke of the Waewaepa Range and water percolating through the limestone above the cave. The water is therefore mixed allogenic-autogenic water with a larger component being allogenic water. Mean hardness values from water sampled within the cave, samples from the surface stream that flows into the cave, and samples at the cave resurgence, indicate an increasing amount of $CaCO_3$ within the water as it flows downstream through the cave system. The $MgCO_3$ values are approximately constant.

At site 6 (surface stream from the Waewaepa Range), mean total water hardness was recorded at 18.95 mg l^{-1}. The mean total hardness increased to 20.69 mg l^{-1} after entering the cave (site 9), and continued to increase downstream from this sampling point. Site 8, the side-stream

sampled within the cave, had a much higher mean total hardness (81.55 mg l^{-1}). This would indicate that the water had been in contact with limestone for a much longer period than the water sampled at site 9. This water was diluted when it mixed with water from the main stream. (The mean total hardness was recorded at 60.27 mg l^{-1}). Mean total hardness levels continued to increase in value downstream, reaching 75.47 mg l^{-1} at the resurgence (site 5).

A marked increase in the mean total hardness occurred over the summer-autumn period of sampling within PT17 Cave, then it decreased during the winter, similar to that recorded at other sites. This marked increase in mean total hardness was only noted within PT17 Cave, and not at other sites examined.

This peak in the hardness values at sites 9 and 10 during the summer-autumn period, may reflect changes in the combined volumes of water, from allogenic and autogenic sources entering the cave, and the degree of hardness of each water source.

3.3 Calculation of Solutional Erosion

Solutional erosion rates have been estimated world-wide in karst areas using one of three methods of investigation: (1) measurement of $CaCO_3$ and $MgCO_3$ within water samples collected from a selected drainage basin over a period of time. This is a measure of the amount of dissolved $CaCO_3$ and $MgCO_3$ removed by solution from a basin; (2) use of a microerosion meter to measure rates of surface lowering of limestone blocks over a period of time; and (3) use of limestone tablets to measure the change in weight (amount solutionally eroded) of the tablets over a period of time, after the initial placement of the tablets in the soil or on the surface of a limestone area.

The first of these methods was used by the author to estimate the solutional erosion rate from a drainage basin within the Puketoi Range. This method required the collection of water samples from a selected drainage basin and the analysis of these samples for $CaCO_3$ and $MgCO_3$. From this data, an estimation of the solutional erosion rate was made.

World-wide results indicate that solutional processes strongly reflect certain environmental factors. Within the Puketoi Range climate, geology and relief are seen as the dominant factors effecting solution, while other factors such as vegetation, soils and drainage are seen as being of less importance.

Long-term variation in climatic conditions within the Puketoi Range influences the amount of solutional erosion to a large degree. This restricts the validity of the temporal extension of the results given below and the inferences that can be made about long-term trends, both in the past and in the future. This is of particular relevance within the Puketoi Range because of the periglacial environment prevailing during the Otira Glaciation and the effect this could have had on the rate of solution.

3.3.1 Computational Techniques in the Estimation of Solutional Erosion

Corbel (1959) was the first to propose a formula for estimating solutional erosion rates in karst areas, namely:

$$X = \frac{4\ E\ T\ n}{100}$$

where X = mean erosion rate in $m^3/km^2/yr$

E = mean annual runoff in decimetres

T = average $CaCO_3$ content of the water in mg l^{-1}

$\frac{1}{n}$ = the proportion of carbonate rock in the drainage basin as a fraction of the total basin area.

Several disadvantages have subsequently been noted in the use of Corbel's formula: (1) the value of E, obtained from the subtraction of evapotranspiration from precipitation, may be inaccurate; (2) magnesium hardness is not taken into consideration; (3) variation in limestone densities are not allowed for; and (4) input of solutes from outside the drainage basin are not taken into account.

Williams (1964, cited in Williams 1968) modified Corbel's karst denudation formula to:

$$X = \frac{E\ T\ n}{10D}$$

where X = carbonate rock dissolved by solution in $m^3/km^2/yr$, or mm/1000 years assuming constancy of conditions

E = mean annual water runoff in decimetres

T = mean total hardness ($CaCO_3$ + $MgCO_3$) in mg l^{-1}

D = density of the limestone

$\frac{1}{n}$ = the proportion of carbonate rock, in the drainage basin as a fraction of the total basin area.

This formula is used when discharge records are unavailable and water surplus is calculated from precipitation less evapotranspiration. Williams (1964, cited in Williams 1968) modified the formula for situations in which discharge records were available:

$$X = \frac{Q\ T\ n}{10^9 AD}$$

where X = limestone removed in solution in millimetres for a specified period

Q = total discharge for the specified period in litres

T = mean total hardness ($CaCO_3$ + $MgCO_3$) in ppm (mg l^{-1}) for the period

$\frac{1}{n}$ = the proportion of carbonate rock in the drainage baisn as a fraction of the total basin area

A = the basin area in square kilometres

D = the density of the carbonate rock in g/cm^3

Since the development of this formula by Williams, many attempts have been made to improve the accuracy of the calculation of solutional erosion rate (Groom and Williams 1965; Douglas 1968; Smith and Newson 1974; Smith and Atkinson 1976; Drake and Ford 1976; Gunn 1978, 1981).

3.3.2 Description of the Towai Drainage Basin

The drainage basin chosen for investigation is situated to the north of Coonoor (Grid Ref. U24/746816). This will be referred to as the Towai drainage basin, named after Towai Road which crosses it. The basin extends from the crest of the Puketoi Range (721 m above sea level) to the Mangatoro Stream (340 m above sea level) (Fig. 3.2 and 3.3), covering an area of 2.2 km^2. The vegetation over the majority of the basin is introduced grasses with small patches of regenerating forest, generally restricted to the deeper dolines and other areas out of reach of stock.

Two limestone beds are present within the basin. In the upper part of the basin, Te Onepu Limestone outcrops. Dry valleys have developed on this limestone. The lower section of the basin comprises Kumeroa Formation limestone with many dolines and a small area of polygonal karst (Fig. 3.2).

These dolines have formed on a plateau which has also been eroded by streams. The boundary between the two limestone areas is quite distinct, with a change from the dry valleys of the upper part of the basin to dolines of the lower section (Fig. 3.2). This boundary is also the area in which many of the surface streams go underground. The landforms developed on each formation may therefore be litholigically contolled.

Subterranean drainage within karst areas may, in some situations, cross topographic divides, therefore topographic boundaries need not conform with the boundary of a drainage basin. To delineate the boundary of a karst basin underground streams must be traced. This is achieved using fluorescent dyes which are easily detectable at resurgences. Limited dye-tracing was undertaken within the Towai drainage basin at Coonoor using Rodamine W.T., a fluorescent dye. The results obtained from the dye-tracing of the basin were inconclusive, as the amounts detected in the analysis of the water samples was very close to the background levels of natural fluorescence in the water. All underground drainage lines shown on figure 3.2 are therefore theoretical.

3.3.3 Estimation of Solutional Erosion

In the estimation of solutional erosion, distinction needs to be made

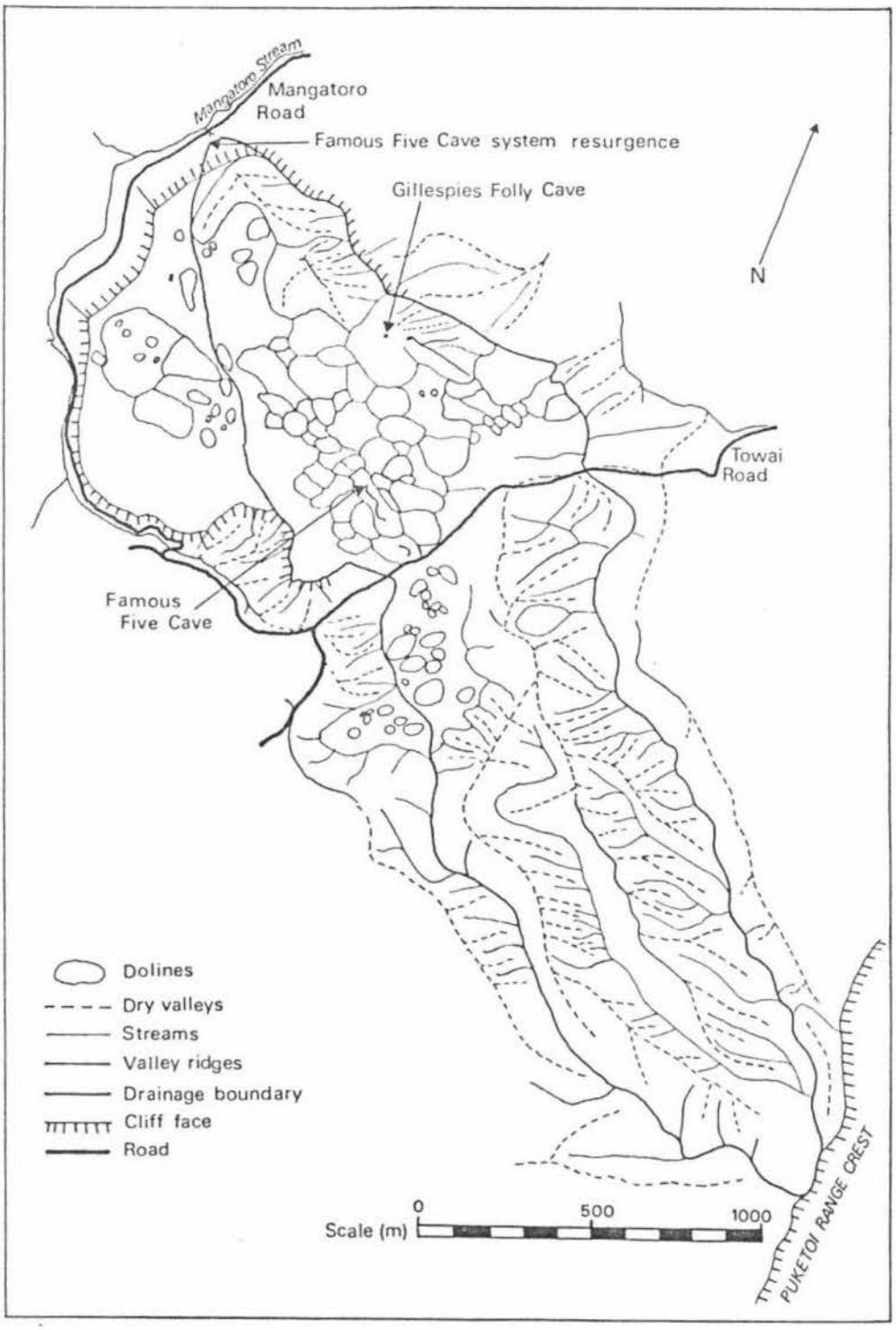

Figure 3.2 Towai drainage basin.

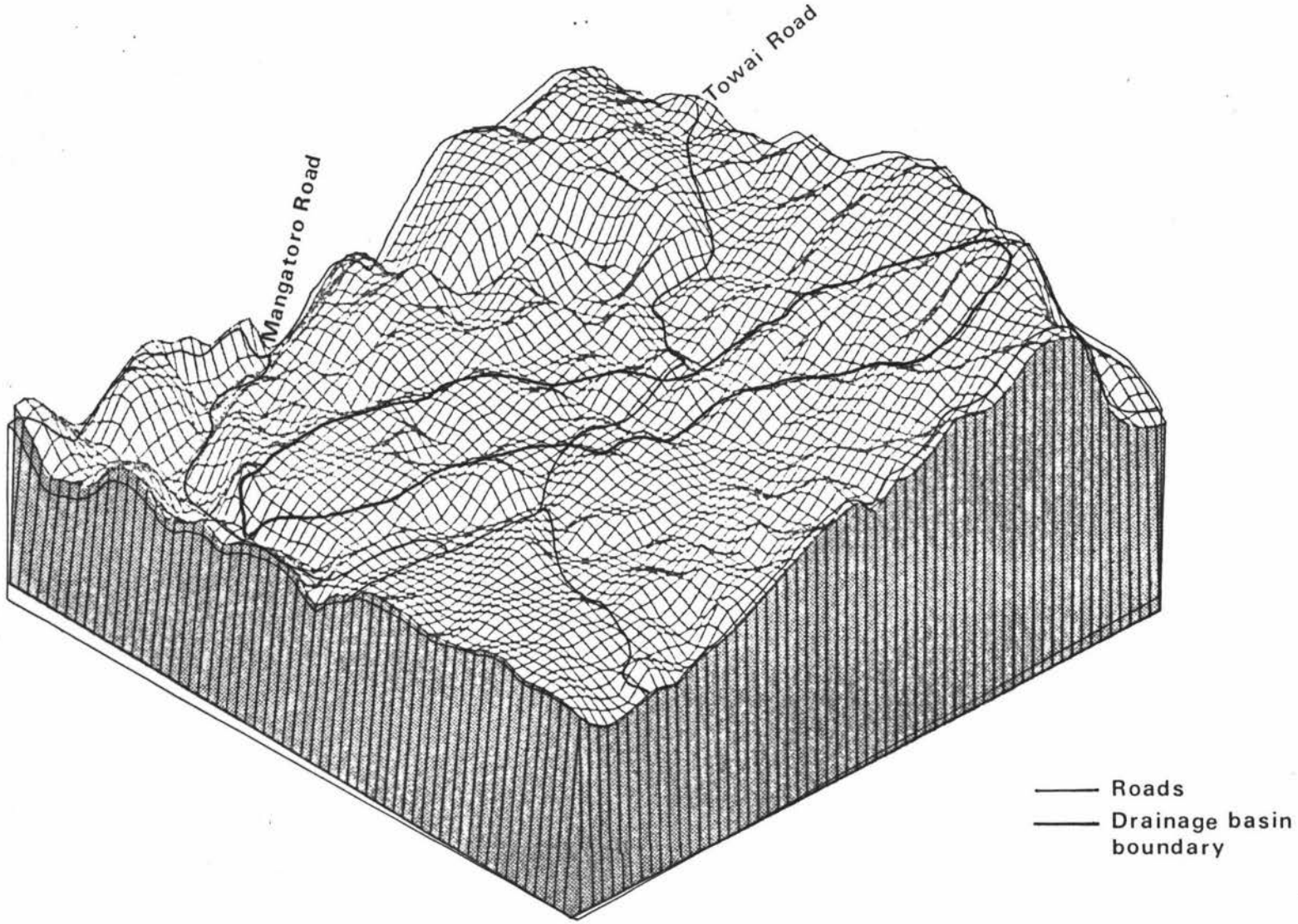

Figure 3.3 3-D computer image of the Towai drainage basin.

between gross solution - the total amount of rock dissolved within the basin, and net solution - the volume of rock removed entirely from the basin. The difference between gross and net solution is accounted for by deposition in the form of speleothems in caves and tufa deposits on the surface. Only net solutional erosion is considered here since deposition is extremely difficult to quantify.

Many of the studies of solutional erosion rates in karst areas are from basins with mixed karst and non-karst rock. This requires the estimation of the input into the system of water and solutes from the non-karst area. The Towai basin is entirely karst, therefore removing errors in the estimation of inputs from non-karst areas in the calculation of the solutional erosion rate. Non-karst rock may, in places, underlie the basin at a shallow depth. The influence of this rock on the solutional erosion rate is unknown.

The original intention of this investigation was to use discharge data collected from the gauging of the stream in the drainage basin. Because of repeated failure of the recorder and the washing away of the weir during floods, the period of discharge record was too small to be considered of any value in the calculation of the solutional erosion.

Instead of using discharge data in the calculation of solutional erosion, the mean annual runoff was estimated by calculating the difference between the annual rainfall and loss through evaporation.

Evaporation was estimated using Penman's formula for the estimation of evaporation from weather data (Penman 1948, cited in Wilson 1974). This was based on information from Mr S.McIntyre's rainfall record at Coonoor; temperature, humidity, and sunshine hours recorded at Dannevirke (Grid Ref. U23/746062) (New Zealand Met. Service 1983); and windspeed data from Ballantrae 1, Woodville (Grid Ref. T24/502962) (New Zealand Met. Service 1983). This information is listed in Table 3.2. The author believes that these figures are representative of the area as a whole. The windspeed recorded at Ballantrae 1 would give the closest approximation of windspeed in the Puketoi Range, as the recorder is situated on the saddle between the Tararua and Ruahine Ranges and is in a direct line with the Puketoi Range.

	J	F	M	A	M	J	J	A	S	O	N	D
T	17.0	17.3	15.8	13.1	10.2	7.8	7.3	8.2	10.1	11.8	13.8	15.6
n/d	0.47	0.50	0.46	0.43	0.37	0.32	0.34	0.35	0.37	0.44	0.44	0.41
R_a	998	963	686	515	358	308	333	453	648	817	994	1033
H	0.76	0.76	0.80	0.82	0.83	0.86	0.86	0.85	0.79	0.75	0.72	0.74
U_2	7.0	6.5	6.0	6.1	7.0	6.1	6.2	6.1	7.0	7.4	7.2	7.0
E_v (per day)	4.9	4.8	3.0	2.0	1.3	0.8	0.9	1.3	2.5	3.7	4.8	4.8
E_v (per month)	151.9	134.4	93	60	40.3	24	27.9	40.3	75	114.7	144	148.8

Total evaporation = 1054.3 mm/year

Table 3.2 Weather data used in the estimation of evaporation. T = temperature (°C); n/d = cloudiness ratio = actual/possible hours of sunshine; R_s = Angots value for solar radiation arriving at the atmosphere (g/cal/cm^2/day); H = humidity; U_2 = wind speed (m/sec); E_v = evaporation (mm/day).

The estimation of evaporation within karst areas has an additional difficulty in that the permeable nature of limestone results in rapid and substantial rainfall infiltration. This results in not only intermittent or absent surface drainage within limestone areas, but there are also losses of water through evaporation. The loss through evaporation for the area is therefore possibly lower than the estimated 1054 mm/yr. This would result in higher mean annual runoff than estimated.

Two samples of rainwater were also collected at Coonoor. These samples were used to establish natural inputs of solutes from precipitation. These two samples yielded $CaCO_3$ and $MgCO_3$ values of 0.0 and 0.4 mg l^{-1}, and 1.42 and 1.24 mg l^{-1} respectively. Rainwater samples collected at Taita, near Wellington, by Blakemore (1973) had mean concentrations of 1.58 mg l^{-1} $CaCO_3$ and 1.94 mg l^{-1} $MgCO_3$, while Claridge (1975) obtained mean concentrations of 1.33 mg l^{-1} and 1.91 mg l^{-1} respectively. The $MgCO_3$ content of rainwater at Coonoor was only slightly lower than that recorded by Blakemore and Claridge at Taita, but the $CaCO_3$ content was much lower.

A total of 28 water samples were collected from Site 3, the resurgence of the Towai drainage basin, between March 1986 and September 1986. To estimate solutional erosion, the $CaCO_3$ and $MgCO_3$ content of the water samples was calculated. Natural inputs of these compounds from rainfall was subtracted from this figure to give the average calcium and magnesium content.

3.3.4 Net Rate of Solutional Erosion

Solutional erosion rate was calculated using William's (1964) equation:

$$X = \frac{E\ T\ n}{10D}$$

This equation was chosen because discharge data is not needed for the calculation of solutional erosion rate.

The values in the equation for the Towai basin are:

Mean annual runoff (E): This is estimated to be 9.56 dm per year (2010 mm yr^{-1} of rainfall less 1054 mm yr^{-1} evaporation).

Total $CaCO_3$ and $MgCO_3$ (T): The average carbonate content of 28 water samples is 142.08 mg l^{-1}. The inputs from rainfall is approximately 1.35 mg l^{-1}, therefore the amount removed from the drainage basin is 140.55 mg l^{-1}.

Density (D): The mean density of eight samples from Te Onepu and Kumeroa Formation limestones collected within the basin is 2.31 g/cm^3.

By substitution of these values in the above equation, net solution (X) in the Towai basin is calculated as:

$$X = \frac{9.56 \times 140.55 \times 1}{10 \times 2.31}$$

$$= 58.2 \text{ m}^3/\text{km}^2/\text{yr}$$

3.3.5 Comparison of Solutional Erosion Rate with Other Areas in New Zealand and World-wide

Two previous estimates of solutional erosion rates have been made in New Zealand. Dowling (1974) and Williams and Dowling (1979) estimated solutional erosion within the Riwaka South catchment, northwest Nelson, to be 100 ± 24 $m^3/km^2/yr$. This catchment is developed on Ordovician marble, and the annual rainfall is 2158 mm.

Gunn (1978, 1981) investigated Oligocene limestone in the Waitomo district. He estimated solutional erosion in the area to be 69^{19}_{8} $m^3/km^2/yr$. The annual rainfall is 2370 mm.

Smith and Atkinson (1976) gave a mean solutional erosion rate of 56.9 $m^3/km^2/yr$ based on 87 estimates in temperate areas world-wide.

The estimated solutional erosion rate of 58.2 $m^3/km^2/yr$ in the Towai drainage basin, Puketoi Range, is extremely close to that recorded by Smith and Atkinson (1976). This figure is also similar to that recorded by Gunn (1978, 1981) in the Waitomo District.

3.4 Conclusions

The analysis of 306 water samples from 15 sampling sites in the Puketoi Range, indicated spatial and temporal changes in the $CaCO_3$ and $MgCO_3$ water content. Three water types were noted: allogenic water from non-karst areas, autogenic water from karst areas, and mixed allogenic-autogenic water. These water types were found to fluctuate in response to storm events and seasonal changes in the supply of water to the area. Each water type has distinctive characteristics to identify it. These characteristics are related to the $CaCO_3$ and $MgCO_3$ content of the water samples, which in turn relates to the geology of the sample sites.

Allogenic water has lower $CaCO_3$ content and is very aggressive to limestone. Autogenic water contains the highest levels of $CaCO_3$, with the water being saturated periods during the year. Mixed allogenic-autogenic water showed the greatest levels of fluctuation in water hardness. This related to storm events and the supply of water from non-karst areas diluting the carbonate concentration from karst areas.

Solutional erosion for the Towai drainage basin was estimated. This basin is developed on Pliocene/Pleistocene limestone at Coonoor. Solutional erosion was estimated at 58.2 $m^3/km^2/yr$, based on the examination of $CaCO_3$ and $MgCO_3$ content in water samples. This estimate is comparable with other solutional erosion estimates in New Zealand and world-wide.

CHAPTER FOUR

KARST LANDFORMS AND CASE-HARDENING WITHIN THE PUKETOI RANGE

4.1 Introduction

Solutional erosion of limestone at or near the surface of the Puketoi Range has resulted in the development of many landforms specific to karst areas. The karst landforms found within the Puketoi Range and on the eastern flanks of the Waewaepa Range have developed on three limestone beds. The uppermost bed is Kumeroa Formation limestone (Pleistocene in age), underlain by the Te Onepu and Awapapa Formation limestones (Pliocene in age) respectively (see chapter 2 for a more detailed discussion of the geology of the range).

This chapter examines the karst landforms developed on these three limestone beds, and the influence changing climatic conditions have had on landform development.

4.2 Fluvial Karst Features of the Puketoi Range

Fluvial features, particularly valleys, take on special characteristics in karst, varying from very steep-sided gorges, to dry valleys, with many intermediate forms. In this section, the variety in valley form found within the Puketoi Range will be examined.

4.2.1 Gorges

Gorges are more frequent and distinctive in limestone than in any other rock type (Jennings 1985). A number of gorges are found on the Puketoi Range. The largest are the Makuri Gorge, in the south-central section of the range, and the gorge formed along parts of the Mangatoro Stream at the northern end. These gorges are more pronounced in karst than elsewhere because of the lack of slope processes to flare back the valley sides (Jennings 1985). This results from limestone directly absorbing water, thereby reducing runoff and minimising slope-wash and mass movement processes that widen valley sides and moderate their steepness

on other rock types (Jennings 1985).

The Makuri and Mangatoro Gorges have developed from mixed allogenic and autogenic waters derived from streams flowing from the Puketoi and Waewaepa Ranges. The water carried by these streams is chemically aggressive, and the gravels derived from the Waewaepa Range are mechanically abrasive to the limestone, resulting in solutional and mechanical erosion of their streambeds.

A smaller gorge has also formed to the north of Coonoor (Grid Ref. U24/747826). This gorge in the headwaters of the Mangatoro Stream has formed entirely from autogenetic water derived from the Puketoi Range. Drainage through this gorge is both surface and subsurface flow, with large sections of the gorge floor dry, except at times of high flow, when the cave systems become full and overflow.

4.2.2 Blind Valleys

The diversion of drainage underground into cave systems in this area has resulted in the development of many blind valleys. Photograph 4.1 shows the entrance to Famous Five Cave (Grid Ref. U24/741817). This is termed a true-blind valley as all the water disappears underground at one locality all the year round. Half-blind valleys occur when, during periods of high flow, water flows beyond the usual point of disappearence into a lower part of the valley. Examples of half-blind valleys in the Puketoi Range are found where streams, derived from the greywacke of the Waewaepa Range, flow a short distance across the limestone surface before disappearing underground. An example of this is found at grid reference U24/719812. Here a stream from the Waewaepa Range flows a minimum of 50 m across the limestone during periods of low flow, but during periods of high flow the surface stream may reach the Mangatoro Stream approximately 2 km downstream.

The distance that these streams flow across the limestone is related to the discharge of the stream and the number of points water is absorbed along a length of streambed.

Photograph 4.1 Blind Valley, Famous Five Cave. The valley is terminated at its downstream end by the sinking of the stream undergroung into the Famous Five Cave system. The stream divides in two along a joint as it disappears underground, to reappear within Famous Five Cave as two waterfalls.

Photograph 4.2 Karst Window, Famous Five Cave system. The surface stream is exposed for approximately 100 m, from its resurgence at the surface (to the right of the photo), to its disappearence underground (to the left of the photo). The brown colour along the length of the stream banks is due to silt deposited during flooding.

4.2.3 Steepheads and Pocket Valleys

Steepheads and pocket valleys are the opposite of blind valleys, occurring in association with the resurgence of water at the surface. Where this water resurges, a valley is cut back into the hillside. If the resurgence is underlain by an impervious basement which has a strong control on the valley form then it is termed a steephead. If this impervious layer is not present the valley is known as a pocket valley. An example of a pocket valley is the resurgence to PT17 Cave. Here a small valley has cut back into the hillside.

4.2.4 Karst Windows

A karst window is defined as "...a large funnel-shaped doline, in the depths of which a short stretch of a cave river is visible" (Bögli 1980, p.64). A karst window has developed within the Famous Five Cave system. Here a surface stream travels a short distance (approximately 100 m) across the surface before going underground again. This stream is entirely enclosed by a large elongated depression (Photo 4.2), similar in shape to a large elongated doline, but with a stream in the bottom of it. Alluvium is deposited along the sides of the depression. This is laid down at times of high flow, when streamflow exceeds the capacity of the cave system, resulting in water backing up and depositing sediment.

This depression may have originated as a doline, which deepened to the local base level, either through solutional erosion of the limestone or collapse into the cave system beneath, thereby exposing the stream. Since that time the depression has developed in the direction of the cave stream to give the present elongated shape.

4.2.5 Dry Valleys

Dry valleys, i.e., valleys without or with only temporary watercourses (Sweeting 1972), are one of the most difficult of karst landforms to assess in terms of their evolution. Dry valleys occur world-wide in all forms of limestone and in virtually all climatic conditions (Smith 1975). Their form is generally similar to that of the normal fluvial valley but they do not have any stream channel developed within their floor.

Because much of the drainage in karst areas is underground, and valleys are essentually the result of fluvial processes of water-flow over the surface, some researchers believe that valleys in karst are not strictly karst landforms (Roglic 1964; Sweeting 1972). In other words, dry valleys are not the result of vertical solution of water entering the karst area and therefore are considered by some to be a fluvial landform.

Dry valleys are generally regarded as relic features formed by past processes and their form is largely unrelated to present process activity (Knighton 1975). Jennings (1982) believes that dry valleys indicate past or present fluvial activities predominant in the erosion of the limestone. These fluvial activities he sees as being particularly subject to change in the Quaternary, because of climatic swings favouring either karst processes or normal surface activities producing, predominantly, valleys rather than dolines. With the dominance of dry valleys within the limestone of the Puketoi Range, the area may be termed fluviokarst in character.

Much of the dip-slope of the Puketoi Range is covered by dry valleys, the area they cover being greater than that of dolines. They are therefore an important landform. In this section dry valleys in the Puketoi Range will be discussed, with some suggestions on their origin and subsequent modification.

4.2.5.1 Dry Valley Formation

Smith (1975) outlined many of the hypotheses for dry valley formation, and divided these theories into three main explanations: (1) differing climatic conditions in the past; (2) superimposition of the drainage net from non-limestone strata; and (3) a fall in the level of the water table. Smith (1975) found that none of these hypotheses were of universal application in the understanding of dry valley development, suggesting instead, that a combination of solutional mechanisms and geohydrological properties of the limestone could result in initial surface dry valley networks and later underground drainage.

Dry valleys in the Puketoi Range form an extensive network over the surface of the range. Surface flow within the valleys only occurs after very heavy rainfall or continual, sustained rainfall. In these situations small streams flow down the centre of the valleys, generally

as a wide flat sheet of water and not as concentrated flow within a stream channel in the valley floor.

Along the crest of the range, many of the valleys have been beheaded (Photo 4.3) indicating that the dry valleys are a relic feature.

Initial formation of the dry valleys within the Puketoi Range may have progressed in a manner similar to that suggested by Smith (1975). After the uplift of the Puketoi Range above sealevel, initial valley development would have commenced upon a thin covering of mud and sand deposited in shallow water just prior to uplift of the area. Erosion of the mud and sand deposited over the limestone would have resulted in initial valley formation quickly eroding down to the underlying limestone beds. Erosion of the limestone would then commence.

Smith believes that the drainage basin morphology of some limestone and non-limestone beds shows the same basic relationships occurring in the initial stages of development. Solutional weathering of the limestone initially occurs at the soil/bedrock interface and then later, deeper in the bedrock along joints and fissures in the rock. In this initial stage, drainage would develop only on the surface of the limestone. Surface drainage would be modified only after a "hydrological jump" has occurred, as described by Atkinson (1968) in the initiation of subterranean drainage. Once this had occurred, true underground drainage would commence and the valleys would become dry as more water is diverted underground.

This process will continue as both the valley system and the underlying bedrock erode down, until such time as non-limestone beds are reached and surface drainage is reestablished. This is seen within the Puketoi Range where the Te Onepu Limestone Formation has been removed, exposing the underlying Raukawa Mudstone Formation.

4.2.5.2 Asymmetrical Dry Valley Shape

Many of the dry valleys developed on the range are asymmetrical in cross-section (Photo 4.4, Fig. 4.1). The asymmetrical shape of dry valleys can result from either structural or climatic controls, or a combination of both. Within the Puketoi Range both have been important in the development of the asymmetrical dry valleys.

Photograph 4.3 Beheaded dry valley (Grid Ref. U24/780838). Beheaded valleys within the Puketoi Range result from retreat of the scarp slope along the eastern edge of the cuesta. The photo was taken looking towards the east.

Photograph 4.4 Asymmetrical dry valley at Pori (Grid Ref. T25/594635). The photo was taken looking towards the east, with north to the left. The steeper valley side is to the left, with a gentle slope to the right.

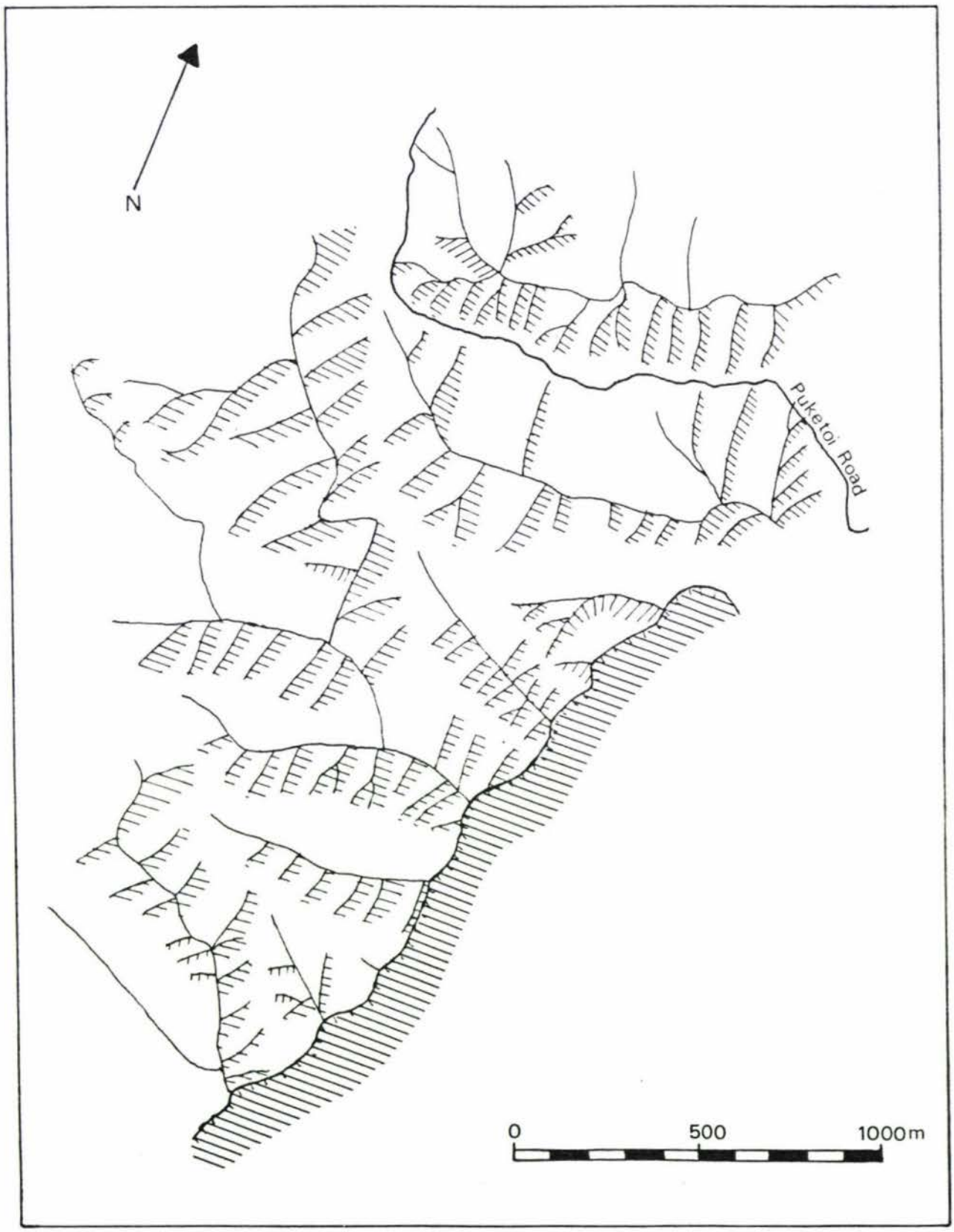

Figure 4.1 Map of asymmetrical dry valleys in the vinicity of Pori. Shading is with the sun in the northwest.

The establishment of a periglacial climate during the Otira Glaciation caused many of the dry limestone valleys along the Puketoi Range to become fluvial, with active streams flowing within them. Evidence of this is seen not only in the solifluction deposits described by Neef (1967, 1984), but also in gravels deposited in Ramsay's Neck Cave, derived from the dry limestone valley in the headwaters of the cave system (discussed in chapter 6), and the limestone gravels exposed in the road-cutting at grid reference T24/699747.

The development of active streams under periglacial environments results from restricted subterranean drainage, with water-flow confined to the surface. The asymmetrical shape of the valleys influenced by a periglacial environment is believed by many (Tricart 1970; Embleton and King 1975), to be the result of differential operations of freeze-thaw on the slopes of a valley (Tricart 1970). Thaw is less likely to occur on the south-facing slope of the valley, as this faces away from the sun. On the north-facing slope of a valley freeze-thaw processes will be more important because of the sunnier conditions.

Other periglacial factors, such as the effect of stream action in basal undercutting of a valley side, the effect of permafrost, and the effect of prevailing winds in snow accumulation, are also considered to be influential in asymmetrical valley development within the Puketoi Range.

Geological structure is also important in the development of asymmetrically-shaped dry valleys. Where valleys are orientated parallel with the strike, an asymmetrical shape in cross-section develops on the down-dip valley side where more erosion occurs.

Within the Puketoi Range the asymmetrical dry valleys are the result of both structure and climate. The degree of modification is dependant on the location and direction of the dry valley.

4.3 Dolines

Apart from caves, the doline is possibly the feature most associated with karst areas. Dolines are found in almost all types of karst irrespective of the climate or altitude, being equivalent in function to the valley in

the non-karst fluvial terrain. Sweeting (1972, p.44) described dolines as "...closed hollows of small or moderate dimensions; they can be cone- or bowl-shaped, with rocky or vegetated sides and a circular or elliptical plan. The diameter is usually greater than the depth, and average dolines vary in size from about 2 m to 100 m deep and from 10 m to 1000 m in diameter. They can occur isolated or in groups in close proximity to one another."

The presence of dolines is considered by many, to create a disorganized drainage system (Chorley et al. 1984), but as Williams states (1978, p.260): "Karst processes and resultant morphologies are merely at one end of a continuum of processes and forms that are found throughout the natural landscape." Williams (1983) recognized the occurrence of dolines more as a reorganization of surface drainage, with the doline acting as a connecting element, between the surface and subsurface components of the drainage system, in the transmission of water though the karst system.

There is considerable variation in the shape, size and means of formation of dolines. A five-fold classification scheme was developed by Cramer in 1941 (cited in Jennings 1985) which has been elaborated as a useful framework for the investigation of dolines (Jennings 1975). This classification is based on the means of formation of the doline: (1) by surface solution of karst bedrock; (2) by cave roof collapse; (3) by subsidence of the surface cover material via pipes or joints in the karst bedrock; (4) by collapse of overlying non-karst bedrock, due to solution of underlying karst rock; and (5) by sinking of streams underground through a cover of alluvium. Jennings (1975) gives a more detailed description of doline types and the ease of distinction. All five types of doline are found along the Puketoi Range, with selected examples shown in photographs 4.5 and 4.6.

Essentially, normal slope hydrological processes occur on the sides of the doline, with drainage down-slope occurring along several paths (Gunn 1978, 1981; Williams 1983) : (1) As a diffuse film of overland flow; (2) As interflow along the contact of permeability discontinuities within the soil profile, including at the interface of the soil and rock; and (3) As subcutaneous flow through the uppermost weathered layers of rock. As the water flows towards the centre of the doline, solution of the

Photograph 4.5 Large solutional doline at Coonoor (Grid Ref. U24/742820), forming part of an area of polygonal karst. Dolines are seen to the left and right of the central doline.

Photograph 4.6 This subjacent doline (Grid Ref. U24/788881) has resulted from the collapse of the thin layer of Kumeroa Formation mudstone overlying Te Onepu Limestone Formation.

limestone occurs, this being aided by eluviation, soil creep and other mass movement processes in the enlargement of the doline.

Progressive karstification of the underlying rock will gradually increase the secondary permeability of the limestone, due to the moisture storage capacity of the soil, allowing the bulk of corrosion to occur in the uppermost layers of the bedrock, beneath the soil. Thus the component of vertical, as opposed to lateral flow within a depression, should increase with time (Williams 1983) . In contrast to solutional dolines, collapse and subjacent dolines will be variable in initial shape because the area and thickness of cave roof collapse is very diverse (Jennings 1975). Equilibrium slope angles will develop on the collapse doline, but not readily on the subjacent doline because of the large amount of insolubles from the non-karst rock, which is difficult to remove through a cave system (Jennings 1975).

4.3.1 Dolines within the Puketoi Range

Dolines are found scattered over much of the limestone of the Puketoi Range, usually singularly or in clusters. However, there is a small area of polygonal karst at Coonoor (Grid Ref. U24/740820). There is great variation in width and depth of the dolines, varying from those that are less than 2 m in diameter and 1 m deep to those that are over 30 m in width and depth (Photo 4.5). In the following discussion some general observations are given on the distribution of dolines within the Puketoi Range.

Dolines do not appear to be favouring any one particular limestone bed in the range and are found on Awapawa, Te Onepu, and Kumeroa Limestone Formations. However, the doline form may be influenced by the individual geological beds. For example, the area of polygonal karst is developed on Kumeroa Formation limestone.

The slope of the surface of the Puketoi Range may also be influentual in the development of dolines. On much of the dip slope of the range (dipping at approximately 15 degrees) dolines are not present, being replaced by dry valleys, but they do occur on more gently sloping surfaces (5 to 10 degrees). The slope of the surface may therefore be a controlling factor in doline and dry valley development.

Two areas of highly clustered dolines are centred at grid references U24/831908 and U24/720790. These dolines are generally small to medium in size, not exceeding 6 m in diameter. The development of doline clusters has attracted much attention, with two theories suggested for their formation. The first, the Mutually Independent Random Processes model (MIRP), was proposed by McConnell and Horn (1972), and the second, the Multigenerational Diffusion and Competition Process model (MDCP), is based on the collective works of Ford (1964), La Valle (1968), Drake and Ford (1972), Williams (1972a, 1972b) and Palmquist (1977, 1979).

Future work is needed on these areas of clustered dolines to determine which of these theories is appropriate.

Dolines in the Puketoi Range are at all stages of development. At one locality (Grid Ref. U24/746818) a series of dolines is seen in the process of coalescing. These dolines are generally water-filled (Photo 4.7), but on occasions are dry (Photo 4.8). The water level within the dolines fluctuates in response to changes in groundwater recharge in the immediate area. During dry periods, heavy rainfall may not cause a rise in the water level within the dolines as all rainfall may be retained within the soil and not reach the groundwater system. However, during the winter there is an almost immediate flow-on effect between rainfall and a fluctuation in water level within the dolines. The existance of these ponds may also indicate an impermeable layer directly beneath the dolines causing a localised high in the water table in this area.

4.4 Karren and Limestone Pavements

The susceptibility of limestone to solutional erosion, has resulted in a greater variety of small-scale solutional features on this rock type, than any other (Jennings 1985). In this section karren and limestone pavements within the Puketoi Range will be discussed.

4.4.1 Karren

The general term used in describing the sculpturing of karst rock is "karren" (German), or less commonly "lapiés" (French). The name karren was originally used to describe solutional runnels cut into limestone,

Photograph 4.7 Solutional dolines coalescing into one large doline (Grid Ref. U24/745815). The ponds within the dolines fluctuate in response to rainfall. The possible existance of an underlying insoluble bed may control the water table in the vinicity of the dolines. This photo was taken in spring.

Photograph 4.8 The same dolines as shown in Photo 4.7; however this photo was taken during the summer. Lowering of the water table during dry periods results in the ponds becoming dry.

but is now used for the whole complex of micro-forms that occur on outcrops of karst rock (Sweeting 1972). Sweeting defined karren as solutional holes and runnels formed directly on bare limestone, or on limestone covered by moss or vegetation. Karren range in size from a few millimetres, to 1 m to 2 m, occasionally reaching 15 m to 20 m in length (Sweeting 1972).

Reference to ideas on karren development date back to Heim in 1878 (cited in Sweeting 1972), who recognised that their formation was essentially the result of chemical solution by water. Further development of theories on karren formation and development did not occur until nearly 50 years later when Cvijic in 1924 published a description of karren in the Dinaric Karst, proposing a cyclic theory of development in Davisian terms. This and other early works in Europe recognised the importance of the presence of soils and vegetation, lithological and structural characteristics of the limestone, and the slope of the rock upon which karren is developed (Gobby 1979).

The next major advancement in the study of the form and genesis of karren came with the publication in 1960 of Bögli's paper entitled "Kalklosung und Karrenbildung" (Solution of Limestone and Karren Formation). In the paper, Bögli developed a detailed classification of karren types and related form to mode of origin. He recognised that chemical solution of the limestone was the fundamental control on karren morphology, with karren-form a direct result of the different phases of solution. His classification was therefore based on solution rates rather than spatial dimensions (Gobby 1979). Since this time, morphometric techniques have been used in the study of karren (Goldie 1973; Lundberg 1976, cited in Gobby 1979), and more recently the effect of lithology on karren has been investigated (Dunkerley 1983).

New Zealand literature on karren is scarce. Morgan (1919) noted the presence of solutional features on the Waro limestone near Hikurangi, while Cotton (1948) gave the first geomorphological account of karren in New Zealand. Zotov (1941) discussed solution cups in North Canterbury, and Bartram and Mason (1948) looked at rills and solution pits in basalts near Hokianga. Purser (1952) used karren features for the identification of limestone members in the Te Kuiti Formation at Port Waikato.

More recently, Dowling (1974) and Gobby (1979), have examined karren in New Zealand. Dowling made reference to the variety of karren types on marble in the Nelson area, while Gobby discussed, in detail, karren morphology in the Waitomo and Port Waikato areas, North Island, New Zealand.

4.4.1.1 Karren Types in the Puketoi Range

Within the Puketoi Range a large variety of karren are found (Photos 4.9 to 4.14). In this section these will be investigated, firstly with a discusssion of the factors affecting karren formation, followed by a description of examples from the Puketoi Range.

Bögli (1960) devised a generic system based on the conditions in which karren develop, that is, the circumstances of runoff of corroding water over the surface of the rock. The system has three basic forms related to the contact time of the water with the surface of the rock: (1) karren produced by free, unhampered runoff; (2) those produced under partial soil or vegetation cover; and (3) those that are formed under a complete soil or vegetation cover. These three groups include all karren forms found on the surface of karst rocks. Associated with them are three further groups: (4) cave karren; (5) surf-zone karren; and (6) lacustrine karren. Of these last three groups, cave karren is found within caves in the Puketoi Range. Karren developed on non-karst rock were also observed by the author (Photo 4.14) and will be discussed at the end of the section.

Of the six factors noted by Sweeting (1972), which influence the development of karren, the more important is possibly the nature of the chemical reaction involving the limestone, carbon dioxide and water (see Sweeting (1972) for a more detailed description of each). Bögli (1960) identified a four phase chemical reaction, in which each solutional phase was associated with a distinctive type of solutional rate, with the different types of solution giving rise to different morphological types of karren. Rillenkarren forms as free karren on bare, exposed rock. Rinnenkarren forms with water of mixed origin, both from the falling rain and from water already flowing down the surface of the rock (Sweeting 1972). This is termed half-free karren. Rundkarren and kamenitzas result from slower chemical reactions, from water that has been in contact with vegetation increasing the supply of biological carbon

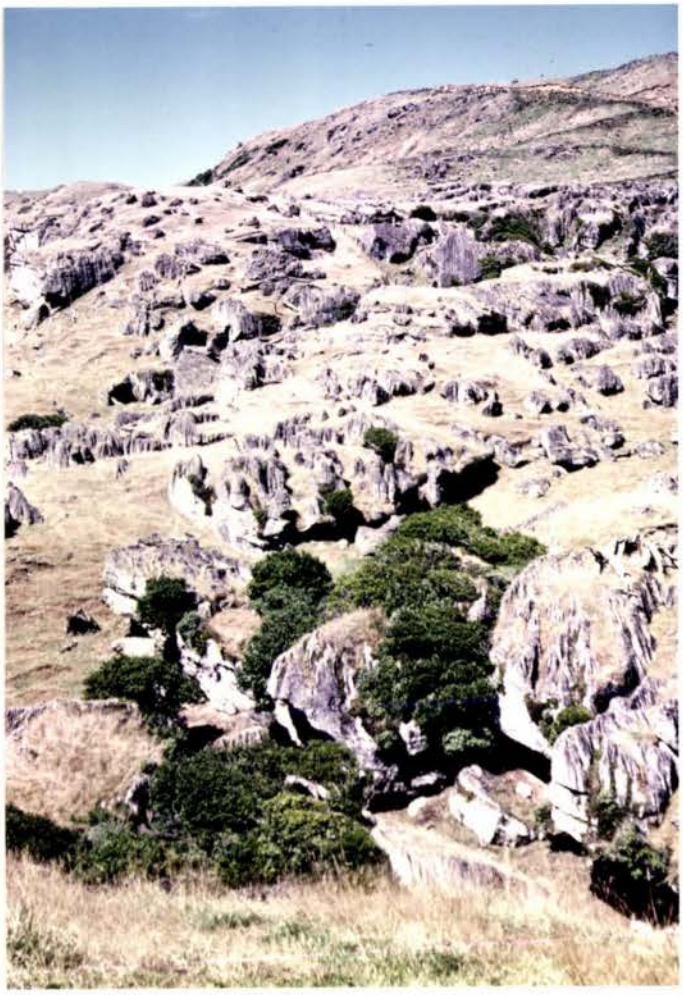

Photograph 4.9 Karren field on the western side of Oporae (Grid Ref. U24/815885).

dioxide, or in contact with the surface of the rock for extended periods of time. This is termed covered karren.

The morphological form of free karren tend to be sharper or finer cut, being rough to the touch, whereas half-free or covered karren are smoother and rounded (Sweeting 1972).

Examples from the Puketoi Range are free, half-free, and covered karren forms. Photograph 4.10 is of a large sloping rock on which rinnenkarren and rundkarren have developed. The rinnenkarren has the sharper ridge crests in the top section of the photograph, forming as half-free karren on bare limestone. The rundkarren in the foreground is covered karren, formed under soil or vegetation. This indicates a former soil cover. The rundkarren are basically drainage features developed under soil or vegetation and are normally influenced by to the slope and dip of the rock (Sweeting 1972). The runnels also have a meandering appearance, termed meanderkarren, formed due to the gentle slope of the rock surface.

Photograph 4.11 is also of rinnenkarren. Here the karren has formed on a nearly vertical rock face. The crest of each ridge is sharp, with rounding towards the base. This again may indicate a former soil cover.

Photograph 4.12 is of solutional basins or kamenitzas. These form on a more or less horizontal surface, with water collecting in pools and basins. Biogenetic carbon dioxide levels are increased by lichens and mosses within the basins, increasing the acidic nature of the water. This is an example of covered karren.

Photographs 4.13 and 4.14 are of karren formed in different situations. The first is of cave karren. The most common cave karren are scalloping and flutes, the result of the petrographic nature of the limestone and the water-flow over the surface of the cave passage. In the example shown (Photo 4.13) the karren is very similar in appearance to rillenkarren formed on subaerial rocks, and not like the scalloping or fluting usually found in caves. The ridges are very sharp crested, with the hollow in which the rills have formed being quite concave. This has possibly resulted from the solution of water percolating through the limestone above, flowing as a sheet down the wall of the passage. The final photograph (Photo 4.14) is of very large rills formed in mudstone.

Photograph 4.10 Large rinnenkarren with sharp crests in the background, with rundkarren with rounded crests in the foreground. This change in karren form indicates former soil levels in the area. Meanderkarren are also present (centre of photo) possibly resulting from the gentle slope of the boulder and the speed of water runoff over its surface.

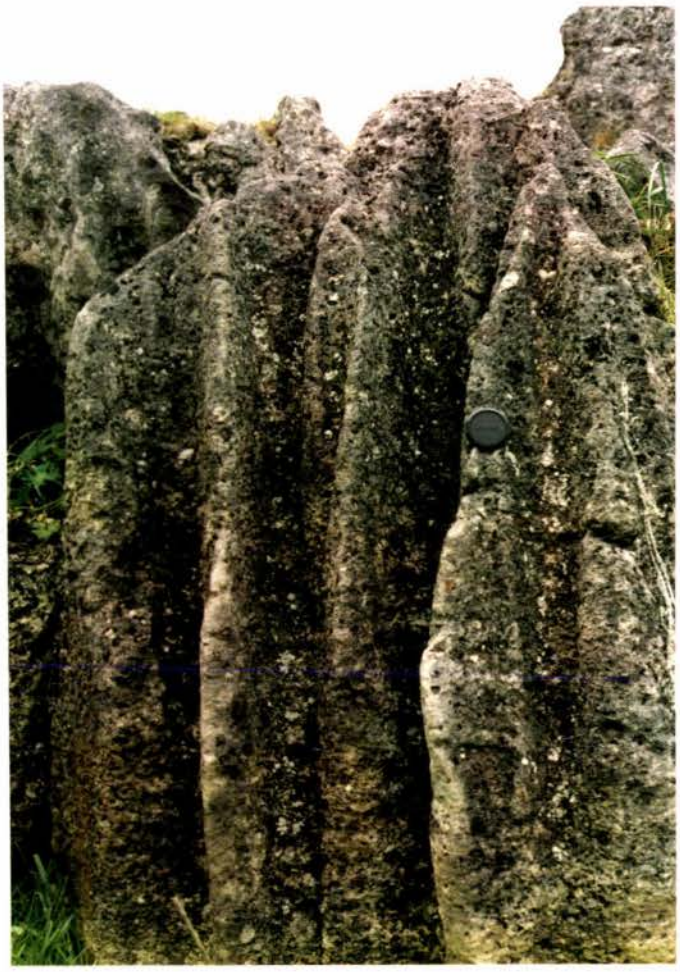

Photograph 4.11 Rinnenkarren and rundkarren on a nearly vertical rock outcrop.

Photograph 4.12 Kamenitzas or cup karren developed on a horizontal rock outcrop. Note moss and lichen growing within the cups, increasing the supply of biogenic CO_2 and hence carbonic acid.

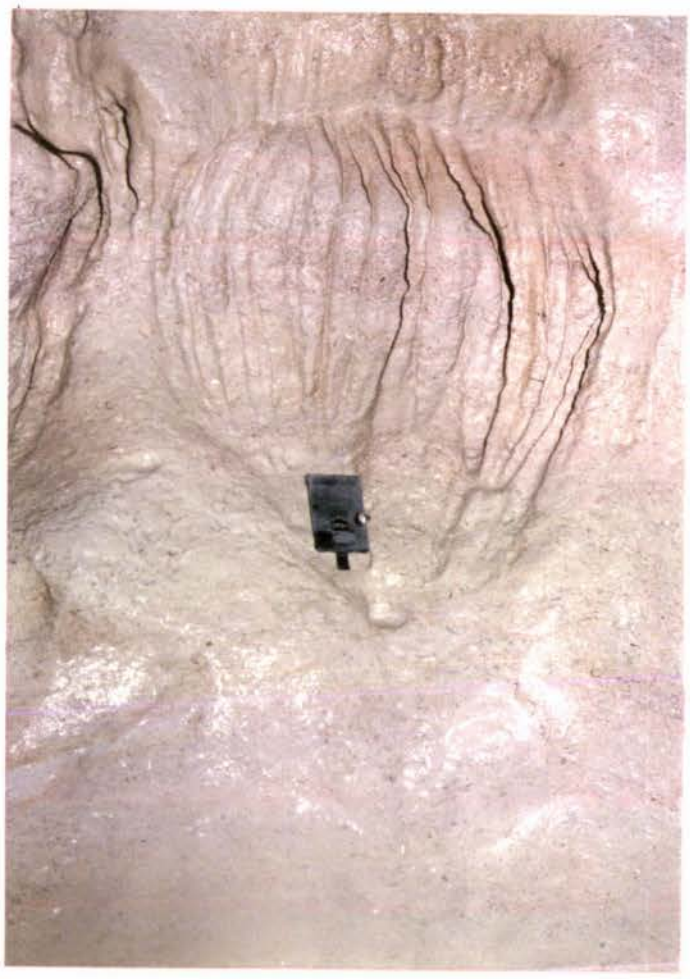

Photograph 4.13 Cave karren within PT17 Cave. The karren has formed as rills, similar to rillenkarren on limestone exposed at the surface. Scale: approximately 40 mm.

Photograph 4.14 Non-karst karren (Grid Ref. T25/638632). The large rills have formed on Raukawa Mudstone Formation.

The mudstone is Raukawa Formation - a massive calcareous, blue-grey silty sandstone and sandy siltstone (Harmsen 1984a, 1985) . The rills are situated at grid reference T25/638632. Their formation is possibly related to the calcareous nature of the mudstone allowing solution to enlarge joints within the mudstone. The radiating nature of the slope may also have been influentual in the formation of the rills, concentrating water-flow down the slope, allowing fluvial erosion to enlarge the joints.

4.4.2 Limestone Pavements

The majority of limestone pavements described in the literature are in cold temperate or alpine areas. Glacial erosion has removed accumulated rock debris and regolith and scoured the limestone, exposing a smooth, flat surface. Subsequently the surface has either been covered by glacial till, restricting the immediate development of the pavement, or developed a soil or peat cover, initiating a pavement beneath. Glacial activity has therefore been considered an essential prerequsite for limestone pavement development (Williams 1966, p.160; Pitty et al. 1985). Only occasional reference has been made to limestone pavements occurring outside of glaciated regions (Day 1978a, cited in Brook 1981). A small area of limestone pavement was found by the author in the Puketoi Range (Grid Ref. U24/794851). This area has not been glaciated in the past, therefore the following discussion is of a non-glacial limestone pavement.

In describing limestone pavements, the terms clints and grikes are used. The clints are the large surface blocks making up the pavement, with the open fissures between the clints called grikes. The top surface of the clints are generally horizontal, with karren sometimes formed on the top of these blocks and down the sides of the grikes (Goldie 1981). The morphology of pavements is probably determined by predominantly one, or a combination of, the following factors: the effect of structure, in particular spatial dip and jointing of the limestone; lithology; topographic position; changes in climate and vegetation; and by the way in which solution takes place on the limestone surface (Williams 1966; Brook 1981; Goldie 1981).

The limestone pavement formed in the Puketoi Range occupies an area

approximately 120 m by 40 m. It is at a height of 700 m above sea level, on an west-facing slope. The pavement is formed on Te Onepu Formation limestone: a well-bedded, coarse-grained, barnacle-rich lime-grainstone (Harmsen 1984a, 1985). This dips eastward at 12 to 17 degrees from horizontal. The pavement is described as inclined, after William's (1966) definition of pavements which have developed on limestone beds dipping between zero and 45 degrees. The pavement has developed parallel to the bedding-plane, with the direction and angle of dip of the limestone coinciding with the ground slope.

At present, the pavement does not appears to be evolving. It is possibly a relic feature, the result of more favourable conditions for development in the past. Grass and soil have formed over much of the pavement area, both on the tops of the clints and in the grikes, as seen in Photo 4.15.

Clints range in size from 2 m to 5 m in length and width, generally tending to be rectangular or triangular in shape. The sides of the clints vary from vertical to a slope of up to 60 degrees from vertical. The sloping nature of some of the clint edges may indicate that part of the pavement formed under a soil cover (as assumed by Brook (1981) from the pavement he examined). Grikes developed between the clints are from 1 m to 1.5 m in width, with depths of 0.3 m to 0.6 m from the top of the clints to the soil formed within them. The soil depth is unknown.

Karren have developed on some of the clints, where the sides slope at less than approximately 45 degrees. On sides steeper than 45 degrees no karren were found.

Clints and grikes are believed to develop through solution along the joints in the limestone, either under a soil cover, or on bare limestone. Intersecting networks of grikes have developed by the solutional enlargement and coalescence along the joints. Brook (1981) found that grikes could also develop through gravitational block-sliding on bedding planes, but only near scarps in stepped karst. Gravitational sliding of clints, on the inclined pavement of the Puketoi Range, may have occurred. Evidence for this is seen in the blocks tilted from their original position (Photo 4.15, to the left of the figure). These blocks appear to have slid into grikes. This may indicate that gravitational sliding has occurred later in the evolution of the pavement, and probably is not an

Photograph 4.15 Limestone pavement (Grid Ref. U24/794851). Large clints and grikes developed within Te Onepu Limestone Formation. Note the small clint to the left of the figure which appears to have fallen into a grike.

important mechanism in the initial formation of the pavement.

The bogaz formed 800 m to the south of the pavement, described in section 4.4, have a very pronounced joint orientation (zero to 40 degrees). This orientation has not been strongly favoured in the development of the pavement. An examination of the orientation of grikes (Fig. 4.2) shows no strong bias towards any one set of joints. Of the 57 measurements taken, the strongest grike orientation was between 300 and 340 degrees, but a full range of angles of orientations were recorded.

During the Otira Glaciation, the Puketoi Range experienced a periglacial climate and not the more severe climatic conditions of a glacial environment. The periglacial climate may have been sufficiently cool to be responsible for the development of the pavement, by restricting vegetation cover to alpine plants, if modern estimates of temperature reduction (Chinn 1983; McGlone 1983) are correct. This could have resulted in the loss of the soil cover because of reduced plant protection, and local stripping of the regolith by solifluction, resulting in an area of bare exposed limestone with a well developed joint system which was readily exploited in the development of the pavement.

Geological factors may be of more importance in the development of the pavement. The ground surface may have developed parallel to that of the dip of the limestone. Under periglacial conditions, the slope would have been steep enough to induce solifluction, removing the regolith covering the pavement surface. Enlargement of the joints within the limestone, by localised solution could then occur resulting in pavement development.

4.5 Bogaz

Water-flow across the surface of limestone concentrates towards vertical or steeply inclined fissures and cracks in the rock. This concentration of water-flow results in higher rates of solution along these lines of weakness which may be bedding planes, joints or other kinds of fissures in the rock (Sweeting 1972). Two areas within the Puketoi Range show large-scale solutional erosion along lines of weakness within the

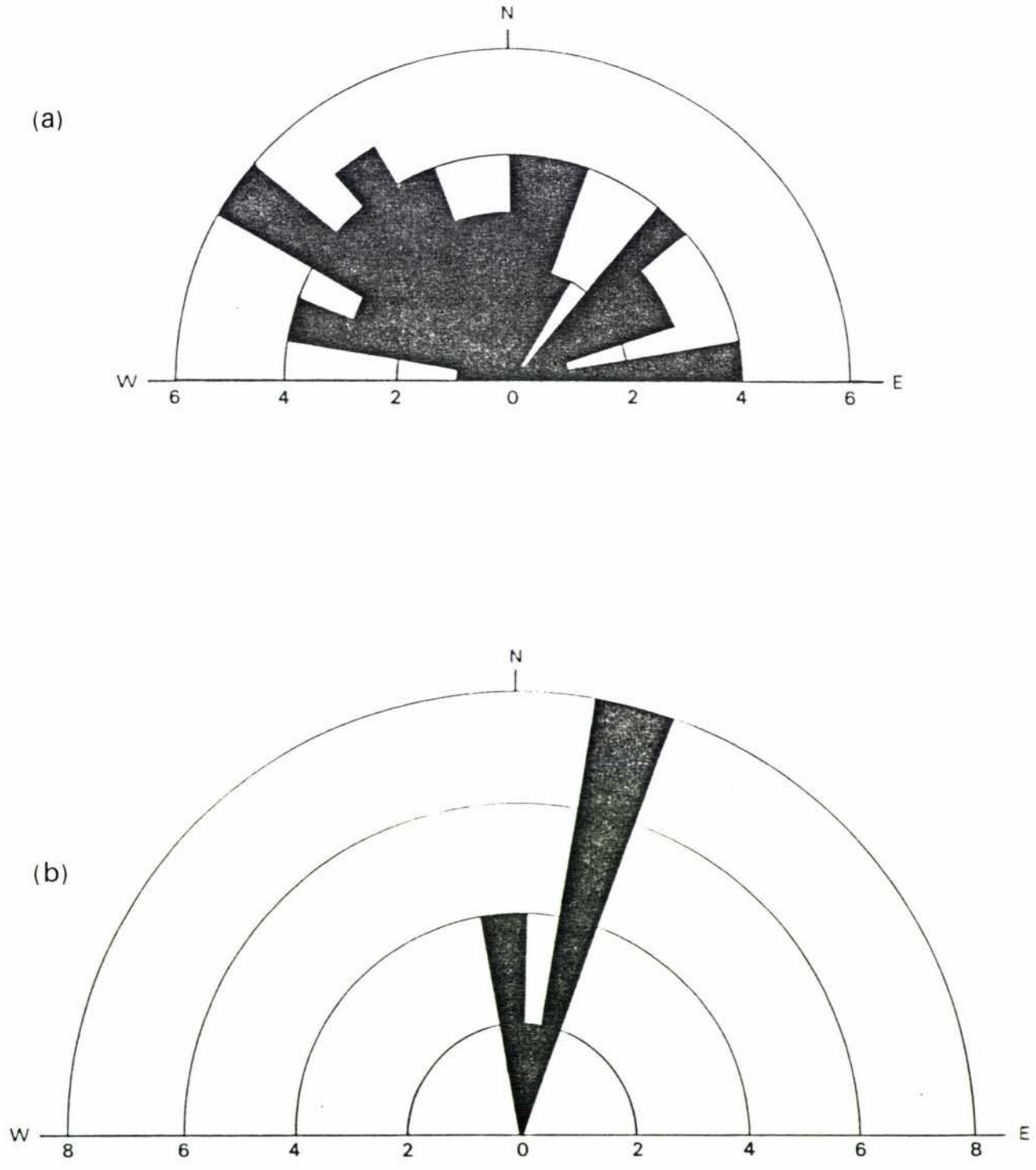

Figure 4.2 Orientation of joints within (a) grikes, and (b) bogaz.

limestone. This has resulted in a series of parallel fissures (Fig. 4.3 and 4.4) up to 30 m in length, 1 m to 4 m in width and 1 m to 8 m in depth. These fissures and their possible mode of origin are described in this section. Features such as these have not been previously described in New Zealand.

4.5.1 Terminology

The world-wide occurrence of fissures within limestone, in almost all climatic conditions, lithologies, and structures, has resulted in a complex variety of terms being used to describe them. These terms, and the suggested methods of development given in the literature, will now be discussed.

The term "kluftkarren" was first introduced by Cvijic in 1893 to describe small-scale features such as grikes. He also described much wider fissures which he believed were formed by the enlargement of kluftkarren. These he called "bogaz" and "strugas" (Sweeting 1972). Bogaz are corridor-like features from 2 m to 4 m wide and tens of metres in length. They are from 1 m to 5 m deep (Sweeting 1972). Cvijic (1924) described bogaz as being solutional enlargements of kluftkarren, while Milojevic (1936, cited in Sweeting 1972) believes that both mechanical and chemical erosion are important in their development.

The term "gull" has been used to describe fissures within limestone in England. This term was first used by Filton (1836, cited in Hollingworth et al. 1944) and has subsequently been defined by Hollingworth et al. (1944) as "...those clefts in the rock which tend normal to the slope of a cambered surface." Cambering of the surface results from the squeezing out of underlying softer material, usually clays, due to the weight of the overlying material. This progressively lowers the upper beds and tension stress opens up zones of weakness such as joints. After the initial opening-up of the joints, continued enlargement is aided by solution and periglacial activity, particularly ice wedging in the continued growth of the fissures. The usage of the term "gull" in England has become associated with areas which have at some stage been influenced by a periglacial climate. For example, Hollingworth et al. (1944); Judson (1947); Kellaway and Taylor (1952); Muskett (1971); Murray and Hawkins (1973). Straw (1966) has used the term to describe

fissures developed along the Niagara Escarpment, Ontario, Canada.

Lattman and Olive (1955) noted joints widened by solution in the semi-arid Stockton Plateau, Trans-Pecos Texas. The widened joints were up to 30 cm across. The joints collected soil and water and subsequently supported dense vegetation. Lattman and Olive considered that these joints were enlarged by the solutional activity of rain water, which moves down the open joints.

Monroe (1964) termed fissures in Puerto Rico "zanjones", a Spanish word for a deep drainage ditch or trench. He described zanjones as "trenches as long as 100 m or more, with vertical sides ranging in width from a few centimetres to about 3 m and in depth from about 1 m to 4 m. They occur as parallel trenches oriented generally in the same direction."

Wilford and Wall (1965) described "corridors" in Sarawak, Malaysia, as "...joint-determined corridors....about 100 feet (30 m) apart and estimated to be from 10 feet (3 m) to 500 feet (150 m) deep". Their maps show group of parallel corridors several hundred feet long.

Sweeting (1972) described kluftkarren and other larger fissures. She noted that zanjones are possibly a variety of Kluftkarren and considers that they might properly be termed "bogaz" or "strugas" using the terms of Cvijic (1893). Monroe (1976) does not agree on the use of the term "struga", as this is a solutionally enlarged bedding plane. He also believes that bogaz, as defined by Sweeting (1972), are posssibly a smaller-scale feature than zanjones

Brook and Ford (1978) introduced the term "labyrinth karst" to describe both large-scale and small-scale solutional enlargement of fissures within limestone. They described "streets" up to 185 m deep and 9 km long and referenced many other examples world-wide both of small-scale and large-scale development of solutionally enlarged fissures. Brook (1981) has suggested that there is a link between the developmental sequence in the origin and evolution of both large-scale and small-scale fissures within limestone. Both Cvijic (1893, 1924) and Jennings and Sweeting (1963) have also questioned possible links between the development of large-scale and small-scale fissures.

Ford (1982, p.348) described bogaz developed within the permafrost areas of Arctic Canada. He states that bogaz are karst landforms developed in this instance by circulation of groundwater to depths of at least 10 m to 15 m in the rock.

Bogaz have recently been described by Odell (1985) in Thailand. Here they range in depth from 5 m to 15 m with some reaching 30 m, and averaging 30 m in length with a maximum of 200 m. Odell gave an evolutionary sequence for their development, with their initial formation as a vertical grike or fissure in the rock which enlarged downwards towards a local water table. At the same time, solutional erosion below the water table created a horizontal fissure. Eventually the grike reaches the horizontal fissure resulting in concentrated enlargement below ground, with a narrow fissure leading to the surface.

The term "bogaz" will be used here in describing medium to large-scale fissuring of limestone within the Puketoi Range. This term has been chosen mainly because of its historical use by Cvijic (1893) in describing solutional enlargement of fissures 2 m to 4 m in width and tens of metres in length.

4.5.2 Bogaz within the Puketoi Range

Two small areas of bogaz have been observed within the Puketoi Range. These are situated at grid references U24/823893 and U24/791847, and shown in figures 4.3 and 4.4 and photograhps 4.16 to 4.18. The northern most area (Grid Ref. U24/823893) will be referred to as "Oporae bogaz", because of the close proximity to Mt. Oporae. The second area (Grid Ref. U24/791847) will be referred to as "Waewaepa bogaz", as this area is on Waewaepa Station.

Figures 4.3 and 4.4 show the most pronounced bogaz recognised from mosaic aerial photograph interpretation (Maps N.Z.M.S. 3 N.150/5 and N.150/8). Field checking revealed many more bogaz. Those not shown on figures 4.3 and 4.4 are generally narrow and short in length. The development of dry valleys has dissected the areas of bogaz, resulting in many gaps within a single bogaz. This is particularly evident in the Oporae area.

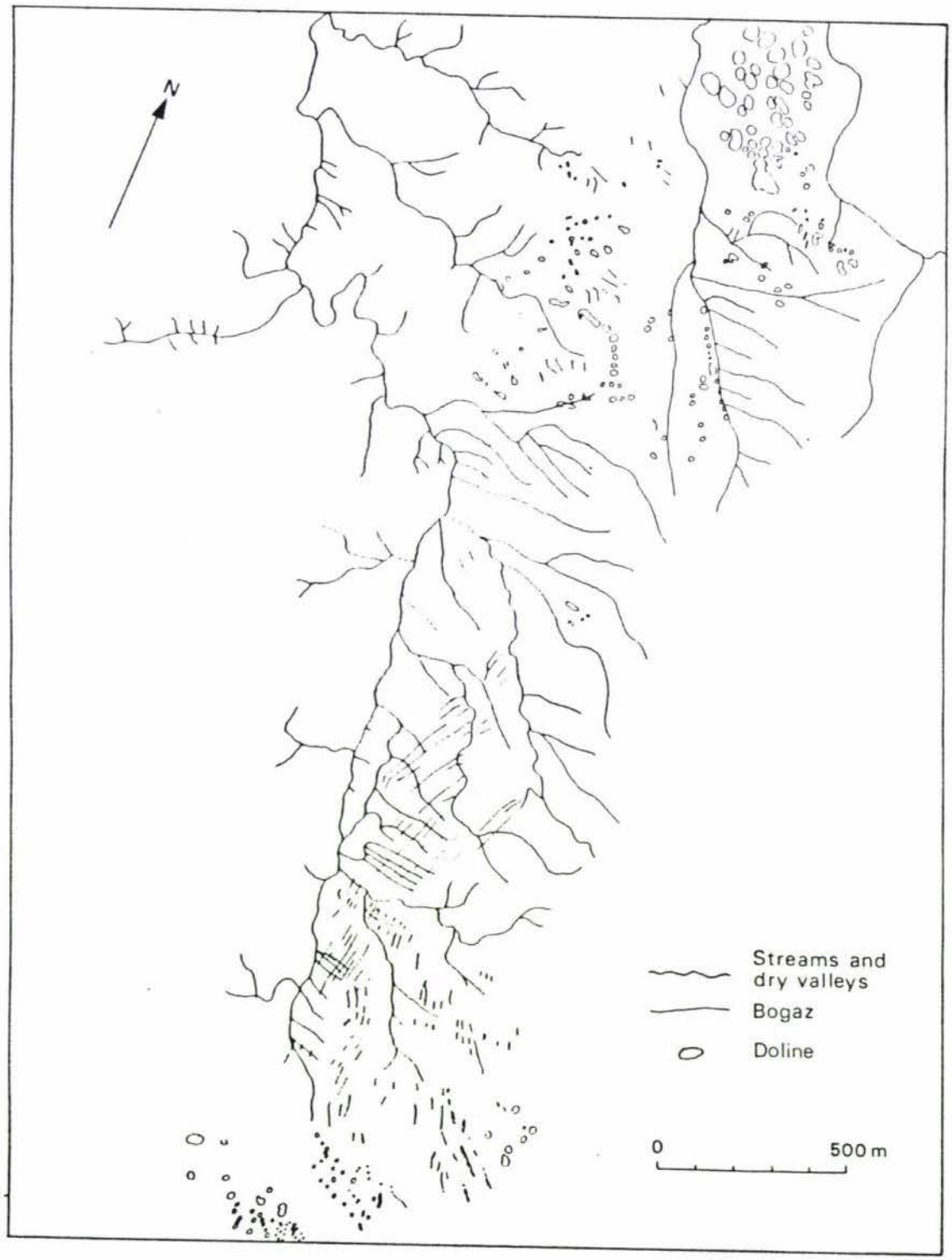

Figure 4.3 Location map of bogaz and dolines at Oporae.

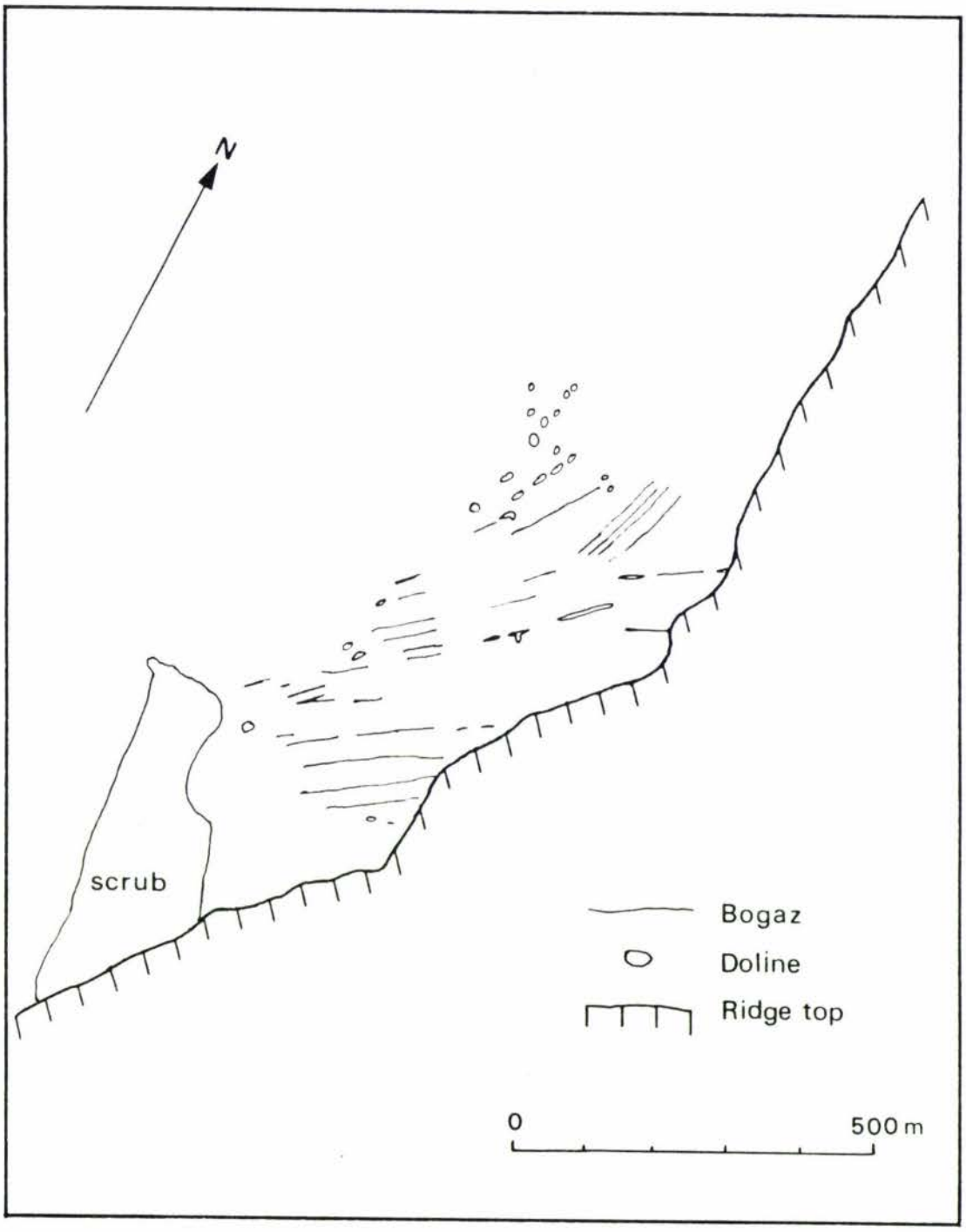

Figure 4.4 Location map of bogaz and dolines at Waewaepa.

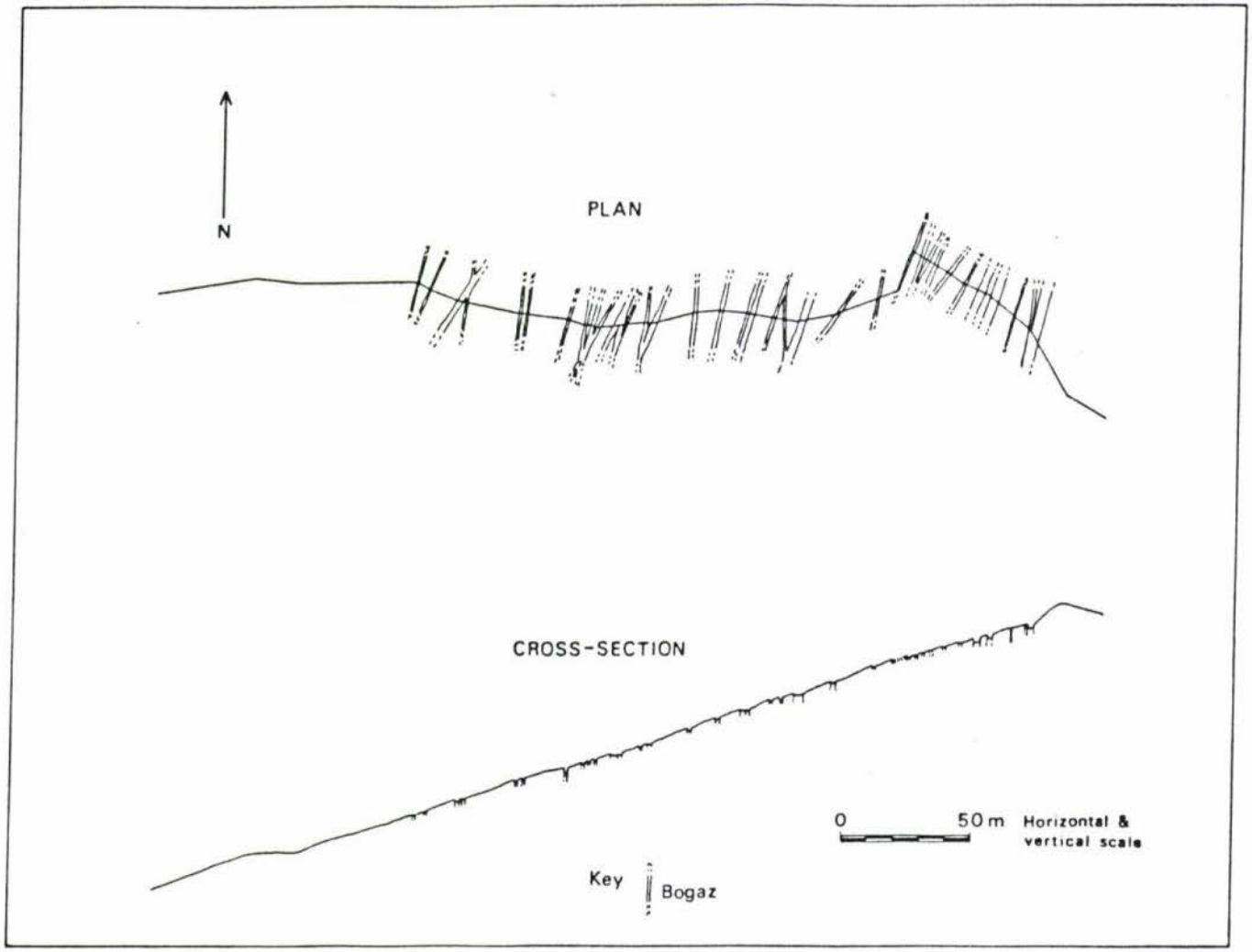

Figure 4.5 Plan and cross-section of bogaz at Oporae.

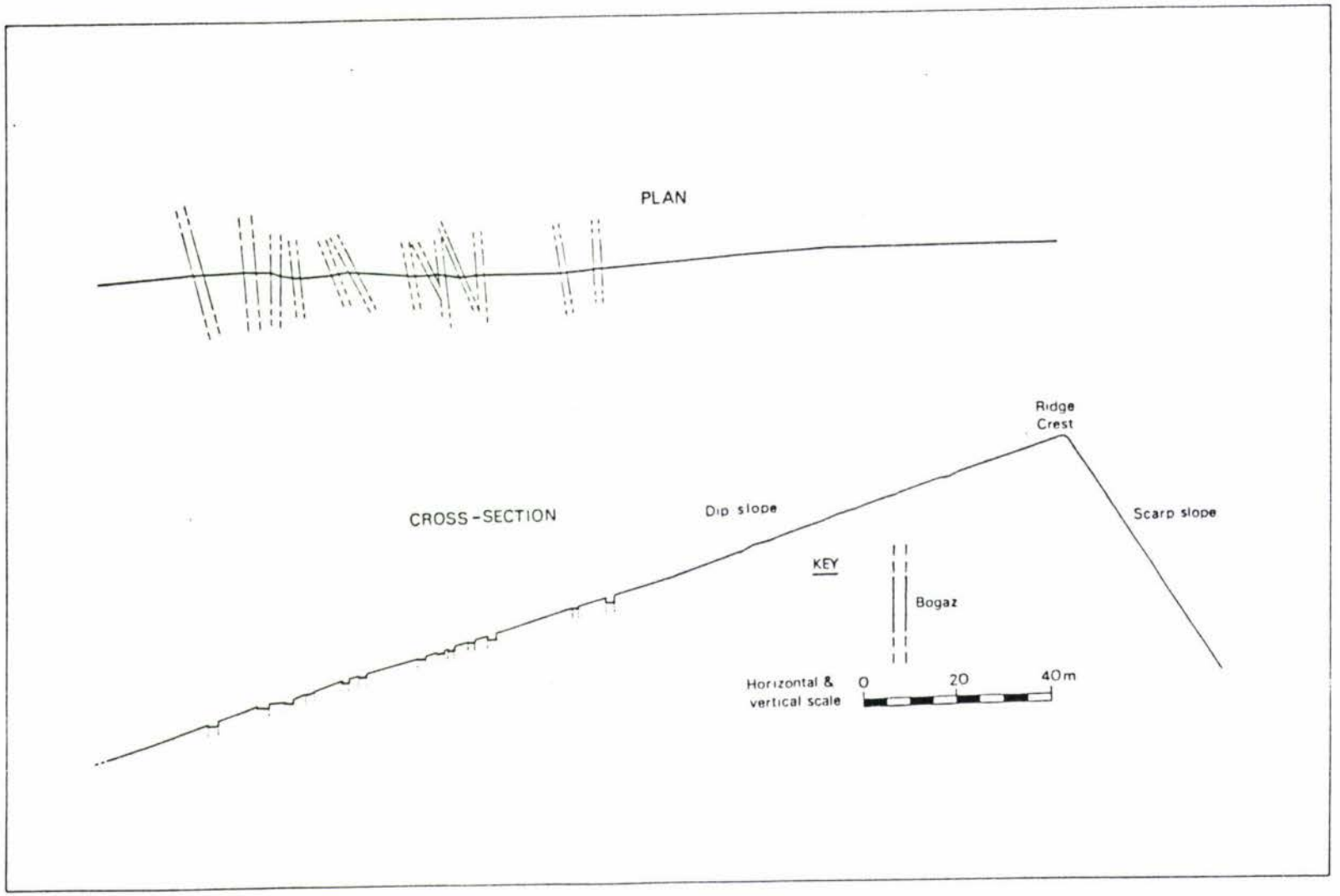

Figure 4.6 Plan and cross-section of bogaz at Waewaepa.

4.5.2.1 Description of Bogaz at Oporae

This is the largest of the two areas of bogaz, covering approximately 1.3 km^2. Bogaz are found along the western limb of the Oporae Anticline (Fig. 4.3, Photo 4.16) on the Awapapa Limestone Formation which is dipping at approximately 15 degrees. This anticline, more correctly termed a monocline, plunges towards the north. The general trend of these bogaz follows the curvature of the hillside - they therefore have a curvilinar appearance. More than one set of joints may be involved in the development of the bogaz. Along the western side of the Oporae Anticline, the bogaz are parallel to the slope of the surface. Further to the north, the bogaz curve towards the east across the plunging monocline, but are still parallel to the slope of the surface. This possibly indicates a secondary set of joints being favoured for bogaz development.

Two distinctive types of bogaz are seen in photograph 4.16. The first type, in the foreground of the photograph, is much larger and deeper, with native shurbs growing at the base (Photo 4.17). These are situated at the southern end of this area of bogaz and are approximately 2 m to 3 m in width and up to 20 m in length. Depth was generally 4 m to 5 m, with some reaching nearly 8 m. Local drainage has been diverted along these bogaz and associated with this is the enlargement of a secondary set of joints which have developed into caves. Springs seen at the bottom of photograph 4.16 are from these caves. During wetter periods streams flow through both the bogaz and caves, the water being derived from the Raukawa Mudstone Formation to the south. Examination of the side and end walls of these bogaz did not reveal any apparent joints or variation in the limestone.

The second type of bogaz are found to the north of this area. They are 20 m to 30 m long, sectioned (up to 100 m in total length), narrow (0.5 m to 2 m) fissures infilled with soil. Figure 4.5 is a surveyed line across this area. The bogaz have vertical or overhung walls with soil-filled floors. The depth of the bogaz is unknown but where they are not soil infilled, depths of up to 4 m are visible.

Further to the north there is a transition from these long narrow bogaz to solutional dolines. In many instances the two have combined to form a fissure with a deep depression at the end. This transitional form is

Photograph 4.16 View of Oporae bogaz area. Photo was taken looking to the north.

Photograph 4.17 Individual bogaz, southern end of Oporae bogaz area (Grid Ref. U24/823893). Streams flow along the bottom of the Bogaz during the summer. (Photo: Mike Shepherd)

illustrated in figure 4.3.

4.5.2.2 Description of Bogaz at Waewaepa

The second area of bogaz is found near the crest of the Puketoi Range, and is much smaller covering only 0.24 km^2. These bogaz have developed within the Te Onepu Limestone Formation and form a series of fissures parallel to the slope. Photograph 4.18 shows one of these bogaz. The form is similar to that of the northern bogaz at Oporae, with the width and depth varying from 1 m to 2 m approximately. These bogaz are also soil-filled. A pit was dug into one of them. A depth of 1.5 m was dug without encountering a floor, and the walls showed no marked narrowing. Occasional limestone pebbles were found.

Figure 4.6 is a surveyed line from the crest of the Puketoi Range, down across the bogaz. Slight depressions were found near the crest (not shown in figure 4.6) and these became more distinctive further down the slope until true bogaz were encountered. These bogaz were less than 1 m in width, and width increased down-slope. At the bottom of the slope bogaz were up to 2 m in width.

4.5.3 Formation of Bogaz within the Puketoi Range

The occurrance of bogaz in different geological beds in two separate areas of the Puketoi Range, may indicate more than one means of formation and development. The initial development of the Oporae bogaz is believed by the author to have resulted from the growth of the Oporae Anticline. This would cause tension along joints within the limestone. When the overlying Raukawa Mudstone Formation was eroded, solutional enlargement of the tension joints began. The continued growth of the bogaz in the northern section of this area was possibly associated with ice-wedging during periglacial conditions.

Tension joints parallel to the anticlinal axis have been noted by De Sitter (1959) in southeast Algeria (Fig. 4.7). These have formed in association with shear joints within limestones underlain by mudstone. De Sitter also noted tension joints forming at right angles to the synclinal axis in the same area. Bogaz observed by the author in the Paporoa National Park are of this form. These have formed in the synclinal basin between Bullock Creek (Grid Ref. K30/779992) and the

Photograph 4.18 Individual bogaz, Waewaepa (Grid Ref. U24/791847). The bogaz is soil infilled.

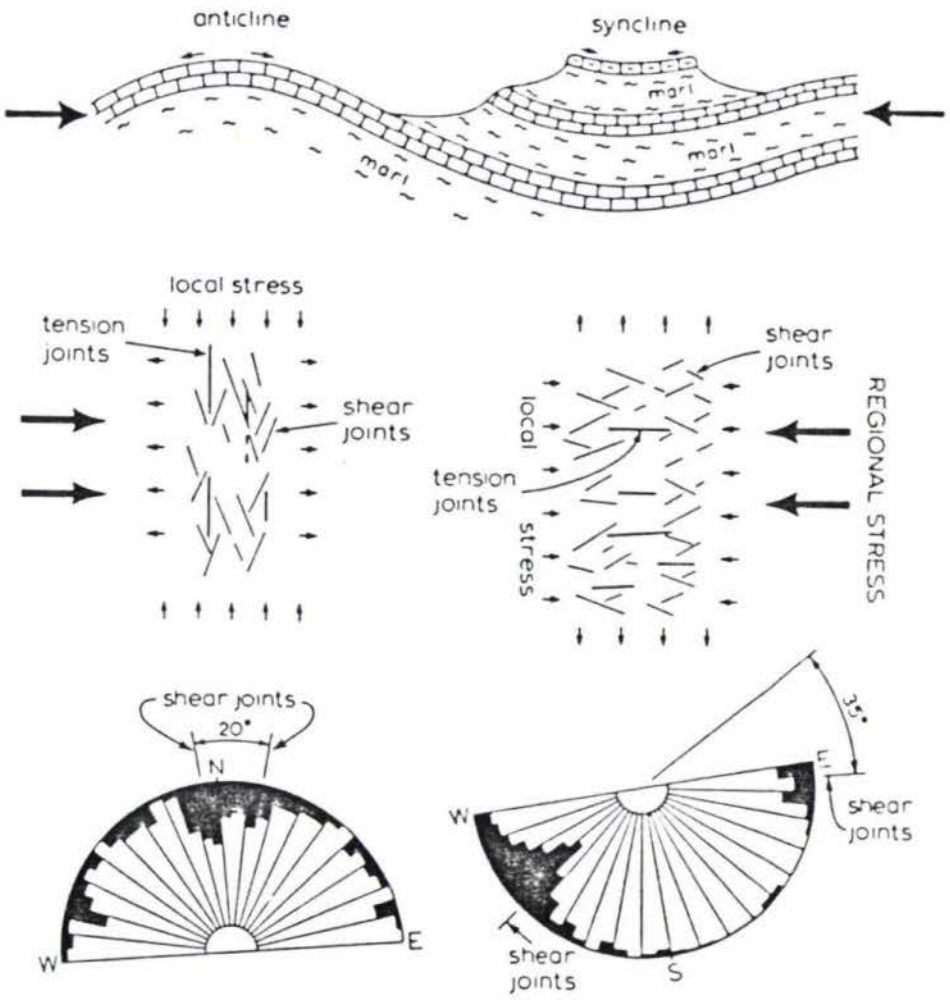

Figure 4.7 Fault patterns in adjoining anticlines and synclines in southeast Algeria. Fault strike frequency diagrams shown below. (From De Sitter 1959).

Pororari River(Grid Ref.K30/754973). These bogaz are up to 30 m in length and 2 m in width.

The bogaz in the southern section of Oporae area may be more recent than those further to the north, their development being related to the recent removal of the overlying Raukawa Mudstone Formation. As this mudstone layer is eroded back, drainage from this area is concentrated towards the bogaz, resulting in localized high rates of solution. This may explain

the larger size of these bogaz compared with the others in the area.

The bogaz at Waewaepa are also believed to have formed from tension applied to joints within the limestone. Here the underlying Raukawa Formation mudstone is possibly being forced out along the scarp slope. This has resulted in the sinking of the top section of the crest causing joints to open up lower down the slope, as this area acts a the pivot point. This is seen in the larger width of the bogaz lower down the dip-slope.

From the above discussion, bogaz development within the Puketoi Range has been controlled largely by the tensioning of joints within the limestone. These joints were more susceptible to solutional erosion and possibly ice-wedging during periods of periglacial climatic conditions, resulting in their enlargement. Solutional enlargement will be continuing today as water flows down these joints, particularly as the water would be acidified by the highly organic soil at their base.

4.6 Case-Hardening of Limestone

4.6.1 Previous Studies

Limestone exposed at the surface may, in certain situations, become harder and purer than the underlying rock. This hardening of the rock has been associated with resistance to erosion, and with differential landform development (Day and Goudie 1977; Day 1981, 1982), with the indurated rock forming more outstanding relief (Sweeting 1972). This induration of the limestone is termed "case-hardening". The indurated layers are also known as calcareous weathering crusts (Panos and Stelcl 1968) and secondary cementation (Sweeting 1980). The phenomenon has been observed world-wide, particularly in humid tropical karst areas, notably in the Caribbean (Weyl 1953, cited in Ireland 1979; Monroe 1966, 1976, 1980; Panos and Stelcl 1968); but also in hot dry climates, for example, the Nullarbor Plain, Australia (Jennings 1971); and in comparatively temperate humid climates, for example, in Canterbury, (Jennings 1971), and on the East Coast of the North Island, New Zealand (Moore and Belliss 1979).

Thickness of the case-hardened layer may vary from a few centimetres to 5 m to 10 m in the case of mogotes (steep-sided hills of limestone generally surrounded by nearly flat alluviated plains) (Monroe 1980). Below this the limestone is much softer and may be quite powdery, chalky and easily eroded (Panos and Stelcl 1968; Monroe 1976).

Development of the case-hardened layer may result from repeated partial solution, of the surface zone of the porous limestone, after wetting, followed by almost immediate reprecipation of the dissolved calcium carbonate, drawn by capillary ascent to the surface (Panos and Stelcl 1968; Monroe 1976). Calcite is deposited either above the surface of the rock, or immediately below, infilling the pores (Panos and Stelcl 1968). Precipitation is the result of either a sudden rise in temperature, which would drive off carbon dioxide, or the circulation of drier air, which would evaporate the water as it reaches the surface (Monroe 1976). Salomons et al. (1978) believe these two processes are also the cause of calcrete formation. These mechanisms would be particularly efficient at shallow depths in the rock, but possibly decrease in efficiency with increasing depth, where other factors may be more important.

Critical factors in case-hardening formation are: the amount, duration and intensity of rainfall on the bare limestone (Jennings 1971); wind direction (blowing rain into rock crevices (Monroe 1976)); and the lithology of the rock. Case-hardening generally occurs on more porous limestones, for example, Oligocene limestone in Canterbury which is chiefly a porous shelly and foraminferal biomicrite (Jennings 1971);and porous coquina limestone along the East Coast of the North Island, New Zealand (Moore and Belliss 1979).

Solution will occur at a greater depth in highly porous rock, than in dense and compact limestone. This strongly influences the formation of case-hardening, with the greatest thickness occurring on the more porous rocks, with high water absorption capacities (Panos and Stelcl 1968; Day 1980). Development of a case-hardened layer over the surface of a rock results in a solid, dense calcareous crust, with low porosity, which is more resistant to erosion than the underlying rock.

Much of the literature on case-hardening is from research into mogote

development in Puerto Rico (Monroe 1966, 1976, 1980; Day 1978b, 1980; Ireland 1979).

4.6.2 Case-hardening in the Puketoi Range

4.6.2.1 Method of Investigation

Case-hardening of limestone along the East Coast was first noted by Moore and Belliss (1979) in the Te Aute Group, and was subsequently observed by Dr. M. Shepherd (pers. comm.) in the Puketoi Range.

The author tested the hardness of limestone exposed along the range, using a Schmidt hammer (type N) described below.

Quantitative comparison of the hardness of case-hardened limestones was first carried out by Day and Goudie (1977). This can be achieved in the field using a Schmidt hammer, also known as an impact hammer, a concrete test hammer, or a Sclerometer. This is considered by Day and Goudie (1977) to be a better measure of the resistance to erosion than the compressive strength, which is a measure of resistance to crushing (Selby 1980).

The Schmidt hammer measures rock hardness in terms of the distance of rebound (recorded as the Rebound Number or R value) of a controlled spring-loaded mass impacting on a rock surface. Because elastic recovery of the rock surface depends on the hardness of the surface, and hardness is related to mechanical strength, the distance of rebound (R) is therefore a measure of the surface hardness or strength.

The following disadvantages, with using the Schmidt hammer have been noted by Selby (1980). It is extremely sensitive to discontinuities in the rock, even hair-line fractures may lower readings by 10 points. The hammer is also very sensitive to water content, especially in weak rock. Full technical details of the hammer's operation and maintenance are given by Day and Goudie (1977).

4.6.2.2 Results

Exposed limestone on the Puketoi Range was selectively tested for rock hardness. Case-hardening was observed predominantly along the top of the range, for example, at Oporae R values averaged 43.9 (n = 19), and in

other exposed situations similar R values were recorded. This may be related to a greater amount of rock outcropping at the surface on the top of the range, than in the valleys. All R value measurements have been adjusted for horizontal readings, from Table 2, Day and Goudie (1977).

Limestone exposed at the surface of sheltered valleys, elsewhere along the top of the range, and lower down on the dip slope, gave much lower R values than recorded at Oporae. For example, to the southwest of Coonoor (Grid Ref. U24/724807), limestone exposed at the surface yielded an average R value of 20.5 (n = 16). Therefore case-hardening appears to be patchy and may only have developed in areas devoid of a soil cover in the past.

An investigation was made of the variation in the nature of the case-hardening along the Puketoi Range. A vertical section of bedrock has been exposed by the bulldozing of a track along the western side of Oporae (Grid Ref. T24/821874). A thin soil cover, approximately 2 cm to 5 cm thick, has developed on the case-hardened limestone (Photo 4.19). The top 20 cm of the exposed rock is case-hardened, with an average R value of 43.9 (n = 19). Between the depths of 20 cm and 25 cm, there is a rapid change, from the upper indurated layer of limestone to very soft, crumbly limestone (R value 13.6 (n = 5)). Inner layers are increasingly softer with R values less than 10 at depths greater than 30 cm (Fig. 4.8).

Case-hardening causes distinctive changes in rock texture, as can be seen in an isolated rock at grid reference U24/785843 (Photo 4.20). Rock hardness decreases rapidly from the hard upper indurated layer, to the inner soft pitted limestone. The average R value of the top section of the rock is 35.8 (n = 8), decreasing to below 15 (n = 10) in the lower section. Many of the nearby exposed rocks are similar in appearance, with a thin indurated top section and a much thicker pitted lower section.

4.6.2.3 Discussion

Although case-hardened limestone within New Zealand has been noted by Jennings (1971) in Canterbury, and by Moore and Bellis (1979) along the East Coast of the North Island, the above investigation is the first detailed description of case-hardened limestone in New Zealand.

Photograph 4.19 Case-hardened limestone at Oporae (Grid Ref. U24/821874). The upper indurated layer is marked by the hammer, with softer limestone beneath.

Photograph 4.20 Case-hardened isolated rock (Grid Ref. U24/785843). Note the change in texture from the upper indurated section to the soft crumbly limestone beneath.

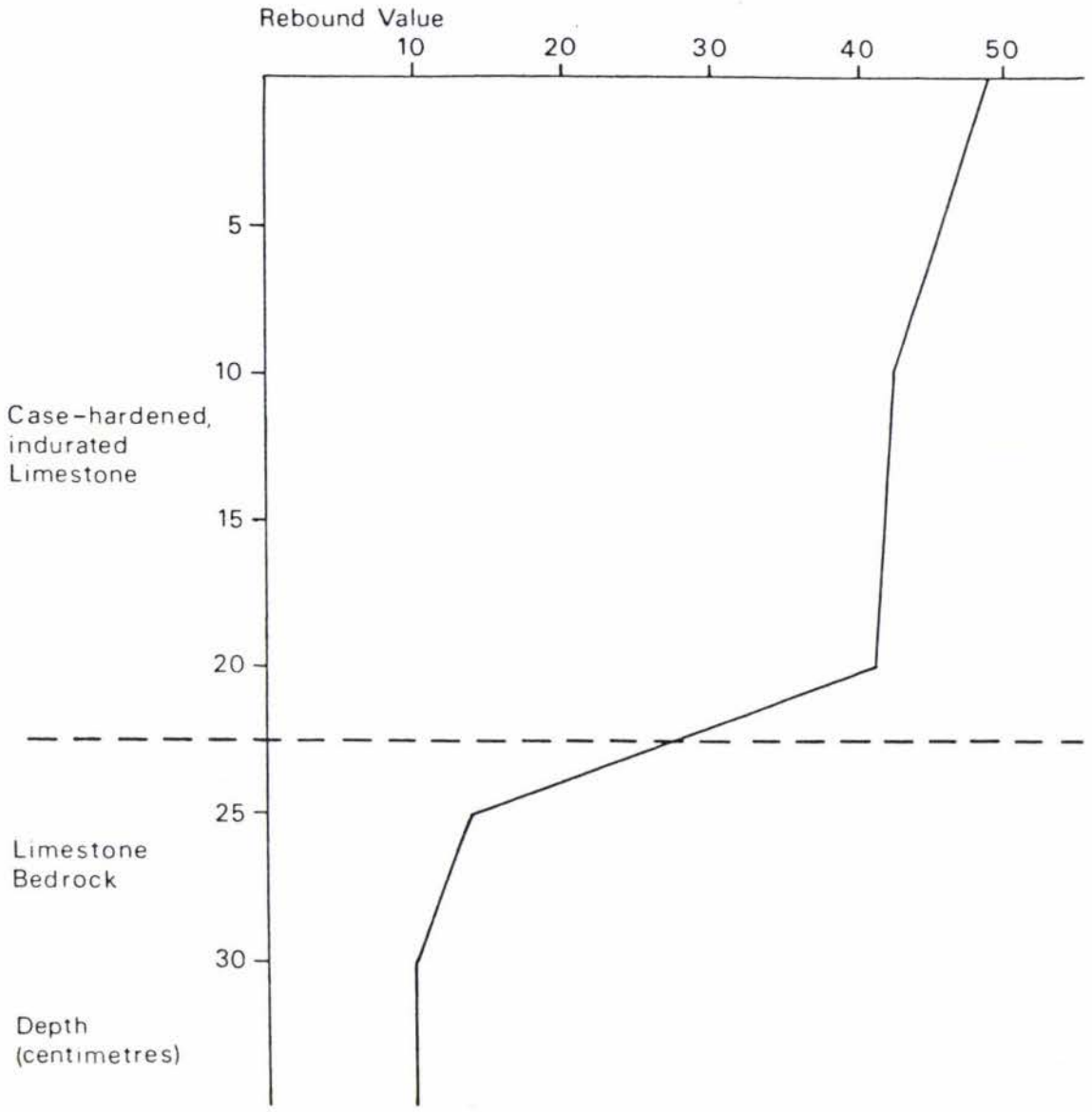

Figure 4.8 Profile of R-values of case-hardened limestone at Oporae (Grid Ref. T24/821874).

Case-hardened limestone found on the Puketoi Range clearly demonstrates the development of an upper indurated layer, with softer underlying rock.

The mechanism for the formation of the case-hardened limestone layers, along the Puketoi Range, is probably related to the frequent strong winds, which draw moisture out of the rock and cause reprecipation of dissolved calcium carbonate at, or near the surface, of the rock.

Case-hardening has been noted as only occurring on limestone exposed at

the surface (Panos and Stelcl 1968; Monroe 1976). If this is so, the case-hardening visible in the vertical section of the rock exposed along the bulldozed track, on the western side of Oporae, as described above, must have developed before the formation of the soil cover. This may indicate that the soil cover is recent in this area. The induration of only the upper section of the isolated rock (Photo 4.20), and other nearby rocks, as described above, could indicate a reduction in soil depth equilavent to the distance between the bottom of the case-hardened layer and the ground surface in this area. These two examples therefore give contradictory clues about the changes in soil depth over time. Localised variation in the formation and development of the soil cover may explain this.

The influence of cooler climatic conditions during the Pleistocene may have been important in the development of the case-hardening. With the establishment of a periglacial climate, the vegetation covering the Puketoi Range would have been alpine and montane, possibly exposing more limestone outcrops to the direct influence of wind, rain and sunshine than would have occurred under a forest cover. Similar work to that carried out by Ivanovich and Ireland (1984) on the dating of case-hardening would be needed to give an age for the formation of the case-hardening within the Puketoi Range, and possible implications for Pleistocene vegetation and soil cover.

4.7 Conclusions

Selected karst landforms within the Puketoi Range have been discussed in this chapter. These landforms range in size from large dry valley systems covering many square kilometres to small karren and case-hardened limestone occuping areas of a few square metres or less.

Many of the landforms discussed above are the result of, or have been influenced by, previous climatic conditions. This is seen particularly in the limestone pavement developed on the range, and has also possibly been influentual in asymmetrical dry valley development. These landforms are relic features formed under periglacial conditions and are not the result of present processes.

Present processes are, however, influential in the continued development of landforms within the range. Karren is believed to be the result of present processes operating in an area and change in the karren form may be in response to changes in the intensity of various geomorphological processes (Dunkerley 1983).

Landforms developed on the range are therefore a reflection of both past and present geomorphological processes.

CHAPTER FIVE
DRAINAGE CHARACTERISTICS

5.1 Introduction

The crest of the Puketoi Range forms a major watershed. It separates rivers which rise on the scarp slope and flow towards the east, from those rivers draining the dip slope, which flow westward into the Manawatu River. The Puketoi Range is on the eastern limit of the Manawatu catchment. The Makuri and Mangatoro Streams flow southward and northward, respectively, to eventually join the Manawatu River. Exceptions to this general pattern of stream flow are the Tiraumea Stream at the southern end of the range, and two streams to the south and southeast of Makuri, which bring water from the eastern side of the range through or around the end of the range to flow westward to the Manawatu River.

Lithology appears to have a strong influence on the development of stream networks and drainage basin morphology in this area. The three main lithological groups are: (1) mudstones, siltstones and sandstones, which will be referred to as mudstones in this chapter; (2) greywacke of the Waewaepa Range; and (3) limestone of the Puketoi Range and the western flanks of the Waewaepa Range. An example from each lithological group will be examined and compared.

This chapter begins with a generalized look at surface drainage on and in the vinicity of the Puketoi Range, followed by a discussion of the drainage basins developed on the three lithological groups mentioned above.

5.1.1 Surface Drainage - a Generalized View

The karst area of the Puketoi Range, like many karst areas, is characterised by few surface streams, with the majority of the drainage underground (see chapters 3 and 4). The two major streams flowing from the range - the Makuri Stream, flowing to the south, and the Mangatoro Stream, flowing to the north - have developed at the contact between the limestone and the less soluble materials found in the area. The headwaters of both of these streams are in the vicinity of Coonoor (Grid ref. U24/738813). This is the highest point in the basin formed between

the Puketoi and Waewaepa Ranges, and accordingly, acts as the drainage basin divide for streams flowing to the south and north.

Both the Makuri and Mangatoro Streams derive water from the limestone covered dip-slope of the Puketoi Range, and the impervious rock of the Waewaepa Range and surrounding area. The water within these rivers, therefore, can carry both high solute and suspended sediment loads, as well as high bedload, where greywacke gravels are being eroded from the Waewaepa Range. The specific proportions of each is dependent on the locality and the spatial distribution of rainfall at the time of measurement. Where the streams are flowing over limestone only, the bedload is relatively low and in many cases is only occasional patches of sand and pebble sized material on an otherwise bare bedrock stream bed. The variation in the solute load of these streams is discussed in chapter 4.

Streams flowing from the eastern scarp slope of the range generally flow to the east coast, with the exceptions to this described below. The scarp slope is predominately Mangatoro Formation, a massive blue-grey, poorly indurated mudstone (Harmsen 1984a, 1985). Only the top section of the scarp is composed of limestone. Owing to the steepness of the scarp here this area of limestone is minimal but the limestone has been extremely influential in the development of the scarp face (see chapter 7 for a discussion on the evolution of the cuesta).

Only two streams from the eastern side of the Puketoi Range flow directly across the range, westwards into the Makuri River. Both have cut gaps through the scarp and dip slopes. These streams are at grid references T25/675685 (see photo 7.2 and T25/635635. These streams carry allogenic water derived from the impervious rocks (Mangatoro Formation) on the eastern side of the range to the Makuri River on the western side (See chapter 7, for a discussion of the development of these streams).

5.2 Drainage Basin Characteristics

The remainder of the chapter will give a brief description of variations found in drainage basin form on limestone, mudstone and greywacke on, or in close proximity to, the Puketoi Range. A drainage basin is defined as

the "...entire area providing runoff to, and sustaining part or all of the stream flow of, the main stream and its tributaries" (Gregory and Walling 1973, p.37).

In the investigation of drainage basin characteristics, three main paths of enquiry may be taken: (1) morphometric analysis to measure the form of the basin; (2) relating the characteristics of the basin to the processes operating in the basin; and (3) the application of methods of landscape description from other branches of study (Gregory and Walling 1973).

In this chapter, the first of these methods will be used in the examination of the drainage basins. In particular, the density of the stream network will be examined as this is a parameter providing a link between the form attributes of a basin, and the processses operating in the streams within the individual drainage basin (Gregory and Walling 1973). The controls placed on drainage-basin form by topography, lithology, pedology and vegetation are all reflected in the density of the drainage network. In this examination of drainage basins, the basins investigated were chosen solely according to the lithology of the bedrock of the individual basins. Other factors such as topography, pedology and vegetation are seen as important in the control of drainage basin form, but in the examples examined the lithological variation between greywacke, mudstone and limestone is likely to be the dominant variable. This is because of the structural control lithology has on denudational processes, that is, the effects of the permeability and massiveness of the rock, and the control on mechanical and chemical weathering.

5.2.1 Method

The density of the drainage network was defined by Horton (1932) as the length of the streams per unit of drainage area. This requires the area of the basin and the total stream length to be measured. This measurement is expressed in km/km^2, allowing a comparison of drainage basins to be made. Drainage density can also be considered a measure of the texture of a landscape. Smith (1950) and Strahler (1957) described areas with drainage density values less than 5.00 as coarse textured,

between 5.00 and 13.78 as medium textured, between 13.7 and 155.3 as fine textured and greater than 155.3 as ultra-fine textured.

Three drainage basins were chosen for examination. These are shown in figures 5.1, 5.2, and 5.3. Figure 5.1 and photograph 5.1 are of the basin developed on Mangatoro Formation mudstone. This is situated on the eastern scarp slope of the Puketoi Range (Grid Ref. U24/790835). Photograph 5.1 is looking from the top of the scarp (marked X on Fig 5.1) eastward across the drainage basin. Figure 5.2 shows the basin developed on Waewaepa Formation greywacke (Grid Ref. U24/782935). This is at the northern end of the Waewaepa Range. The lower section of this basin is close to the boundary with Kumeroa Formation mudstone. This was not field checked, therefore the exact position of the boundary is unknown; mudstone may therefore be present in the lower section of the catchment.

Figure 5.3 is the basin developed on Te Onepu Formation limestone (Grid Ref. U24/752805). The distinctive nature of karst, with much of the drainage underground, and with surface drainage often directed into dolines rather valleys, makes the comparison between karst and non-karst drainage basins difficult. Also, the physical boundaries of karst drainage basins need not be restricted to surface features, with underground drainage paths crossing the surface boundaries of the basin. Field checking was carried out to identify streams and dry valleys. No dye testing was undertaken, but it is assumed that the boundary of the basin is the watershed boundary around the basin. Two drainage density figures are given for the karst basin. The first is for streams alone, and the second is for streams and dry valleys combined. The differentation between stream valleys and dry valleys is made on the presence or absence of a stream channel. Where a stream channel is present the valley was identified as a stream valley. This may lead to the omission of first order stream valleys where flow may be rare.

The examination of the drainage basin densities was achieved using aerial photograph mosaic maps at a scale of 1:15 840. The scale of these maps was sufficently large to allow easy identification of drainage basin watersheds and stream channels. All streams and streamlets visible on the aerial mosaic maps were drawn onto each figure.It was difficult to identify streamlets in the basin developed on mudstone, (Fig 5.1) as the top of this basin was covered in regenerating forest. This is clearly

Photograph 5.1 Drainage basin developed on Mangatoro Mudstone Formation along eastern scarp slope of the Puketoi Range. The photo was taken from the crest of the range, looking towards the east.

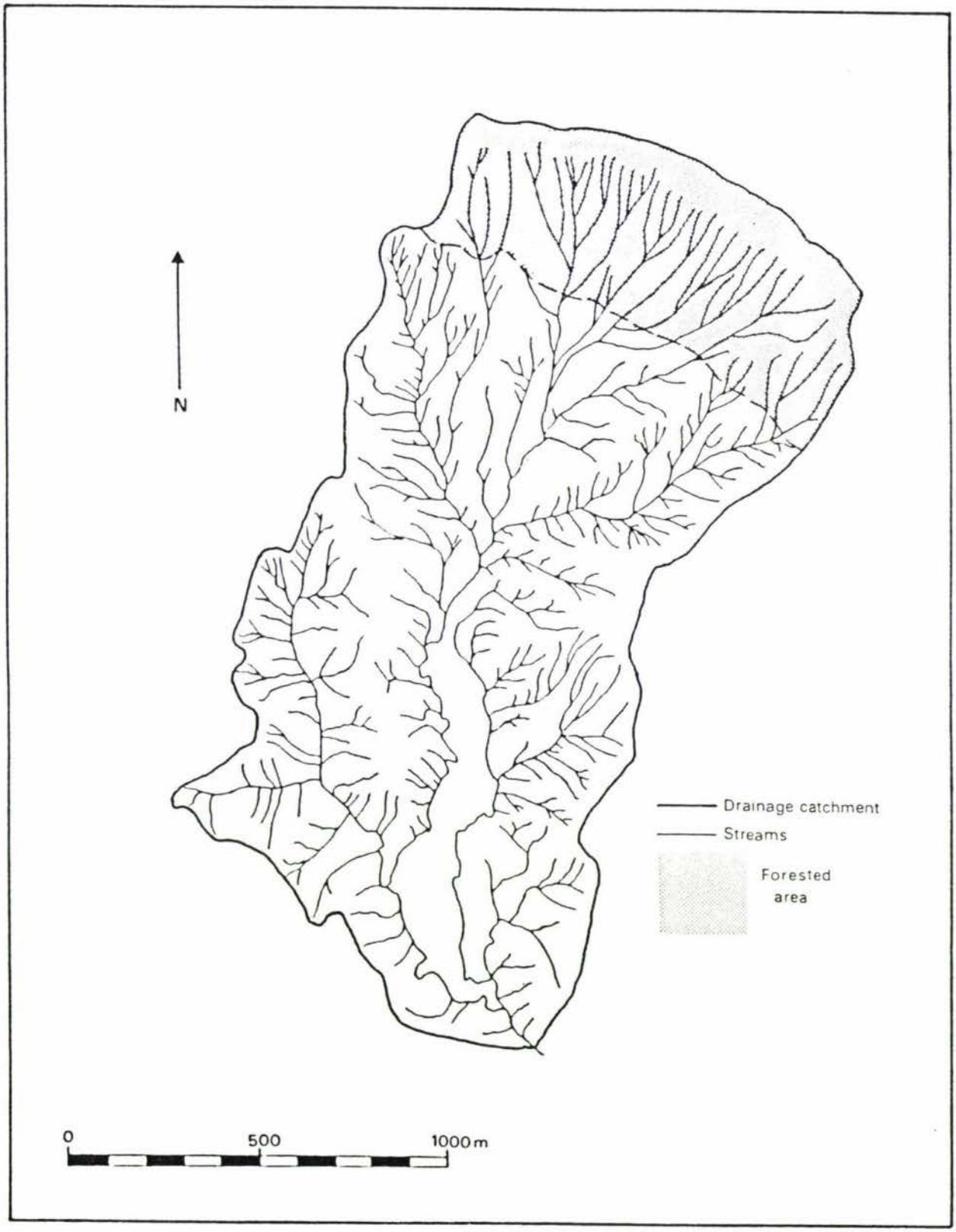

Figure 5.1 Mudstone drainage basin on the eastern scarp slope of the Puketoi Range.

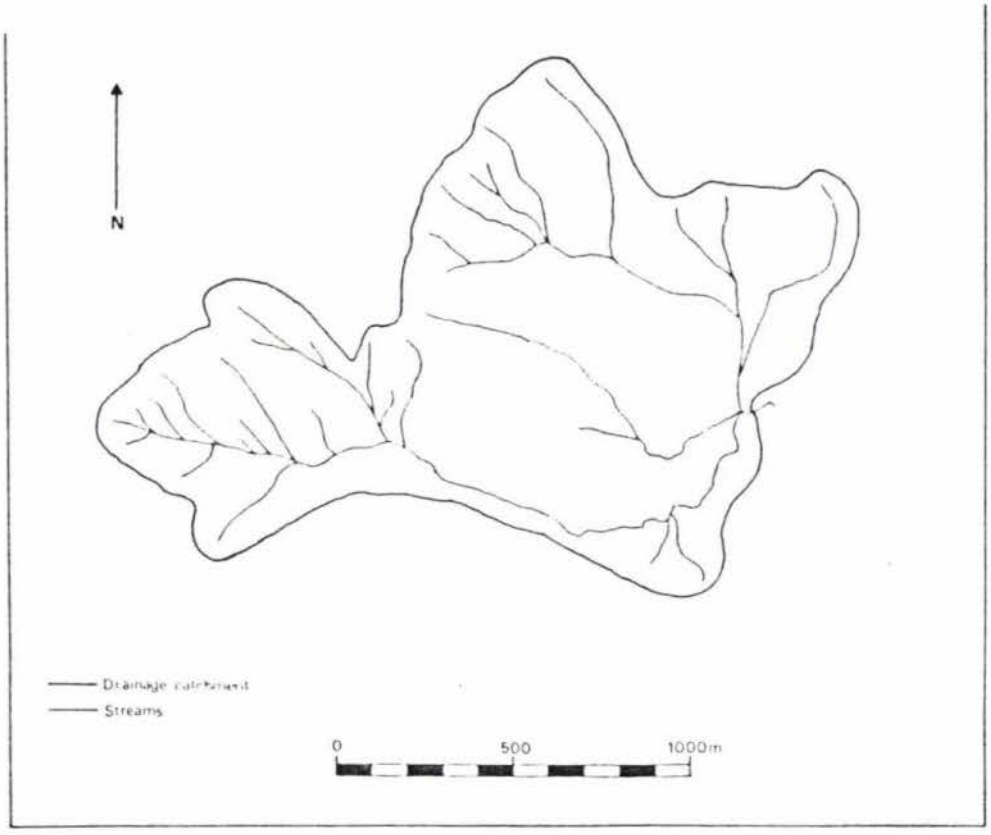

Figure 5.2 Greywacke drainage basin on the eastern flanks of the Waewaepa Range.

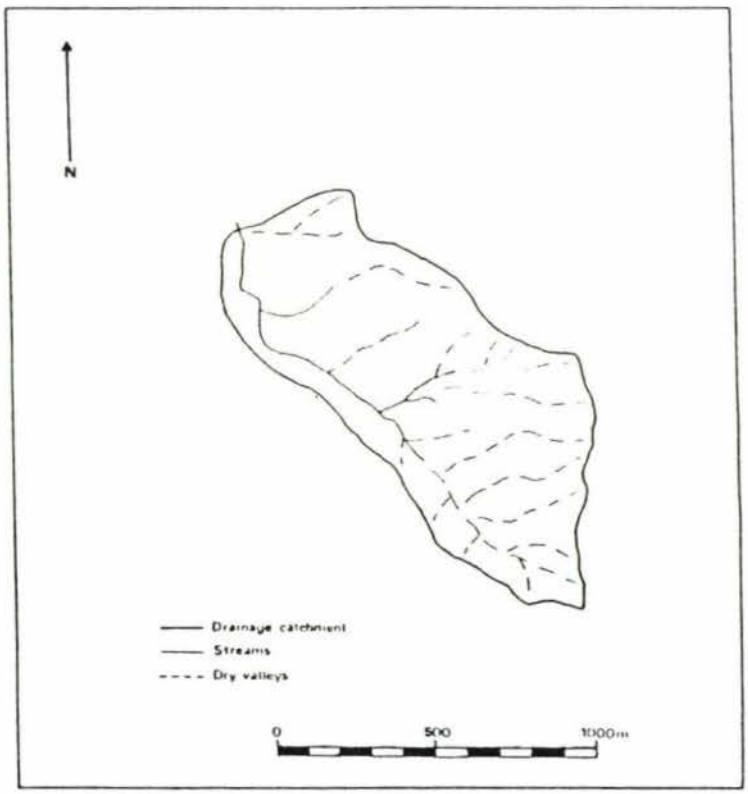

Figure 5.3 Limestone drainage basin to the north of Coonoor, Puketoi Range.

noticable on figure 5.1, as the density of the drainage decreases in the forested section. Other factors such as the change in the lithology in this basin may also have been influentual in the decrease in streamlet density (see conclusion).

5.2.2 Results

Considerable variation was found in the drainage basin density of the three basins examined. This is summarised in Table 5.1. The basin developed on mudstone had the highest drainage density (16.92 km/km^2). The textural ratio classification is fine for this basin, according to Smith (1950) and Strahler (1957). The other two basins, in contrast to the mudstone basin, were similar in density (6.12 km/km^2 for greywacke and 7.94 km/km^2 for limestone (stream and dry valley combined)). These two basins are classified as having a medium texture. If only surface streams are considered in the calculation of drainage density on limestone, the density falls to 2.09 km/km^2. This would classify the basin as having a coarse texture.

Table 5.1 Drainage density figuresfor three basins in the Puketoi Range.

	DRAINAGE BASIN TYPE		
	Mudstone	Greywacke	Limestone
Basin area (km^2)	2.45	1.73	0.79
Stream length (km)	41.46	10.58	1.65 (streams only) 6.27 (stream + dry valleys)
Drainage density (km/km^2)	16.92	6.12	2.09 (streams only) 7.94 (stream + dry valleys)

5.2.3 Conclusion

This examination of drainage density has shown that there is variability in drainage basins developed on mudstone, limestone and greywacke. This variation in density is probably related to the differing lithologies of each basin, and the control this has on rates and types of denudational processes. Other influences such as topography, pedology and vegetation will effect the drainage basins but in this investigation the lithology of the bedrock is assumed to be of greater importance than the other three variables.

The higher drainage density within the mudstone basin reflects the softer nature of this material and the ease with which it is eroded when compared with the other two basins. The gradient of this basin is steep, related to its position on the scarp slope of the Puketoi Range. This will allow more rapid rates of transport of material from the basin. Material removed from the basin will be sand sized and smaller. Much of this material is deposited at the base of the scarp when the gradient of the stream becomes gentle.

Greywacke is much harder than the other two lithologies investigated. This makes it much harder to erode, except where it is closely jointed or shattered by faulting. This is reflected in the density of the drainage basin, that is, the basin has a much coarser texture than the mudstone drainage basin. The shattered nature and close jointing of much of the greywacke contributes to slipping and other mass movements occuring within the basin.

Denudation within the limestone basin is primarily controlled by solution of chemically aggressive water. Very little mass movement occurs on the slopes of the valleys within the drainage basin, the land here being more stable than the other two basins examined. This results from the soluble nature of limestone, reducing subsurface saturation because of the primary and secondary permeability of the limestone, which contributes to reducing mass movement. The surface drainage density reflects the solubility of the limestone, with a surface stream drainage density of 2.09 km/km^2.

When comparing the drainage density of a karst drainage basin with that

of basins formed on other rock types it must be recognised that the true density of the underground stream network on karst cannot be assessed, and may in fact be quite high. The use of streams and dry valleys combined probably gives a better measure of the drainage density than when streams alone are used. Gregory (1966), in his examination of drainage density on limestone in southeast Devon, found the density for streams to be 1.72 km/km^2 and density for streams and dry valleys to equal 2.43 km/km^2. His results were not as extreme as those found for the Puketoi Range, but they do illustrate the contrasting drainage densities obtained by the two different methods.

CHAPTER SIX
CAVE SEDIMENT

6.1 Introduction

Some caves offer an unique opportunity in the study of landscape evolution as they may function as sediment traps, preserving a continuous record of sedimentation which is usually undisturbed. This overcomes the difficulty with the analysis of surface deposits, which have been laid down in a dynamic geological environment, where over long periods of time undisturbed sediment records are unlikely (Harmon 1980). The examination of New Zealand cave sediment is still in its infancy, and as Williams has noted "...their fossil record undoubtedly hold[s] the key to much of the Upper Quaternary natural history of many regions of the country..." (Williams 1982a, p.125). In this chapter sediment from caves in the Puketoi Range is examined.

The analysis of cave sediment began well over 100 years ago, with much of the early work directed towards cave entrance facies analysis, because of the archaeological importance of these deposits (for example, Brain 1958). There was also early work on interior sediment, for example, Pengelly (1864) examined false floors of flowstone and their relationship to clastic fill stratigraphy. This early work could only produce relative chronologies of events occurring within and around the cave. It was not until the later development of carbon-14 dating in the 1950's, and uranium-series dating techniques in the late 1960's and early 1970's that any means of absolute dating of ancient deposits was available (Cherdyntsev et al. 1965; Fornaca-Rinaldi 1968, cited in Harmson et al. 1975; Ford et al. 1972).

With the development of uranium-series dating techniques, and the more recent development of palaeomagnetic dating methods (Latham et al. 1979; Schmidt 1982; Schmidt et al. 1984), the absolute chronological dating of sediment can now be extended back well beyond one million years.

Cave sediment classification has developed with no generally accepted criteria, with various authors grouping cave sediment in accordance with their personal interests of study (Wolfe 1972a). For example, they have been based on the source and position of the material, (Kukla and Lozek 1958, cited in Wolfe 1972a), the texture of the sediment (Link 1966), the

nature of the deposit (White 1964; Frank 1965, cited in Wolfe 1972a), and the processes operating on the sediment (Wolfe 1972a).

In the broadest sense, all material found in caves, other than the host rock in situ, can be considered to be "cave sediment" (Wolfe 1972a). Bögli (1980, p. 165) has developed his definition along similar lines defining cave sediment as: "...embracing all clastic, organic and chemical deposits occurring in subterranean cavities and cave entrances...". This definition has been used by Bull (1983), and Schroeder and Ford (1983). Bögli's definition will be used here, combined with Kukla and Lozek's (1958) classification of sediment on the basis of its original source (autochthonous: derived from within the cave, and allochthonous: derived from outside the cave) and their position within the cave, that is, entrance facies and interior facies.

A better understanding of sedimentation and sedimentary histories within caves, has led to the publication of many recent papers about cave and landform evolution, and palaeoclimatic models. Many of these are based on information gained from the dating of speleothems (Harmon et al. 1975; Atkinson et al. 1978; Ford et al. 1981; Latham et al. 1982; Gascoyne et al. 1983) while others have utilized clastic and chemical sediment. For example, Bull (1978) used electron microscope analysis of quartz grain sediment from Agen Allweld Cave, South Wales, to develop a picture of past events, both within the cave and on the surface. Clastic sediment within Castleguard Cave, Canada, was studied by Schroeder and Ford (1983), who identified up to nine distinct episodes of sedimentation within the cave. Bull (1983) has summarised recent work on the use of chemical sediment, as an aid to the reconstruction of palaeoenvironments, and geomorphological development of caves and landforms.

Within New Zealand there are very few examples of the use of cave sediment as an indicator of past geomorphological events. Barrett (1963) examined sediment in Kairimu Cave, southwest Auckland, which he used in determining the development and age of the last three stages of the cave's development. Hendy and Wilson (1968) used oxygen isotope analysis, combined with carbon-14 dating, of speleothems from the Waitomo district, to produce a palaeoclimatic graph of the last 35 000 years. Williams (1982b) combined thorium/uranium and carbon-14 age-data from speleothems to investigate the relationships between cave levels, emerged

coastal terraces and uplift rates in the northwest of the South Island. More recently, Lyons (1983, 1984) examined the palaeomagnetism of cave sediment, both clastic and chemical, to determine the ages of caves and geomorphological development of land surfaces.

This chapter is divided into five sections: (1) a description of the two caves in which detailed study of cave sediment was carried out; (2) chemical deposits; (3) clastic deposits; (4) organic deposits; and (5) an examination of sediment deposition within Ramsay's Neck Cave.

6.1.1 Description of Caves Investigated in the Puketoi Range

In the following chapter two caves will be investigated in detail. The first, Ramsay's Neck Cave, contains clastic sediment probably deposited during the last stadial of the Otira Glaciation when a periglacial environment prevailed. Information from the examination of these clastic deposits, the dating of speleothems from the cave, and the geology and drainage of the area, allow the likely sequence of events which have occurred within the cave, to be determined (see section 6.5). The second cave, PT17 Cave, is situated at the boundary between the greywacke of the Waewaepa Range, and Kumeroa Formation limestone flanking the range. Present sedimentary patterns in the cave are discussed below.

6.1.1.1 Ramsay's Neck Cave

Ramsay's Neck Cave is situated at the southern end of the Puketoi Range (Grid Ref. T25/589638), and has developed in Te Onepu Limestone. This limestone has formed a synclinal basin (The Pori Syncline), and is infilled with younger Nukumaruan siltstones and sandstones. Ramsay's Neck Cave developed as a drainage path leading out of this syncline. Because of the solubility of the limestone, this drainage path has been underground, and not via surface drainage. Ramsay's Neck Cave, and one other cave further to the south, provide the only paths out of the synclinal basin for streams within it. Ramsay's Neck Cave is the largest known cave in the Puketoi Range, with a surveyed length of 744 m.

Ramsay's Neck Cave has two stream passages (A and B on Fig. 6.1) which join to form one main stream passage. The main stream flows through the

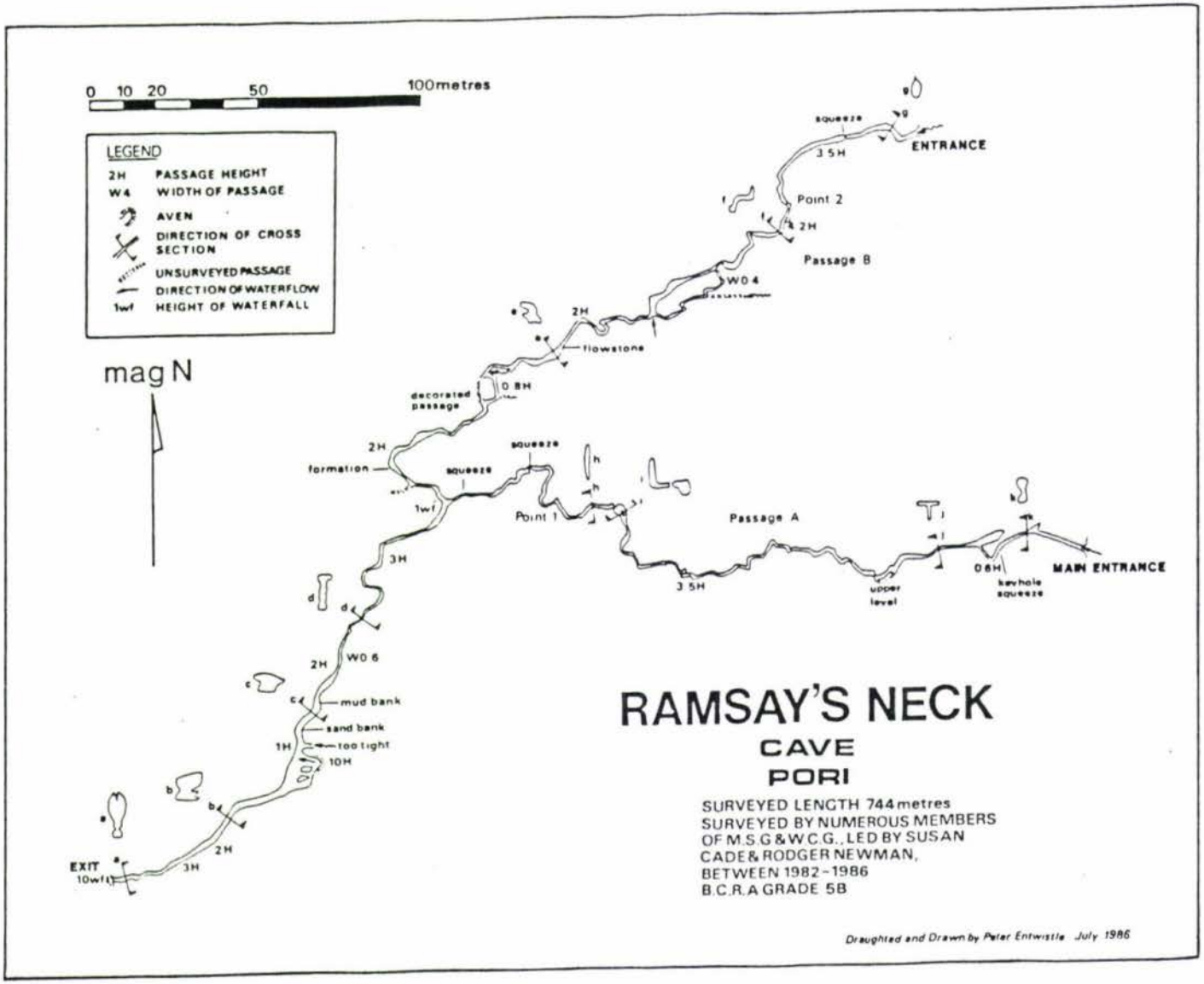

Figure 6.1 Ramsay's Neck Cave.

western limb of the syncline, and reappears at the surface as a 10 m waterfall.

Along much of passage A, Raukawa Mudstone (see cross-section C - C', Geological Map of the Puketoi Range - back pocket; and Fig. 6.2) is exposed on the floor. Contact with this will result in rapid entrenchment of the passage, continuing the present trend of narrow vadose passage development. This passage possibly was phreatic in origin, with remnants of a phreatic tube evident in parts of the passage.

Passage B, in places, is keyhole in shape. This is characteristic of two distinctive phases of development. The first phase was phreatic, and resulted in a circular passage approximately 3 m in diameter. In the second phase, a vadose notch was eroded into the floor of this passage. Ancient clastic sediment is found along the bottom of this circular phreatic tube (Photo 6.1), with contemporary sediment in the active stream bed in the bottom of the vadose notch.

6.1.1.2 PT17 Cave

PT17 Cave (Fig. 6.3) is situated on Makairo Road, approximately 2 km from the Coonoor Junction (Grid Ref. U24/725814). The cave has developed in Kumeroa Formation limestone, where it flanks the greywacke of the Waewaepa Range. Streams flowing down from the range carry chemically aggressive water which solutionally erodes the limestone, resulting in the cave's development.

Passage development has strongly favoured jointing in the limestone, resulting in a network of passages, many of which have been abandoned in the development of the cave. The abandoned passages reflect the changing position of surface streams and/or their ability to supply water to the cave.

6.2 Chemical Deposits

The study of chemical sedimentation products in caves can be useful in the reconstruction of the geomorphological history of both cave and surface landforms. Certain cave minerals, and the radiometric and palaeomagnetic dating of chemical cave sediment, are useful in the

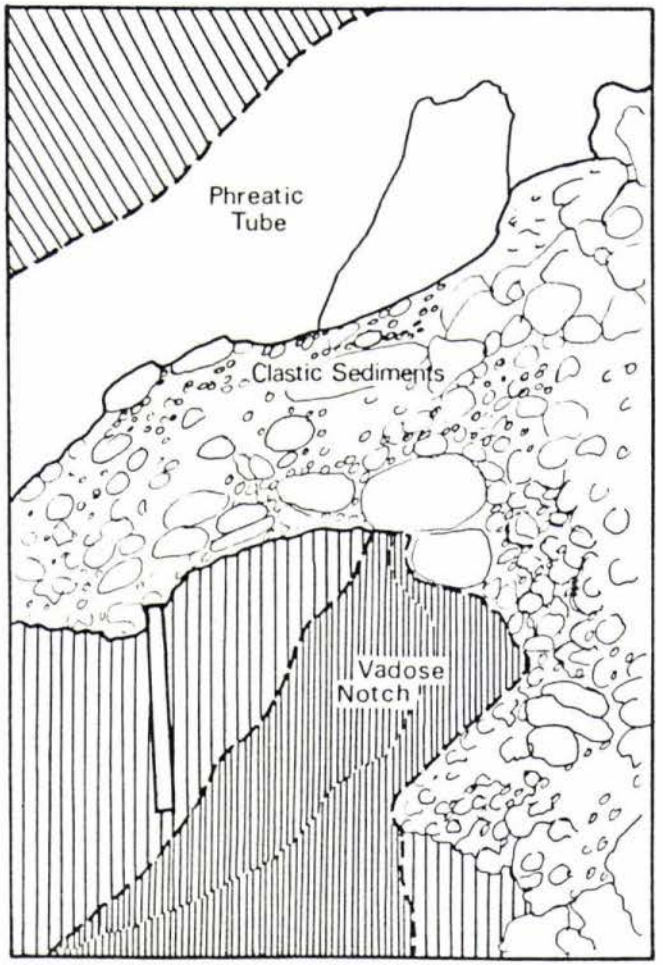

Photograph 6.1 Phreatic tube and vadose notch within Ramsay's Neck Cave. Ancient sediment is found along the botton of the phreatic tube.

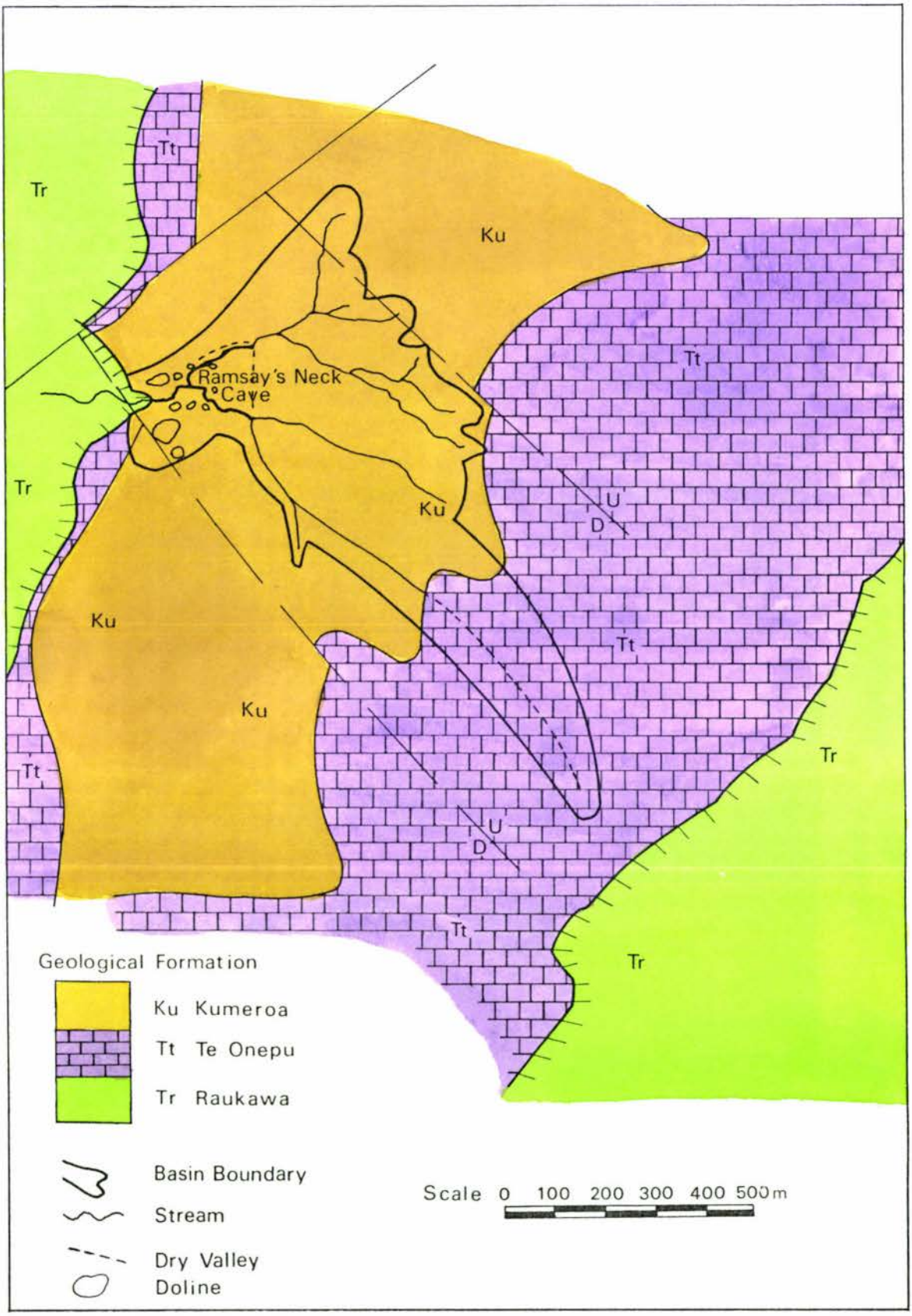

Figure 6.2 Geology and drainage of Ramsay's Neck Cave and surrounding area.

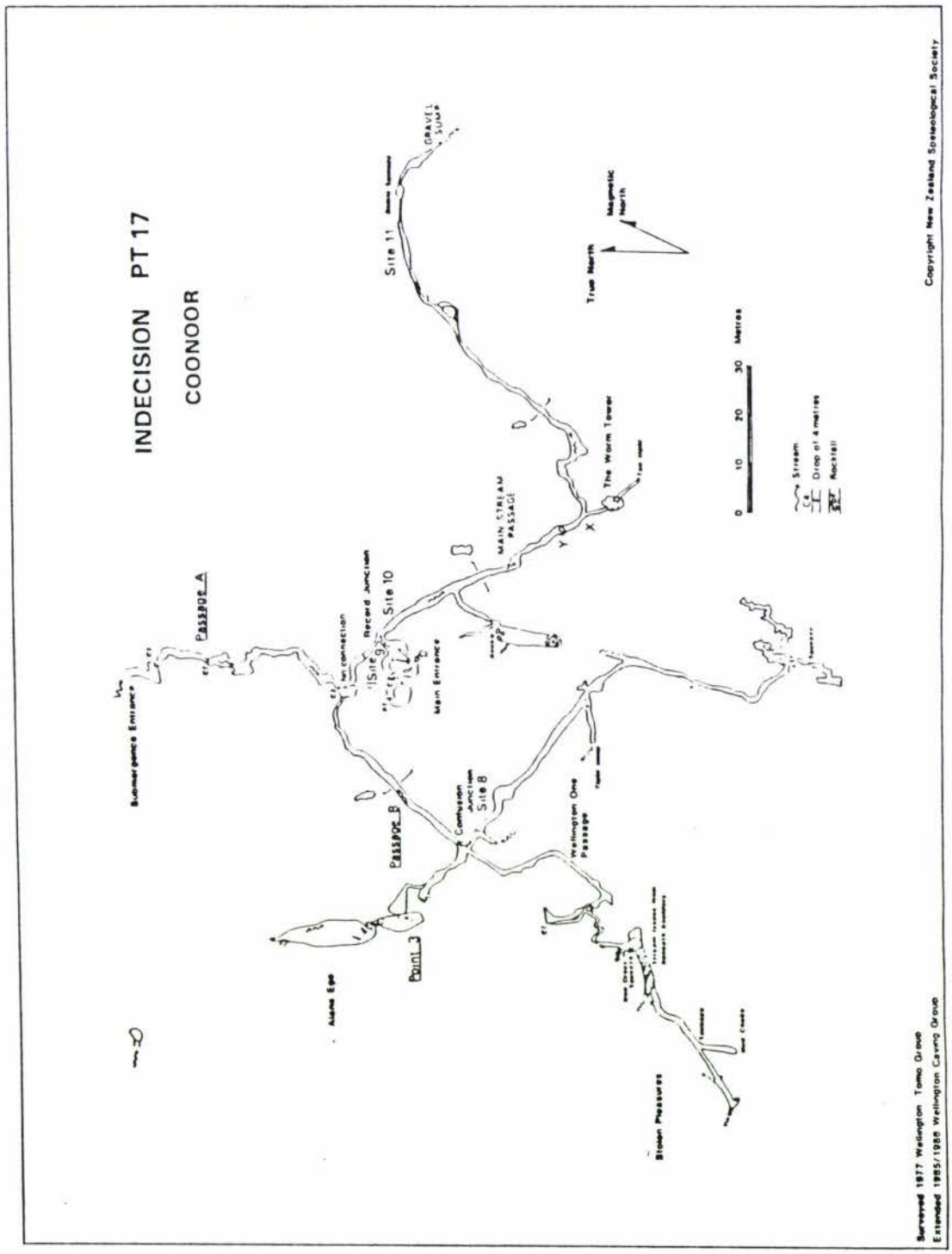

Figrue 6.3 PT17 Cave.

understanding of cave and landform genesis (Bull 1983). White (1976) lists appromimately 80 cave minerals but considers "...only about 20 of these are found in the 'normal' cave environment. The rest are mainly the result of very special conditions of mineralization..." (White 1976, p. 270). Bögli (1980) extended the list to over 100, with additional minerals such as marcasite (Peck 1979) and applelite (Ash 1975) recently being added. Most of these cave minerals only occur as traces within clastic or chemically sedimented deposits, or represent polymorphs which are metastable, or theoretically unstable, in the cave environment. Others are the result of cavity invasion by ore-forming solutions and occur only in isolated situations (Bull 1983).

Only two types of chemical deposits have been observed within caves in the Puketoi Range. The first and most common are calcite deposits, with the chemical composition $CaCO_3$, which form stalactites, stalagmites, and flowstones. These are found in all the known caves in the area. The second type, known as moonmilk or rock milk, has been noted in three caves in the Puketoi Range: Ramsay's Neck (Grid Ref. T25/589638), Gillespies Folly (Grid Ref. U24/725816) and Soggy Gummy Part 1 (Grid Ref. U24/799872).

Moonmilk found within caves is in a variety of forms. It can occur as either a soft crumbly white powder or chalky material, as a white paste, or as a thick jelly-like substance.

Formation has been attributed to the effects of micro-organisms, and impurities of magnesite, dolomite, and other minerals containing magnesium and calcite (Sweeting 1972). The majority of moonmilk samples analysed in New Zealand have been pure calcite, the few exceptions to this have contained aragonite. No micro-organisms have been found in any of the samples (Cody pers. comm.). The sample from Soggy Gummy Cave Part 1, submitted by the author to Dr A.Cody for analysis, was pure calcite.

The formation of moonmilk is believed by Cody (pers. comm.) to be controlled by environmental factors such as rapid changes in humidity and possibly temperature. These factors may interfere with the nucleation of the calcite, restricting the growth of the calcite to a micro-crystalline form.

6.2.1 Speleothem Development

The term "speleothem" is applied to mineral deposits in caves which are precipitated by water, which has seeped through the overlying limestone. Classification is based on the method of deposition and morphology, with four basic forms: stalactites (Gr. stalaktos = dripping, growing downwards from the roof), stalagmites (growing upwards from the floor), flowstones (growing over the floor, walls and roof), and rimstones (formed in water,creating pools), as well as a number of less common varieties.

Speleothem development is governed by a variety of geologic, hydrologic, geochemical and climatic factors, which interact to allow water containing calcium carbonate, and carbonate species (or other cave minerals), to seep through the limestone and into the cave. The degassing of carbon dioxide, from the percolating water, results in precipitation and speleothem growth. The deposition mechanism depends on a supply of water, with a higher partial pressure of carbon dioxide (pCO_2) in comparison with the cave atmosphere. The water-CO_2-carbonate liquid/solid interface controls sedimentation (Bull 1983).

The growth rate of speleothems (and hence their age) is not uniform, even for speleothems of the same mineral composition (Bull 1983). Bögli (1980) states: "There are no rules which reveal a relationship between age and length (of a speleothem). There are periods of rapid growth and others of slow growth, even periods of inactivity" (Bögli 1980, p. 191). Bögli cites two examples to illustrate this: a stalactite, in a cave in the city of Buxton (south Pennines, Great Britain) took 100 years to grow 10 cm, while in Grotte des Demoiselles (southern France) a stalactite grew 10 cm in 20 years.

6.2.2 Uranium-Series Dating of Speleothems

Uranium-series dating has developed out of the need for an absolute dating technique, suitable for materials deposited within the Pleistocene and Holocene. The carbon-14 method of dating is considered reliable only within the past 40 000 to 50 000 years. The potassium/argon method is of limited application because suitable deposits are scarce (Harmon et al. 1975), while the recent development of magnetic reversal dating has been

applied mainly to older deposits (Schmidt 1982). The range of uranium-series disequilibrium methods cover portions of most of the Holocene and Pleistocene, but only the thorium/uranium ($^{230}TH/^{234}U$) method has been developed to the point of reliability (Harmon et al. 1975).

Studies by Thurber et al. (1965) concluded that four conditions need to be met before carbonate material can be reliably dated by the $^{230}TH/^{234}U$ method. These are: (1) sufficient uranium concentration must be present in the sample to allow accurate determination of activity ratios in a relatively short counting time; (2) the initial isotopic state of the system must be known; (3) no loss or gain of uranium or thorium can have occurred since the time of deposition; and (4) disequilibrium ratios of the radioisotopes must exhibit a progression towards secular equilibrium with time.

Experimental tests can be performed to determine whether or not specific samples meet the above requirements. Pure calcite speleothems, with well defined and preserved internal stratigraphy, which show no signs of diagenetic alterations and post-depositional erosion, are described by Thompson et al. (1974) as generally meeting these conditions.

For a summary of the theory behind, and the application of, the thorium/uranium dating method see Appendix Seven. The analytical methods used to accurately determine the $^{230}TH/^{234}U$ activity ratio are outlined in Harmon et al. (1975), and Gascoyne et al. (1978), and will not be discussed here.

6.2.3 Speleothems Removed for Dating

Three speleothem samples were removed from caves in the Puketoi Range for thorium/uranium dating, in an attempt to gain more information on cave development and history. This dating method covers a range of 1000 to 350 000 years (Harmon et al. 1975). Two samples were removed from Ramsay's Neck Cave (Grid Ref. T25/589638), and a third from PT17 Cave (Grid Ref. U24/725816).

6.2.3.1 Description of Samples

All samples removed for dating had been broken from their point of attachment to the cave passage. This was the result of either natural causes, such as earthquakes or rockfall, or by accidental human interference.

(1) Sample from Passage A, Ramsay's Neck Cave:

This was a small column 50 cm long, with a maximum diameter of 12 cm. This had originally developed as a straw (sinter tube), which had thickened due to the deposition of calcite around the straw. Thickening had occurred mainly in the middle section with thinning towards both ends (Photo 6.2). The column was also curved along the axis of the cut. The column had been dislodged from its original position and was lying across a ledge, below the point of detachment, and was partially recemented onto this ledge. Point 1 on Figure 6.1 shows the position in the cave from which the column was removed.

(2) Sample from Passage B, Ramsay's Neck Cave:

This was a medium sized stalactite approximately 1.0 m long (the end section had been broken off). In cross-section (Photo 6.3), a cluster of six straws can be seen. These formed the original growth points of the stalactite, and had subsequently thickened and merged together. Growth around some of the straws appears to have been asymmetrical, possibly resulting from a draft in the passage causing uneven deposition of calcite. The original straws had been infilled with calcite crystals. Point 2 on Figure 6.1 shows the position in the cave from which the stalactite was removed.

Thickening of the stalactite had occurred below the point of attachment, as in the column described above (see Fig. 6.4). This resulted in the weight of the stalactite being supported by a relatively small area. The stalactite fell from the roof when accidently knocked by a caver. The point of attachment was approximately 5 m downstream from the site where clastic sediment was removed for analysis (see below). No part of the stalactite showed signs of post-depositional erosion, even though it occurred at the level of the gravel fill, therefore its growth is assumed to have occurred after the deposition of the limestone gravels within the passage (see below).

Photograph 6.2 Longitudinal section of speleothem column removed from passage A, Ramsay's Neck Cave. A core was cut from the central section of the speleothem for dating. Scale: 300 mm.

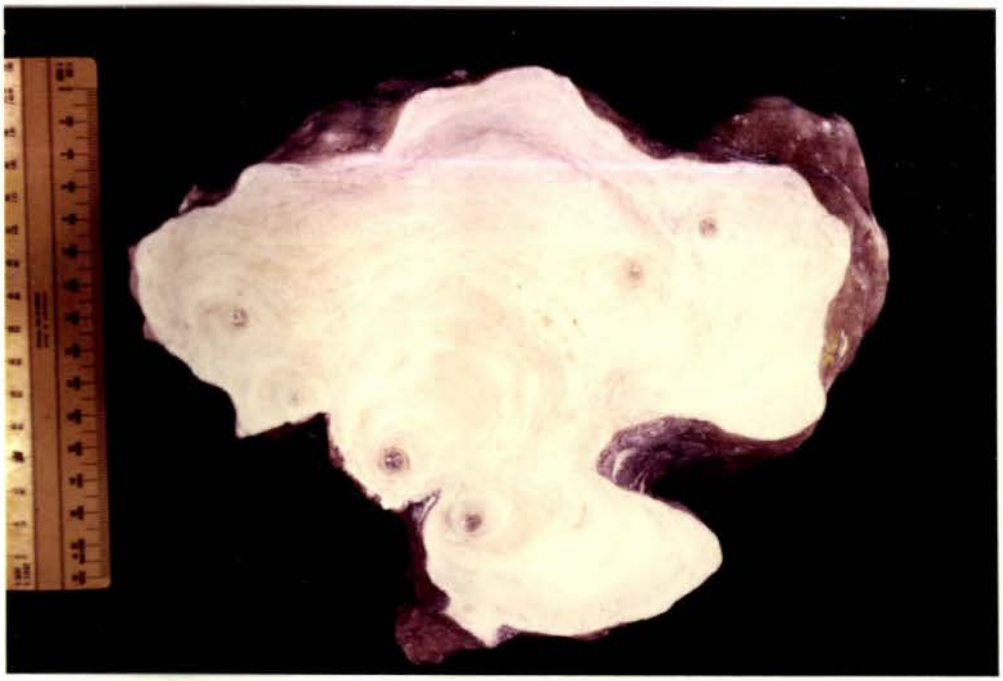

Photograph 6.3 Cross-section of speleothem removed from passage B, Ramsay's Neck Cave. A core was cut from the most central straw for dating. Note growth rings around each straw. Scale: 300 mm.

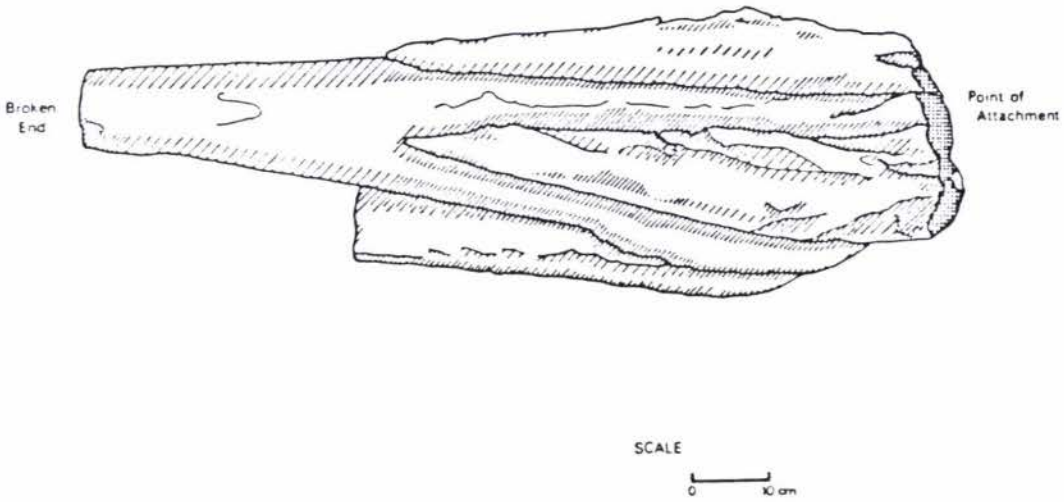

Figure 6.4 Sketch of speleothem removed from Ramsay's Neck Cave for dating.

(3) Sample from PT17 Cave:

This cave contains very little speleothem material, although there are many abandoned stream passages which suggest that more than a brief period of cave development must have occurred. The sample removed was from Alans Ego chamber. This chamber is the highest known point in the cave, other than the present active stream passage (Passage A, Fig. 6.4), and may have been one of the original streamways in the cave.

The sample removed for dating was a piece of flowstone (Photo 6.4) which had been dislodged from its original position and was jammed in the rockfall leading into the chamber. (See Figure 6.3 for the position (Point 3) of the flowstone in the cave). Its original position was probably on the wall of this chamber, where a sheet of flowstone has formed. The flowstone shows two distinct phases of deposition (seen in Photo 6.4). The first formed a thin sheet attached to the wall. This was then covered with a film of mud. At some later stage, a second thicker layer of flowstone was deposited over the layer of mud. The portion dated was from the inner, thinner layer of flowstone.

Photograph 6.4 Speleothem flowstone removed from Alans Ego Chamber, PT17 Cave. A section was cut from the inner most layer (closest to scale) for dating. Scale: 150 mm.

6.2.4 Dates From the Speleothem Samples Removed

At the time of completion of this thesis, the dates from the samples sent for dating (in April 1986) had not been received. The information on the speleothem samples has been included so that a record of the samples is available. This will facilitate any later interpretation of the dates, when they become available.

6.3 Clastic Deposits

Clastic cave sediment has drawn much attention since late last century. The emphasis continues to be on the gaining of information on the evolution of caves and the surrounding land surface, and in the development of palaeoclimatic models. In the following sections ancient sediment from Ramsay's Neck Cave and modern sediment from PT17 Cave are discussed.

6.3.1 Description of Clastic Sediment From Ramsay's Neck Cave

In Ramsay's Neck Cave, ancient clastic cave-stream sediment has been deposited along a section of passage B, from approximately the oxbow passage upstream to the squeeze (see Fig. 6.1). The sedimentary sequence for this section of cave is given in Table 6.1 and Figure 6.5.

Table 6.1 Sedimentary sequence in passage B, Ramsay's Neck Cave, with related cave environmental conditions.

Sedimentary unit	Cave environment
stalactite/flowstone	sub-aerial
fine-grained sediment	ponded, vadose
ancient cave stream sediment	fluvial, vadose

The ancient cave stream sediment is overlain at a sharp boundary by laminated fine-grained sediment. The sequence is capped in places by

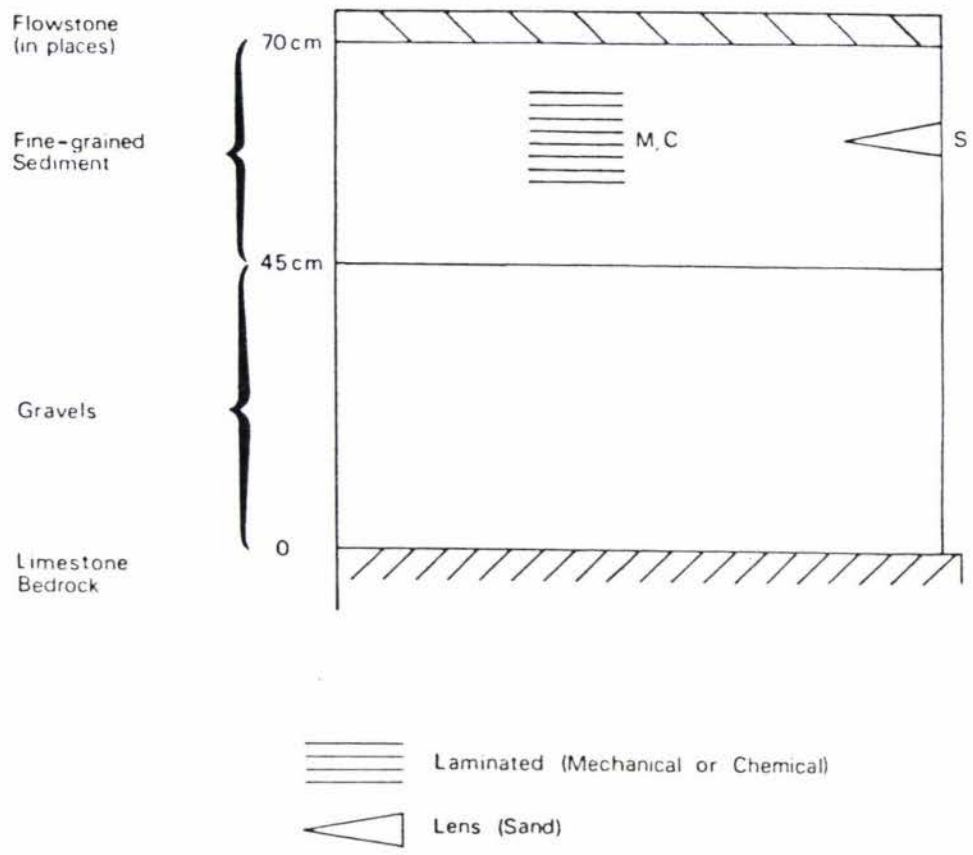

Figure 6.5 Generalized sedimentary section from passage B, Ramsay's Neck Cave.

flowstone and stalactites (Photo 6.5). This deposit, with the exception of the in situ speleothem deposition, is surface derived material, deposited in the passage in response to changing hydrological conditions in the cave. Each unit therefore has a different mechanism of deposition, but not necessarily deposited in a single event. The ancient cave stream sediment is indicative of higher energy deposition than the overlying fine-grained sediment, which was deposited in a low energy environment.

Particle size analysis was carried out on samples of ancient sediment and contemporary cave stream sediment within Ramsay's Neck Cave, and surface stream sediment upstream from the cave (Figure 6.6). As Collcutt (1979) noted, the accuracy of particle size analysis is highly sensitive to sample size. On theoretical grounds he recommended that a 2 kg sample be taken for particles of up to -4.5 phi (20 mm) in diameter, and that 1 kg be added for every increase of 1 mm. An 82 kg sample would therefore be required for -6.5 phi (100 mm) particles. Collcutt considers that even

Photograph 6.5 Sedimentary sequence examined within Ramsay's Neck Cave.

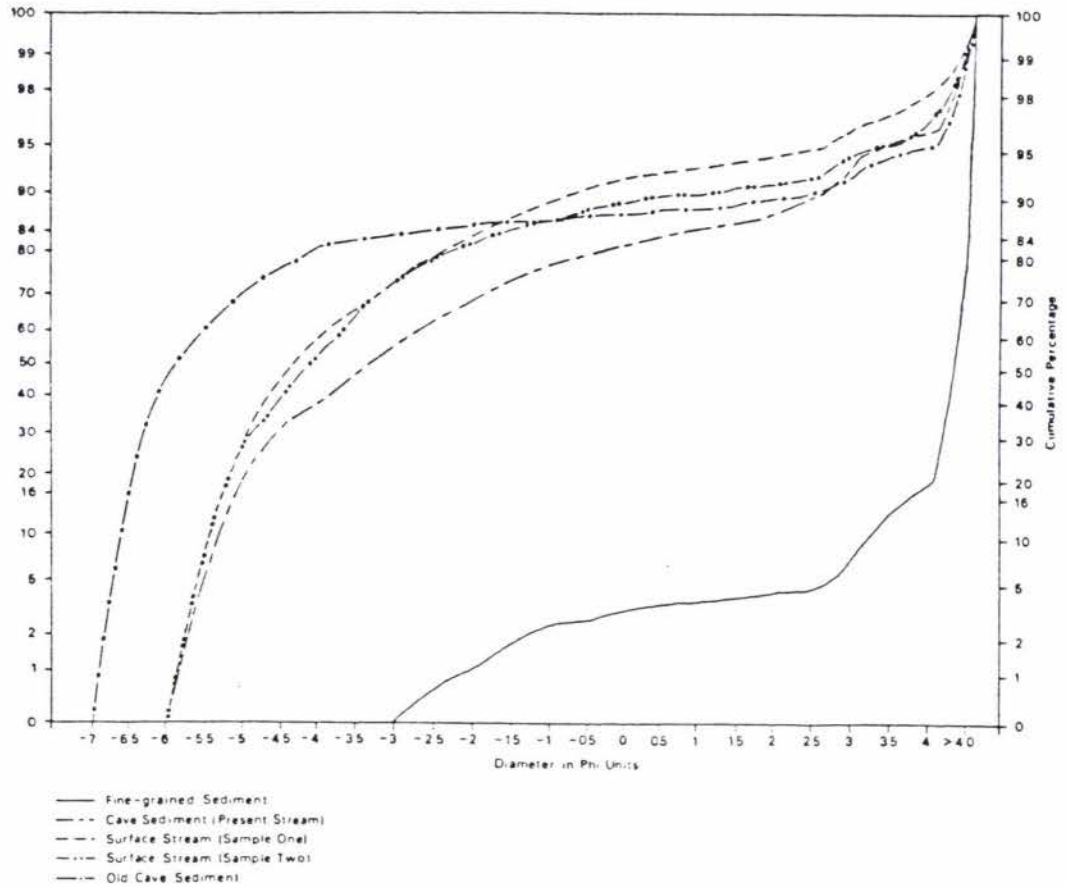

Figure 6.6 Graph of particle size analysis for cave and surface sediment associated with Ramsay's Neck Cave.

this amount of sample material would probably be an underestimate of the true weight needed for accuracy.

Due to the extreme difficulty in the removal of material from Ramsay's Neck Cave, no attempt was made to remove the weight of material recommended by Collcutt (1979). The maximum weight of the samples analysed was 5 kg and they contained material up to -6.5 phi. This is well below the 82 kg recommended by Collcutt (1979), therefore the data given in Appendix Eight and Figure 6.6 cannot be considered an accurate measure of particle size of the sediment. Use of the Folk-Ward statistics (a widely used statistical method of particle size analysis) does, however, allow an approximate comparison of the differences in mean sizes of material removed from each site (Table 6.2). Refer to Appendix Eight for Folk-Ward statistics methodology. No Folk-Ward analysis was carried out on the sample of fine-grained sediment (see below).

The sediment samples removed from the cave are considered by the author to be representative of the population as a whole. No stratification was

found in the ancient cave stream sediment along the length of the passage, neither was there any apparent variation in sediment size in the contemporary cave and surface stream sediment.

Table 6.2 Folk-Ward statistics of mean and standard deviation of cave and surface stream sediments.

Sample	Phi Mean	Phi Standard Deviation (Inclusive graphic)
Surface Stream Sediment (sample 1)	-3.90	2.05
Surface Stream Sediment (sample 2)	-3.78	2.25
Cave Stream Sediment	-2.70	2.74
Ancient Cave Stream Sediment	-5.16	2.48
Fine-grained Sediment	----- NOT ASSESSED	----

6.3.1.1 Ancient Cave Stream Sediment

The ancient cave stream sediment was deposited as a basal gravel unit within the passage. This is comprised of clast-supported limestone gravels, with a small sand, silt and clay component (see Appendix Eight and Photo 6.5). The thickness of the gravels varies from approximately 45 cm to 1 m. This variation in depth is the result of the uneven nature of the floor of the original phreatic tube, with greater thickness in the hollows and thinning on the highs. This resulted in an approximately flat gravel stream bed in the cave. The clasts range in size up to -6.5 phi, with a mean of -5.12 phi. They show no sign of *in situ* weathering.

The gravels were deposited under vadose conditions. Deposition is assumed to have occurred during the last stadial of the Otira Glaciation when spring or early summer meltwater from the winter snows flowed through the cave causing seasonal flooding. This resulted in the gradual increase in the thickness of the gravels, over a succession of years, until the passage became choked. Water velocity, at the time of deposition, can be approximated by a comparison of the maximum and mean sizes of clasts found in each sample analysed. From Figure 6.7, the

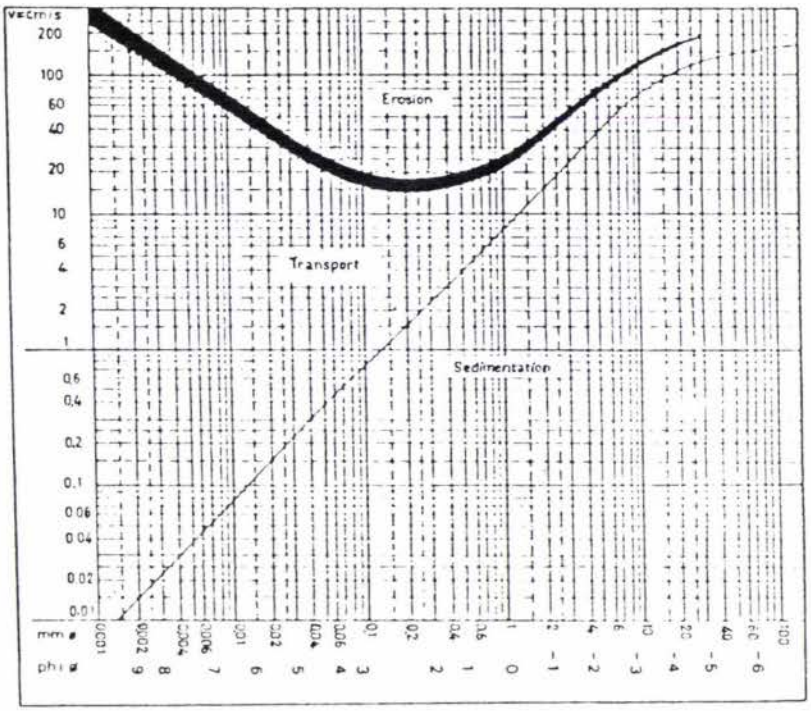

Figure 6.7 Relationship between velocities of erosion, transportation, and sedimentation according to Hjulström (1935). Mean values. (From Bögli 1980).

approximate velocity of waterflow at the moment of sedimentation of the gravel unit, can be determined. With the maximum clast size of the sample -6.5 phi, water velocities would have exceeded 150 cm per second to transport the material, with a mean velocity of 125 cm per second required (-5.12 phi).

6.3.1.2 Fine-Grained Sediment

A distinctive change occurred in the sedimentation pattern within the passage, from the ancient cave stream sediment described above, to the overlying fine-grained laminated sediment (Photo 6.5). This deposit is distinctly laminated, with lighter coloured bands of sand-sized material between darker red to black bands of silt and clay-sized material.

A sample was analysed for particle size, which was randomly selected. This contained a small autochthonous component (small pieces of calcite derived from the roof). This is not included in the size analysis data. The mean size of the sediment could not be calculated without further

analysis, but 79.5 percent of the sample was finer than 4.0 phi in size (silt and clay-sized). This fraction of the sediment, combined with the fine-sand fraction, means that 95.4 percent of the sample is 3.0 phi or smaller. Flow velocities at the moment of sedimentation were very slow moving, or ponded water, the velocity being at a maximum 0.1 cm per second (3.0 phi material) or slower. The stilling of the water within the cave is believed by the author to have resulted from the partial or complete blockage of the passage by the ancient cave stream sediment, resulting in the fine-grained sediment being laid down.

6.3.1.3 Analysis of Fine-grained Sediment

The following data (Table6.3) was provided by Dr. R. Stewart, Soil Science Department, Massey University, who analysed the fine-grained sediment supplied by the author.

Table 6.3 Analysis of fine-grained sediment from Ramsay's Neck Cave.

	Red Sample (Oxidised)	Black Sample (Reduced)
Water Content:		
Water as percent dry solid	229	247
Water as percent wet sample	69.9 to 70.0	71.0 to 71.2
Percentage loss, Organic Matter: (Peroxide Treatment)	2.2	1.2

From his analysis, Dr. Stewart described the red sample as having been oxidised, and the black sample as having been reduced, in situ. The losses from peroxide treatment approximate organic matter content, but the treatment also removes any manganese oxide present. The apparent higher percentage organic matter loss for the red sample, could be attributed to a loss of manganese oxide.

Dr. Stewart also carried out X-ray diffraction analysis of the sample. No detectable peaks were found on X.R.D. traces to indicate any clay mineral present. This suggests the sample is a non-crystalline material. Quartz does occur, probably as silt-sized material.

From the high water content and non-crystalline nature of the sample, Dr. Stewart concluded that the sample was predominantly allophane - a short range order aluminium oxide/silica colloid.

Allophane was first described by Stromeger in 1809, from material lining cavities in marl and caves in limestone, in southern Germany. The word allophane is derived from the Greek words "to appear", and "other", due to its change, with the loss of water on standing, from a glassy material to an earthy material. Allophane is generally found in volcanic ash soils in New Zealand and its presence in the cave has possibly resulted from a heavy volcanic ash shower falling over the drainage basin of the streams flowing into the cave. The ash deposit was then washed from the surface down into the cave, where it was deposited by slow moving or ponded water, stilled by the gravel blockage of the passage. Smart et al. (1985) identifed allophane in Clearwater Cave, Gunung Mulu National Park, Sarawak, East Malaysia. Here it formed a waxy-white layer, locally up to 1 m thick. This layer was used as a marker bed in the investigation of cave sedimentary patterns.

6.3.1.4 Contemporary Cave and Surface Stream Sediment

One sample of the contemporary cave stream sediment, and two samples from the surface stream flowing into Ramsay's Neck Cave, were also analysed to determine particle size. This would allow the comparison between ancient and contemporary hydrological processes occurring within the cave to be made (see Appendix Eight and Table 6.2). Due to the proximity of the road to this stream, greywacke gravel roading chips had found their way into the surface stream and into the cave. This and the possibility of other material dumped into the stream in the making of the road may have influenced the mean size of the samples analysed. No attempt was made to remove this material from the samples.

The maximum size of the contemporary cave and surface stream sediment samples was -5.0 phi, requiring a water velocity of approximately 112 cm per second to transport this sediment, with a mean velocity of 60 cm per

second(-2.70 to -3.90 phi) (Table 6.2). This is half the mean velocity that was required for the transportation of the ancient cave sediment (see Fig. 6.7). However, the small size of the sediment may reflect smaller material at the source rather than weaker currents.

6.3.1.5 Discussion of Sediment Size in Ramsay's Neck Cave

A marked secondary mode at 3 phi was found in all the samples examined, excluding the fine-grained sediment. This secondary mode accounted for 1.6 to 3.8 percent of the sediment in the samples examined (see Appendix Eight).

Neef (1984) in describing the beds of the Kumeroa Formation in the vicinity of Pori, found that the formation varied from a sandy siltstone to a fine to medium sandstone, with rarer thin, very fine-grained sandy horizons. The secondary mode of fine sand found in the sediment samples examined is probably derived from the sand within the Kumeroa Formation. This sand has possibly been eroded from the Kumeroa Formation beds and transported into the surface streams, and then into the cave.

Loess, windblown silt derived from glacial outwash and other alluvium (Bloom 1978), may also contribute to the secondary mode found in the samples. This would have been deposited in the soils in the area during the Otira Glaciation.

Flood events, occurring during the deposition of the ancient sediment, may have been of a greater magnitude than at present, based on the difference in size of material carried by the cave stream today, compared with what was carried in the past. There are two factors which could influence changes in the sediment size being transported by the cave stream, other than the magnitude of flood events. Firstly, variation in passage size and shape may be important in determining the water velocity as it moves down the passage. The influence of this factor is unknown, although there is no buildup of larger clasts at the entrance to the cave, which would be expected if water velocities diminished on entering the cave. Secondly, a change in the size of the material being transported may have occurred. In particular, maximum size of clasts appears to have been greater in the past. Nearly 50 percent of the ancient cave stream sediment is greater than -6.0 phi, while none of the contemporary cave sediment is. (The influx of roading material was all

smaller than -4.0 phi therefore this has not influenced the comparison between the ancient cave stream sediment and the contemporary sediment). This could have resulted from climatic change, with a periglacial climate during the last stadial of the Otira Glaciation favouring mechanical weathering, producing larger clasts than under the temperate climate of today.

6.3.2 Gravel Fluctuations in PT17 Cave

The position of PT17 Cave on the boundary between the limestone of the Puketoi Range and the greywacke of the Waewaepa Range has not only enabled the cave to be supplied with chemically aggressive water via the streams that flow from the Waewaepa Range but the same streams also supply greywacke gravels eroded from the range.This sediment has had a significant effect on the development of PT17 Cave. Past and present effects of gravel fluctuations will be discussed in the following section. The word gravel in this section, unless otherwise stated, refers to greywacke gravels derived from the Waewaepa Range.

6.3.2.1 Surface Evidence of Previous Gravel Levels within PT17 Cave

Surface features above PT17 Cave indicate that in the past the cave has been completely infilled with gravel. These features are: (1) a series of alluvial terraces have formed directly above the entrance to the cave and further upstream; and (2) a dry valley infilled with gravel continues downstream past the cave (Photo 6.6).

The highest of these terraces starts upstream of the cave and continues down past the cave in the dry valley. All lower terraces extend upstream from the cave entrance, indicating that flushing out of gravel from within the cave has occurred, causing the stream to downcut upstream of the cave, abandoning the valley downstream from the cave.

The present entrance to PT17 Cave is via a collapsed doline partially infilled with gravel. During the maximum period of gravel aggradation in the cave this doline was completely gravel-filled, with the stream flowing over the top. The gravel aggradation was caused either by localised blockage of the passages, for example, by rockfall, or by increased gravel supply resulting from changing climatic conditions.

Photograph 6.6 Abandoned stream bed and terraces downstream of PT17 Cave. The stream now enters the cave to the left of the photo.

The author believes the latter is the more likely explanation for gravel fluctuations in the past, with climatically induced gravel deposition at the foot of the Waewaepa Range infilling the cave.

6.3.2.2 Contemporary Gravel Fluctuations within PT17 Cave

Contemporary gravel level fluctuations have been restricted to the section of passage, from the junction of the two streams in PT17 Cave (Record Junction) down the main passage to the gravel sump (Fig. 6.3). Gravel fluctuations have been observed in PT17 Cave, by cavers who regularly visit the cave, since its discovery in the early 1970's, (R. Newman pers. comm.).

The author has observed rapid fluctuations in the gravel levels in PT17 Cave, in the 20 month period up to February 1987. At present, gravel enters the cave mostly via the main stream passage (marked A on Fig. 6.3), with a smaller amount derived from the side-stream (marked B on Fig. 6.3). Gravel levels in this side-stream passage, are presently not fluctuating rapidly, compared with gravel levels in the main stream passage. The presence of an old gravel bank within this side-stream passage, however, indicates that gravel levels in the past were higher, and that gravel has been moving down this passage. The reduced volume of gravel at present possibly indicates that the supply has diminished or ceased, presumably by localised blockage upstream of the stream's appearance in the cave.

In the 12 months up until July 1985, the gravel level in PT17 Cave appeared to be stable with possibly a gradual lowering of the stream bed. This was despite a number of heavy rainfalls during this time which would have caused flooding in the cave. For example, between 9.12.84 and 14.12.84, 142.2 mm of rain fell but this had little or no effect on the gravel levels in the cave. (All rainfall data was recorded by Stuart McIntyre, a farmer at Coonoor.)

Heavy rainfall between 20.06.85 and 21.06.85, and again on the 24.06.85 through to 28.06.85, resulted in a total of 310.0 mm of rain. Debris lines of wood in the cave passages indicate both storms caused severe flooding in the cave, with water backing up behind the gravel sump to a height of approximately 5 m. Associated with this flooding was the movement of a large quantity of gravel into the cave. This resulted in

the bed of the cave stream being elevated by approximately 2 m at 'Record Junction', and the increase in elevation decreasing downstream to 0.5 m at 'Bottle Neck Squeeze', leaving only a 10 cm gap remaining for water flow. Photograph 6.7, taken in March 1985, shows the stream passage at point X, marked on Figure 6.3. Photograph 6.8 was taken from the same position in late August 1985, after the deposition of the gravel.

The depth of gravel deposited varied along the passage, owing to localized changes in passage shape and blockages in the passage. A boulder, marked Y on Figure 6.3, is jammed between the passage walls. Before the rise in the gravel level, a clearance of approximately 1.4 m had developed between the bottom of the boulder and the stream bed, allowing a person easy passage beneath. The boulder is approximately 1.5 m in vertical length. The boulder was almost completely covered by gravel after the flooding, with approximately 25 cm remaining above the stream bed. This would give an increase in the gravel depth, around the boulder, of between 2.6 m to 2.7 m. These observations were made three weeks after the flood, by which time the gravel level appeared already to be lowering. This was indicated by gravel remaining in places along the passage wall approximately 5 cm higher than the stream bed. This could have resulted from either compaction of the gravel, or its transport down the passage by the receding flood waters.

When the cave was revisited, in late August 1985, the gravel level had receded 15 cm to 20 cm and this trend has continued.

Over the two week period from 26.06.86 to 09.07.86, 183 mm of rain fell causing the cave to flood again. This had a very different effect from the flood of July 1985. A thickness of approximately 50 cm of gravel was removed from the section of passage below 'Record Junction' and transported downstream, to raise the stream bed by 30 cm to 40 cm upstream of 'Bottle Neck Squeeze'.

This rise in the gravel level may have been caused by one of the following three factors: (1) the gravel sump past 'Bottle Neck Squeeze' may have been too constricted during the flood event, resulting in a build-up of gravel above this point; (2) the storage capacity of gravel past the gravel sump may have reached its limits, stopping any further gravel from moving down the passage; and (3) the gravel may be moving as

Photographs 6.7 and 6.8 Main stream passage PT17 Cave. Photo 6.7 was taken in March 1985 before flooding of the cave. Photograph 6.8 was taken in August 1985 from the same position after flooding and deposition of gravel within the cave. Line indicates same position on cave wall in both photos. (Photo 6.7: Jeff Archer)

a true pulse, similar to that described by Brougham and O'Connor (1982) for the Pohangina River. Gravel pulses have been observed in that river to respond to the size of floods occurring. Any one of these mechanisms could explain the observed gravel movements, and therefore more detailed investigation is required before fluctuations in gravel levels can be better understood.

It would appear that very little new gravel entered the cave during these, and immediately subsequent periods of heavy rain, as any new gravel entering the cave would presumably have been deposited in the vicinity of 'Record Junction'. This did not appear to happen, although infilling, after removal of material downstream, could have occurred.

The depth of the gravel at PT17 Cave resurgence does not appear to be changing in relation to the inputs at the submergence. This could possibly be the result of a long lag-time between the input and output of the gravel, the result of a large storage capacity within the cave system, between the gravel sump and the resurgence.

The sudden rise in the gravel level, in July 1985, is probably the result of a landslide in the Waewaepa Range (approximately 1 km upstream from PT17 Cave) which was triggered by the heavy rain occurring in that month, supplying the stream with gravel. The transportation of the gravel, down into the cave, resulted in the deposition of between 209 m^3 (assuming an average depth of 1 m) and 314 m^3 (assuming an average depth of 1.5 m) of gravel between 'Record Junction' and 'Bottle Neck Squeeze'. As no increase in the depth of the gravel has occurred in subsequent periods of heavy rain, this is considered to be an isolated occurrence resulting from this one major landslide.

Gravel levels in PT17 Cave have been observed to fluctuate over the past 15 years. This may be the result of such landslides, as described above, occurring once every five to ten years, increasing the depth of gravel during one storm event; then over the period of a number of years this gravel being transported through the cave.

From the above discussion on contemporary gravel fluctuations within PT17 Cave, some possible deductions with respect to past events, may be made. Assuming the level of gravel within the cave is controlled by the amount

carried by the streams feeding into the cave, and that no localised blockages have occurred, fluctuations are the result of erosion occurring within the Waewaepa Range. At present, the subterranean drainage system can just cope with the gravel supply but the gravel level is low in comparison with past periods, when the gravel completely infilled the cave and re-established surface drainage over the cave entrance. This could have resulted from more intense slope processes in the past moving gravel down into the streams flowing into the cave.

Evidence of increased gravel supply during the Pleistocene has also been found by Mosley (1977) in the Ruahine Range, 30 km to the west of the Puketoi Range. Here large gravel terraces aggraded at the foot of the range during cooler phases of the Pleistocene.

Climatic cooling, during the last stadial of the Otira Glaciation, may have resulted in increased erosion rates from the periglacial processes. If the increased supply of gravel continued over a sufficiently long period, the development of fluvial deposits overlying the cave, and the re-establishment of the drainage system on the surface, as seen in the geomorphological evidence, would have been caused solely by climatic change during this period of time. Climatic warming, at the end of the last stadial of the Otira Glaciation and through to the present, would have decreased erosion rates and hence the supply of gravel to the cave. Drainage would have continued over the surface, until such time as the gravel within the cave was flushed out. As this flushing out process continued, the drainage would have been diverted back through the cave, as is occurring today.

6.4 Organic Deposits

Organic deposits can be placed into two main groups: (1) Floral, and (2) Faunal remains. Both are allochthonous deposits brought into the cave environment through a variety of mechanisms: fluvial transportation, especially at times of high streamflow; falls down potholes and shafts; and deposition of excrement (guano) by colonies of animals, such as bats and birds, which feed outside the cave but use it as shelter. Within New Zealand the most commonly observed organic deposits consist of the bones of animals, particularly birds, which have

either fallen down shafts or have been washed into the cave (Worthy 1982, 1984).

The caves within the Puketoi Range are no exception and many caves contain bone deposits. For example, Ramsay's Neck Cave contains a wide variety of bird bones including moa, weka and takahe (for a full list of subfossil remains identified from caves in the area, see Appendix One).

Plant remains are usually less obvious, as many are small fragments, but may range upwards in size to large logs. Palynology is an important analytical technique in the reconstruction of past vegetational and climatic regimes (Faegri and Iverson 1964). It was hoped that the finding of pollen trapped in fine-grained sediment (as described in section 6.3.1.2), and a subsequent palynological study, could be used in conjunction with the dating of speleothems, associated with this sediment, to give a possible reconstruction of the vegetation and climate at the time of deposition of the sediment. A test for the presence of pollen was therefore undertaken. The only other report of pollen examined within caves in New Zealand, is by Harris (in Barrett 1963). This listed pollen identified from sediment taken from Kairimu cave, south-west Auckland.

The peroxide treatment of the fine-grained sediment sample (see section 6.3.1.3) resulted in a loss of between 1.2 percent (reduced sample) and 2.2 percent (oxidised sample) as organic matter, by weight. The result would suggest that pollen may be present as it is one of the organic substances more resistant to decay. Two samples from the sediment were analysed by the method described in Appendix Nine. The material remaining, after the extraction process, was placed on to microscopic slides and examined under 400x magnification . The cave samples contained no pollen. Therefore it is unlikely that pollen is present in the cave sediment.

Peterson (1976), in his examination of pollen from sediment within Mammoth Cave, Central Kentucky, USA, also found older sediment devoid of pollen, while contemporary sediment contained countable numbers of pollen grains.The five hypothesis he proposed, to explain the absence of fossil pollen, will be examined in relation to the situation found in Ramsay's Neck Cave:

(1) Pollen did not enter the cave: No attempt was made to examine contemporary cave sediment within Ramsay's Neck Cave for pollen, therefore this cannot be proved or disproved. Contemporary pollen was found in Mammoth Cave, however, and it is also likely to be found in Ramsay's Neck Cave.

(2) Pollen entered the cave but was mechanically destroyed during transport: Peterson could find no evidence to support this, as mechanical abrasion of modern pollen grains was not significant in the samples he examined. This would seem unlikely to affect any pollen entering Ramsay's Neck Cave, as Peterson observed pollen transported for distances of at least 800 m (0.5 miles) within Mammoth Cave. The sediment deposited 50 m to 75 m from the present entrance, within Ramsay's Neck Cave, is well within this range.

(3) Pollen entered the cave, but flow velocities were too slow to keep it in suspension: This was found to be true in some areas within Mammoth Cave. Clay and silt-sized material which settled out of ponded water, were found to contain insufficient pollen for counting, whereas all successful cave pollen samples, examined by Peterson, came from areas where sand was also deposited. He therefore considered that areas accumulating only finer sediment (clays and silts) do not accumulate large quantities of pollen. These areas, however, have the potential for supplying more information, as clays and silts are less permeable than sandy sediment and therefore the pollen is less likely to be oxidised or physically removed by water. Secondly, the finer cave sediment tends to be laminated and therefore provide a better time-stratigraphic record, as compared with sandy sediment.

Flow velocities, at the time of deposition of the fine-grained sediment in Ramsay's Neck Cave, were sufficiently slow to have enabled the deposition of predominantly fine sediment (clays and silts) (see section 6.3), and not large quantities of sand-sized sediment and pollen. This possibly resulted from the ponding of water and the settling out of the fine material still in suspension. This method of sediment deposition is different to that observed in Mammoth Cave, where clays and silts are deposited in upper level passages and are not the result of a blockage in the passage. In both situations the effect on pollen transport is likely

be the same, with water velocities too slow to transport pollen present in the water any great distance.

(4) Pollen entered the cave, but flow velocities were too high to permit deposition: This was found to be true in some situations within Mammoth Cave, where there was a continuous flow of water and occasional flooding, resulting in the flushing out of sediment. The possibility of water flows being too high to permit deposition of pollen within Ramsay's Neck Cave, would seem unlikely, as evidence of flow velocities at the time of deposition of the fine sediment (see section 6.3) indicate that the velocity of the water would have been low, due to the gravel blockage in the passage.

(5) Pollen was deposited in the cave, but was subsequently destroyed by oxidation or removal by percolating groundwater: This could not be proved or disproved in Peterson's study, although it is known that pollen is presently entering Mammoth Cave. The oxidation or removal of the pollen is possible in Ramsay's Neck Cave. The sediment sample has undergone both reduction and oxidisation in the past, and Thomkins (pers. comm.) considered the sediment too dry to allow the pollen to survive, therefore destruction of pollen deposited in the sediment is likely.

The absence of pollen in the fine-grained sediment within Ramsay's Neck Cave may therefore be attributed to hypotheses 1, 3, or 5. The pollen wasn't present at the site examined within the cave, possibly as a result of it not entering the cave; or it wasn't transported owing to low flow velocities; or alternatively oxidation of the sediment sample has occurred, resulting in the destruction of any pollen that was present. This third explanation is probably more likely, as the deposition of all pollen present in the flowing water, before reaching the site examined, is doubtful, with such a short distance between the entrance and the sampling site. It is highly likely that pollen did enter the cave, although this cannot be proven.

6.5 Sedimentation within Ramsay's Neck Cave

From the above discussion on sediment within Ramsay's Neck Cave, a sequence of events occurring within the cave can be reconstructed. This

sequence is based on the examination of the clastic sediment, the geology of the surrounding area, and the drainage network upstream from the cave (Fig. 6.2).

Development of the cave possibly began late in the Oturi interstadial or more probably in the Otira Glaciation. Drainage from the eastern limb of the Pori Syncline, flowed westward over the impervious sandstone and siltstone beds overlying the Te Onepu Limestone, across the western limb of the syncline and into the headwaters of the Hirinakitu Stream. As the stream eroded downwards, karstification of drainage began, probably first with the development of passage B, and later, drainage from the south forming passage A in Ramsay's Neck Cave. This is indicated by the relative passage sizes, evidence that greater solution has occurred in passage B, compared with passage A. This is based on the assumption that other factors which could affect solution rates such as agressiveness and flow rates have been similar during the development of the two passages. The water table at this time was perched above the base level of the surrounding area, being confined by the impervious Raukawa Mudstone, directly below the limestone in which Ramsay's Neck Cave is formed. This resulted in the initial phreatic character of passage B (seen in the keyhole shape of the passage (see Photo 6.1)). It was not until the erosion of the Raukawa Mudstone, on the western side of the syncline, that the water table would have been lowered, resulting in vadose development of the cave.

With the onset of the maximum of the last stadial in the Otira Glaciation, climatic conditions in the area would have been very harsh, with a periglacial environment being established. This resulted in formation of an active stream in the southernmost dry valley of the drainage basin of the Ramsay's Neck Cave, which transported limestone gravels into the cave during spring and summer snow-thaw flooding. This supply was sufficient to block passage A, and then divert the flow to passage B, eventually choking this as well.

The gravel blockage of passage B resulted in a change in the hydrological conditions within Ramsay's Neck Cave. Coarse gravels formed the ancient cave stream sediment throughout this passage, eventually blocking it. This resulted in a spatial pattern of deposition of the overlying material with coarse material deposited at, or near, the entrance and

finer material settling out of slow moving or ponded water deeper within the cave. As a consequence, the sediment has a graded appearance.

The supply of finer silt/clay material was increased by volcanic ash showers depositing material over the drainage basin. This was washed into the cave to form the laminated fine-grained sediment overlying the gravels.

Eventually the cave passages were completely sealed, with all drainage diverted over the surface. The sealing of the passage resulted in the growth of stalactites and false floors of flowstone.

Passage A contains no old gravels. Indirect evidence, however, provided by false floors of flowstone formed approximately 1 m below the roof, and the remains of a layer of fine-grained material above these false floors, similar to that observed overlying the gravels in passage B, indicates that this passage underwent a similar sedimentary history to that seen in passage B.

Streamsink dolines, which have developed between the present submergences and resurgence of the cave, are the direct result of the gravel blockages in the passages diverting the stream across the surface and then down into the cave. This diversion of the drainage resulted in the formation of the chamber within the cave (see Fig. 6.1).

As the last stadial of the Otira Glaciation ended, the supply of gravel was reduced, and finally ceased as the valleys to the south, on the limestone, once again became dry. The streams flowing from the siltstone and sandstone beds continued to supply water, cutting down into the limestone and re-establishing drainage through the cave. The sinking of the streams was via new entrances, with the older, original entrances completely sealed. This second phase of development within the cave is vadose in nature resulting in stream entrenchment in the previously formed passages. This phase of development continues today.

To allow the survival of the clastic sediment within passage B, the initial re-entry of the stream into the passage must have been rapid for the sediment to survive. This could have been either through strong solutional erosion or rapid mechanical incision, or a combination of

both. If rapid entrenchment had not occurred the sediment would have been washed from the cave. Wolfe (1972b), from his study of sediment within caves, concluded that sediment is probably deposited in the latter stage of passage evolution, and if deposited at an earier stage, little evidence would remain. The situation within Ramsay's Neck Cave would appear to contradict this, as passage B still retains significant deposits of ancient sediment, with this passage still containing an active stream.

6.6 Conclusions

In this chapter sediment from two caves within the Puketoi Range has been investigated. The two caves, Ramsay's Neck Cave and PT17 Cave, contain sediment deposited under differing climatic conditions. The sediment in Ramsay's Neck Cave is predominantly ancient sediment deposited under periglacial conditions, with smaller amounts of contemporary sediment deposited under present climatic conditions. PT17 Cave has predominantly contemporary sediment, fluctuating in response to present climatic conditions.

In Ramsay's Neck Cave the ancient sediment was possibly deposited during the maximum of the Otira Glaciation. Results from the analysis of this sediment indicate that valleys that are presently dry in the catchment of this cave contained streams that carried sediment into the cave. This possibly indicates that the climate at this time was periglacial, with mechanical erosion of the limestone being of greater importance than solutional erosion of today. This sediment was deposited as basal gravel, overlain by a fine-grained sediment. The fine-grained sediment contains allophane, possibly derived from a volcanic ash shower during the Otira Glaciation.

The second cave, PT17 Cave, contains predominantly contemporary gravels. These gravel fluctuate in response to present hydrological conditions. The examination of these gravels, and geomorphological surface features in the vinicity of the cave, indicate that the gravel supply to the cave in the past was much greater than at present. This is possibly due to an increased supply of gravel eroded from the Waewaepa Range under periglacial climatic conditions. This gravel was carried down into the

cave completely infilling it. With climatic warming at the end of the Otira Glaciation, through to the present, the supply of gravel decreased and was flushed from the cave. The gravel level within the cave today fluctuates in response to present hydrological conditions and the supply of gravel from the Waewaepa Range.

CHAPTER SEVEN
CUESTA DEVELOPMENT

7.1 Introduction

The Puketoi Range can geomorphologically be termed a cuesta. This is a landform which has a gently sloping surface bounded on one edge by an escarpment (Simonett 1968). The shape of a cuesta results from a gently dipping layer of relatively resistant rock (in the case of the Puketoi Range, predominantly Te Onepu Limestone Formation), which is underlain by softer, easily eroded strata (Mangatoro Mudstone Formation). This results in a steeper scarp slope.

The term cuesta is a Spanish word meaning hill or slope. According to Hill (1896, cited in Simonett 1968) this term was applied to tilted structural plains, and to other asymmetrical features including tilted fault block mountains, in Texas and New Mexico, U.S.A.. Davis (1899) adopted the term and restricted its usage to the definition given in the first paragraph.

Cuestas are related to several other landforms, forming part of a graduational series from hogbacks through to homoclinal ridges and cuestas to mesas. Cuestas are differentiated from the other forms (except homoclinal ridges) by the migration of the crestline in the direction of dip, a process defined by Cotton (1948) as homoclinal shifting.

The escarpment, or scarp, is defined as a cliff or steep rock face of great length. Two general types are recognized: structural and erosional escarpments. The Puketoi Range scarp is erosional in form. No pronounced faults are found along the length of the scarp.

In this chapter, the geomorphological development of the Puketoi Range will be discussed. This begins by describing the development of the Puketoi Range cuesta, then the subsequent development of geomorphological features on the range are examined.

7.2 Development of the Puketoi Range Cuesta

From Lewis's (1980) investigation of the present accretionary ridge and slope system offshore of the East Coast, North Island, inferences can be made about the initial formation of the proto-Puketoi Range. Lithological variation in the geological beds laid down during the Pliocene and Pleistocene have been very influential in the subsequent development of the range. The resistant nature of the limestone beds, and the structural control these beds have placed on the development of the range, are particularly important. Inference about deposition and uplift of these beds can be made from the examination of the present accretionary ridge and slope along the East Coast of the North island.

The proto-range formed as one of a series of ridge and basin systems, which are generally 5 km to 30 km wide and 10 km to 60 km long (Lewis 1980). These ridges are either seaward-faulted or sharply dipping asymmetrical anticlinal ridges (Lewis 1973a; Katz 1974b) with flat-floored, sediment-filled synclinal basins aligned more or less parallel to the slope (Pantin 1963; Lewis 1976). Calcareous sedimentary material, from the current-swept and sediment-free anticlinal ridges, is at present deposited in greatest thickness in the off-shore basins (Kamp 1982). The sediment thins towards the crest of the anticlines, and in some places, it drapes over the growing anticlinal ridges (Lewis 1980).

This pattern of sedimentation is believed by the author to be similar what was occurring when sediment was laid down in the vicinity of the proto-Puketoi Range. This sediment varies in thickness from 200 m to 2000 m along the East Coast (Lewis 1980). The Pliocene sediments on which the Puketoi Range has formed, reaches a maximum thickness of 300 m at the northern end of the range (Harmsen 1984a, 1985).

From early Waipipian times onwards the area to the east of the Puketoi Range, and the Waewaepa Range to the west, was uplifted above sealevel and subsequently began to erode. This supplied sediment to the basin formed between the proto-Puketoi Range and the Waewaepa Range resulting in the Kumeroa Formation. By early Pleistocene time, the proto-Puketoi Range had been uplifted above sealevel and was beginning to erode. The initial form of the range was an asymmetrical anticline, the western side of which was a succession of alternating limestone and terrigenous beds

(Te Aute Group). These beds thinned to the east, with the crest of the anticline probably Mangatoro Formation, or very thin beds of overlying Te Aute Group sediments.

After uplift of the proto-Puketoi Range above sealevel, an erosional breach developed along the crest of the asymmetrical anticlinal axis of the range. This would have resulted in more rapid erosion and removal of the steeply-dipping and softer Mangatoro Formation mudstone on the eastern side of the anticline, than the more resistant alternating beds of limestone and softer terrigenous deposits to the west. This differentiation in erosion rates within the range resulted in the development of the Puketoi Range cuesta, with the steeply dipping eastern scarp slope and gently-dipping western dip slope. As erosion on the eastern side of the range continued, increased thicknesses of Te Onepu and Awapawa Limestones would have been exposed along the scarp slope, influencing the development of the scarp slope to a greater degree.

Schumm and Chorley (1966) classified the scarp slope of a cuesta on the basis of a combination of the lithology, climate and vegetation cover. This classification identified three basic forms: simple, composed of one main rock type; compound, composed of two major rock types, a resistant caprock and a weaker underlying rock; or complex, possessing more than one caprock over less resistant rock.

The form of the three scarp types described above is primarily determined by the character of the rock of which they are composed, and the manner in which the rocks are eroded. Schumm and Chorley (1966) identified four geological variables important in the development of the scarp form: (1) Rock resistance as controlled by cementation and porosity; (2) The orientation and spacing of joints and bedding planes; (3) The directions of dip; and (4) The proportion of the scarp slope composed of caprock.

The scarp of the Puketoi Range is a complex scarp, with the Te Onepu and Awapapa Limestones forming resistant caprocks between Raukawa and Mangatoro Mudstone Formations. The Kumeroa Formation further down the dip slope of the range does not, at present, influence the development of the scarp slope.

The thickness of the interbedded limestone and mudstone beds is possibly

the primary control in determining the nature of the scarp slope, and the range as a whole. The range is therefore a structurally controlled landform, the result of the interbedded limestone and terrigenous beds on which it is developed.

The form of the scarp ranges from a single scarp slope (Photo 7.1), where the thickness of the upper Te Onepu Limestone is controlling the scarp form and slowing the erosion of the underlying beds, to a triple scarp slope, where three limestone beds in the northern section of the range have created three scarp slopes. Here again the erosion of the underlying mudstone beds is controlled by the rate of erosion of the overlying limestone.

7.3 Drainage Development

Drainage and relief within the Puketoi Range is strongly controlled by the structure of the range, with the Puketoi Range itself a structurally controlled landfrom as described above.

Using the nomenclature of Ollier (1981), streams developed on the Puketoi Range may be termed strike, dip and anti-dip streams. Strike streams run in the strike direction, and are separated from each other by strike ridges. Dip and anti-dip streams, which are tributaries of strike streams, commonly enter the strike streams at approximately right angles. Dip streams flow down the dip slope, whereas anti-dip streams flow down the scarp slope. Where the dip is gentle, as in the Puketoi Range, dip streams are longer than anti-dip streams.

The above nomenclature was developed by Ollier (1981) to describe structurally controlled streams in regions of dipping strata, and replaces an older nomenclature system for such areas. This older system identified four stream types; consequent, subsequent, secondary consequent, and obsequent streams. This system presumed a time sequence for the origin of the various streams (Ollier 1981). In reality, drainage is initiated over the whole of the area at once, with no part of the surface not developing drainage. This contradicts with the old system which presumed a time sequence in the development of drainage (Ollier 1981).

Photograph 7.1 Aerial oblique view along the Puketoi Range looking towards the south. The scarp slope is a single slope in this section of the range. (Photo: Richard Heerdegen)

There are differences in drainage density values for dip and anti-dip streams within the Puketoi Range. This is related to the nature of the geological beds in which they have developed. The anti-dip streams are developed on Mangatoro Formation mudstone. This is much softer and less permeable than the overlying limestone beds, resulting in lower infiltration and higher runoff than observed in the limestone forming the dip slope. This results in the drainage density on mudstone being much higher than that of limestone (16.92 km/km^2 and 7.94 km/km^2 respectively). This variation in drainage denisity with respect to the geology of the underlying rock is also seen in the greywacke of the Waewaepa range, where the density is similar to the limestone of the Puketoi Range. Drainage characteristics of the area are described in more detail in chapter 5.

The overall stream pattern for the Puketoi Range consists of two strike streams formed within the basin between the Waewaepa and Puketoi Ranges, the Mangatoro Stream flowing to the north, and the Makuri Stream flowing to the south. Widely spaced dip streams have developed on the dip slope of the range, and relatively short and closely spaced anti-dip streams on the scarp slope. Many of the dip streams developed within the Puketoi Range are dry valleys reflecting the permeable nature of limestone. The stream pattern developed on the range is known as a trellis pattern.

Dip streams within the range can become a significant feature when eroded into the underlying mudstone beds. Photograph 7.2 illustrates the end result of stream erosion through the limestone beds and into the underlying Mangatoro Mudstone. The photograph is of the stream flowing from behind Makuri township. Here it has cut a gap into the range. The stream has eroded down through the Te Onepu and Awapapa Limestones, and into the Mangatoro Mudstone Formation.

A developmental sequence of gap formation in the range can be observed along its length. At grid reference T25/619645 the initial stages of development are seen. Here the stream has cut down through the Te Onepu Limestone and into the underlying Raukawa Mudstone. The basin developed in the mudstone has become much wider than valleys found on limestone only, with the sides cut back in the central part of the basin to give an oval appearance to it. The rate of development of this basin is possibly controlled by the contact with the limestone at the downstream end of the

Photograph 7.2 Stream gap behind Makuri. Note asymmetrical mudstone ridges to the centre-right of the photo.

basin. The stream would not be able to erode into the mudstone faster than the downcutting of the limestone at the downstream end.

Development of the valley will continue with the enlargement of the basin and the removal of limestone along the crest of the range. This is seen at grid reference T24/690705, where a wide flat triangle shaped basin has formed. Mechanical erosion by the stream will continue until the Awapapa Limestone is reached. Contact with this limestone will change the hydrological conditions within the basin, with the stream becoming dry. This would slow the rate of mechanical erosion and increase the rate of solutional erosion within the basin.

Solutional erosion will continue until the Mangatoro Mudstone is reached. Contact with this mudstone bed will result in the repetition of the process described above.

The drainage basin shown in photograph 7.2 has a series of asymmetrical ridges cut into the mudstone to the east of the scarp slope. These ridges indicate that the basin formed at a time when the scarp slope was further to the east and possibly higher than today. As the stream eroded down and homoclinal shifting of the crestline to the west occurred, this area was left untouched by streams from the scarp slope. The pattern of three predominant asymmetrical ridges developed on the mudstone is the result of erosion of the crest down to this level over time.

The anti-dip streams which have formed along the scarp slope possibly result from runoff down the scarp slope rather than headward erosion of the streams. This conclusion is based on the survival of the area to the east of the the stream described above. If headward erosion was occurring, this area of Mangatoro Mudstone would have been eroded quickly by headward erosion of streams flowing to the east in this area.

7.4 Mass Movement and Gravity-sliding on the Scarp Slope

The Puketoi Range scarp has formed predominantly by runoff of streams from the scarp slope as mentioned above.

Large-scale mass movement and gravity-sliding has also been influential in the development of the scarp. This is seen today in the northern and

southern sections of the range, where the scarp slope has been effected by large-scale slumping and gravity-sliding.

In the northern section of the range, to the south of Oporae (Grid Ref. U24/820865), a large slump/earthflow has occurred (Photo 7.3). It consists of a number of large limestone-covered slump blocks which have been rotated backwards, and a considerable area of earthflow, which has moved southward as seen in the photograph.

The slump was generated from the scarp slope of the range, where Awapapa Limestone overlies Mangatoro Formation mudstone. The slump was possibly generated by the permeability of the limestone allowing rainfall to percolate through it and collect within the comparatively impervious mudstone layers. This weakened the mudstone bed and generated the slump.

Along this section of the range, the Oporae Anticline has a very gentle dip to the east and dips steeply to the west. The area of the slump is across the anticlinal axis, requiring the Mangatoro Formation to be very mobile at the time the slump was generated, as the dip of the beds is not favourable for movement because the original dip of the beds is in the wrong direction.

Possible gravity-sliding of large blocks of limestone at the southern end of the range has also occurred (Photo 7.4) Along the scarp slope in this section of the range large blocks of limestone have moved down the scarp slope to become separated from the scarp.

Neef (1967, 1974, 1984), in his investigation of the geology of this area identified these blocks as a limestone lens within the Makuri Sandstone Formation (reclassified by the author as Mangatoro Formation). The author believes that Neef made an incorrect geological interpretation of the area, as no thin limestone beds are found further to the north past the area the author believes to have been effected by gravity-sliding.

The drainage for this area also appears irregular. Streams flow down the contact area between the Mangatoro Formation and the dislocated limestone blocks, with no indication of present or past drainage on the limestone blocks, as would be expected if overlying material had been eroded off. The drainage also appears to have been funnelled in behind the dislocated

Photograph 7.3 Large scale mass movement on the southeastern side of Oporae.

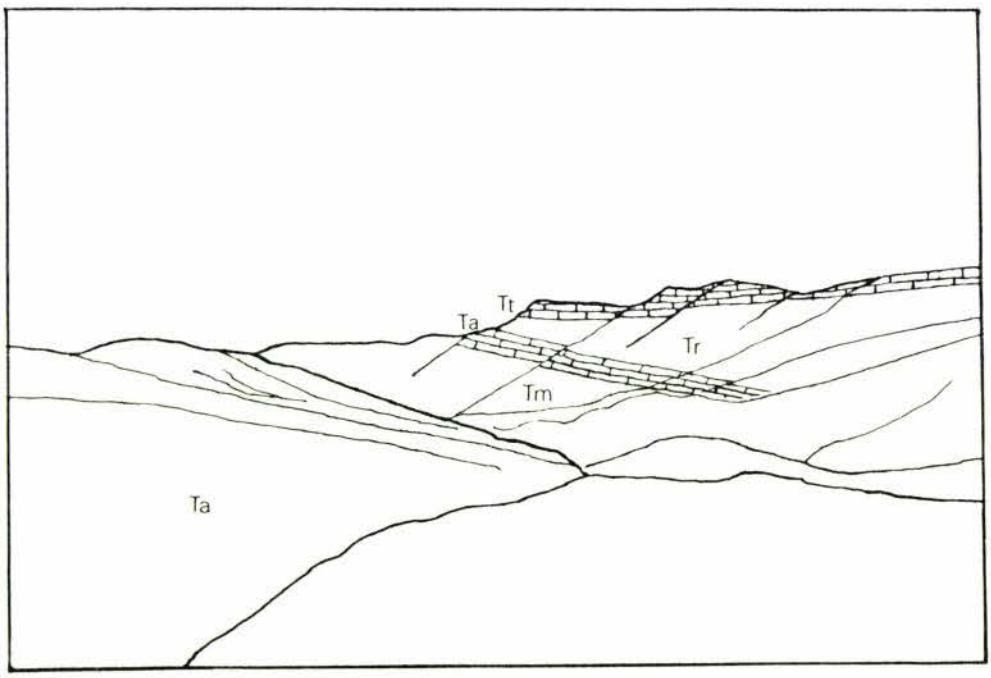

Photograph 7.4 Gravity-sliding at the southern end of the Puketoi Range. The limestone block in the foreground has moved down from the the lower limestone bed marked Ta.

blocks and then outward between them.

Further evidence for gravity-sliding is seen in the asymmetrical valley shape developed between dislocated blocks and the scarp slope. This would be expected by the movement down slope of large blocks of material from higher up.

Contorted, and near vertical beds of Mangatoro Mudstone Formation were also found in areas in which gravity-sliding had occurred. This possibly indicates flow of the material downslope associated with gravity-sliding.

7.5 The Significance of the Limestone Beds within the Puketoi Range

The limestone beds of the Puketoi Range are thin alternating beds, 20 m to 70 m thick, between terrigenous beds 60 m to 240 m thick. These limestone beds are sufficently thick and pure in $CaCO_3$ to allow the development of karst features within the limestone as described in chapter 4. The karst landforms developed are similar in their form and extent to those developed on more massive limestones in other parts of the country. The existence of these karst features on the limestone of the Puketoi Range indicates that this is an area of karst, developed in relatively young Pliocene/Pleistocene limestone.

The erosion of the limestone was estimated in chapter 3 at 58.2 $m^3/km^2/yr$. Assuming constant and even rates of solution, 10m of limestone would be removed in approximately 170 000 years. The lateral extention of this solutional erosion rate is very approximate. Changing climatic conditions, especially the establishment of periglacial conditions during glacial periods would have a major influence on the type and rate of erosion of the limestone. A change to more pronounced mechanical erosion during periglacial periods is evident from sediments within Ramsay's Neck Cave. This is discusssed in chapter 6.

The limestone beds of the Puketoi range form a protective barrier over the underlying mudstones. Once the limestone has been removed the cuesta would soon disappear as the mudstones would erode rapidly. The Puketoi Range therefore has a limited life controlled by the rate of erosion of the limestone.

The much greater rate of erosion of the mudstone is seen in the country to the east. This area was originally much higher than the Puketoi Range when uplifted above the sea but has rapidly eroded away. Uplift of the range is therefore much greater than erosion, with the limestone covering the range forming a protective barrier to rapid erosion rates. The cuesta may therefore reach much greater heights before it is destroyed. This is especially so if greater thicknesses of limestone are exposed to the west, in the basin between the Puketoi and Waewaepa Ranges.

7.6 Conclusions

The development of the Puketoi Range as a cuesta is structurally controlled by the Te Onepu and Awapapa Limestone beds. These two beds have formed a protective barrier over the underlying mudstones, reducing the rapid rates of erosion associated with mudstones.

Drainage development, and large scale mass movement and gravity-sliding have modified the shape of the cuesta. This is especially so along the eastern scarp slope of the range where large areas of the range has been effected by mass movement and gravity-sliding.

Karst landforms have developed on the limestone of the range. These landforms are similar to karst landforms developed in more massive limestones elsewhere in New Zealand.

CHAPTER EIGHT

CONCLUSIONS

This thesis has examined specific aspects of the karst geomorphology of the Puketoi Range. This range forms part of the much larger Kahurangi Karst, an area of karst developed on relatively young (Pliocene to Pleistocene) limestone on the East Coast of the North Island.

Detailed mapping of the beds on which the range has developed, was undertaken. This allowed the investigation of the structure/landform relationships between alternating beds within the range. Three limestone beds and three terrigenous beds were identified. These are (from youngest to oldest) the Kumeroa Formation (Pleistocene in age), with an upper limestone member and a lower mudstone member; Te Aute Group (Pliocene in age) consisting of four formations: Te Onepu Limestone, Raukawa Mudstone, Awapapa Limestone, and Mangatoro Mudstone.

These beds form a sucession of thin, 20 m to 70 m thick beds of barnacle-rich coquina limestone and calcareous sandstones interbedded between 60 m to 240 m thick terrigenous deposits of siltstone and mudstone.

The Puketoi Range forms part of the highest wedge of Tertiary sediment uplifted by the subduction of the Pacific Plate beneath the Indian Plate. The wedge has been pushed upwards and landwards by the movement of the plates. This resulted in the proto-Puketoi Range forming as an asymmetrical anticlinal ridge which has subsequently been eroded into a cuesta. This cuesta consists of a western limestone-capped dip slope of predominantly Te Onepu Limestone, and a steeply dipping scarp slope on the eastern side, exposing alternating limestone and mudstone beds.

Solutional processes and erosion within the Puketoi Range were investigated. Examination of 306 water samples collected over 8 months indicates considerable variation in solution, both spatially and temporally. Three types of water were identified: allogenic water derived from non-karst areas, autogenic water derived from limestone, and mixed allogenic-autogenic water.

Solutional erosion rate for the Towai drainage basin at Coonoor was estimated at 58.2 $m^3/km^2/yr$. This is comparable with other temperate areas in New Zealand (Waitomo, 69^{19}_{8} $m^3/km^2/yr$), and also world-wide estimates of solutional erosion in temperate areas.

Selected karst features within the Puketoi Range were examined. These features range from large dry valley systems to small areas of karren and case-hardened limestone. Case-hardening and bogaz, two features found within the limestone of the Puketoi Range, have not previously been described in detail in New Zealand.

Many of these features, for example, dry valleys, limestone pavements and case-hardened limestone, have formed, or have been modified by periglacial processes during the Otira Glaciation. This climatic influence is seen in the development of a limestone pavement through solifluction processes (pavements are generally associated with glaciated areas), and the exposure of limestone at the surface to harsh environmental conditions in the past resulting in case-hardening of the limestone.

Bogaz are fissures within limestone resulting from solutional erosion along lines of weakness within the rock. Bogaz are found within two areas of the Puketoi Range. They form a series of parallel fissures up to 30 m in length, 1 m to 4 m in width, and 1 m to 8 m in depth. Their formation within the Puketoi Range has resulted from tension placed on joints in the limestone. These joints are more susceptible to solutional erosion, and possibly to ice-wedging, during periods of periglacial climatic conditions. Solutional erosion of the bogaz continues today through water flowing down into the joints, acidified by organic material within the soil of the bogaz.

Case-hardening of limestone within the Puketoi Range was observed. This forms an upper indurated layer over limestone exposed at the surface. Case-hardening within the Puketoi Range appears to be patchy in its development. It forms predominantly in areas more exposed to strong winds which draws moisture out of the rock, causing reprecipitation of the dissolved calcium carbonate at, or near the surface of the rock.

Case-hardened limestone is assumed to form only on limestone exposed at

the surface. The position of the case-hardened layer of limestone may therefore indicate changes in the soil level. At Oporae, case-hardened limestone was found beneath a soil cover. This soil cover has possibly formed since the development of the case-hardening. At another locality the case-hardened layer is well above the soil level, exposing soft pitted limestone beneath. In this situation the soil level may have been lowered.

Drainage basin characteristics within the Puketoi Range were found to be strongly influenced by the lithology of the rock type within individual basins.

The drainage density was calculated for three different basins formed on mudstone, limestone and greywacke lithologies. The mudstone drainage basin was found to have the highest drainage density (16.92 km/km^2). This is classified as a fine-textured basin. In contrast, the densities within the greywacke and limestone basins were found to be similar, 6.12 km/km^2 and 7.94 km/km^2 (stream and dry valleys) respectively. These two basins are classified as medium-textured.

Variation in the drainage densities within the three basins is attributed to variation in the weathering, erosion and mass movement of the underlying rock within each basin.

Sediment from Ramsay's Neck Cave and PT17 Cave was investigated. The sediment within Ramsay's Neck Cave is predominantly ancient, consisting of ancient cave stream sediment deposited as a basal unit, overlain by a fine-grained unit, and in places by speleothems.

This ancient sediment, and the contemporary sediment within the cave and surface stream, were examined. The ancient cave stream sediment was deposited during periods of higher water velocity than is found today. This conclusion is based on the mean size of ancient and contemporary sediment. The higher water velocity may have resulted from seasonal snowmelt when the area experienced a periglacial climate during the Otira Glaciation. The ancient cave stream sediment eventually choked the cave reducing the water velocity so that it became very slow moving or ponded. Fine-grained material transported by the stream was deposited over the ancient cave stream sediment. This sediment contains a large amount of

allophane - a volcanically derived material found in many volcanic soils in New Zealand. Speleothem samples sent for dating will give a minimum age for the sediment.

Contemporary gravel fluctuations within PT17 Cave were also investigated. These gravels, derived from the greywacke of the Waewaepa Range, fluctuate in response to present day hydrological conditions within the cave. Heavy rainfall in July 1985 generated a large landslide approximately 1 km upstream from the cave, resulting in the deposition of between 209 m^3 and 314 m^3 of gravel within the cave. Since this time, the gravel level within the cave has lowered. These fluctuations may have a 5 to 10 year cyclic effect, which is associated with mass movement within the Waewaepa Range.

Surface evidence indicates that in the past the volume of gravel transported by the cave stream has been considerably greater, filling the cave and re-establishing surface drainage. This may have been associated with periglacial processes, which increased the supply of gravel from the Waewaepa Range to the cave.

The evolution of the Puketoi range as a cuesta has been strongly influenced by the two limestone beds on which it has developed. These two beds control the development of the scarp slope along the eastern side of the range. The scarp is a complex scarp, with variation in the thickness of the limestone beds controlling the form of the scarp.

Drainage, and mass movement and gravity-sliding has influenced the development of both the dip and scarp slopes of the range. A trellis drainage pattern has developed. This drainage pattern is controlled by the structure of the range with strike, dip, and anti-dip stream developed.

Large-scale mass movement and gravity-sliding have occurred in places along the scarp slope of the range. In these areas, sections of the scarp slope have moved downward and to the east, away form the general dip of the range.

This investigation has examined an area of relatively thin Pliocene/Pleistocene limestone, varying from 20 m to 70 m in thickness,

and interbedded between much thicker terrigenous deposits. The limestone has strongly controlled the development of the range and the continued existence of the range as a geomorphological feature.

The limestone of the range supports many karst landforms and features. Karstification of the limestone has and is occurring. The thin nature of the limestone is not restricting karst landform development, with many of the karst landforms found in this area also developed on more massive limestones elsewhere in New Zealand.

APPENDIX ONE

PLANTS OF THE ORIGINAL FOREST OF THE "FORTY MILE BUSH" AREA AND SUBFOSSIL BONES FROM CAVES WITHIN THE PUKETOI RANGE

The following list of native plants is taken from Carle (1980, p.3-4), from his book on the "Forty Mile Bush" area, of which the Puketoi Range formed a part. The list is not intended as a full botanical list of all plant species in the area, but does give some indication of the diversity of native plants before the bush was cleared.

NOTE: The names given in single brackets are the common English name for the plants.

TOTARA	Podocarpus totara
RIMU (Red pine)	Dacrydium cupressinum
RATA	Metrosideros robusta
MATAI (Black pine)	Podocarpus spicatus
KAHIKATEA (White pine)	Dacrycarpus dacrydioides
MIRO	Podocarpus ferrugineus
PUKATEA	Laurelia novae-zelandiae
TAWA	Beilschmiedia tawa
HINAU	Elaeocarpus dentatus
REWAREWA (Honeysuckle)	Knightia excelsa
MAIRE	Nestigis spp. probably N. cunninghamii
TOWAI (Silver Beech)	Northofagus menziesii
TETOKI	Alectryon excelsus
KOWHAI	Sophora spp.
MANUKA	Leptospermum scorparium
KONINI (Fuschia)	Fuschia excorticata
KARAKA	Corynocarpus laevigatus
MAHOE (Whiteywood)	Melicytus ramiflorus
WHAWHA PAKU (Fivefinger)	Pseudopanax spp. probably P. arborea
POPORAMU (Broadleaf)	Griselinia littoralis
KARAMU	Coprosma lucida
MAKOMAKO (Wineberry)	Aristotelia serrata
HOROEKA (Lancewood)	Pseudopanax crassifolium
OWHERIA (Lacebark)	Hoheria spp. probably H. sexytlosa
KOROMIKO	Hebe spp. probably H. stricta
RAMARAMA	?
RANGIORA	Brachyglottis repanda
MATIPO (red)	Myrsine australis
MATIPO (silver)	Myrsine divaricata
AKEAKE	Dodonaea viscosa
TUTU (BuliBuli)	Coriaria spp. probably C. arborea
KEIKEI	Freycinetia baueriana
TIKAUKA (Cabbage tree)	Cordyline spp. either C. australis or C. banksii
TOITOI (Pampas grass)	Cortaderia richardii
RAPO (Raupo)	Typha orientalis
NIKAU (Palm)	Rhopnostylis sapida
HARAKEKE (Flax)	Phormium tenax
PUAWANANGA (Clematis)	Clematis paniculata
RATA	Metrosiderus spp.
KAREAO (Supplejack)	Ripogonum scandens
TATARAMOA (Lawyer)	Rubus spp.

Subfossil bones identified from caves within the Puketoi Range

The following list is of sub-fossil bones removed from caves within the Puketoi Range. This list is as complete as possible. Information about

the bones removed from the area in 1952-53 by the Dominion Museum is incomplete. The bones are held by the Manawatu, National, and Canterbury Museums. The numbers beside each name represents: Number of bones/ Number of individuals. Where a single number is given, this represent the minimum number of individuals present.

RAMSAYS NECK CAVE Bones removed and/or identified by T.Worthy 9.6.85:

Moas: Pachyornis mappini 5/5; Anomalopteryx didiformis 1/1; Dinornis sp.? 1/1; Dinornis struthoides 1/1; Euryapteryx sp. 1/1; several bones in situ of A. didiformis and Euryaptheryx; Anomalopteryidae 1/1.

Weka Gallirallus australis 4 skeletons; Takahe Notornis mantelli 1/1.

GILLESPIES FOLLY CAVE Bones removed and/or identified by T.Worthy 2.11.86:

Moas: Dinornis struthorides 22/6; D. nouaezealandiae 9/3; D. giganteus 9/2; Anomalopteryx didiformis 32/10; Pachyornis mappini 10/3.

Kakapo Strigops habroptilus 2+/1; Rail Aptornis sp. 2/1; Weka Gallirallus asutralis 1/1.

SITE 12 (Manawatu Museum)

Moas: Dinornis sp. 1

SITE 22 (Manawatu Museum)

Bird and rat bones - not identified

SITE 25 (Manawatu Museum)

Weka Gallirallus australis 1; Kakapo Strigops habroptilus 1; Wren (identified by P.R.Milliner); Frog bones; Mouse bones; Freshwater crayfish Paranephrops.

Bones removed and/or identified by T.Worthy 2.2.85:

Moas: Anomalopteryx didiformis x/2; Pachyornis mappini x/1;

Kiwi Apteryx sp. 2/1; Takahe Notornis (Porphyrio) mantelli 15/1; Kakapo Strigops habroptilus 14/1; Weka Gallirallus australis 24<<+>/4; Laughing owl Sceloglaux albifacies 4/1; Kokako Callaeas cinerea 3/1; A. chloris 2/1; Wren Xenicas sp. 3/1.

Frogs: Leiopelma n.sp.1 9/2, 27/3; Leiopelma n.sp.3 10/2, 3/1, 10/1; Leiopelma hamiltoni 6/2; Leiopelma extant sp. indet. 5/2;

Lizards: Cyclodina ornata 1 skeleton; Cyclodina alani 1/1; Leiolopisma sp. 2/1.

Snail Fauna: Cytora lignara 1; Laoma marina 1; Therasiella neozelanica 2; Cavellia anguicula 2; Fectola trilamellata 32; Potamopyrgus antipodarum 3; "Geminoropa" moussoni 39; "Flammoconcha" compressivoluta 1; Lairea lepida 6; Allairea tullia 8; Charopa coma many.

SITE 30 (Manawatu Museum)

Moas: 11 bones removed - not identified.

SITE 44 Tresspass Tomo Cave

Moas: 32 bones removed - not indentified.

Site 47 (Manawatu Museum)

Magpie Gymnorthina tibicen 1.

Site 54 (Manawatu Museum)

Kaka Nestor meridionalis 1; Kakapo Strigops habroptilus 1.

80 ACRE CAVE (PT6) - also known as The Hole the Bullock Fell Down

Bones removed 1971, identified by P.R.Millener:
Moas: Dinornis giganteus 1; Anomalopteryx didiformis 4; Euryapteryx geranoides 1.

Kakapo Strigops habroptilus 2; Pterodroma cookii 1; Weka Gallirallus australis 1; Kokako Callaeas cinerea 1; Grey Duck Anas superciliosa 1; Pigeon ?Hemiphaga novaeseelandiae 1; Little Shag Phalacrocorax melanoleucos 1.

Bones removed 1973, identified by P.R.Millener:
Kakapo Strigops habroptilus 1; Weka Gallirallus australis 1.

Bones removed 1983, identified by T.Worthy:
Moas: Pachyornis mappini 1; Anomalopteryx didiformis 9; Euryapteryx geranoides 2; Dinornis giganteus 1; D. struthioides 1; Juvenile 1.

Finsch's Duck Euryanas finschi; Kiwi Apteryx sp. 1; Kokako Callaeas cinerea 2; Kakapo Strigops habroptilus 1; Weka Gallirallus australis 1.

Bones identified by R.J.Scarlett:
Cook's Petral Pterodroma cooki 1; Grey Duck Anas superciliosa 1; Pigeon Hemiphaga novaeseelandiae 1; Little Shag Phalacrocorax melanoleucos 1.

COONOOR Bones removed 1914, identified by P.R.Millener:

Moas: Pachyornis mappini 4; Euryapteryx geranoides 1; Dinornis giganteus 4; D. novaezealandiae 4; Anomalopteryx didiformis 13.

Rail Aptornis otidiformis 28; Kiwi Apteryx australis 5; A. owenii 5; Apteryx sp. 5; Pterodroma cookii 2, ?Hymenolaimus malacorhynchos 1; Finsch's Duck Euryanas finschi 5; Anas sp. 10; Weka Gallirallus australis 5; Takahe Porphyrio mantelli 2; Gallinula hodgeni 1; Capellirallus karamu 2; Pigeon Hemiphaga novaeseelandiae 3; Kakapo Strigops habroptilus 7; Kaka Nestor meridionalis 2; Cyanoramphus novaezealandiae 2; Megaegotheles novaezealandiae 1; Kakako Callaeas cinerea 3; ?Philesturnus carunculatus 1; Tui Prosthemadera novaeseelandiae 2; Anthornis melanura 1.

WAEWAEPA CAVE NO 1 Bones removed in 1952-1953. (National Museum) Identified by P.R.Millener.

Moas: Anomalopteryx didiformis 3; Dinornis giganteus 1; D. novaezealandiae 2.

Kiwi Apteryx australis 2; Weka Gallirallus australis 1; Gallinula hodgeni 2; Rail Aptornis otidiformis 1.

WAEWAEPA CAVE NO 2 Bones removed in 1952-1953. (National Museum) Identified by P.R.Millener.

Moas: Dinornis novaezealandiae 1.

Kiwi Apteryx australis 1; Weka Gallirallus australis 6; Takahe Porphyrio mantelli 1; Rallidae indet. 1; Finsch's Duck Euryanas finschi 1; Kakapo Strigops habroptilus 3.

WAEWAEPA CAVE NO 5 Bones removed in 1952-1953. (National Museum) Identified by P.R.Millener.

Moas: Dinornis novaezealandiae 1; Anomalopteryx didiformis 1.

Rail Aptornis otidiformis 1.

WAEWAEPA CAVE NO 6 Bones removed in 1952-1953. (National Museum) Identified by P.R.Millener.

Moas: Anomaloptryx didiformis 1.

Rail Aptornis otidiformis 1; Takahe Porphyrio mantelli 1; Kokako Callaeas cinerea 1.

WAEWAEPA CAVE NO 7 Bones removed in 1952-1952. (National Museum) Identified by P.R.Millener.

Moas: Dinornis giganteus 1.

WAEWAEPA CAVE NO 9 Bones removed in 1952-1953. (National Museum) Identified by P.R.Millener.

Moas: Dinornis novaezealandiae 1; D. struthoides 2; Dinornis sp. 1; Anomalopteryx didiformis 3.

Goose Cnemiornis septentrionalis 2; Rail Aptornis otidiformis 1; Takahe Porphyrio mantelli 1; Pigeon Hemiphaga novaeseelandiae 2; Kakapo Strigops habropilus 1; Megaegotheles novaezealandiae 1; Kakako Callaeas cinerea 1.

MANGATORO VALLEY Bones removed 1914. Identified by P.R.Millener.

Dinornithidae indet. - "three skeletons, nearly complete, in cave 1400 feet above sea-level" - Hill 1914.

PUKETOI RANGE Bones identified by P.R.Millener:

Moas: Anomalopteryx didiformis 4.

PORI Bones identified by P.R.Millener:

Moas: Dinornis sp. 1; Dinornis novaezealandiae 1.

References:

Millener P.R. 1981 The Quaternary Avifauna of the North Island, New Zealand. Unpub. Ph.D. thesis, University of Auckland. xxviii + 897 pp. 2 vols.

Worthy T. 1986 pers. comm.

APPENDIX TWO

LITHOSTRATIGRAPHY OF THE PUKETOI RANGE

The following section describes the stratigraphy of the Puketoi Range. This is mainly based on the work of Harmsen (1984a, 1984b, 1985), who differentiated stratigraphic units of the Te Aute Group on the basis of gross lithology, independent of any age control. Some formation boundaries, however, coincide with stage boundaries. Harmsen (1984b) measured and described three stratigraphic sections within the range (Appendix Three). These sections were used by the author to trace beds along the range, and for the subsequent drawing of the geology map (see back pocket).

Waewaepa Formation (adapted from Ongley 1935)

Definition: Ongley (1935), in describing the greywacke of the southern end of the Waewaepa Range, first termed this formation the Waewaepa Series. Lillie (1953) elevated the greywackes in the range to the Greywacke Group. Kingma (1962) named the greywacke, Wakarara Greywacke, based on the occurrence of upper Jurassic plant spores and the identification of the fossil Buchia hochstetteri Fleming. The greywacke has subsequently been reclassified by Neef (1967, 1974, 1984) as the Waewaepa Formation, when he described greywacke and argillites exposed at Castle Hill in the Eketahuna district. This is the oldest rock exposed in the area, forming the basement rock of the region and is covered unconformably by younger sediments.

Distribution and thickness: The greywacke forms the basement rock of the area, with the Waewaepa Range representing a basement high uplifted by plate tectonic movement. Within the study area, the greywacke is confined to the Waewaepa Range. The thickness of the greywacke is unknown.

Lithology: Greywacke of the Waewaepa Range is characterised by true greywacke forming a large part of the rock, but with sandstones, jasperites, argillites, mudstone, shales, and limestones also present (Lillie 1953).

Contact relationship: The greywacke forms the basement rock, overlain by Mangatoro Formation of the Te Aute Group, along the eastern flanks of the Waewaepa Range and western side of the Puketoi Range.

Known age range: Kingma (1962) identified upper Jurassic plant spores and the Lamellibranch, Buchia hochstetteri Fleming in the greywacke. This indicated a Jurassic age of the rock.

Te Aute Group (adapted from Hector 1887)
(Individual formations are described separately below)

Definition: The group's name is derived from the township of Te Aute (Grid Ref. V22/210458) at the foot of the Raukawa Range. Te Aute limestone was first mentioned by Hector (1887) and formally defined as Te Aute Formation by Lillie (1953). Harmsen formally defined the Te Aute Group as "...all marine sediments overlying the regional unconformity, at places at uppermost Miocene or within the Pliocene, and underlying mostly with angular unconformity, the Kumeroa Formation of southern Hawke's Bay, and Petane Formation or Kidnappers Group of central Hawke's Bay. At a few places it is concordant with the Kumeroa or Petane Formation, but its upper boundary is marked by a lithologic change from barnacle-rich limestone to muddy sandstone or sandy mudstone." (Harmsen 1985, p. 416-417) She identified six formations and one member within the group. Of these, four formations are found in the Puketoi Range.

Neef (1967, 1974, 1984) mapped the southern end of the Puketoi Range. He identified the Eketahuna and Makuri Groups, Kapitean to Nukumaruan in age (early Pliocene to early Pleistocene). This is approximately equivalent to the Te Aute Group formally identified by Harmsen (1984a, 1985).

Distribution and thickness: The Te Aute Group crops out discontinuously along the eastern hill country and coastline of central and southern Hawke's Bay. Small remnants remain along the eastern side of the Ruahine Range. The group covers the majority of the Puketoi Range shown in the geology map (back pocket). Isopachs of the Te Aute Group give thicknesses of 300 m along the northern and central sections of the Puketoi Range (Fig. A.1).

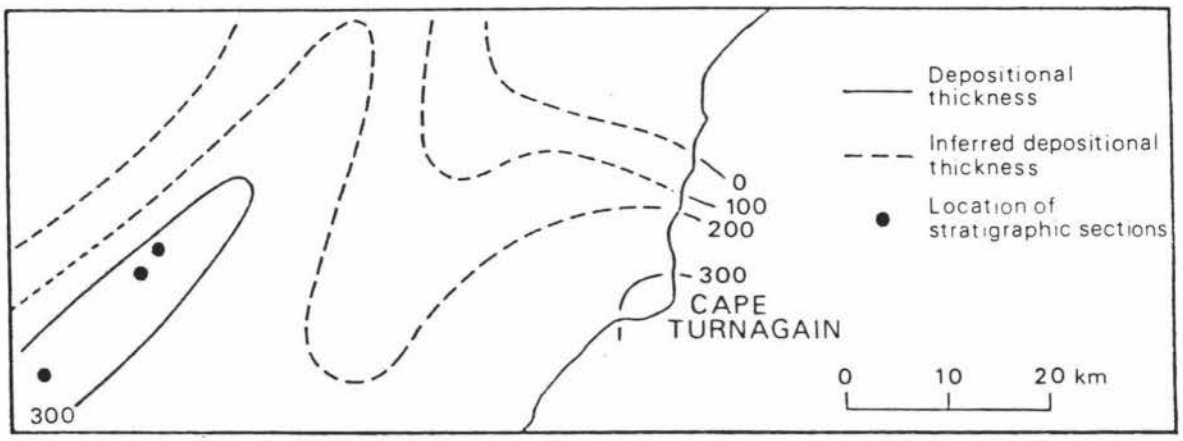

Figure A.1 Isopach map (in metres) of the Te Aute Group in southern Hawke's Bay. (From Harmsen 1985).

Lithology: The Te Aute Group is characterised by barnacle-rich coquina limestone and calcareous sandstone, interbedded in thicker terrigenous deposits of siltstone and mudstone, occasionally sandy or carbonaceous, but generally homogenous, and fine to medium-grained sandstone (Harmsen 1984a, 1985). Rapid vertical and lateral facies changes are also characteristic of the group. Harmsen (1984a, 1985) believes this possibly reflects tectonic deformation, and glacio-eustatic fluctuations in sea levels, during the deposition of the sediment.

Contact relationships: The Te Aute Group rests unconformably on strata ranging in age from Jurassic to late Miocene. Along the eastern scarp slope of the Puketoi Range, the underlying rocks are Tongaporutuan sandstones and mudstones, while on the western side the group laps on to the basement greywacke of the Waewaepa Range which is Jurassic in age.

The Te Aute Group is concordantly overlain by muddy sandstones, and sandy mudstones of the Kumeroa Formation, along the Puketoi Range and eastern flanks of the Waewaepa Range.

Known age range: Using molluscan and foraminiferal fossils, Lillie (1953) and Beu et al. (1980) indicated that the Te Aute Group ranges in age from Kapitean to Mangapanian, that is, late Miocene to Pliocene in age, 6.0 to 2.0 million years.

Mangatoro Mudstone Formation (adapted from Lillie 1953)

Definition: Lillie (1953) named the formation after the Mangatoro River, which drains the northern end of the Puketoi Range, but did not indicate any type sections. Harmsen (1984a, 1985) designated an exposure along the Mangahei Road (Grid Ref. V23/926057 - 920062) as the type section. The Mangatoro Formation is the oldest and thickest of the Te Aute Group and consists predominantly of a mudstone unit. It rests unconformably on strata ranging in age from Jurassic to late Miocene, and is unconformably overlain by the Awapapa Limestone.

Distribution and thickness: The Mangatoro Formation overlies the Mapiri Formation on the eastern side of the Puketoi Range, and overlies Jurassic or older rock on the western side and on the eastern flanks of the Waewaepa range. Along the Puketoi Range, thickness varies from 209 m at Coonoor (Grid Ref. U24/784827-773833) to 238 m at Makuri (Grid Ref. T25/690671-680682).

Lithology: Mangatoro Formation is dominated by blue-grey, poorly indurated mudstone with abundant foraminiferal fossils and sparse, poorly preserved macrofossils (Harmsen 1984a, 1985). Along the eastern margin of the range, the formation is typically massive blue-grey mudstone with sparse macrofossils (Harmsen 1984a, 1985).

Contact relationships: Mangatoro Formation unconformably overlies Tongaporutua flysch strata (upper Miocene - not exposed in the Puketoi Range) or lateral equivalents with angular discordance of between two and eight degrees (Harmsen 1984a, 1985). On the western side of the Puketoi Range, and eastern flanks of the Waewaepa Range, it laps onto the Mesozoic basement high of the Waewaepa Range. The top of the formation along the Puketoi Range is taken to be immediately below the massive calcareous sandstone, at the base of the Awapapa Limestone (Harmsen 1984a, 1985).

Known age range: Fossils identified by Lillie (1953), Beu et al. (1980) and Hornibrook (cited in Harmsen 1985) indicate that the Mangatoro Formation ranges in age from Kapitean to mid-Waipipian, that is late Miocene to mid-Pliocene in age - approximately 6.0 to 3.0 million years.

Awapapa Limestone Formation (adapted from Sporli and Pettinga 1980)

Definition: Sporli and Pettinga (1980) introduced the informal name, Awapapa member, for interbedded coquina limestone, and crossbedded sandstone, which outcrop along the western part of the Maraetotara Plateau, north of Mount Kahuranaki (Grid Ref. V22/405495). Beu et al. (1980) mapped this unit as Te Mata Limestone in the Te Aute Subdivision. The Awapapa member was elevated by Harmsen (1984a, 1985) to formation status and formalised as Awapapa Limestone. The type section was defined as the uppermost sequence of limestone, exposed in the face below the northeastern ridge of Te Mata Peak (Grid Ref. V22/450596).

Awapapa Limestone is a thick limestone and calcareous sandstone unit, that unconformably overlies Mesozoic to Opoitian strata, and is concordantly overlain by Raukawa Formation along the Puketoi Range.

Distribution and thickness: Awapapa Limestone is developed extensively within the Puketoi Range. The formation thickness is highly variable, being thickest in the middle of the range - Coonoor, 50 m (Grid Ref. T24/784827-773833); Makuri, 76 m (Grid Ref. T25/690671-680682) - and thinning to the north and south.

Lithology: Awapapa Limestone consists of sandy and skeletal limestone, calcareous sandstone, minor conglomerates, and shellbeds. It is characterised by a variety of sedimentary structures, mainly well-developed tubular cross-bedded or trough cross-bedded units. Large-scale contemporaneous slump pockets and convolutions are common (Harmsen 1985). In the northern section of the range, a 10 m thick sandstone bed has developed between the upper and lower limestone beds. This wedges out to the south. This had not been noted by Harmsen (1984a, 1985) in her examination of the Te Aute Group, and is therefore considered by the author, to be a localised occurrance within the Puketoi Range.

Contact relationship: Awapapa Limestone in the Puketoi Range rests unconformably on the Mangatoro Formation and is concordantly overlain by Raukawa Mudstone. The upper boundary is marked by a distinctive lithological change from limestone, or calcareous sandstone, to massive siltstone, or silty sandstone (Harmsen 1984a, 1985).

Known age range: From the identification of macrofossils and foraminifera, Harmsen (1984a, 1985) concluded the Awapapa Limestone was mid-Waipipian in age, that is mid-Pliocene, approximately 3.0 to 2.6 millian years.

Raukawa Mudstone Formation (adapted from Harmsen 1984a)

Definition: The name Raukawa Mudstone is derived from the Raukawa Range, with the type section found along the Te Onepu Road (Grid Ref. V22/206484 - 119490) (Harmsen 1984a, 1985).

Raukawa Mudstone consists predominantly of mudstone. It concordantly overlies Awapapa Limestone, and is concordantly overlain by Te Onepu Limestone.

Distribution and thickness: The formation is exposed along the eastern scarp slope of the Puketoi Range. Thickness varies along the range, from 40 m at Makuri (Grid Ref. T25/690671-680682) to 59 m at Coonoor (Grid Ref. T24/784827-773833) (Grid Ref. T24/654704).

Lithology: The formation in the Puketoi Range, consists of massive, calcareous, blue-grey silty sandstone and sandy siltstone, with a few thin oyster beds and concretionary layers mostly near the top of the formation (Harmsen 1984a, 1985).

Contact relationship: Raukawa Mudstone concordantly overlies Awapapa Limestone along the Puketoi Range, and is in turn concordantly overlain by Te Onepu Limestone. Along Towai Road, the formation is sharply overlain by sandy grainstone of Te Onepu Limestone (Harmsen 1984a, 1985).

Known age range: Macrofossils indicate an age range of mid-Waipipian to mid-Mangapanian for the Raukawa Formation (Harmsen 1984a, 1985). This is mid to late Pliocene, approximately 2.6 to 2.2 million years.

Te Onepu Limestone Formation (adapted from Harmsen 1984a)

Definition: The name Te Onepu Limestone is derived from Te Onepu village (Grid Ref. V22/166513) and the type section on Te Onepu Road (Grid Ref.

V22/198493 - 195494) (Harmsen 1984a, 1985).

Te Onepu Limestone is a thick, predominantly limestone unit. It rests concordantly on Raukawa Mudstone, and unconformably underlies Kumeroa Formation, along the Puketoi and Waewaepa Ranges.

Distribution and thickness: Te Onepu Limestone forms the caprock over much of the dip slope of the Puketoi Range, being overlain in places by Kumeroa Formation. Much of the original surface has been eroded. Thickness at Makuri (Grid Ref. T25/690671-680682) is 30 m, and at Coonoor (Grid Ref. T24/784827-773833) 29+ m (eroded).

Lithology: The formation along the Puketoi Range is characterised by well-bedded, coarse-grained, barnacle-rich lime-grainstone, with less common cross-bedded barnacle, or skeletal-rich grainstone, and bioturbated fine-grained calcareous sandstone (Harmsen 1984a, 1985)

Contact relationships: The lower boundary of Te Onepu Limestone is concordant with the underlying Raukawa Mudstone. The upper contact is rarely seen because of erosion. The exception is where it is concordantly overlain by siltstone, followed by limestone of Kumeroa Formation (Harmsen 1984a, 1985).

Known age range: Macrofossils indicate that the Te Onepu Limestone as Mangapanian in age (Kingma 1971; Beu et al. 1980), that is late Pliocene to early Pleistocene(approximately 2.2 to 1.85 million years).

Kumeroa Formation (adapted from Lillie 1953)

Definition: Named after beds at Kumeroa (Grid Ref. T24/643920), on the western side of the Waewaepa Range, this formation consists largely of argillaceous sandstones, sandy mudstones, and detrital limestones (Lillie 1953). The formation was divided by Lillie (1953) into upper and lower Kumeroa Formations, with a lithological break at the base of the upper Kumeroa Formation.

Distribution and thickness: The Kumeroa Formation outcrops discontinuously over much of the Puketoi and Waewaepa Ranges. Thickness varies from approximately 40 m, on Waewaepa Station (Grid Ref.

U24/795875), to over 150 m at grid reference U24/713780.

Lithology: Lillie (1953) identified two limestone horizons, separated by argillaceous sandstones and sandy mudstones, within the formation. The base of the formation is usually represented by a shelly, detrital limestone, which rests on Te Aute beds.

Contact relationship: The lower boundary of the formation is precise, with faunal and lithological changes. Lillie (1953) identified an unconformity between this formation, and the underlying Te Aute Group, but Harmsen (1984a, 1985) states that the Kumeroa Formation is concordant with the underlying Te Onepu Limestone, along the Puketoi Range. The upper boundary has been eroded away.

Known age distribution: Faunal evidence indicates that the Kumeroa Formation is Nukumaruan in age Lillie (1953), that is early to mid-Pleistocene, approximately 1.85 to 1.15 million years in age.

APPENDIX THREE

STRATIGRAPHIC SECTIONS OF THE TE AUTE GROUP IN THE PUKETOI RANGE

From Harmsen,F.J. 1984 Stratigraphic sections of the Pliocene Te Aute Group in Southern Hawke's Bay, N.Z.. Publication of Geology Department, Victoria University of Wellington. No. 29.

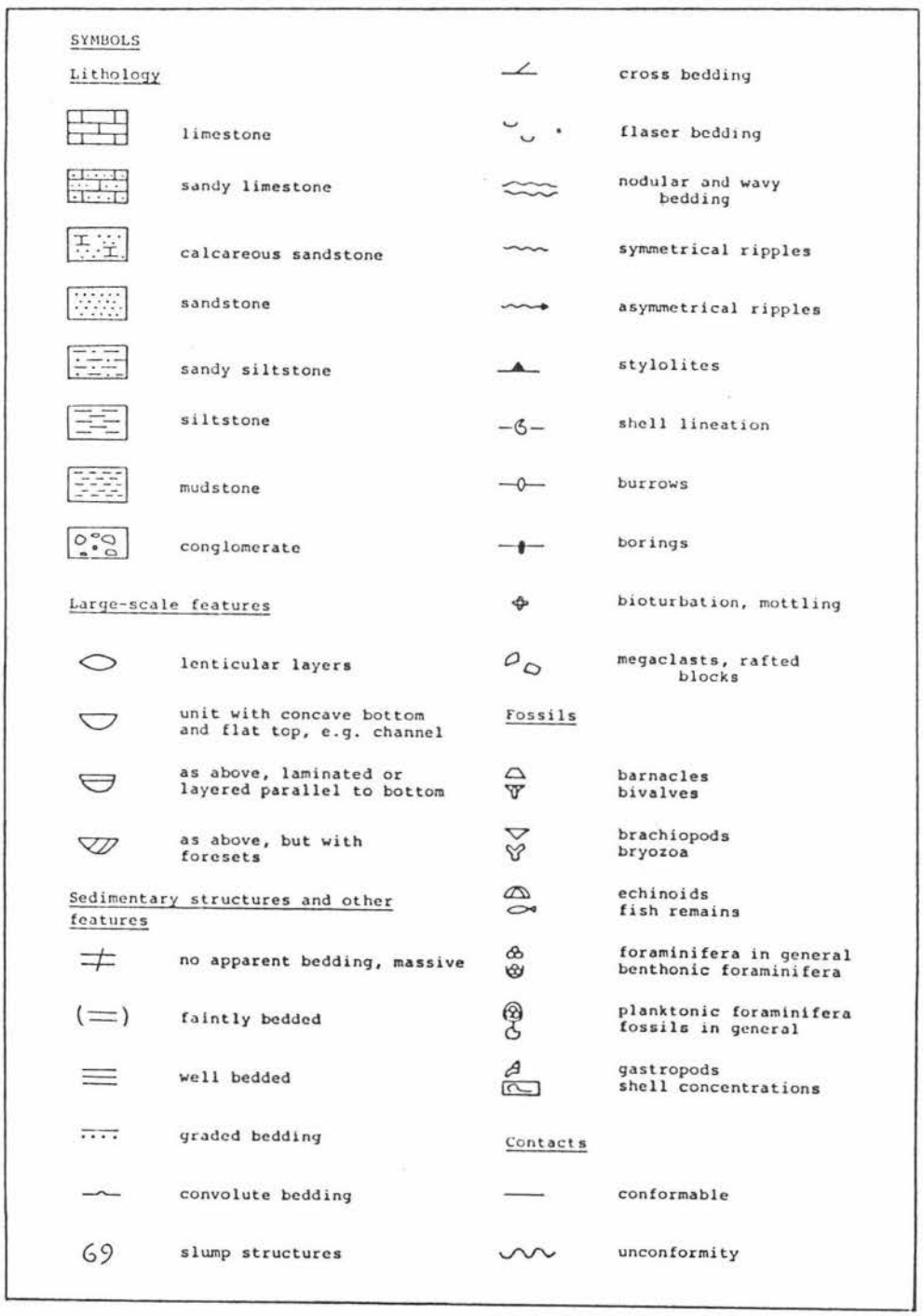

COONOOR (CO) REFERENCE SECTION

N150/616273-604279; U24/784827-773833 SCALE 1:1000

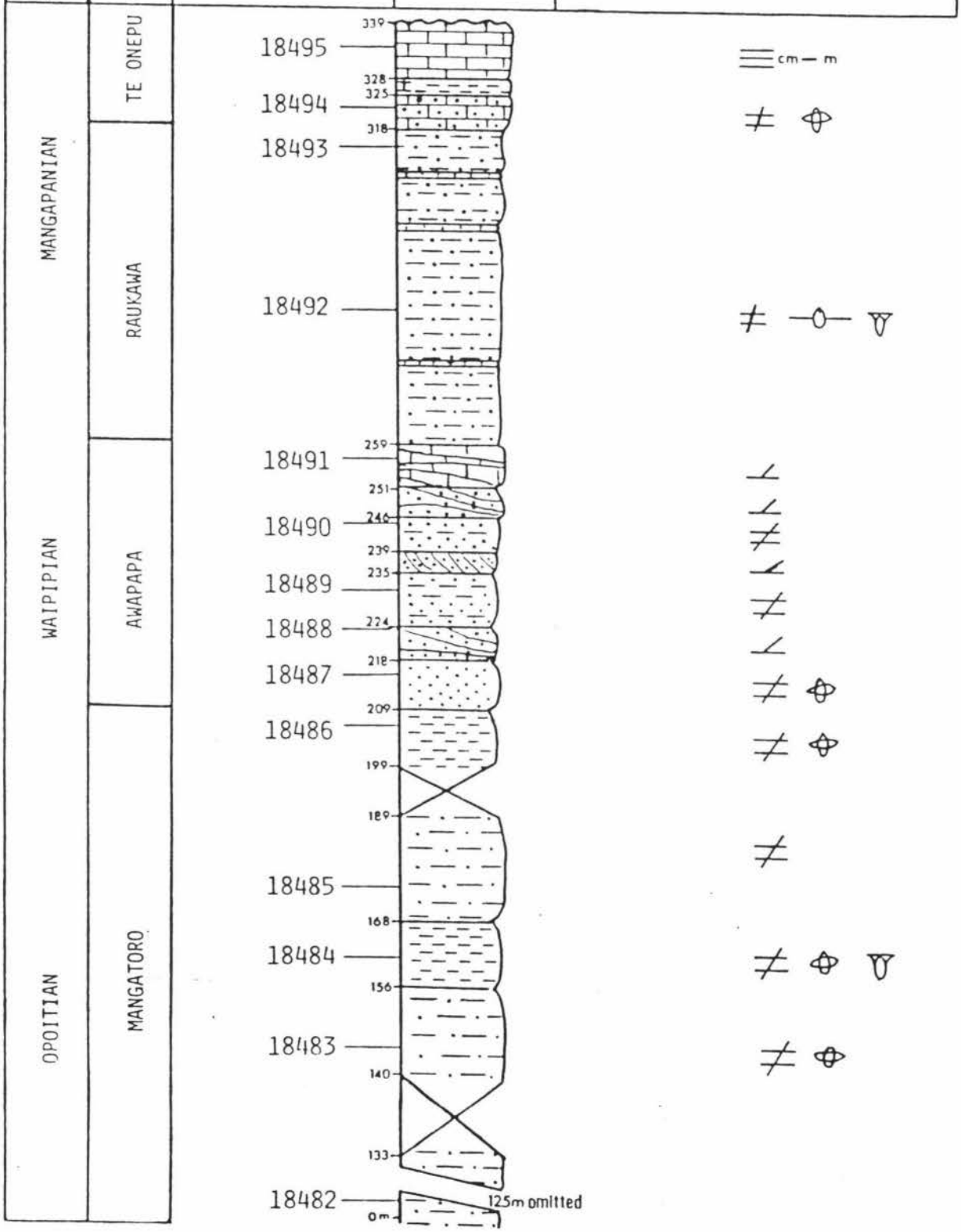

DESCRIPTION

- eroded surface -

328-339m
Barnacle-rich grainstone, grey-yellow, fine-grained, poorly cemented, in beds from 0.2 to 1.8m.

- sharp contact -

325-328m
Calcareous sandy siltstone, grey, moderately soft, generally poorly cemented but with some layers, up to 20cm thick, well-cemented and harder. Abundant macrofossils, mainly bivalves.

- sharp contact -

318-325m
Terrigenous sandy grainstone, light grey to yellow-grey, very fine-grained, homogeneous. Strongly bioturbated.

- sharp contact -

259-318m
Silty sandstone, blue-grey, moderately hard, homogeneous in which bedding can be recognised only by irregular layers of fossils, mainly Ostrea valves. Abundant mud-infilled burrows, up to 1cm across. Occasional concretionary layers, up to 40cm thick, becoming more common towards top of unit. Rare lenses of mudstone.

- sharp contact -

251-259m
Barnacle/mollusc-rich grainstone, grey-yellow, coarse-grained, well-sorted, moderately well-cemented. Large-scale, low-angle planar cross-bedding.

- sharp contact -

246-251m
Sandstone, brown, moderately soft, fine to medium-grained, containing large-scale planar to tangential cross-beds.

- gradational contact -

239-246m
Sandstone, brown, soft, fine to medium-grained, laminated. Common mudstone beds, up to 4cm thick.

235-239m - gradational contact -
Sandstone, yellow-brown, soft, medium-grained, with high-angle, large-scale planar to tangential cross-beds.

224-235m - sharp contact -
Sandstone, brown, soft, fine to medium-grained, laminated. Common mudstone beds, up to 2cm thick.

- gradational contact -

218-224m
Sandstone, brown, moderately soft, fine to medium-grained. Low-angle, large-scale planar cross-beds

- gradational contact -

209-218m
Sandstone, brown to grey-brown, soft, medium-grained, massive.

- sharp contact -

199-209m
Mudstone, blue-grey, soft, massive, rare, scattered fossils.

189-199m
Covered interval.

168-189m
Sandy siltstone, blue-grey, soft, massive, sparsely fossiliferous.

- sharp contact -

156-168m
Mudstone, grey and blue-grey, soft, massive, with common, scattered molluscs.

- sharp contact -

0-156m (small intervals not exposed).
Sandy siltstone, blue-grey, soft to moderately soft, massive, rare, scattered macrofossils.

- lower boundary not exposed -

MOANUI (MU) — REFERENCE SECTION

N150/566238; U24/738796 — SCALE 1:500

NZ STAGE	FORMATION	SAMPLE NUMBER	GRAPHIC LOG	ADDITIONAL GRAPHICS
MANGAPANIAN	TE ONEPU	18497 18496	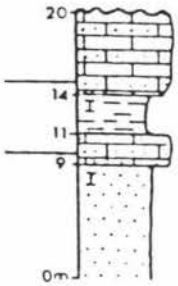	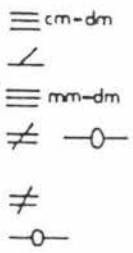

DESCRIPTION

- eroded surface -

14-20m

Alternating barnacle-rich grainstone, yellow-grey, coarse-grained, moderately well-sorted, massive, well-cemented, and terrigenous sandy grainstone, light yellow, fine-grained, moderately sorted, small-scale planar cross-bedding, poorly cemented.

- sharp contact -

11-14m

Calcareous siltstone, grey, sandy, fossiliferous. Preferentially cemented beds.

- sharp contact -

9-11m

Terrigenous sandy grainstone, grey-yellow, fine-grained, unbedded. Common mud-infilled burrows, up to 1cm across and 4cm long. Moderately cemented.

- sharp contact -

0-9m

Calcareous sandstone, brown-grey, moderately soft, massive, fossiliferous.

- lower contact not exposed -

MAKURI (MK) — REFERENCE SECTION

N154/518100-506112; T25/690671-680682 — SCALE 1:1000

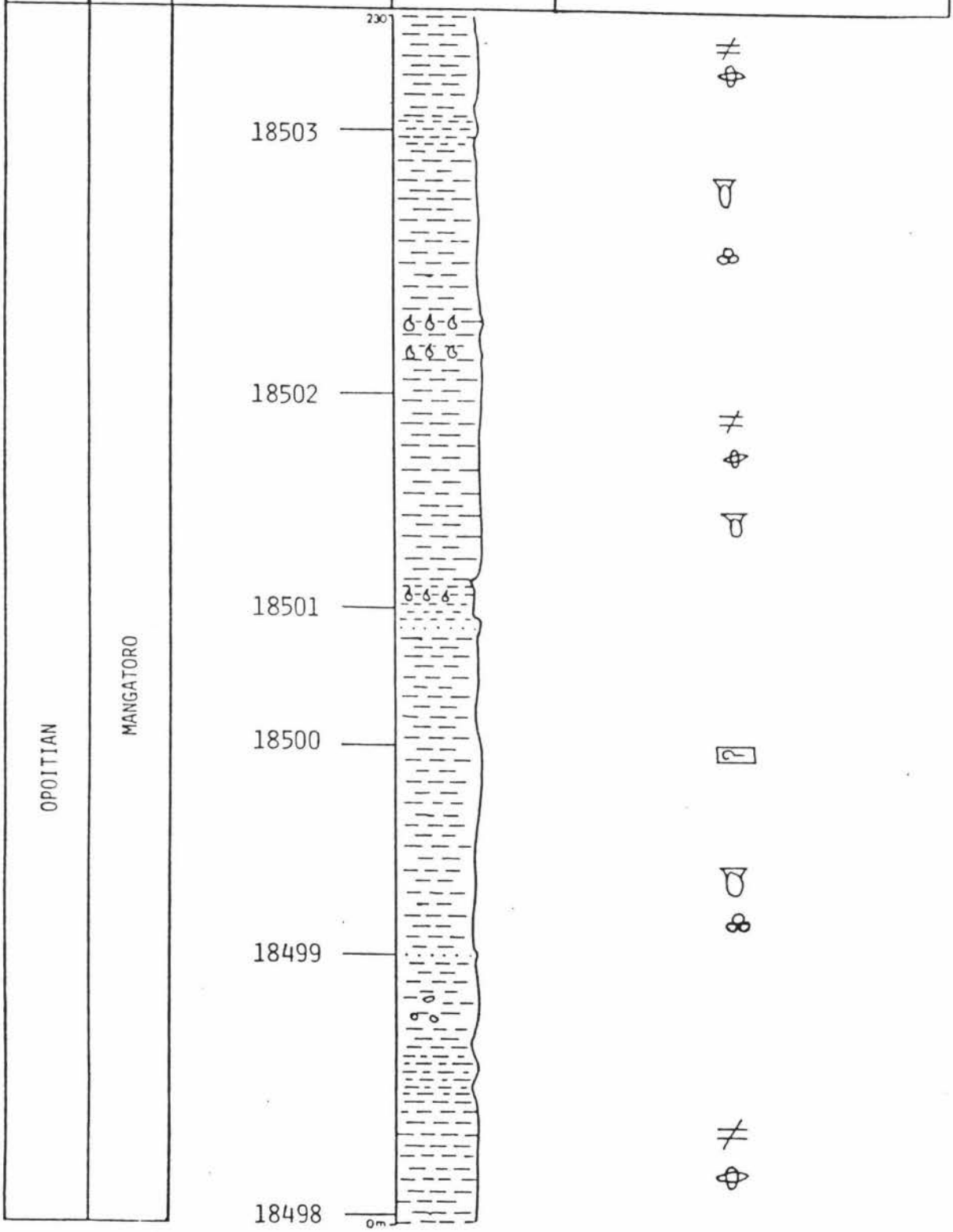

DESCRIPTION

- gradational, indistinct contact -

0-238m

Siltstone, blue-grey to medium grey, moderately soft to moderately hard, generally massive but with rare indistinct to laminated horizons. Contains common, thick (5 to 8m) beds of massive, medium-grey clayey siltstone, and occasional, thin (1 to 4cm) sandstone layers. A few irregular layers of fossils, mainly specimens of Ostrea, Phialopecten, and Dentalium. Occasional scattered, discoidal concretions, and rare, thin (0.5 - 5cm) concretionary layers. Very rare carbonaceous horizons. Vertical and sub-horizontal burrows containing spreiten, up to 2cm across and 9cm long, are common in a few horizons. Some scattered macrofossils, mainly thin-shelled bivalves.

- lower contact not exposed -

MAKURI (MK) — REFERENCE SECTION

N154/518100-506112; T25/690671-680682 — SCALE 1:1000

NZ STAGE	FORMATION	SAMPLE NUMBER	GRAPHIC LOG	ADDITIONAL GRAPHICS
MANGAPANIAN	TE ONEPU	18513		
		18512		
		18511		
	RAUKAWA			
		18510		
WAIPIPIAN	AWAPAPA	18509		
		18508		
		18507		
		18506		
		18505		
	MG	18504		

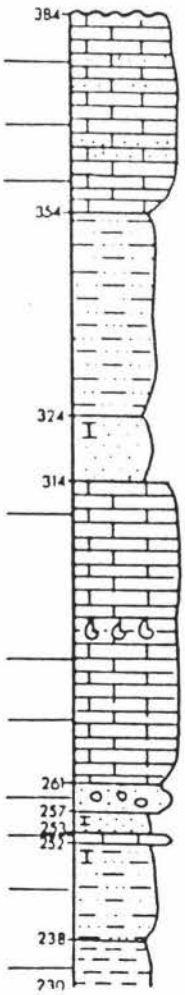

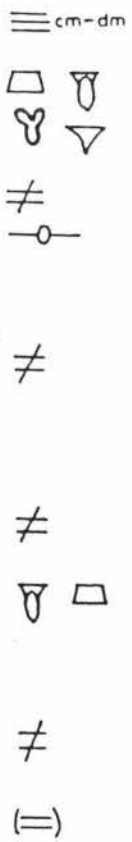

DESCRIPTION

- concordant contact with Kumeroa Formation -

354-384m
Alternating barnacle-rich grainstone, yellow-grey, fine-grained, moderately well-sorted, laminated, well-cemented, in beds from 5-20cm, and terrigenous sandy grainstone, brown-yellow, fine to medium grained, moderately sorted, massive, poorly to moderately well-cemented, in beds from 5 to 15cm.

- sharp contact -

324-354m
Silty sandstone, blue-grey, soft to moderately hard, massive, common, scattered bivalves.

- sharp contact -

314-324m
Calcareous sandstone, orange-brown, weathered, soft, massive.

- sharp contact -

261-314m
Barnacle-rich grainstone and mollosc-rich packstone/grainstone. Barnacle-rich grainstone is brown-yellow, coarse-grained, very well-sorted, massive, well-cemented. Mollusc-rich packstone/grainstone is yellow-brown, fine to very coarse-grained, poorly sorted, massive, moderately to well-cemented, packed full of small bivalves and a few gastropods. Occasional shell beds (10-30cm) of mainly Ostrea and Phialopecten valves in a coarse sandy, bioclastic matrix.

- sharp contact -

257-261m
Pebbly rustone, containing abundant angular to subangular limestone clasts up to 5cm long, and common, small bivalves in a coarse, moderately cemented, sandy matrix.

- erosional contact, relief 2 to 5cm -

253-257m
Calcareous sandstone, grey-yellow, soft, massive.

- highly irregular eroded contact, relief up to 8cm -

252-253m
Mollusc-rich packstone, grey, fine-grained, very well-cemented. Only moulds and castes of molluscs preserved due to preferential leaching of aragonitic shells.

- highly irregular eroded contact, relief up to 5cm -

238-252m
Calcareous silty sandstone, brown-yellow, weathered in places to orange-brown, soft, massive, though very rare muddy laminations.

APPENDIX FOUR

DATA COLLECTED FROM EXAMINATION OF WATER SAMPLES

The data given in this appendix was collected from the 15 water sampling sites in the Puketoi Range. The following abbreviations have been used:

DBT: Dry Bulb Temperature

WBT: Wet Bulb Temperature

RH: Relative Humidity

WT: Water Temperature

$CaCO_3$: Calcium carbonate content of the water sample

$MgCO_3$: Magnesium carbonate content of the water sample

Total H: Total Hardness of the water sample. This is $CaCO_3$ and $MgCO_3$ combined

*: No information collected.

Site 1 - Mangatoro Stream

(Grid Ref. U24/799927)

Date	Time	DBT (°C)	WBT (°C)	RH %	WT (°C)	$CaCO_3$ (mg l^{-1})	$MgCO_3$ (mg l^{-1})	Total H (mg l^{-1})	pH
7 3 86	1015	15.0	13.3	84	14.5	179.8	9.70	191.3	7.6
15 3 86	1520	22.7	20.5	82	21.0	107.3	8.07	116.9	7.7
22 3 86	908	13.8	11.1	73	13.0	134.8	9.53	146.2	8.0
2 4 86	910	14.4	12.5	81	12.2	151.0	9.01	161.7	8.1
6 4 86	1000	20.5	13.8	47	14.0	113.6	9.01	124.3	8.1
13 4 86	930	15.0	12.2	74	12.0	146.0	7.97	155.5	7.9
20 4 86	1045	14.1	12.7	89	12.3	122.3	9.70	133.8	7.8
26 5 86	1500	23.3	17.2	53	17.7	88.6	9.25	99.6	7.6
5 5 86	1015	11.3	10.0	85	11.0	110.6	8.32	120.4	7.4
11 5 86	1050	17.5	13.0	61	12.2	107.3	10.05	119.3	8.0
24 5 86	940	5.2	4.1	85	7.2	101.8	9.29	112.9	7.2
5 6 86	925	10.5	7.5	65	8.4	82.4	8.04	91.9	7.4
8 6 86	1010	12.5	10.8	85	9.9	111.8	8.84	122.3	7.3
15 6 86	1015	8.3	6.1	73	7.8	87.4	8.46	97.4	7.8
22 6 86	900	11.9	9.4	74	9.4	92.4	8.39	102.3	7.3
27 6 86	1050	9.4	7.7	79	8.3	86.9	8.66	97.1	7.5
15 7 86	1010	3.3	3.3	100	6.0	94.8	9.56	106.2	7.5
22 7 86	1025	5.5	4.7	90	6.5	119.8	9.01	130.5	7.6
27 7 86	1030	10.5	9.1	84	8.2	84.9	8.35	94.8	7.3
6 8 86	950	7.5	6.6	89	7.9	90.4	8.66	100.6	7.4
14 8 86	1000	7.5	6.9	93	7.6	72.4	8.14	82.0	7.2
19 8 86	1015	10.0	8.3	80	8.6	92.4	9.39	103.5	7.3

Site 2 - Mangatoro Stream

(Grid Ref. U24/762842)

Date	Time	WBT (°C)	DBT (°C)	RH %	WT (°C)	$CaCO_3$ (mg l^{-1})	$MgCO_3$ (mg l^{-1})	Total H (mg l^{-1})	pH
7 3 86	1040	15.2	13.3	81	14.5	144.8	8.01	154.3	8.2
15 3 86	1535	22.5	18.3	66	18.0	102.3	8.07	111.9	7.7
22 3 86	930	13.8	11.1	73	13.0	117.3	8.39	127.3	8.1
2 4 86	930	13.8	11.6	78	12.0	129.8	8.32	139.7	8.1
6 4 86	1020	19.1	14.7	62	14.0	115.6	7.97	125.0	8.2
13 4 86	940	14.4	11.6	73	12.5	132.8	7.45	141.6	8.0
0 4 86	1100	15.8	13.8	81	13.1	122.3	8.49	132.4	7.9
6 4 86	1520	20.5	15.0	54	15.1	110.3	8.46	120.4	7.5
5 5 86	1040	10.2	9.1	87	11.1	99.8	7.97	109.3	7.5
1 5 86	1110	16.1	13.0	72	12.3	99.8	9.01	110.5	7.5
4 5 86	1005	6.6	4.7	75	8.5	92.4	8.32	102.2	7.3
5 6 86	938	9.1	6.1	63	8.5	78.4	7.62	87.4	7.6
8 6 86	1030	11.6	10.0	82	10.1	106.1	8.11	115.7	7.4
5 6 86	1035	8.6	6.3	72	8.8	87.4	8.14	97.0	7.6
2 6 86	913	10.8	9.1	82	9.5	90.9	7.97	100.3	7.4
7 6 86	1105	8.3	6.6	79	8.7	83.6	8.32	93.5	7.5
15 7 86	1035	8.6	8.0	94	8.6	84.9	8.56	95.0	7.6
22 7 86	1048	6.1	5.0	85	7.8	106.3	7.66	115.4	7.7
27 7 86	1047	14.1	9.1	52	8.8	84.9	7.28	93.5	7.6
6 8 86	1018	8.8	7.7	86	8.1	80.9	7.38	89.6	7.4
15 8 86	1015	6.6	6.1	93	8.0	75.1	7.97	84.6	7.2
19 8 86	1040	9.1	7.7	83	9.2	79.4	8.39	89.3	7.1

Site 3 Cave Resurgence, Mangatoro Stream

(Grid Ref. U24/737827)

Date	Time	DBT (°C)	WBT (°C)	RH %	WT (°C)	$CaCO_3$ (mg l^{-1})	$MgCO_3$ (mg l^{-1})	Total H (mg l^{-1})	pH
7 3 86	1055	13.8	11.3	75	11.5	194.7	7.30	203.5	7.9
15 3 86	1550	21.1	17.2	67	12.5	152.3	6.58	160.1	7.9
22 3 86	945	13.3	10.5	72	11.5	149.8	6.93	158.0	8.1
31 3 86	1045	11.3	9.7	82	11.0	143.5	7.10	152.0	8.2
2 4 86	940	13.6	11.3	78	11.2	137.3	6.93	145.5	8.1
6 4 86	1030	19.1	14.7	62	11.7	130.8	6.76	138.8	8.1
13 4 86	950	13.3	10.5	72	11.2	156.0	5.89	163.0	8.0
16 4 86	1415	16.6	14.4	79	11.3	152.8	6.58	160.6	7.8
20 4 86	1112	15.8	13.8	82	11.2	152.8	6.58	160.6	7.8
24 4 86	1515	16.3	13.8	76	11.7	142.8	7.35	151.5	7.5
26 4 86	1535	*	*	*	11.6	143.5	7.45	152.4	7.5
5 5 86	1050	9.7	9.1	94	10.9	145.3	6.93	153.5	7.5
11 5 86	1117	16.6	13.3	70	11.2	122.3	8.04	131.9	7.9
24 5 86	1015	7.2	6.6	93	10.4	133.8	7.28	142.4	7.7
1 6 86	1040	10.5	8.8	81	9.5	136.1	6.93	144.3	7.4
5 6 86	950	9.1	6.1	63	10.2	104.8	6.72	112.8	7.8
8 6 86	1040	11.1	9.7	85	10.6	152.8	6.93	161.0	7.4
15 6 86	1045	7.5	5.2	72	10.0	98.6	7.69	107.7	7.8
22 6 86	918	11.1	9.7	85	10.6	124.8	7.28	133.5	7.4
27 6 86	1110	8.3	6.6	79	10.2	118.3	7.28	127.0	7.6
15 7 86	1115	9.1	7.7	83	10.0	143.0	7.14	151.5	7.7
22 7 86	1105	5.5	4.4	85	10.0	147.3	7.07	155.7	7.7
27 7 86	1100	9.4	8.6	90	10.2	127.8	6.44	135.5	7.3
6 8 86	1025	7.7	6.1	79	9.9	112.8	6.51	120.6	7.3
15 8 86	1030	6.1	4.7	82	9.7	109.8	8.14	119.5	7.5
19 8 86	1047	8.8	7.7	86	10.3	108.3	6.72	116.3	7.0
14 9 86	1315	10.2	8.0	74	10.2	105.1	6.58	112.9	*

Site 4 - Spring, Mangatoro Stream

(Grid Ref. U24/737824)

Date	Time	DBT (°C)	WBT (°C)	RH %	WT (°C)	$CaCO_3$ (mg l^{-1})	$MgCO_3$ (mg l^{-1})	Total H (mg l^{-1})	pH
7 3 86	1110	15.8	13.8	81	12.5	112.3	7.94	121.3	7.6
15 3 86	1600	21.6	18.0	70	13.5	77.4	7.28	86.0	7.5
22 3 86	955	12.7	9.7	69	12.5	87.4	8.49	97.4	8.0
2 4 86	947	13.8	11.6	78	11.8	88.6	8.49	98.7	7.8
6 4 86	1040	18.8	14.7	64	12.0	90.4	8.39	100.3	8.1
13 4 86	1000	13.3	12.2	89	11.7	102.3	8.73	112.7	7.8
20 4 86	1123	15.2	13.8	87	11.7	114.3	8.66	124.6	7.6
26 4 86	1540	*	*	*	11.8	103.6	9.70	115.1	7.6
5 5 86	1100	9.7	9.1	94	10.8	83.6	7.14	92.1	7.1
11 5 86	1125	15.8	12.5	68	11.2	84.9	9.18	95.8	7.9
24 5 86	1020	7.5	6.3	86	10.2	74.9	8.04	84.4	7.7
5 6 86	1015	9.7	6.6	63	10.1	69.4	7.45	78.2	7.8
8 6 86	1055	11.1	10.0	88	10.2	86.4	8.32	96.2	7.4
15 6 86	1105	6.9	5.0	75	9.8	68.6	8.14	78.3	7.7
22 6 86	930	11.1	9.4	82	9.8	76.4	8.04	85.9	7.4
27 6 86	1125	8.0	6.9	85	9.5	69.4	7.55	78.3	7.4
15 7 86	1135	9.4	7.7	80	9.0	73.4	8.00	82.9	7.6
22 7 86	1115	5.8	5.5	96	9.0	84.9	7.97	94.3	7.7
27 7 86	1110	8.8	8.6	97	9.0	76.6	7.21	85.2	7.3
6 8 86	1045	7.5	6.3	86	8.6	59.9	6.96	68.2	7.4
15 8 86	1107	6.3	5.2	86	7.9	57.4	6.83	65.5	7.6
19 8 86	1105	8.3	7.5	89	8.8	59.9	7.66	69.0	7.1

Site 5 PT17 Cave Resurgence, Mangatoro Stream

(Grid Ref. U24/731820)

Date	Time	DBT (°C)	WBT (°C)	RH %	WT (°C)	$CaCO_3$ (mg l^{-1})	$MgCO_3$ (mg l^{-1})	Total H (mg l^{-1})	pH
7 3 86	1125	12.7	11.3	86	12.0	97.3	7.30	106.1	7.5
15 3 86	1605	21.6	17.7	67	13.5	62.4	6.86	70.5	7.6
22 3 86	1007	14.4	11.1	68	12.5	82.4	8.25	92.1	7.9
2 4 86	----------			STREAM NOT FLOWING				----------	
6 4 86	----------			STREAM NOT FLOWING				----------	
13 4 86	----------			STREAM NOT FLOWING				----------	
20 4 86	----------			STREAM NOT FLOWING				----------	
26 4 86	----------			STREAM NOT FLOWING				----------	
5 5 86	1110	10.0	8.8	87	10.8	66.9	6.76	74.9	7.1
11 5 86	----------			STREAM NOT FLOWING				----------	
24 5 86	1030	5.0	4.4	93	10.1	69.9	7.48	78.8	7.7
5 6 86	1025	9.1	6.1	63	9.8	63.9	7.17	72.4	7.7
8 6 86	----------			STREAM NOT FLOWING				----------	
15 6 86	----------			STREAM NOT FLOWING				----------	
22 6 86	1715	10.2	8.8	84	9.6	69.9	7.28	78.5	7.4
27 6 86	1140	8.3	*	*	8.8	56.1	6.76	64.2	7.6
15 7 86	1140	8.6	6.1	69	9.0	58.6	7.66	67.7	7.5
22 7 86	1135	6.1	5.0	85	8.7	77.9	7.66	87.0	7.6
27 7 86	1115	8.8	7.7	86	8.4	53.6	6.76	61.7	7.3
15 8 86	1045	6.3	5.8	93	8.6	70.6	6.83	78.7	7.6
19 8 86	1056	8.8	7.5	82	9.2	69.4	7.80	78.6	7.1

Site 6 - Stream from the Waevaepa Range

(Grid Ref. U24/724817)

Date	Time	DBT (°C)	WBT (°C)	RH %	WT (°C)	$CaCO_3$ (mg l^{-1})	$MgCO_3$ (mg l^{-1})	Total H (mg l^{-1})	pH
7 3 86	1200	13.3	11.3	80	11.0	5.7	11.78	19.4	7.5
15 3 86	1430	20.0	18.8	90	13.5	3.9	7.07	12.3	7.4
22 3 86	1205	12.2	10.0	77	10.5	8.2	8.25	18.0	7.8
1 4 86	1645	10.2	8.6	81	9.7	8.7	8.46	18.7	8.2
6 4 86	1240	16.9	14.1	75	11.3	8.7	8.32	18.6	8.0
13 4 86	1217	12.2	9.7	74	10.4	9.7	7.62	18.7	7.8
20 4 86	1330	14.4	13.3	89	9.8	11.2	8.49	21.3	7.9
26 4 86	1430	16.1	14.1	81	11.3	8.4	9.18	19.3	7.8
5 5 86	1330	9.7	8.3	83	9.1	7.9	8.32	17.8	7.5
11 5 86	1350	15.2	13.3	81	9.8	11.2	8.49	21.3	8.0
24 5 86	1335	7.7	7.2	93	7.0	12.4	8.04	22.0	7.9
5 6 86	1205	8.3	6.6	78	7.5	10.4	7.69	19.6	7.9
8 6 86	1234	10.0	9.1	90	8.4	9.2	8.32	19.1	7.6
15 6 86	1235	3.3	2.7	92	6.6	6.4	8.66	16.7	7.8
22 6 86	1530	9.4	8.3	87	7.5	8.4	9.01	19.1	7.3
27 6 86	1307	7.2	*	*	6.6	8.7	8.49	18.8	7.5
15 7 86	1400	7.2	6.1	86	6.0	11.4	8.32	21.3	7.5
22 7 86	1520	3.8	2.7	83	5.7	15.9	8.49	26.0	7.7
27 7 86	1325	7.5	7.2	97	6.7	3.7	8.00	13.2	7.3
6 8 86	1330	7.5	6.9	93	5.9	9.9	8.32	19.8	7.6
17 8 86	1330	8.6	7.2	82	6.8	7.9	6.96	16.2	7.7
19 8 86	1255	8.3	8.3	100	7.0	10.7	7.80	19.9	7.3

Site 7 - Stream from the Waewaepa Range

(Grid Ref. U24/719812)

Date	Time	DBT (°C)	WBT (°C)	RH %	WT (°C)	$CaCO_3$ (mg l^{-1})	$MgCO_3$ (mg l^{-1})	Total H (mg l^{-1})	pH
7 3 86	1225	14.4	11.6	73	12.0	6.4	6.83	14.4	7.2
15 3 86	1410	22.7	18.3	65	14.5	4.9	6.31	12.4	7.4
22 3 86	1145	13.0	9.7	66	11.5	6.2	7.24	14.8	7.6
1 4 86	1630	10.0	8.6	83	10.0	6.9	7.62	16.0	8.1
6 4 86	1300	17.5	13.8	68	11.8	7.9	7.35	16.7	7.9
13 4 86	1200	12.7	9.4	66	11.1	8.4	7.10	16.9	7.7
20 4 86	1312	14.4	12.7	84	11.0	9.4	7.45	18.3	7.8
26 4 86	1405	19.7	14.4	59	12.4	7.4	8.32	17.3	7.8
5 5 86	1315	9.4	8.3	87	9.3	7.9	7.76	17.2	7.5
11 5 86	1335	14.4	12.5	81	10.4	10.4	7.76	19.6	8.0
24 5 86	1313	9.1	6.6	63	7.2	8.9	6.65	16.8	7.8
5 6 86	1150	8.3	6.1	72	7.3	11.4	6.86	19.6	7.9
8 6 86	1217	9.4	8.8	93	8.6	7.7	7.14	16.2	7.6
15 6 86	1225	3.0	2.5	92	6.6	6.9	7.83	16.2	7.7
22 6 86	1513	10.0	8.3	80	7.5	8.7	8.18	18.4	7.3
27 6 86	1250	7.5	*	*	6.5	7.9	7.45	16.8	7.5
15 7 86	1340	7.7	6.6	79	6.0	9.9	7.07	18.3	7.5
22 7 86	1500	3.8	2.7	83	5.4	14.7	7.42	23.5	7.7
27 7 86	1305	8.3	7.7	93	7.8	2.2	6.24	9.6	7.4
6 8 86	1315	7.7	6.6	86	6.2	8.9	7.24	17.5	7.5
17 8 86	1315	9.4	7.2	73	7.0	6.4	6.17	13.8	7.7
19 8 86	1234	9.4	7.7	79	7.1	11.9	6.72	19.9	7.3

Site 8 - PT17 Cave, Coonoor

(Grid Ref. U24/725814)

Date	Time	DBT (°C)	WBT (°C)	RH %	WT (°C)	$CaCO_3$ (mg l^{-1})	$MgCO_3$ (mg l^{-1})	Total H (mg l^{-1})	pH
7 3 86	1330	11.6	11.6	100	11.5	84.9	7.07	93.2	7.4
15 3 86	1300	11.6	11.6	100	11.8	69.9	7.28	78.5	7.3
22 3 86	1230	11.6	11.6	100	11.5	69.9	7.97	79.3	7.6
1 4 86	1720	11.9	11.3	95	11.2	71.1	8.07	80.7	7.5
6 4 86	1330	11.9	11.6	97	11.6	90.4	8.32	100.2	8.1
13 4 86	*	11.6	11.3	97	11.2	88.6	8.14	98.3	7.4
20 4 86	1400	11.9	11.3	95	10.8	106.1	7.69	115.2	7.5
26 4 86	1030	11.6	11.1	92	10.8	90.4	9.01	101.0	7.5
5 5 86	*	12.2	11.6	95	11.4	59.9	7.62	68.9	7.3
11 5 86	1415	12.2	11.9	97	10.7	73.6	8.39	83.6	7.6
24 5 86	1345	11.9	11.6	97	10.6	68.6	6.93	76.8	7.6
5 6 86	1230	11.1	10.8	97	10.2	62.4	7.17	70.9	7.5
8 6 86	1300	11.1	10.8	97	10.4	64.9	7.55	73.8	7.3
15 6 86	1300	10.0	10.0	100	10.1	62.9	8.14	72.5	7.5
22 6 86	1330	10.8	10.5	97	9.8	57.9	7.55	66.9	7.3
27 6 86	*	10.5	*	*	9.8	48.9	7.45	57.7	7.4
15 7 86	1420	10.0	10.0	100	10.0	70.1	7.45	79.0	7.5
22 7 86	1550	10.0	9.4	94	9.6	69.4	7.42	78.2	7.5
26 7 86	*	10.2	9.7	94	9.4	69.4	6.86	77.5	7.1
17 8 86	1400	11.3	11.3	100	9.4	70.6	6.93	78.8	7.4

Site 9 PT17 Cave, Coonoor

(Grid Ref. U24/725814)

Date	Time	DBT (°C)	WBT (°C)	RH %	WT (°C)	$CaCO_3$ (mg l^{-1})	$MgCO_3$ (mg l^{-1})	Total H (mg l^{-1})	pH
7 3 86	1330	12.7	12.2	95	12.5	9.9	7.94	19.4	7.3
15 3 86	1300	13.3	13.3	100	14.3	10.9	7.10	19.4	7.1
22 3 86	1230	11.6	11.6	100	11.5	6.4	8.32	16.3	7.6
1 4 86	1725	10.5	10.5	100	10.2	13.7	8.46	23.7	8.1
6 4 86	1340	12.5	11.6	92	11.6	11.2	8.73	21.6	8.0
13 4 86	*	11.6	11.6	100	10.7	14.9	8.73	25.3	7.6
20 4 86	----------	----------	----------	STREAM NOT FLOWING			----------	----------	
26 4 86	----------	----------	----------	STREAM NOT FLOWING			----------	----------	
5 5 86	*	10.8	10.2	95	9.5	9.4	7.90	18.8	7.5
11 5 86	1425	9.7	9.7	100	9.1	15.4	8.66	25.7	7.8
24 5 86	1355	7.7	7.7	100	7.2	11.7	7.62	20.7	7.8
5 6 86	1240	8.3	8.3	100	7.6	10.9	7.62	20.0	7.7
8 6 86	1310	9.1	8.8	97	8.6	10.9	7.80	20.2	7.5
15 6 86	1310	6.6	6.6	100	6.6	10.4	8.66	20.7	7.7
22 6 86	1340	9.4	9.4	100	7.1	12.9	8.39	22.9	7.3
27 6 86	*	7.2	*	*	7.0	9.4	8.66	19.7	7.4
15 7 86	1430	7.2	7.2	100	6.0	12.4	7.80	21.7	7.6
22 7 86	1600	5.5	5.5	100	5.7	15.9	8.25	25.7	7.5
26 7 86	*	6.6	6.6	100	5.5	4.2	7.66	13.3	7.2
17 8 86	1410	8.8	8.6	95	7.2	8.7	7.31	17.4	7.6

Site 10 - PT17 Cave, Coonoor

(Grid Ref. U24/725814)

Date	Time	DBT (°C)	WBT (°C)	RH %	WT (°C)	$CaCO_3$ (mg l^{-1})	$MgCO_3$ (mg l^{-1})	Total H (mg l^{-1})	pH
15 3 86	1300	12.2	12.2	100	13.9	26.2	7.23	34.6	7.1
22 3 86	1230	11.6	11.6	100	11.5	44.9	8.25	54.7	7.5
1 4 86	1730	11.3	10.5	92	11.0	53.6	7.97	63.1	8.1
6 4 86	1350	11.6	11.1	96	11.2	68.6	7.97	78.1	7.9
13 4 86	*	11.6	11.3	98	11.0	79.4	8.25	89.2	7.4
20 4 86	1420	10.0	10.0	100	10.7	106.1	7.80	115.3	7.5
26 4 86	1200	11.1	10.8	97	10.9	94.8	9.01	105.5	7.5
5 5 86	*	11.1	10.5	94	10.2	28.9	7.90	38.3	7.3
11 5 86	1430	10.5	10.5	100	10.4	66.4	8.39	76.3	7.6
24 5 86	1400	8.3	8.3	100	8.3	40.4	7.48	49.3	7.6
5 6 86	1250	8.8	8.3	94	8.5	*	*	*	*
8 6 86	1315	9.4	9.1	97	9.7	45.7	7.45	54.5	7.3
15 6 86	1320	7.7	7.7	100	8.8	44.4	8.25	54.2	7.5
22 6 86	1350	8.3	8.3	100	8.8	41.4	8.04	50.9	7.3
27 6 86	*	8.6	*	*	7.3	37.4	7.90	46.8	7.4
15 7 86	1440	6.9	6.6	97	8.0	33.9	7.97	43.4	7.6
22 7 86	1610	6.6	6.6	100	7.8	52.4	7.62	61.4	7.5
26 7 86	*	7.2	6.6	94	6.6	18.9	7.03	27.3	7.2
17 8 86	1415	8.3	8.3	100	7.6	33.7	7.00	42.0	7.5

Site 11 - PT17 Cave, Coonoor

(Grid Ref. U24/725814)

Date	Time	DBT (°C)	WBT (°C)	RH %	WT (°C)	$CaCO_3$ (mg l^{-1})	$MgCO_3$ (mg l^{-1})	Total H (mg l^{-1})	pH
15 3 86	1300	14.1	14.1	100	13.2	31.2	7.10	39.5	7.2
22 3 86	1230	12.5	12.2	98	11.5	42.4	8.39	52.4	7.6
1 4 86	1740	12.7	11.6	88	11.0	54.9	8.14	64.6	8.0
6 4 86	1400	12.2	11.9	98	11.0	71.9	8.39	81.8	7.9
13 4 86	*	13.3	12.2	89	11.0	80.4	8.32	90.2	7.4
20 4 86	1430	12.2	12.2	100	11.0	101.8	7.80	111.1	7.5
26 4 86	930	12.4	12.2	98	11.0	87.6	9.18	98.5	7.4
5 5 86	*	11.6	11.6	100	10.8	37.2	7.45	46.0	7.3
11 5 86	1440	11.6	11.6	100	10.6	69.9	8.66	80.2	7.6
24 5 86	1410	10.8	10.8	100	9.8	40.4	7.48	49.3	7.5
5 6 86	1300	10.8	10.0	92	9.6	*	*	*	*
8 6 86	1325	11.6	10.8	92	9.9	53.4	7.55	62.4	7.3
15 6 86	1330	10.5	10.2	98	9.8	59.1	7.83	68.4	7.5
22 6 86	1350	10.8	10.0	92	9.5	46.9	7.62	55.9	7.2
27 6 86	*	10.0	*	*	9.0	40.9	7.90	50.3	7.4
15 7 86	1450	9.4	8.3	87	8.0	36.4	7.97	45.9	7.6
22 7 86	1620	9.4	8.8	94	8.1	57.4	7.62	66.4	7.4
26 7 86	*	8.6	8.3	97	*	29.9	7.66	39.0	7.1
17 8 86	1420	9.4	8.8	94	8.2	38.9	6.93	47.1	7.4

Site 12 - Famous Five Cave Submergence

(Grid Ref. U24/741817)

Date	Time	DBT (°C)	WBT (°C)	RH %	WT (°C)	$CaCO_3$ (mg l^{-1})	$MgCO_3$ (mg l^{-1})	Total H (mg l^{-1})	pH
7 3 86	1455	15.5	13.3	78	11.5	167.3	6.52	175.0	7.7
15 3 86	1645	20.0	16.6	72	12.5	119.8	5.72	126.6	7.4
22 3 86	1045	13.8	11.1	73	11.0	137.3	6.93	145.5	7.7
2 4 86	1020	15.0	12.2	68	11.0	134.8	6.65	142.7	8.2
6 4 86	1150	19.1	14.7	62	11.3	142.3	6.58	150.1	7.9
13 4 86	1112	13.8	10.8	70	11.1	136.1	6.58	143.9	7.5
20 4 86	1223	15.0	14.1	92	11.0	154.8	5.82	161.7	7.6
26 4 86	1610	*	*	*	11.4	148.0	7.35	156.8	7.4
5 5 86	1225	10.2	8.3	77	10.8	140.8	7.10	149.2	7.4
11 5 86	1216	15.0	12.2	74	10.9	122.3	7.38	131.1	7.6
24 5 86	1240	10.5	7.5	65	10.7	129.8	5.96	136.9	7.4
5 6 86	1100	8.6	6.9	82	10.4	106.1	6.86	114.2	7.5
8 6 86	1132	10.5	9.4	88	10.6	152.8	6.24	160.2	7.9
15 6 86	1135	5.2	4.7	93	10.2	109.8	7.10	118.3	7.6
21 6 86	1150	10.2	9.7	94	10.3	126.1	7.45	134.9	7.4
15 7 86	1245	10.2	7.7	71	10.0	143.0	6.93	151.3	7.7
22 7 86	1324	5.5	4.4	85	10.2	152.8	6.89	161.0	7.6
27 7 86	1215	8.8	7.7	86	10.0	133.1	6.24	140.5	7.7
6 8 86	1207	7.2	6.1	86	10.0	111.8	6.58	119.6	7.2
19 8 86	1140	10.0	8.3	80	10.4	109.8	6.72	117.8	6.9
14 9 86	1210	10.5	8.3	75	10.2	106.1	5.89	113.1	*

Site 13 - Famous Five Cave Resurgence

Grid Ref. U24/740822)

Date	Time	DBT (°C)	WBT (°C)	RH %	WT (°C)	$CaCO_3$ (mg l^{-1})	$MgCO_3$ (mg l^{-1})	Total H (mg l^{-1})	pH
7 3 86	1520	15.5	12.2	68	11.5	157.3	6.14	164.7	7.6
15 3 86	1710	18.6	15.5	74	12.0	124.8	6.76	132.8	7.6
22 3 86	1107	14.7	11.9	78	12.0	132.3	6.58	140.1	7.7
2 4 86	1040	15.0	12.2	73	11.0	101.1	6.31	108.6	8.1
6 4 86	1212	18.6	14.7	66	11.7	144.8	5.82	151.7	7.7
13 4 86	1130	13.3	10.2	70	11.2	136.1	6.31	143.5	7.6
20 4 86	1245	16.1	14.1	81	11.7	159.3	5.61	165.9	7.6
26 4 86	1625	*	*	*	11.2	144.3	6.76	152.3	7.4
5 5 86	1245	9.7	8.0	80	10.6	139.3	6.58	147.1	7.4
11 5 86	1225	14.7	11.9	74	11.0	123.6	6.93	131.8	7.6
24 5 86	1237	9.7	6.9	66	10.4	135.8	5.54	142.4	7.5
5 6 86	1115	8.8	6.1	66	10.1	111.3	6.31	118.8	7.6
8 6 86	1148	10.0	8.8	87	10.4	156.3	6.10	163.5	7.8
15 6 86	1150	4.4	3.6	87	10.0	109.8	6.24	117.2	7.6
21 6 86	1000	9.1	8.8	97	10.2	124.8	6.93	133.0	7.5
15 7 86	1305	7.7	6.1	78	10.0	149.8	6.93	158.0	7.7
22 7 86	1345	5.8	4.1	77	10.0	147.3	6.55	155.1	7.7
27 7 86	1235	9.1	7.5	79	9.9	130.8	6.10	138.0	7.7
6 8 86	1224	7.2	6.1	86	10.1	118.3	6.51	126.1	7.2
19 8 86	1200	11.6	9.4	76	10.4	120.8	6.55	128.6	7.0
14 9 86	1225	9.7	7.7	76	10.2	112.1	6.10	119.3	*

Site 14 - Makuri River

(Grid Ref. T24/654704)

Date	Time	DBT (°C)	WBT (°C)	RH %	WT (°C)	$CaCO_3$ (mg l^{-1})	$MgCO_3$ (mg l^{-1})	Total H (mg l^{-1})	pH
8 3 86	1620	20.0	16.1	67	17.0	127.3	6.62	135.7	7.9
15 3 86	1745	20.0	17.2	76	18.0	89.9	6.24	97.3	7.8
22 3 86	1350	17.2	12.5	58	15.0	112.3	7.69	121.5	8.0
2 4 86	1120	16.1	12.5	66	12.3	94.8	7.28	103.5	8.1
6 4 86	1440	14.7	13.3	86	14.0	130.3	6.76	138.3	8.0
13 4 86	1750	12.7	11.1	82	13.0	124.3	7.28	133.0	8.0
20 4 86	1500	16.6	11.6	55	13.3	134.8	6.37	142.4	8.1
26 4 86	1720	*	*	*	14.6	127.3	7.90	136.7	7.7
5 5 86	1530	12.2	9.1	68	11.5	97.8	6.93	106.1	7.5
11 5 86	1520	16.6	13.8	75	12.5	102.3	7.76	111.6	7.9
24 5 86	1530	10.2	8.3	77	9.4	112.3	6.17	119.6	7.6
5 6 86	1353	12.2	8.3	59	9.6	88.4	7.07	96.7	7.8
8 6 86	1355	11.9	10.2	83	10.4	118.6	6.65	126.5	7.9
15 6 86	1418	5.5	4.4	85	8.0	92.4	7.28	101.0	7.9
27 6 86	*	10.5	*	*	8.6	84.4	6.93	92.6	7.5
15 7 86	1530	10.2	8.0	74	7.0	105.8	7.66	114.9	7.6
22 7 86	1710	4.4	3.3	83	7.3	130.8	7.66	139.9	7.6
27 7 86	1456	10.5	8.6	78	8.4	79.9	7.03	88.2	7.7
6 8 86	1420	11.3	9.4	79	8.8	92.4	6.96	100.6	7.3
15 8 86	1400	8.8	7.7	86	8.2	84.4	7.00	92.7	7.5
19 8 86	1325	12.5	10.0	74	8.9	96.8	7.42	105.6	7.7

Site 15 - Makuri River

(Grid Ref. T25/627688)

Date	Time	DBT (°C)	WBT (°C)	RH %	WT (°C)	$CaCO_3$ (mg l^{-1})	$MgCO_3$ (mg l^{-1})	Total H (mg l^{-1})	pH
8 3 86	1550	17.7	16.1	85	15.5	119.8	7.06	128.7	8.2
22 3 86	1405	16.6	12.7	64	13.5	112.3	7.45	121.2	8.1
2 4 86	1135	15.8	13.3	76	11.7	92.4	7.62	101.4	8.3
6 4 86	1450	15.0	13.3	83	13.3	140.3	6.76	148.3	8.0
13 4 86	1805	11.3	11.1	97	13.0	130.8	7.45	139.6	8.1
20 4 86	1515	16.1	13.6	76	11.6	146.3	6.79	154.4	8.1
26 4 86	1730	*	*	*	13.5	134.8	8.14	144.5	7.7
5 5 86	1545	11.6	9.7	79	11.0	99.8	7.35	108.6	7.6
11 5 86	1535	13.6	13.0	95	11.3	86.9	7.90	96.2	8.0
24 5 86	1545	8.8	7.7	86	8.5	101.8	6.31	109.3	7.7
5 6 86	1515	10.0	8.8	87	9.0	88.4	7.62	97.4	7.9
8 6 86	1415	11.6	11.1	95	10.1	121.3	7.14	129.8	7.9
15 6 86	1430	5.5	5.0	93	7.8	92.4	7.69	101.5	8.0
27 6 86	*	8.6	*	*	8.4	98.8	8.18	108.5	7.4
15 7 86	1545	6.6	6.6	100	7.0	107.6	8.56	117.7	7.6
22 7 86	1725	3.3	3.3	100	7.4	128.8	8.11	138.4	7.7
27 7 86	1510	9.7	8.8	90	7.9	77.4	7.83	86.7	7.7
15 8 86	1415	7.5	6.1	82	7.3	92.4	7.35	101.1	7.4
19 8 86	1335	11.1	9.7	85	8.6	99.8	7.66	108.9	7.1

APPENDIX FIVE

GRAPHS OF VARIATION IN CARBONATE CONTENT OF WATER SAMPLES AT EACH SAMPLING SITE

SITE 1 Mangatoro Stream (Grid Ref. U24/799927)

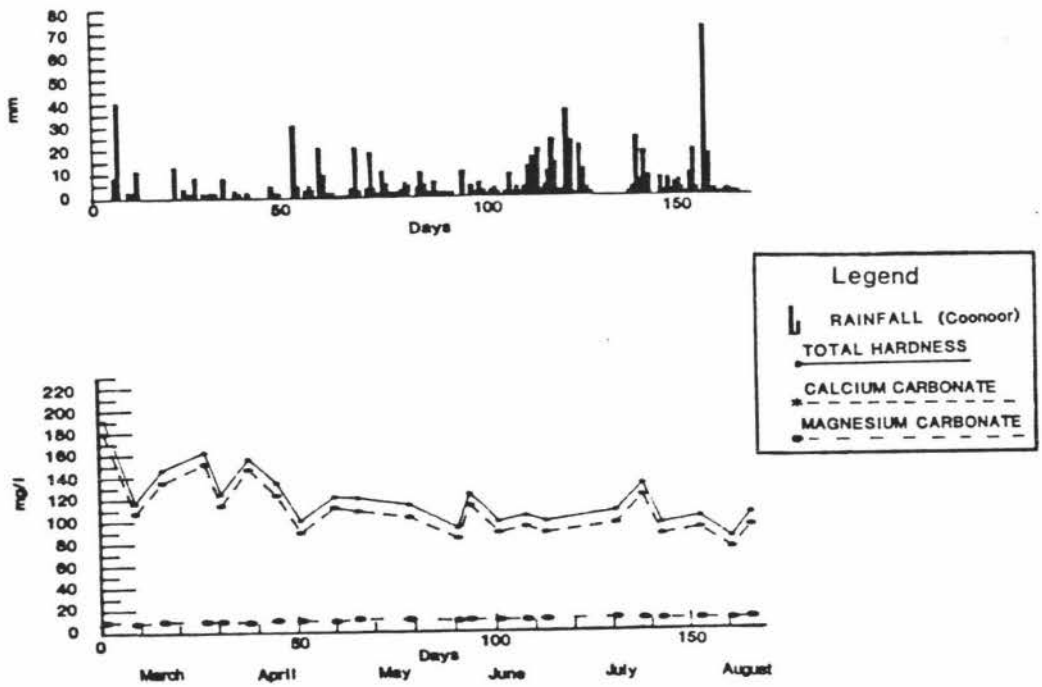

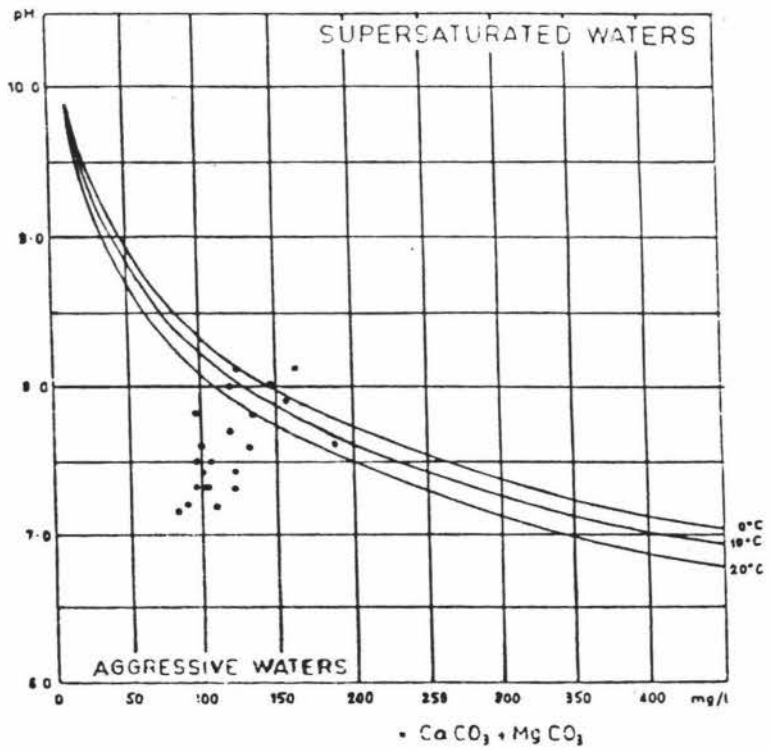

SITE 2 Mangatoro Stream (Grid Ref. U24/762842)

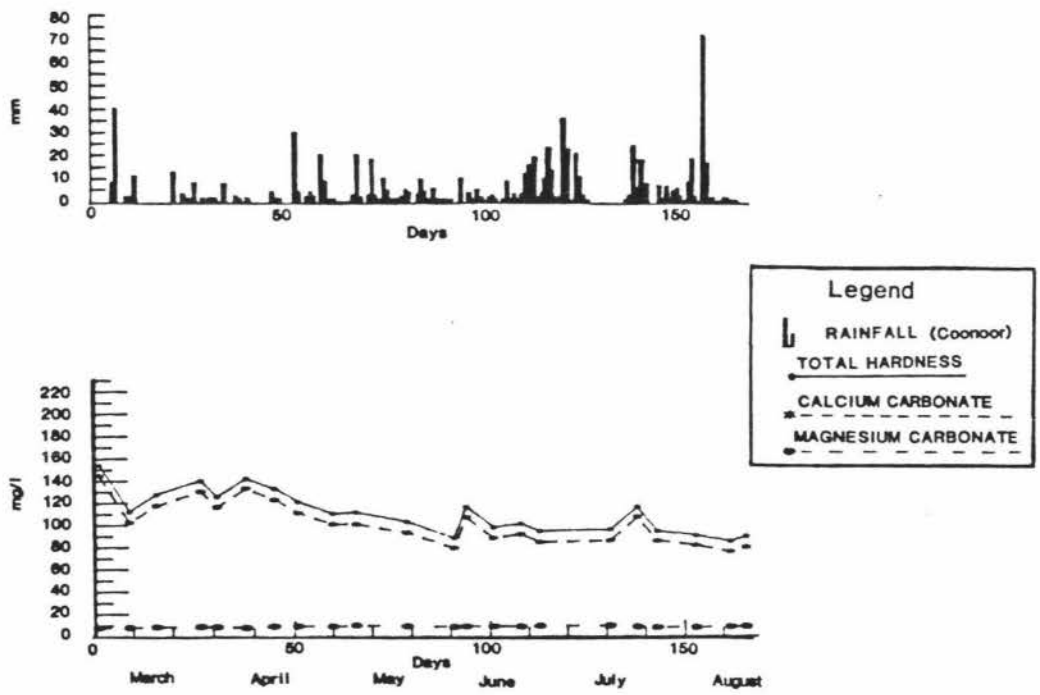

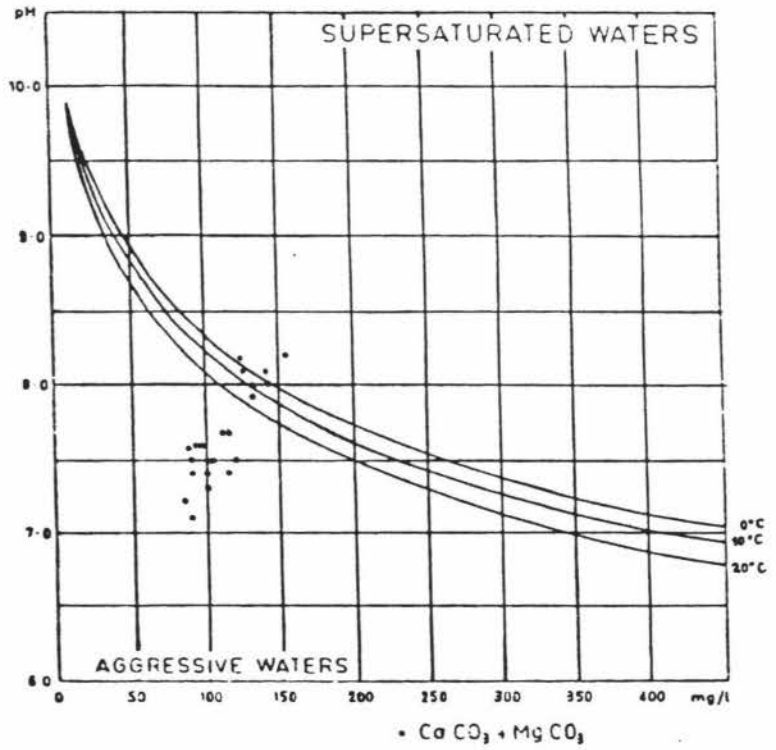

SITE 3 Cave Resurgence, Mangatoro Stream (Grid Ref. U24/737827)

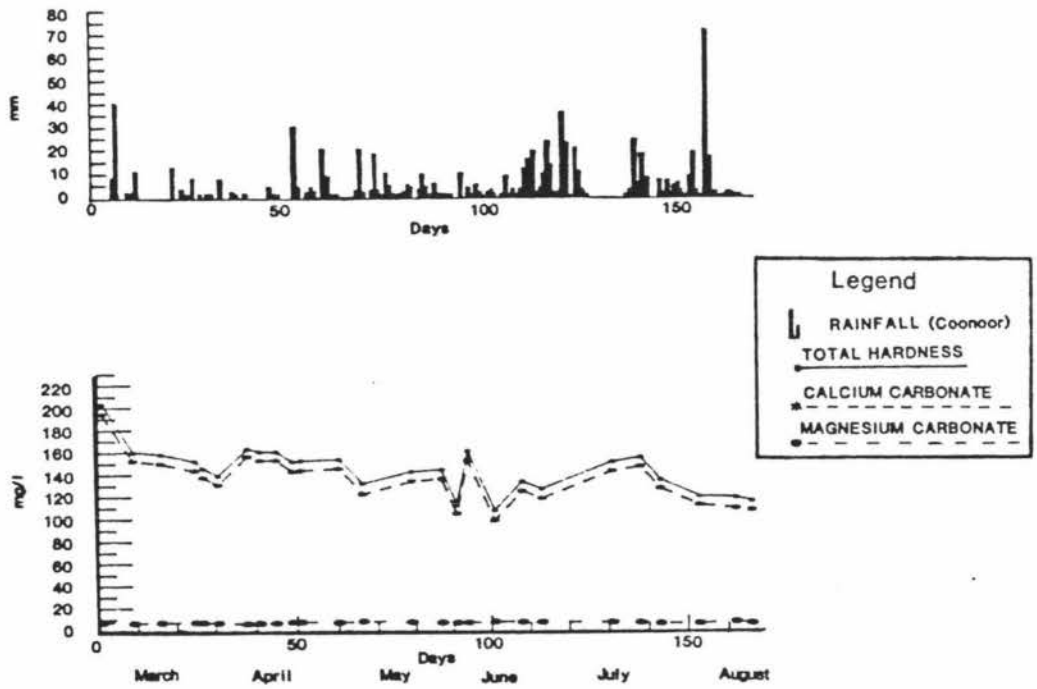

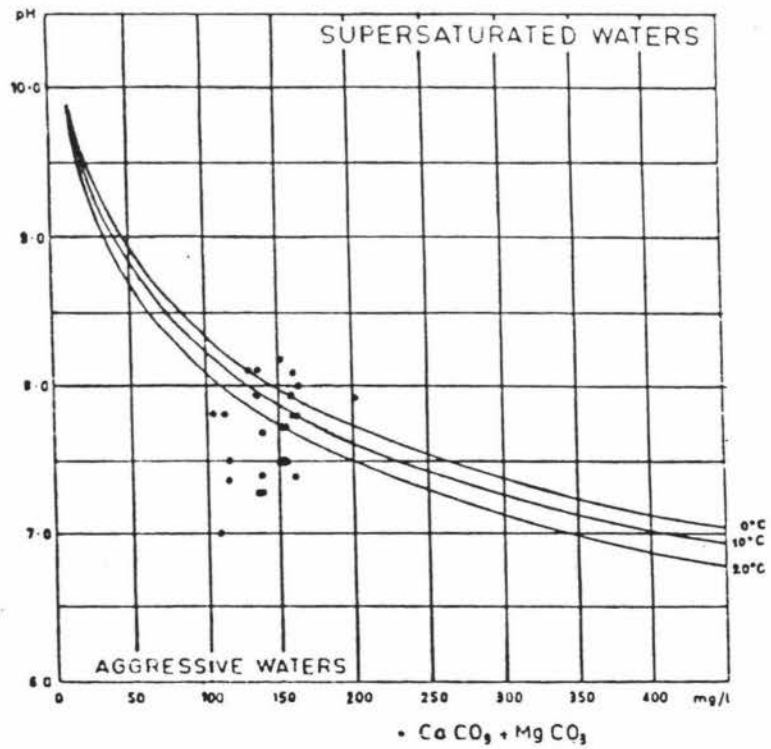

SITE 4 Spring, Mangatoro Stream (Grid Ref. U24/737824)

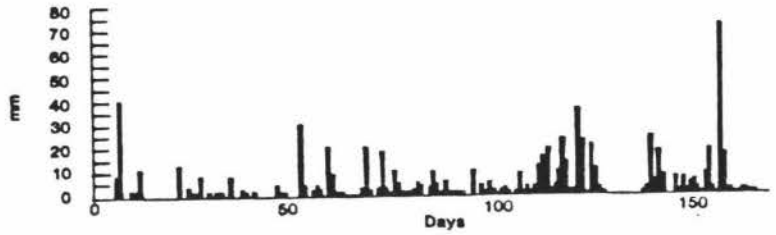

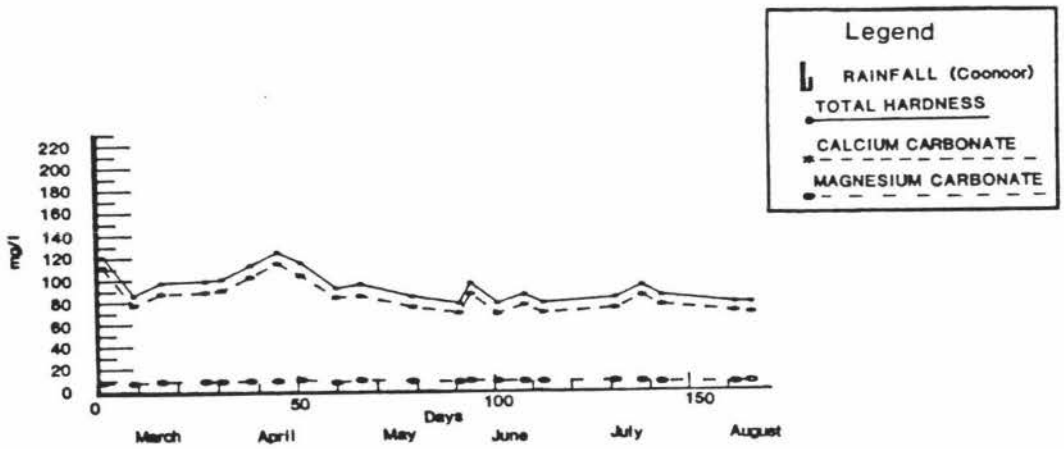

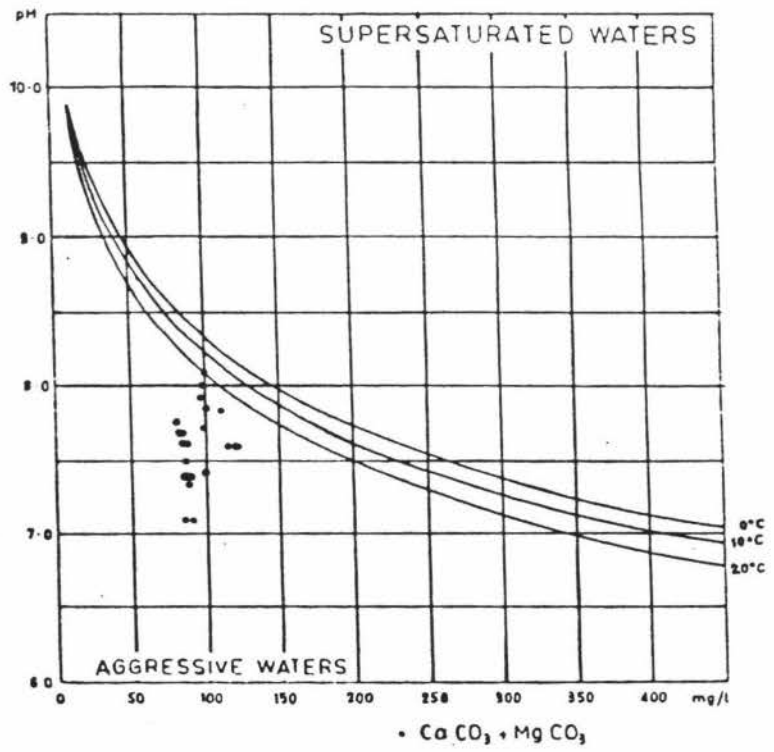

SITE 5 PT17 Cave Resurgence, Mangatoro Stream (Grid Ref. U24/731820)

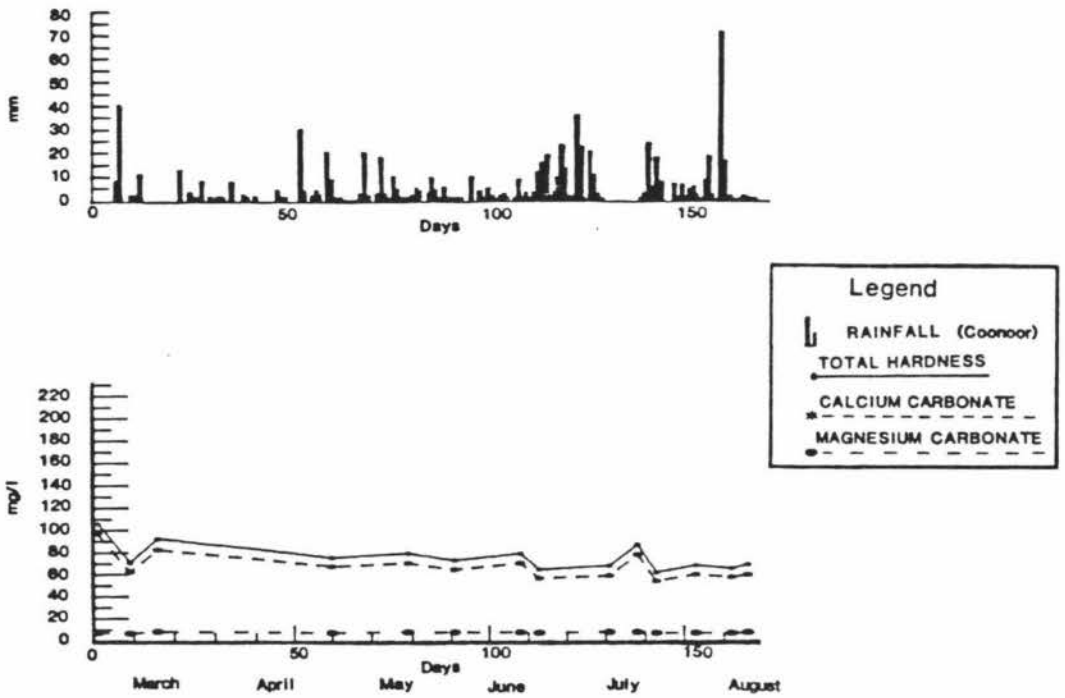

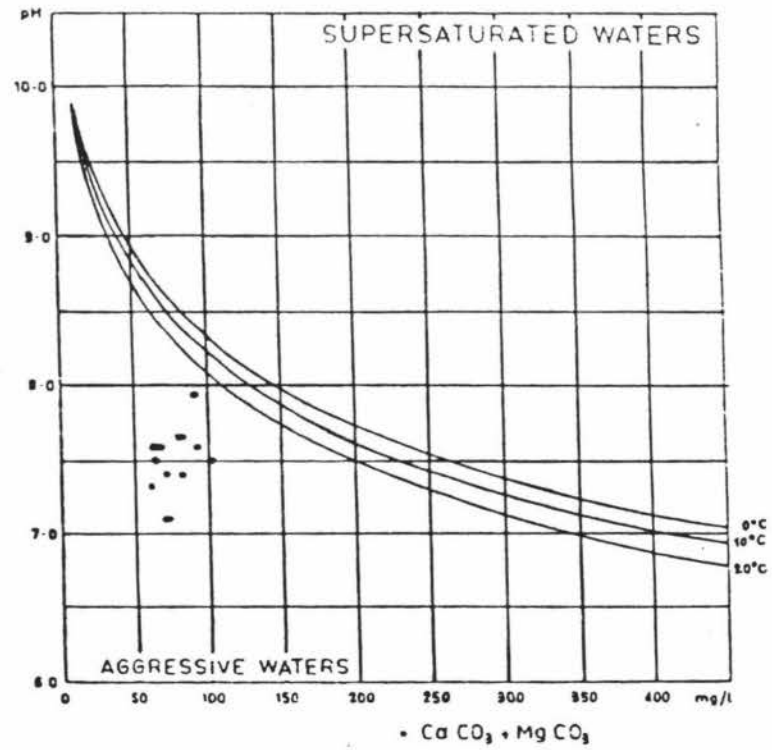

SITE 6 Stream from the Waewaepa Range (Grid Ref. U24/724817)

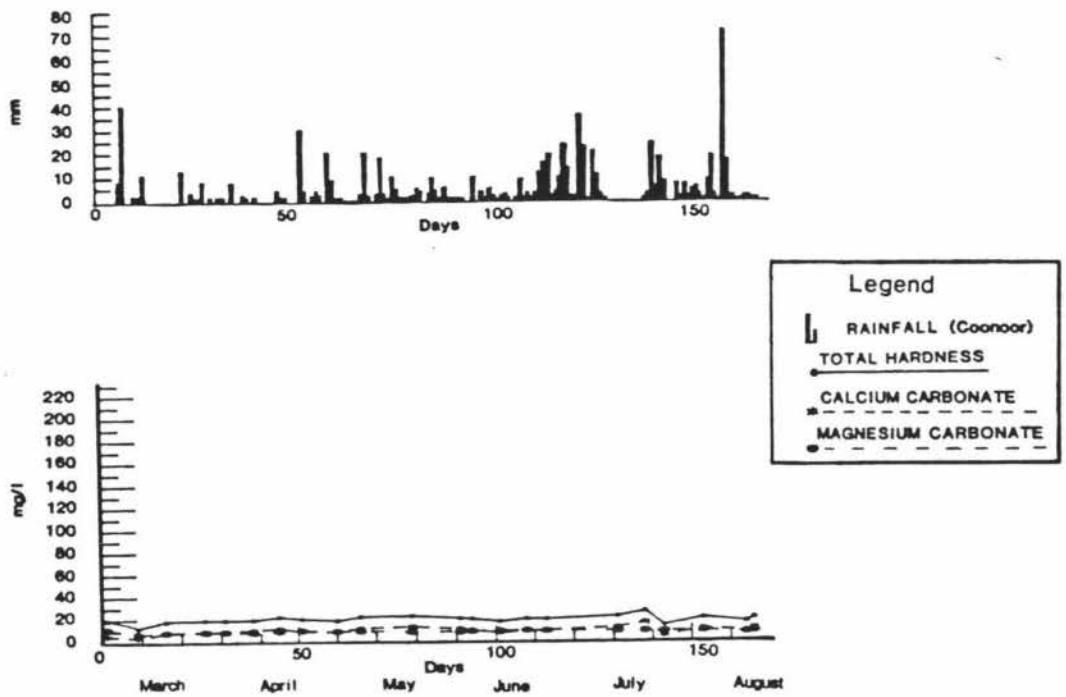

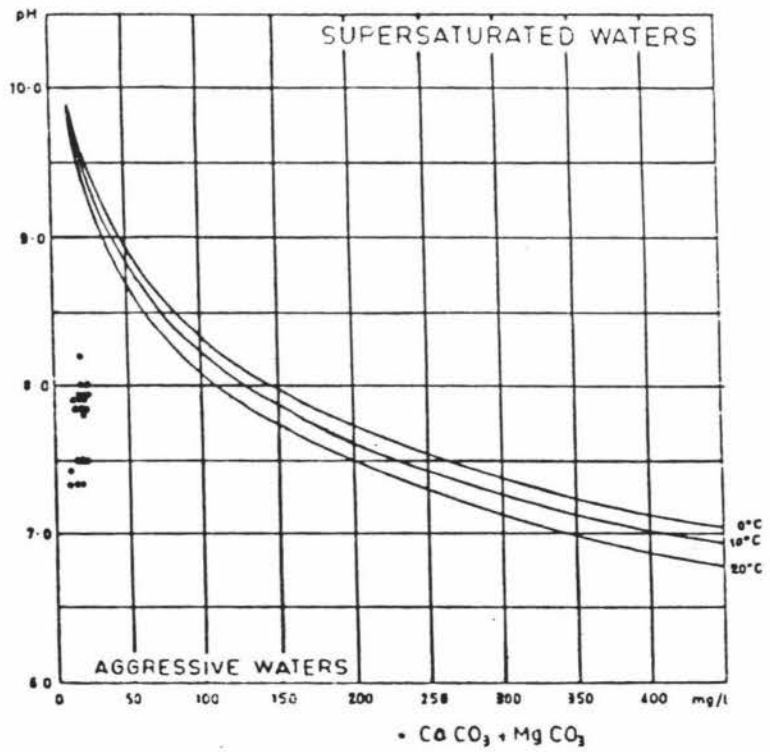

SITE 7 Stream from the Waewaepa Range (Grid Ref. U24/719812)

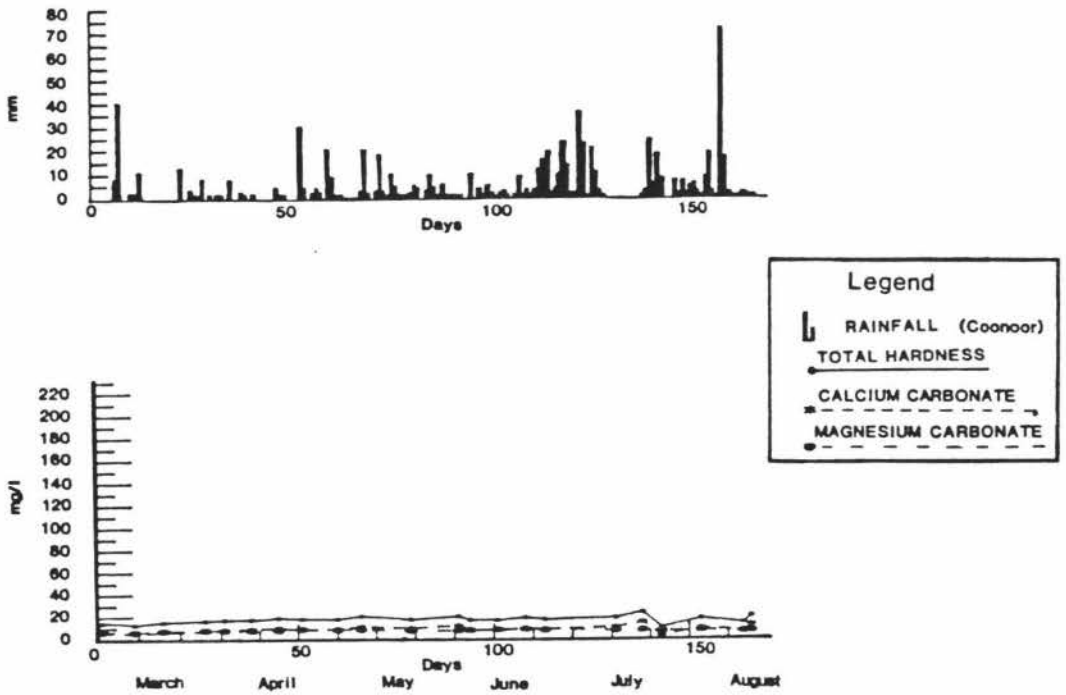

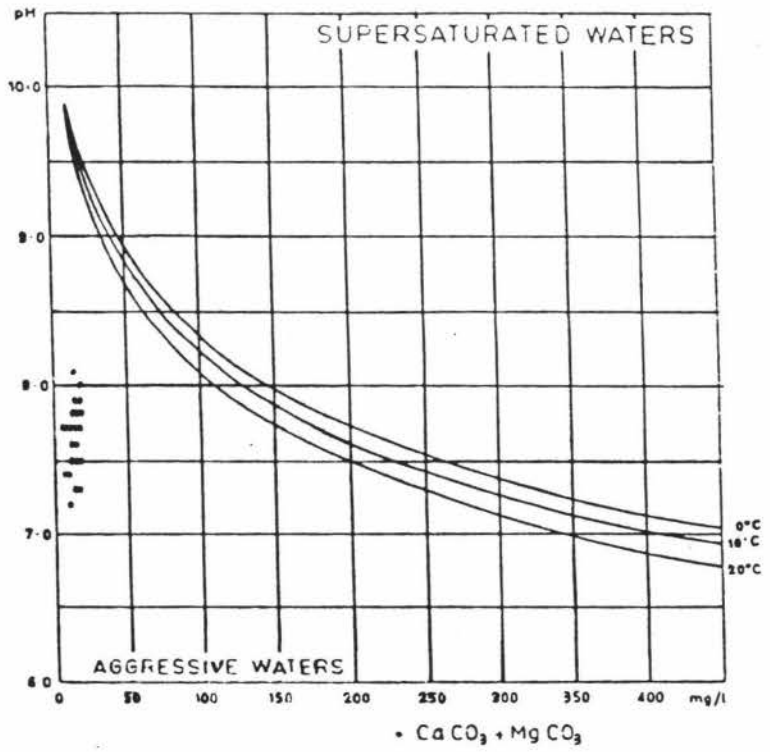

SITE 8 PT17 Cave, Coonoor (Grid Ref. U24/725814)

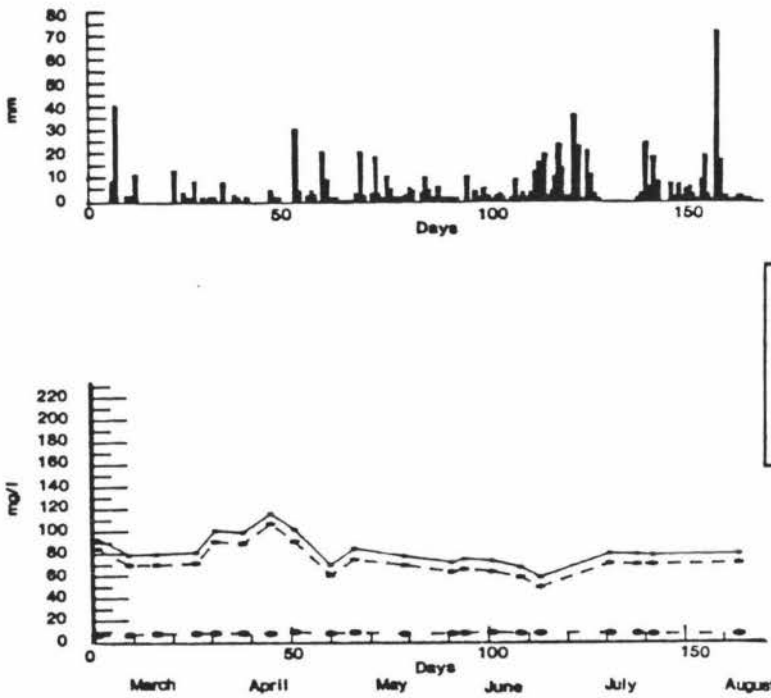

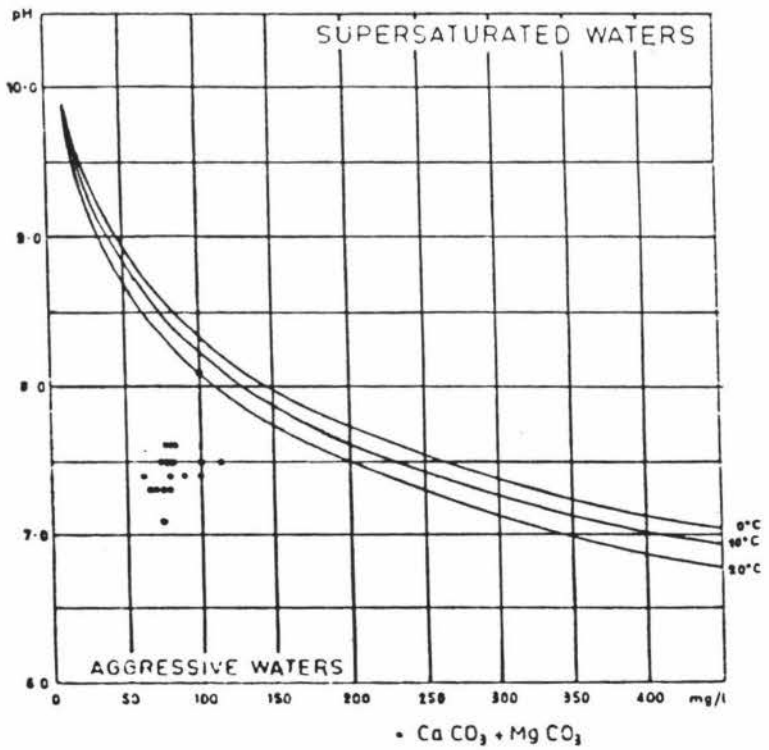

SITE 9 PT17 Cave, Coonoor (Grid Ref. U24/725814)

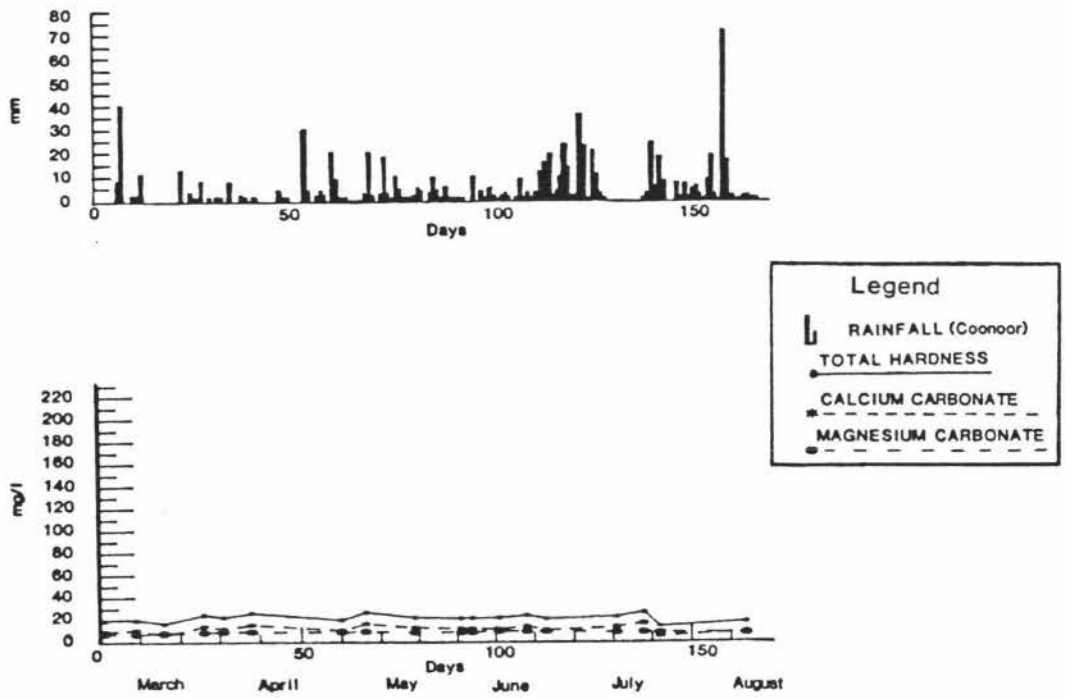

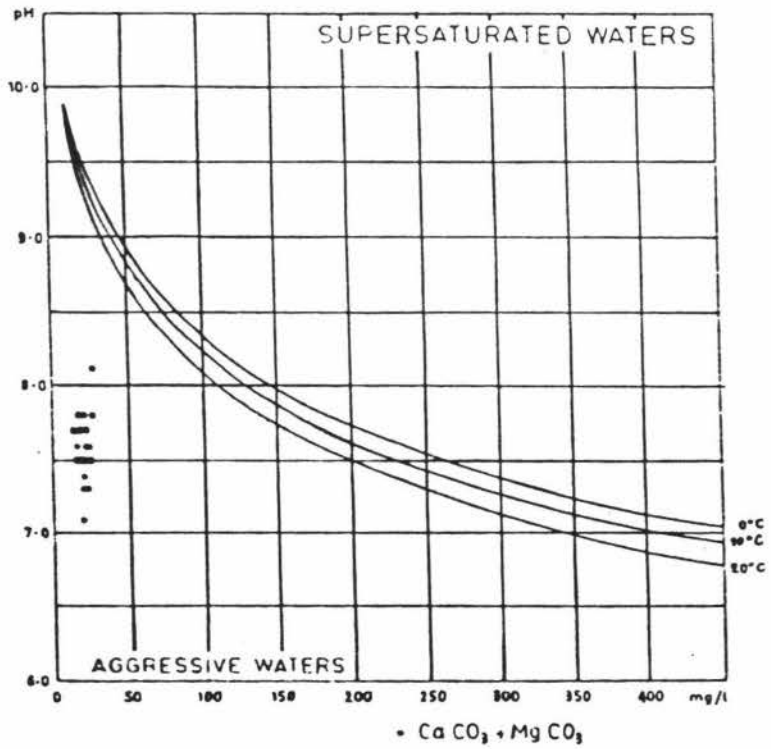

SITE 10 PT17 Cave, Coonoor (Grid Ref. U24/725814)

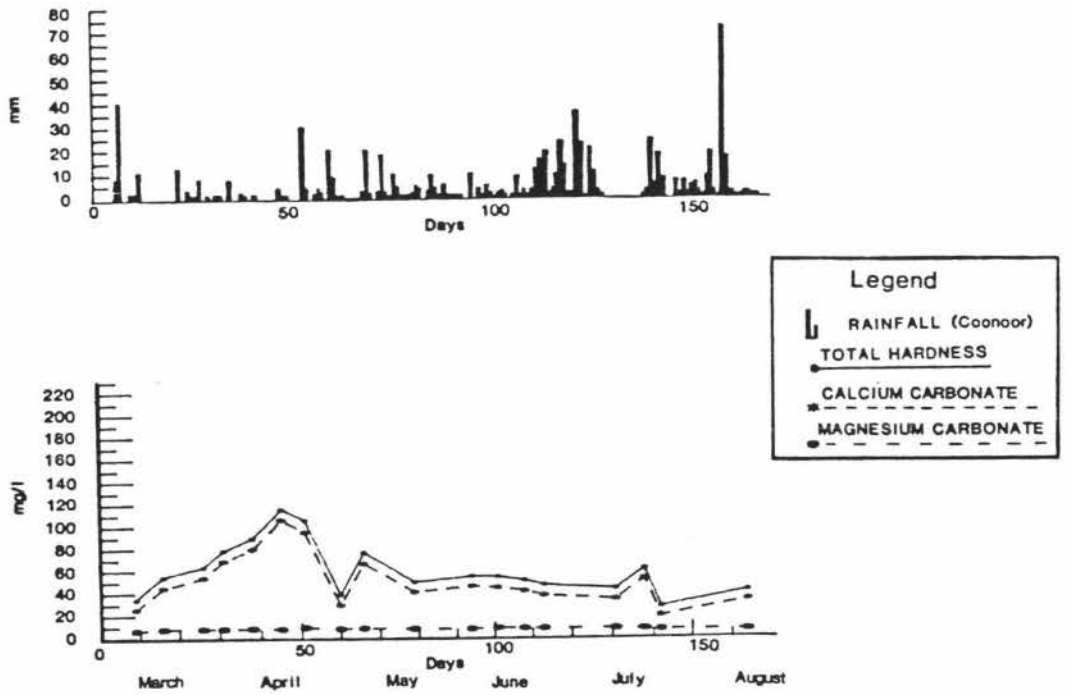

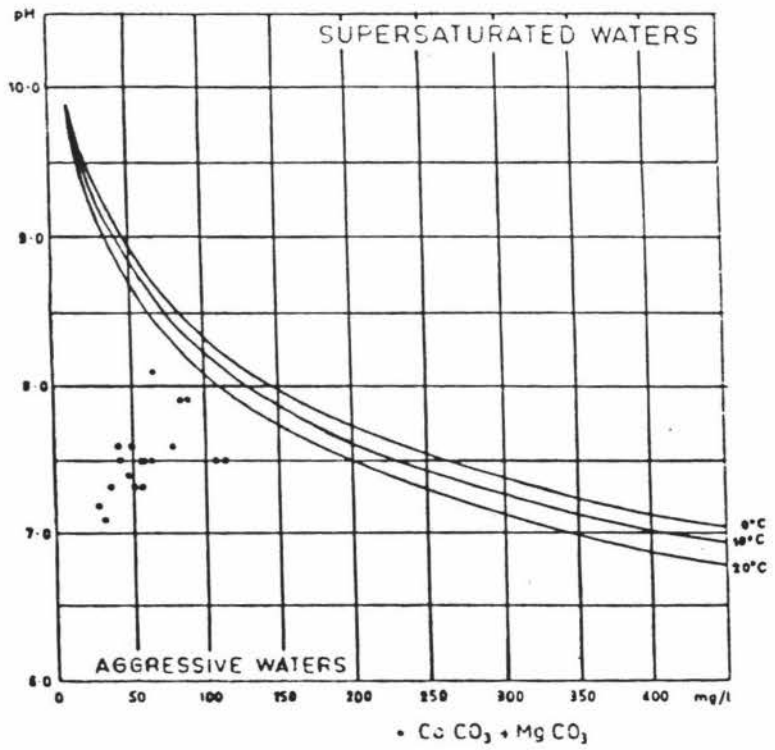

SITE 11 PT17 Cave, Coonoor (Grid Ref. U24/725814)

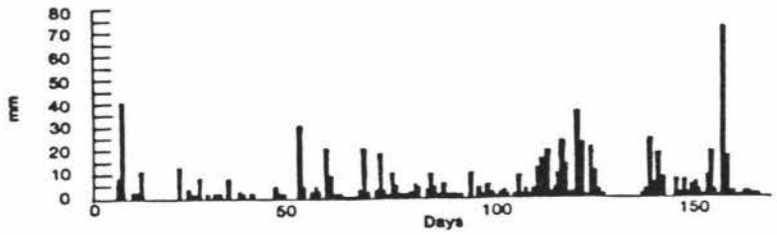

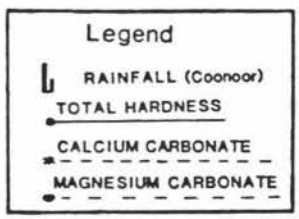

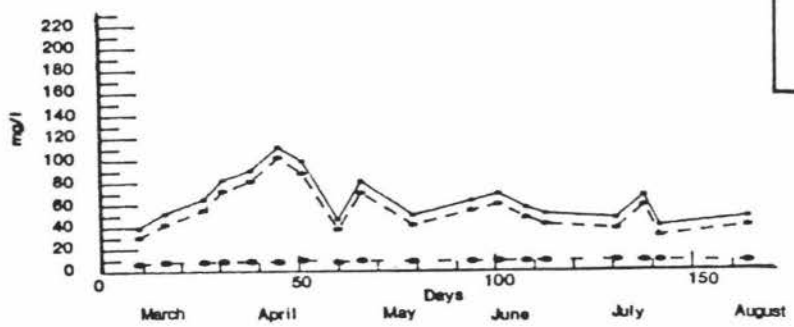

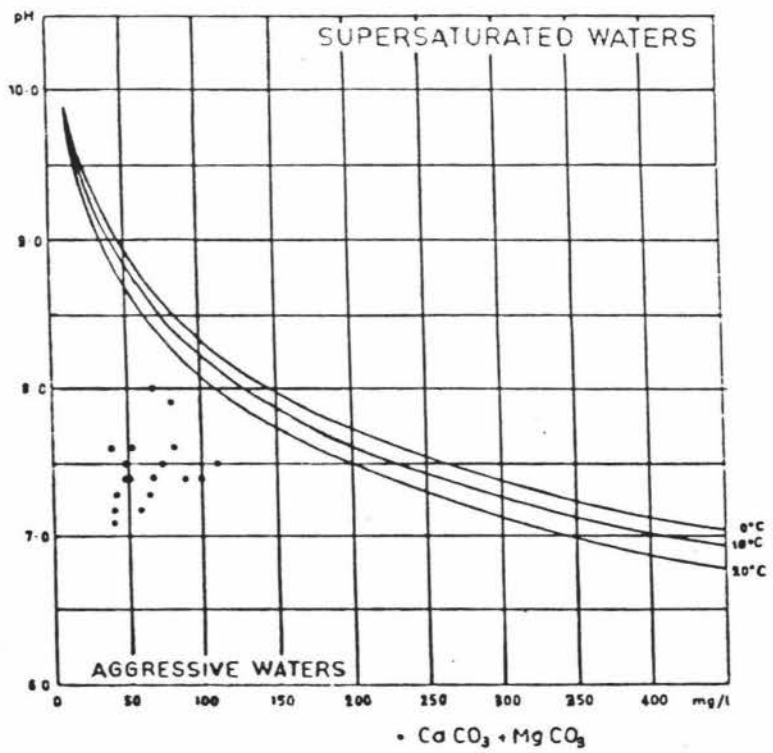

SITE 12 Famous Five Cave Submergence (Grid Ref.U24/741817)

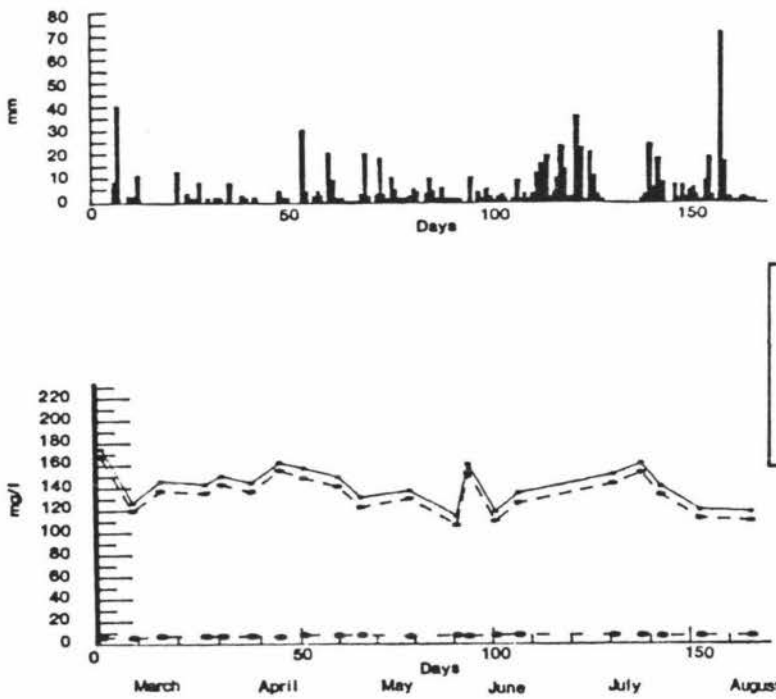

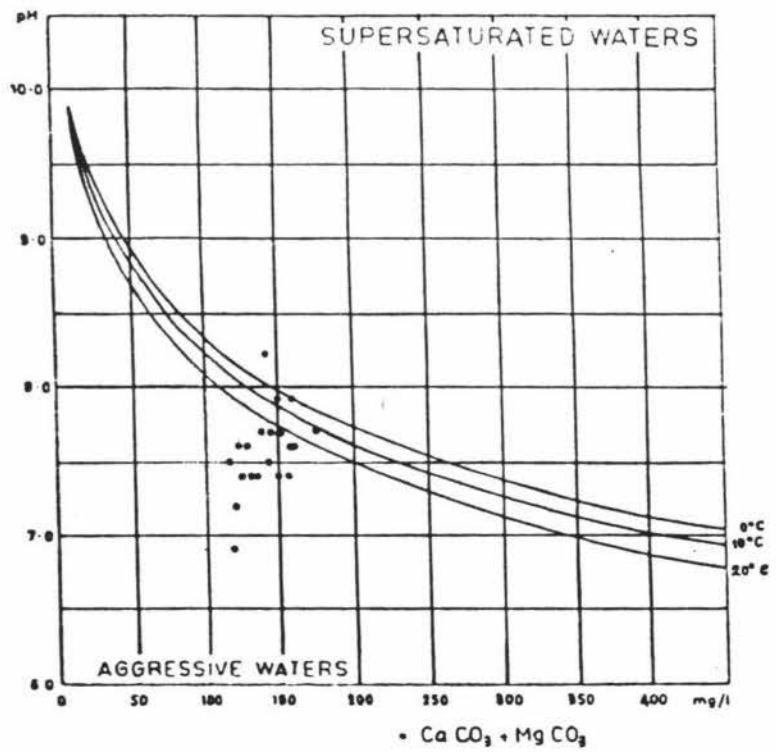

SITE 13 Famous Five Cave Resurgence (Grid Ref. U24/740822)

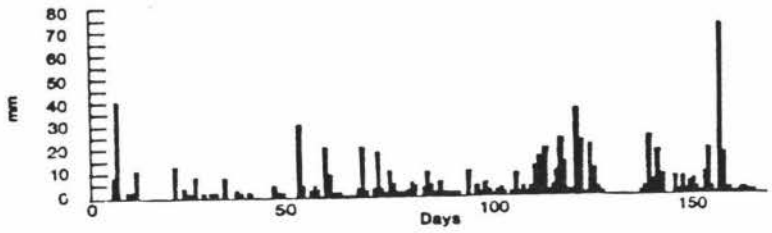

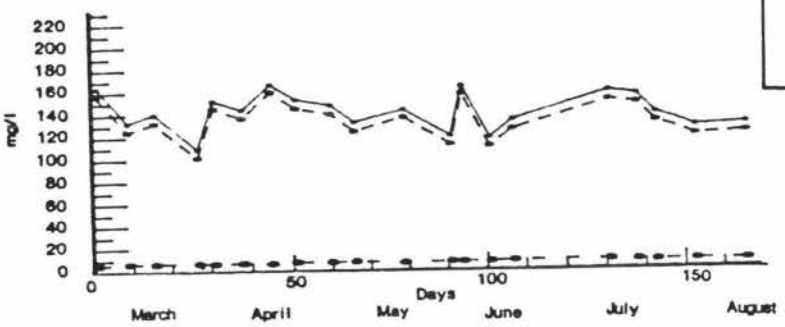

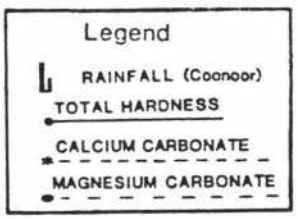

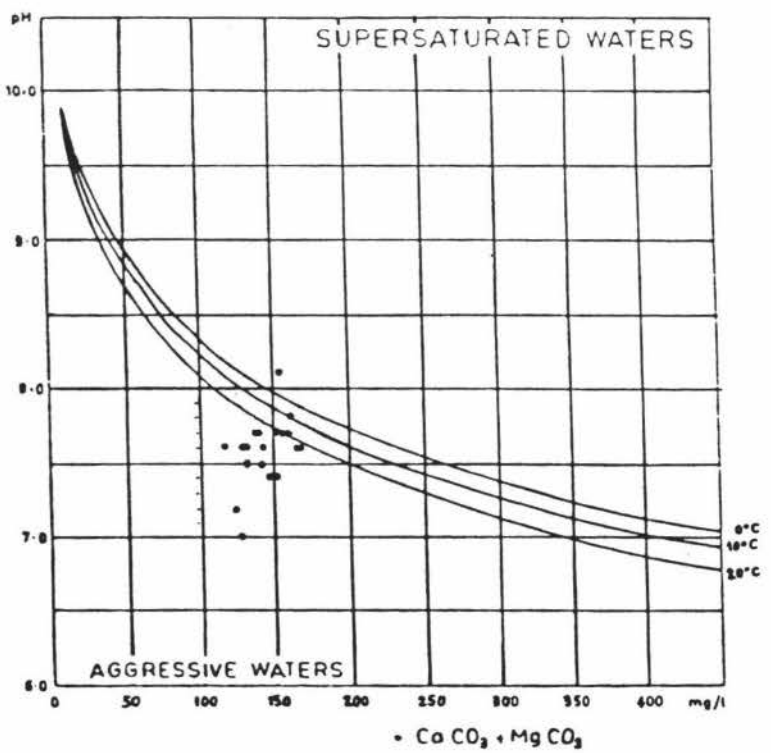

SITE 14 Makuri River (Grid Ref. T24/654704)

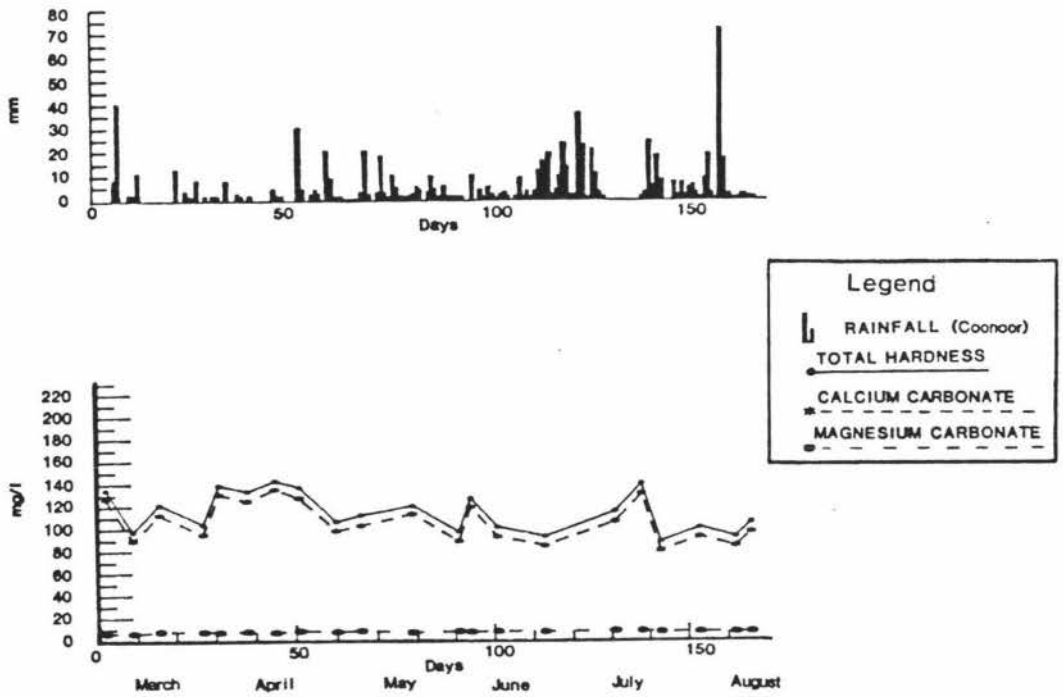

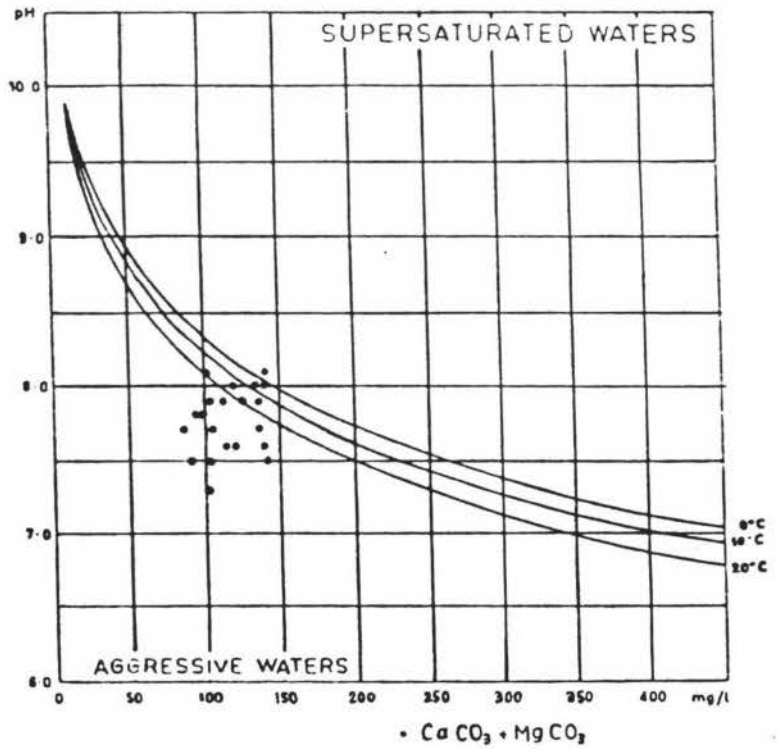

SITE 15 Makuri River (Grid Ref. T25/627688)

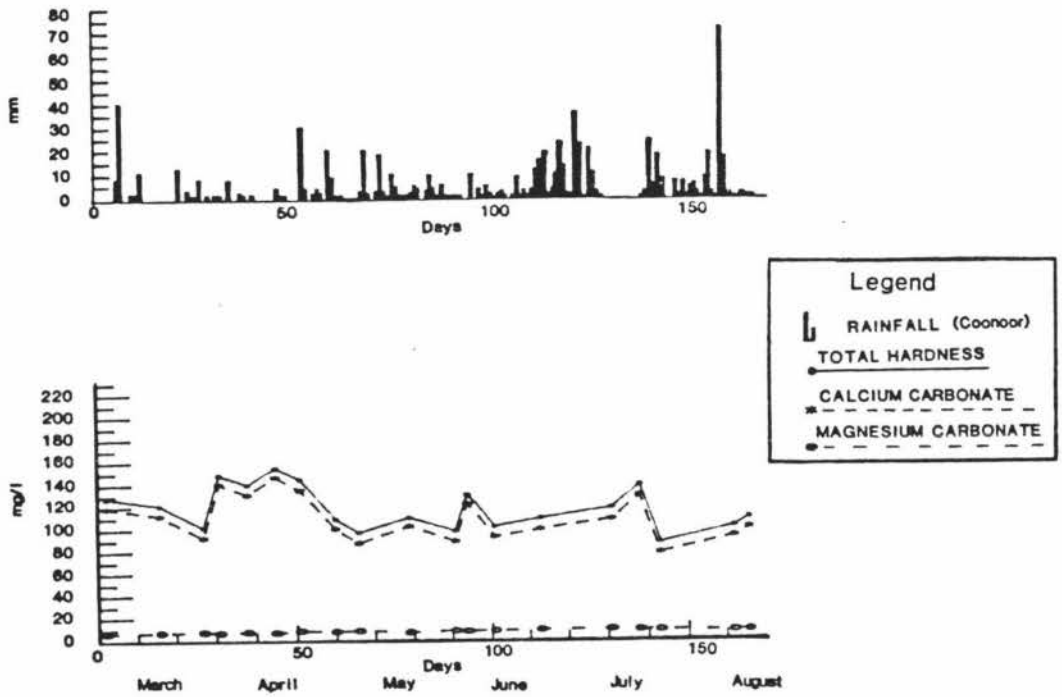

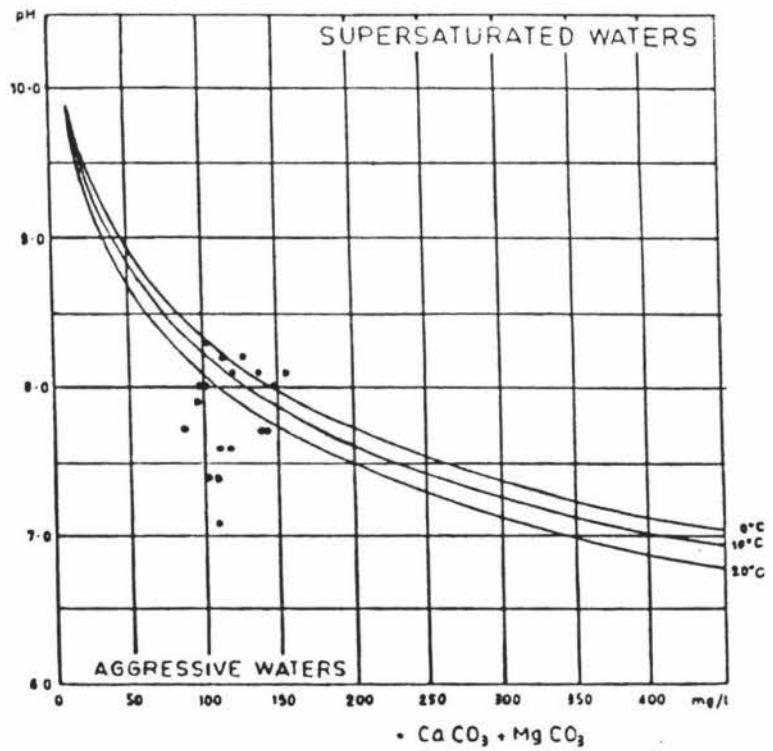

APPENDIX SIX

STATISTICAL DATA AND CORRELATION MATICES FOR WATER SAMPLING SITES

The following abbrevations have been used:

WT: Water Temperature

$CaCO_3$: Calcium carbonate content of the water samples

$MgCO_3$: Magnesium carbonate content of the water samples

Total H: Total Hardness of the water samples. This is $CaCO_3$ and $MgCO_3$ combined.

++: Significant at the 99.95 % confidence level

+: Significant at the 95.00 % confidence level

SITE 1

	N	MEAN	MEDIAN	TRMEAN	STDEV	SEMEAN	MIN	MAX	Q1	Q3
WT	22	10.71	9.65	10.43	3.75	0.80	6.00	21.00	7.87	12.47
$CaCO_3$	22	108.12	104.55	106.32	26.07	5.56	72.40	179.80	88.30	120.42
$MgCO_3$	22	8.88	8.92	8.86	0.62	0.13	7.97	10.05	8.34	9.42
Total	22	118.66	114.90	116.86	26.36	5.62	82.00	191.30	99.05	131.32
pH	22	7.59	7.55	7.58	0.29	0.62	7.20	8.10	7.30	7.82

	WT	$CaCO_3$	$MgCO_3$	Total H
WT	1.000			
$CaCO_3$	0.397*	1.000		
$MgCO_3$	0.072	0.347	1.000	
Total H	0.396*	1.000**	0.372*	1.000
pH	0.491*	0.548*	0.303	0.551*

SITE 2

	N	MEAN	MEDIAN	TRMEAN	STDEV	SEMEAN	MIN	MAX	Q1	Q3
WT	22	10.91	9.80	10.72	2.82	0.60	7.80	18.00	8.57	13.02
$CaCO_3$	22	101.14	99.80	100.26	19.60	4.18	75.10	144.80	84.57	116.02
$MgCO_3$	22	8.08	8.09	8.07	0.42	0.09	7.28	9.01	7.89	8.39
Total H	22	110.72	109.90	109.85	19.67	4.19	84.60	154.30	93.50	125.57
pH	22	7.64	7.60	7.64	0.31	0.06	7.10	8.20	7.40	7.92

	WT	$CaCO_3$	$MgCO_3$	Total H
WT	1.000			
$CaCO_3$	0.677**	1.000		
$MgCO_3$	0.266	0.094	1.000	
Total H	0.683**	1.000**	0.119	1.000
pH	0.567*	0.820**	-0.064	0.816**

SITE 3

	N	MEAN	MEDIAN	TRMEAN	STDEV	SEMEAN	MIN	MAX	Q1	Q3
WT	27	10.75	10.60	10.73	0.74	0.14	9.50	12.50	10.20	11.30
$CaCO_3$	27	135.08	137.30	134.16	21.12	4.06	98.60	194.70	118.30	149.80
$MgCO_3$	27	7.00	6.93	7.00	0.49	0.09	5.89	8.14	6.58	7.28
Total H	27	143.41	145.50	142.44	21.02	4.04	107.70	203.50	127.00	158.00
pH	26	7.68	7.70	7.69	0.29	0.05	7.00	8.20	7.47	7.90

	WT	$CaCO_3$	$MgCO_3$	Total H
WT	1.000			
$CaCO_3$	0.576*	1.000		
$MgCO_3$	-0.144	-0.193	1.000	
Total H	0.574*	1.000**	-0.166	1.000
pH	0.515*	0.357*	-0.031	0.359*

SITE 4

	N	MEAN	MEDIAN	TRMEAN	STDEV	SEMEAN	MIN	MAX	Q1	Q3
WT	21	10.66	10.20	10.62	1.41	0.30	8.60	13.50	9.35	11.80
$CaCO_3$	21	84.04	83.60	83.26	14.01	3.06	68.60	114.30	72.00	89.50
$MgCO_3$	21	8.06	8.04	8.04	0.69	0.15	6.83	9.70	7.50	8.49
Total H	21	93.57	92.10	92.75	14.48	3.16	78.20	124.60	80.80	99.50
pH	21	7.60	7.60	7.60	0.26	0.05	7.10	8.10	7.40	7.80

	WT	$CaCO_3$	$MgCO_3$	Total H
WT	1.000			
$CaCO_3$	0.637*	1.000		
$MgCO_3$	0.421*	0.586*	1.000	
Total H	0.638*	0.999**	0.624*	1.000
pH	0.401*	0.252	0.478*	0.271

SITE 5

	N	MEAN	MEDIAN	TRMEAN	STDEV	SEMEAN	MIN	MAX	Q1	Q3
WT	14	9.89	9.30	9.75	1.70	0.45	7.90	13.50	8.67	11.10
$CaCO_3$	14	66.86	63.15	65.43	12.04	3.22	53.60	97.30	58.30	71.90
$MgCO_3$	14	7.24	7.22	7.19	0.45	0.12	6.76	8.25	6.81	7.66
Total H	14	75.47	71.45	74.07	12.32	3.29	61.70	106.10	67.15	80.85
pH	14	7.50	7.55	7.50	0.22	0.06	7.10	7.90	7.37	7.62

	WT	$CaCO_3$	$MgCO_3$	Total H
WT	1.000			
$CaCO_3$	0.562*	1.000		
$MgCO_3$	0.207	0.503*	1.000	
Total H	0.557*	0.999**	0.533*	1.000
pH	0.307	0.303	0.372	0.311

SITE 6

	N	MEAN	MEDIAN	TRMEAN	STDEV	SEMEAN	MIN	MAX	Q1	Q3
WT	22	8.55	7.95	8.44	2.18	0.46	5.70	13.50	6.67	10.42
$CaCO_3$	22	9.02	8.70	8.95	2.73	0.58	3.70	15.90	7.90	10.82
$MgCO_3$	22	8.36	8.32	8.26	0.93	0.19	6.96	11.78	7.95	8.49
Total H	22	18.95	19.10	18.94	2.84	0.60	12.30	26.00	17.95	20.25
pH	22	7.68	7.70	7.67	0.25	0.05	7.30	8.20	7.50	7.90

	WT	$CaCO_3$	$MgCO_3$	Total H
WT	1.000			
$CaCO_3$	-0.407*	1.000		
$MgCO_3$	0.152	-0.094	1.000	
Total H	-0.340	0.930**	0.279	1.000
pH	0.246	0.350	-0.052	0.321

SITE 7

	N	MEAN	MEDIAN	TRMEAN	STDEV	SEMEAN	MIN	MAX	Q1	Q3
WT	22	8.96	8.20	8.86	2.54	0.54	5.40	14.50	6.90	11.20
$CaCO_3$	22	8.24	7.90	8.22	2.56	0.54	2.20	14.70	6.77	9.52
$MgCO_3$	22	7.21	7.24	7.21	0.58	0.12	6.17	8.32	6.80	7.65
Total	22	16.82	16.85	16.85	2.84	0.60	9.60	23.50	15.70	18.32
pH	22	7.63	7.65	7.63	0.23	0.05	7.20	8.10	7.47	7.80

	WT	$CaCO_3$	$MgCO_3$	Total H
WT	1.000			
$CaCO_3$	-0.420*	1.000		
$MgCO_3$	0.051	0.272	1.000	
Total H	-0.368*	0.972**	0.492*	1.000
pH	0.103	0.218	0.273	0.271

SITE 8

	N	MEAN	MEDIAN	TRMEAN	STDEV	SEMEAN	MIN	MAX	Q1	Q3
WT	20	10.59	10.65	10.58	0.77	0.17	9.40	11.80	9.85	11.35
$CaCO_3$	20	72.49	69.90	71.94	13.42	3.00	48.90	106.10	63.40	82.07
$MgCO_3$	20	7.65	7.55	7.61	0.56	0.12	6.86	9.01	7.19	8.12
Total H	20	81.55	78.65	81.01	13.68	3.06	57.70	115.20	72.82	90.80
pH	20	7.46	7.50	7.45	0.19	0.04	7.10	8.10	7.33	7.50

	WT	$CaCO_3$	$MgCO_3$	Total H
WT	1.000			
$CaCO_3$	0.425*	1.000		
$MgCO_3$	0.386*	0.373	1.000	
Total H	0.435*	0.999**	0.415*	1.000
pH	0.355*	0.374	0.462*	0.389*

SITE 9

	N	MEAN	MEDIAN	TRMEAN	STDEV	SEMEAN	MIN	MAX	Q1	Q3
WT	18	8.77	8.10	8.63	2.55	0.60	5.50	14.30	6.90	10.90
$CaCO_3$	18	11.06	10.90	11.19	2.98	0.70	4.20	15.90	9.40	13.10
$MgCO_3$	18	8.08	8.09	8.11	0.51	0.12	7.10	8.73	7.65	8.66
Total H	18	20.69	20.45	20.84	3.25	0.76	13.30	25.70	19.25	23.10
pH	18	7.57	7.60	7.56	0.26	0.06	7.10	8.10	7.37	7.72

	WT	$CaCO_3$	$MgCO_3$	Total H
WT	1.000			
$CaCO_3$	0.015	1.000		
$MgCO_3$	-0.011	0.374	1.000	
Total H	0.015	0.985**	0.529*	1.000
pH	-0.018	0.374	0.441*	0.420*

SITE 10

	N	MEAN	MEDIAN	TRMEAN	STDEV	SEMEAN	MIN	MAX	Q1	Q3
WT	19	9.58	9.70	9.51	1.83	0.42	6.60	13.90	8.00	11.00
$CaCO_3$	18	50.95	44.65	49.51	23.69	5.58	18.90	106.10	33.85	66.95
$MgCO_3$	18	7.86	7.93	7.84	0.50	0.11	7.00	9.01	7.47	8.25
Total H	18	60.27	54.35	58.89	24.05	5.67	27.30	115.30	43.05	76.75
pH	18	7.48	7.50	7.47	0.23	0.05	7.10	8.10	7.30	7.60

	WT	$CaCO_3$	$MgCO_3$	Total H
WT	1.000			
$CaCO_3$	0.376	1.000		
$MgCO_3$	0.321	0.598*	1.000	
Total H	0.324	1.000**	0.614*	1.000
pH	0.076	0.347	0.314	0.351

SITE 11

	N	MEAN	MEDIAN	TRMEAN	STDEV	SEMEAN	MIN	MAX	Q1	Q3
WT	18	10.16	10.25	10.11	1.33	0.31	8.00	13.20	9.37	11.00
$CaCO_3$	18	54.48	50.15	53.06	20.55	4.84	29.90	101.80	38.47	70.40
$MgCO_3$	18	7.88	7.81	7.86	0.55	0.13	6.93	9.18	7.53	8.33
Total H	18	63.83	59.15	62.43	20.96	4.94	39.00	111.10	46.82	80.60
pH	18	7.46	7.40	7.45	0.22	0.05	7.10	8.00	7.30	7.60

	WT	$CaCO_3$	$MgCO_3$	Total H
WT	1.000			
$CaCO_3$	0.226	1.000		
$MgCO_3$	0.241	0.600*	1.000	
Total H	0.229	1.000**	0.620*	1.000
pH	0.061	0.316	0.453*	0.325

SITE 12

	N	MEAN	MEDIAN	TRMEAN	STDEV	SEMEAN	MIN	MAX	Q1	Q3
WT	21	10.73	10.70	10.68	0.62	0.13	10.00	12.50	10.20	11.05
$CaCO_3$	21	132.60	134.80	132.17	17.69	3.86	106.10	167.30	115.80	145.50
$MgCO_3$	21	6.64	6.65	6.64	0.51	0.11	5.72	7.45	6.24	7.01
Total H	21	140.50	142.70	140.12	17.68	3.86	113.10	175.00	123.10	154.05
pH	20	7.56	7.60	7.56	0.27	0.06	6.90	8.20	7.40	7.70

	WT	$CaCO_3$	$MgCO_3$	Total H
WT	1.000			
$CaCO_3$	0.305	1.000		
$MgCO_3$	-0.236	-0.019	1.000	
Total H	0.296	0.999**	0.016	1.000
pH	0.118	0.480*	-0.086	0.479*

SITE 13

	N	MEAN	MEDIAN	TRMEAN	STDEV	SEMEAN	MIN	MAX	Q1	Q3
WT	21	10.74	10.40	10.72	0.71	0.15	9.90	12.00	10.10	11.35
$CaCO_3$	21	132.38	132.30	132.61	16.86	3.68	101.10	159.30	119.55	146.05
$MgCO_3$	21	6.36	6.31	6.37	0.40	0.08	5.54	6.93	6.10	6.67
Total H	21	139.93	140.10	140.21	16.76	3.66	108.60	165.90	127.35	153.70
pH	20	7.58	7.60	7.58	0.22	0.05	7.00	8.10	7.50	7.70

	WT	$CaCO_3$	$MgCO_3$	Total H
WT	1.000			
$CaCO_3$	0.286	1.000		
$MgCO_3$	-0.094	-0.206	1.000	
Total H	0.285	1.000**	-0.179	1.000
pH	0.178	0.044	-0.186	0.038

SITE 14

	N	MEAN	MEDIAN	TRMEAN	STDEV	SEMEAN	MIN	MAX	Q1	Q3
WT	21	11.22	10.40	11.09	3.22	0.70	7.00	18.00	8.50	13.65
$CaCO_3$	21	106.06	102.30	105.93	17.83	3.89	79.90	134.80	91.15	125.80
$MgCO_3$	21	7.07	7.03	7.08	0.50	0.10	6.17	7.90	6.70	7.54
Total H	21	114.50	111.60	114.41	17.90	3.91	88.20	142.40	98.95	134.35
pH	21	7.76	7.80	7.77	0.22	0.04	7.30	8.10	7.60	7.95

	WT	$CaCO_3$	$MgCO_3$	Total H
WT	1.000			
$CaCO_3$	0.395*	1.000		
$MgCO_3$	-0.226	0.013	1.000	
Total H	0.389*	0.999**	0.045	1.000
pH	0.551*	0.432*	-0.020	0.431*

SITE 15

	N	MEAN	MEDIAN	TRMEAN	STDEV	SEMEAN	MIN	MAX	Q1	Q3
WT	19	10.33	10.10	10.22	2.59	0.59	7.00	15.50	7.90	13.00
$CaCO_3$	19	109.06	101.80	108.73	20.07	4.60	77.40	146.30	92.40	128.80
$MgCO_3$	19	7.52	7.62	7.53	0.55	0.12	6.31	8.56	7.14	7.90
Total H	19	118.01	109.30	117.71	19.92	4.57	86.70	154.40	101.40	138.40
pH	19	7.81	7.90	7.82	0.31	0.07	7.10	8.30	7.60	8.10

	WT	$CaCO_3$	$MgCO_3$	Total H
WT	1.000			
$CaCO_3$	0.519*	1.000		
$MgCO_3$	-0.341	-0.278	1.000	
Total H	0.515*	1.000**	-0.249	1.000
pH	0.630*	0.276	-0.310	0.269

APPENDIX SEVEN

THORIUM/URANIUM DATING METHOD

The following is a summary from Harmon et al. (1975), of the theory behind, and application of, the thorium/uranium dating method. The actinide series contains elements with atomic numbers 89 to 103, all of which are radioactive. Only uranium and thorium have sufficiently long-lived nuclides to occur naturally in large quantities. Oceanic concentrations of uranium and thorium average 2 ppb and 0.2 ppb respectively (Adams et al. 1959). Because thorium has a high ionic potential, the Th^{4+} ion is quickly absorbed or precipitated as insoluble hydrolysats when in solution, hence the strong depletion of thorium with respect to uranium. Uranium is readily oxidized during weathering to the uranyl ion (UO_2^{2+}), which contains uranium in the 6+ valence state and forms several soluble complexes.

During karstification, the uranium tends to form soluble complexes and to remain in solution, whereas thorium, with it strong affinity for clay minerals, is quickly removed from solution. It is therefore important, for this dating method, that speleothems samples are not contaminated with clay minerals. During weathering uranium isotopes are fractionated, ^{234}U being enriched in groundwater with respect to its parent ^{238}U. Once in solution the uranium is transported as the soluble anionic carbonate complex $(UO_2(CO_3)_3)^{4-}$. The CO_2-charged groundwater may become supersaturated, on entering the cave environment, due to the degassing of CO_2. This causes the uranyl carbonate complex to dissociate to UO_2^{2+} and CO_2 resulting in coprecipitation of the uranyl ion UO_2^{2+} with calcite, forming a thorium-free closed system enriched in ^{234}U to the same extent as the parent water. This results in uranium concentrations within speleothems in the range of 10 ppb to 100 ppb (Harmom et al. 1974).

Uranium series dating depends on spontaneous transmutation of a certain amount of the unstable uranium nuclide to another form, over a fixed period of time, at a fixed rate, according to the general law:

$$N_t^d = N_t^p(e^{\lambda_p t} - 1) \qquad \text{equation 1}$$

where N_t = the number of atoms of a certain nuclide at some time t, N_0 = the number of atoms of that nuclide at t = 0, and λ = the decay constant given in terms of sec^{-1} (which is a measure of the probability of the nuclide decaying within a certain period of time).

When the daughter product is absent initially from the host material, as with the $^{230}Th/^{234}U$ dating method, the radioactive decay of the parent nuclide is described by equation 1, and the age of the deposit can be simply determined from the relationship:

$$N_t = N_o^x e^{-\lambda t} \qquad \text{equation 2}$$

where N_t^d and N_t^p are the respective amounts of daughter and parent nuclides at time t.

Only ^{234}U and ^{238}U are co-precipitated with calcite from water essentially free of thorium; any ^{230}Th subsequentally found is the product of radioactive decay of the ^{234}U and ^{238}U. Thus, the amount of ^{230}Th present is a direct measure of the age of the sample at any subsequent time t. Taking into account the initial disequilibrium of ^{234}U, the age of a sample is determined from the relationship:

$$[\frac{^{230}Th}{^{234}U}]_t = (\frac{1-e^{-\lambda_{230}t}}{1-\frac{^{234}U}{^{238}U}_t}) - (\frac{\lambda_{230}}{\lambda_{230}-\lambda_{234}})(1-\frac{1}{[\frac{^{234}U}{^{238}U}]_t})(1-e^{-(\lambda_{230}-\lambda_{234})t}) \qquad \text{equation 3}$$

where $[\frac{^{230}Th}{^{234}U}]_t$ and $[\frac{^{234}U}{^{238}U}]_t$ are measured activity ratios at time t,

λ_{230} is the decay constant of ^{230}Th, and λ_{234} is the decay constant of ^{234}U. The ^{230}Th half-life is the time required for the original number of atoms of a nuclide present to decrease by one-half. The half-life is related to the inverse of the decay constant. Thus, the longer the half-life, the greater the range of the method. This method has a potential range of about 1000 - 350 000 years B.P. (Harmon et al. 1975).

APPENDIX EIGTH

PARTICLE SIZE ANALYSIS OF SEDIMENT FROM RAMSAY'S NECK CAVE AND STREAM FLOWING INTO THE CAVE

Three sediment samples were removed from Ramsay's Neck Cave and two from the stream flowing into the cave for particle size analysis. Each sample was first wet-sieved to remove the silt/clay component. The material coarser than 4 phi was then oven dried at 60 degrees Celsius for two days. Each sample was then dry sieved through 0.5 phi division sieves for 30 minutes. The fraction remaining on each sieve was then weighed to one decimal place. When large quantities of finer sediment were found on a sieve, the sample was subdivided and then resieved so as not to overload the sieve.

Folk-Ward statistics were used for a statistical analysis of the samples. The computational methods were as follows:

Mean

$$M_z = \frac{P_{16} + P_{50} + P_{84}}{3}$$

Inclusive graphic standard deviation

$$\sigma_1 = \frac{P_{84} - P_{16}}{4} + \frac{P_{95} - P_5}{6.6}$$

Inclusive graphic skewness

$$Sk_1 = \frac{P_{16} + P_{84} - 2P_{50}}{2(P_{84} - P_{16})} + \frac{P_5 + P_{95} - 2P_{50}}{2(P_{95} - P_5)}$$

Graphic kurtosis

$$K_1 = \frac{P_{95} - P_5}{2.44(P_{75} - P_{25})}$$

where P_i is the diameter in σ units at the ith percentile [$\sigma = -\log_2$ (diameter in mm)]

SURFACE STREAM SEDIMENT sample 1

FOLK-WARD STATISTICS

MEAN	=	-3.90
VARIANCE	=	4.20
STD. DEVN.	=	2.05
SKEWNESS	=	0.53
KURTOSIS	=	1.51

DATA FOR DRAWING FREQUENCY CURVES

SIEVE	WEIGHT	WT. PCT.	CUM. WT. PCT.
-6.0	0.0	0.0	0.0
-5.5	363.0	9.2	9.2
-5.0	814.9	20.7	29.9
-4.5	645.2	16.4	46.2
-4.0	468.3	11.9	58.1
-3.5	345.5	8.8	66.8
-3.0	291.7	7.4	74.2
-2.5	231.2	5.9	80.1
-2.0	159.0	4.0	84.1
-1.5	124.0	3.1	87.2
-1.0	84.1	2.1	89.3
-0.5	68.0	1.7	91.1
0.0	44.0	1.1	92.2
0.5	28.2	0.7	92.9
1.0	21.9	0.6	93.5
1.5	20.8	0.5	94.0
2.0	21.0	0.5	94.5
2.5	28.0	0.7	95.3
3.0	61.2	1.6	96.8
3.5	19.8	0.5	97.3
4.0	36.0	0.9	98.2
>4.0	70.3	1.8	100.0

SURFACE STREAM SEDIMENT sample 2

FOLK-WARD STATISTICS

MEAN	=	-3.78
VARIANCE	=	5.08
STD. DEVN.	=	2.25
SKEWNESS	=	0.47
KURTOSIS	=	1.66

DATA FOR DRAWING FREQUENCY CURVES

SIEVE	WEIGHT	WT. PCT.	CUM. WT. PCT.
-6.0	0.0	0.0	0.0
-5.5	536.5	13.5	13.5
-5.0	641.4	16.1	29.6
-4.5	491.3	12.4	42.0
-4.0	469.5	11.8	53.8
-3.5	530.3	13.4	67.2
-3.0	298.8	7.5	74.7
-2.5	184.4	4.6	79.3
-2.0	134.5	3.4	82.7
-1.5	102.6	2.6	85.3
-1.0	68.1	1.7	87.0
-0.5	55.7	1.4	88.4
0.0	38.5	1.0	89.4
0.5	28.9	0.7	90.1
1.0	24.1	0.6	90.7
1.5	20.9	0.5	91.2
2.0	24.3	0.6	91.8

2.5	38.1	1.0	92.8
3.0	89.5	2.3	95.0
3.5	22.0	0.6	95.6
4.0	57.6	1.4	97.0
>4.0	118.0	3.0	100.0

CAVE STREAM SEDIMENT

FOLK-WARD STATISTICS

MEAN	=	-2.70
VARIANCE	=	7.48
STD. DEVN.	=	2.74
SKEWNESS	=	0.42
KURTOSIS	=	1.08

DATA FOR DRAWING FREQUENCY CURVES

SIEVE	WEIGHT	WT. PCT.	CUM. WT. PCT.
-6.0	0.0	0.0	0.0
-5.5	118.0	7.0	7.0
-5.0	233.8	13.9	20.9
-4.5	194.6	11.5	32.4
-4.0	108.4	6.4	38.8
-3.5	148.0	8.8	47.6
-3.0	164.6	9.8	57.4
-2.5	112.4	6.6	64.0
-2.0	100.0	6.0	70.0
-1.5	84.5	5.0	75.0
-1.0	52.0	3.0	78.0
-0.5	46.2	2.8	80.8
0.0	31.3	1.9	82.7
0.5	25.3	1.5	84.2
1.0	21.3	1.2	85.4
1.5	22.1	1.3	86.7
2.0	28.5	1.7	88.4
2.5	41.3	2.5	90.9
3.0	64.2	3.8	94.7
3.5	20.6	1.2	95.9
4.0	12.1	0.7	96.6
>4.0	57.0	3.4	100.0

ANCIENT CAVE STREAM SEDIMENT

FOLK-WARD STATISTICS

MEAN	=	-5.16
VARIANCE	=	6.14
STD. DEVN.	=	2.48
SKEWNESS	=	0.73
KURTOSIS	=	2.46

DATA FOR DRAWING FREQUENCY CURVES

SIEVE	WEIGHT	WT. PCT.	CUM. WT. PCT.
-7.0	0.0	0.0	0.0
-6.5	937.2	18.5	18.5
-6.0	1482.7	29.3	47.8
-5.5	695.2	13.7	61.5
-5.0	502.2	9.9	71.4
-4.5	257.7	5.1	76.5
-4.0	230.3	4.5	81.0

-3.5	91.5	1.8	82.8
-3.0	56.5	1.1	83.9
-2.5	44.3	0.9	84.8
-2.0	39.4	0.8	85.6
-1.5	33.8	0.7	86.3
-1.0	29.7	0.6	86.9
-0.5	29.2	0.6	87.5
0.0	25.5	0.5	88.0
0.5	23.1	0.4	88.4
1.0	24.6	0.5	88.9
1.5	24.8	0.5	89.4
2.0	32.1	0.6	90.0
2.5	43.1	0.9	90.9
3.0	138.1	2.7	93.6
3.5	66.3	1.3	94.9
4.0	36.4	0.7	95.6
>4.0	221.8	4.4	100.0

FINE-GRAINED SEDIMENT

DATA FOR DRAWING FREQUENCY CURVES

SIEVE	WEIGHT	WT. PCT.	CUM. WT. PCT.
-3.0	0.0	0.0	0.0
-2.5	0.3	0.8	0.8
-2.0	0.1	0.3	1.1
-1.5	0.3	0.8	1.9
-1.0	0.2	0.5	2.4
-0.5	0.1	0.3	2.7
0.0	0.2	0.5	3.2
0.5	0.1	0.3	3.5
1.0	0.1	0.3	3.8
1.5	0.1	0.2	4.0
2.0	0.1	0.3	4.3
2.5	0.1	0.3	4.6
3.0	1.3	3.5	8.1
3.5	2.2	5.9	14.0
4.0	2.4	6.5	20.5
>4.0	29.5	79.5	100.0

APPENDIX NINE

POLLEN EXTRACTION METHOD

The following process extracts pollen from a sample and prepares it for permanent mounting.

(1) Treatment with KOH:

This removes any humic acid that may be present. One to five grams of the sample is placed into a Nalgen centrifuge tube with 7 ml of 10 percent KOH. This is placed in a water bath and kept at just below boiling, for 10 minutes, and is stirred occasionally with a glass rod to ensure the sample is disaggregated.

(2) Removal of plant fragments:

The contents of each centrifuge tube are poured through a fine sieve (100 mesh brass) into a 100 ml beaker. This is then rinsed several times with distilled water. The volume of the rinsings is then reduced in volume by centrifuging several times, at 2000 revolutions per minute for four minutes each time, and decanting the supernatant fluid into the sink. This is then finally rinsed with distilled water, centifuged and decanted and repeated once more. Five millilitres of glacial acetic acid is added and stirred. This is then centrifuged and decanted.

(3) Removal of cellulose by Acetolysis:

In a fume cabinet 22.5 ml of acetic anhydride is poured into a dry beaker and 2.5 ml of concentrated sulphuric acid slowly added. The acetolysis solution is then poured into each centifuge tube containing the pollen analysis samples. The tubes are then placed in a fast boiling water bath which is allowed to come to the boil again and left for exactly 4 minutes. The tubes are then removed, centrifuged, and decanted into the sink with running water. Five milliletres of glacial acetic acid is stirred in and the tubes centrifuged and decanted again.

Note - If any extraneous inorganic material can be seen in the sample, this must be removed with hydrofluoric acid.

(4) Staining:

The sample material is put in suspension with distilled water and three

drops of 10 percent KOH added. This is stirred, centrifuged, and decanted. Basic Fuchsin solution is added and the suspension is allowed to stand for 10 minutes, but stirred occasionally. This is then centrifuged and decanted, rinsed once more with distilled water, and centrifuged and decanted again.

(5) Mounting:

Glycerine jelly is gently warmed in a warm water bath. One drop of the pollen sample is pipetted onto the microscope slide, with two drops of glycerine. The slide is then warmed and a cover slip is lowered over the drop. This is left until the glycerine hardens before examination under the microscope.

REFERENCES

ADAMS,C.S. and A.C.SWINNERTON 1937: The solubility of calcium carbonate. Transactions of the American Geophysical Union 11(2):504-508.

ADKIN,G.L. 1912: The discovery and extent of former glaciation in the Tararua Ranges, North Island, New Zealand. Transactions of the New Zealand Institute 44:308-316.

ASH,D.W. 1975: Appletite: A new calcite structure from Apple Cave, Orange County, Indiana. NSS Bulletin 37:35-39.

ASTON,B.C. 1915a: Limestone - North Island analysis. The Journal of Agriculture 11(3):235-240.

ASTON,B.C. 1915b: Limestone of the Wairarapa and Manawata. The Journal of Agriculture 11(5):403-410.

ASTON,B.C. 1918: Limestones of New Zealand - further analysis. New Zealand Journal of Agriculture 17(2):98-101.

ATKINSON,T.C. 1968: The earlist stages of underground drainage in limestone - a speculative discussion. Proceedings of the British Spelaeological Association 6:53-70.

ATKINSON,T.C.; P.L.SMART; R.S.HARMON and A.C.WALTHAM 1978: Palaeoclimatic and geomorphic implications of 230TH/234U dates on speleothems from Britain. Nature 272:24-28.

BAGNALL,A.G. 1976: Wairarapa: An historical excursion. Hedley's Bookshop for the Masterton trust Lands Trust. 607 p.

BARRETT,P.J. 1963: The development of Kairimu Cave, Marakopa district, south-west Auckland. New Zealand Journal of Geology and Geophysics 6:288-98.

BARTRAM,J.A. and A.P.MASON 1948: Lapiés and solution pits in basalts at Hokianga, New Zealand. New Zealand Journal of Science

and Technology 30B:165-172.

BEU,A.G.; T.C.GRANT-TAYLOR, and N.de B.HORNIBROOK 1980: The Te Aute limestone facies, Poverty Bay to Northern Wairarapa. New Zealand Geological Survey Miscellaneous Series Map 13 34 p. + 2 maps.

BIROT,P. 1954 Problemes de morphologie karstique. Annls. Geogr. 63:161-92.

BLAKEMORE,L.C. 1973 Element accessions in rainwater at Taita, New Zealand, 1963-1971. New Zealand Soil Bureau Scientific Report No.17 16 p.

BLOOM,A.C. 1978: Geomorphology: A systematic analysis of late Cenozoic landforms. Prentice-Hall, New Jersey 510 p.

BÖGLI,A. 1960: Solution of limestone and karren formation. ("Kalkosung und karrenbilding") Translated by Mary Fargher. In SWEETING,M.M. (ed.) 1981 Karst Geomorphology Benchmark papers in geology No.59 pp. 64-89.

BÖGLI,A. 1980: Karst Hydrology and Physical Speleology. Translated by J.C.Schmid. Springer-Verlay Berlin 284 p.

BRAIN,C.K. 1958: The Transvaal Ape-Man-Bearing Cave Deposits. Transvaal Museum Memoir No.11, 131 p.

BROOK,G.A. 1981: The limestone pavements of Nahanni: An example of micro-scale labyrinth karst. South African Geographical Journal 63(1):35-46.

BROOK,G.A. and D.C.FORD 1978: The origin of labyrinth and tower karst and the climatic conditions necessary for their development. Nature 275:493-96.

BROUGHAM,G.G and E.C.O'CONNOR 1982: Pohangina River: A gravel resource and sediment study. Manawatu Catchment Board and Regional Water Board, Palmerston North (N.Z.). 21 p.

BROWNE,G.H. 1978: Wanganui strata of the Mangaohane Plateau, Northern Ruahine Range, Taihape. Tane 24:199-210.

BULL,P.A. 1978: A quantitative approach to scanning electron microscope analysis of cave sediments. In WHALLEY,W.B. (ed.) Scanning electron microscopy in the study of sediments. Geo Abstracts, Norwich pp. 201-226.

BULL,P.A. 1983: Chemical sedimentation in caves. In GOUDIE,A.S. and K.PYE (ed.) Chemical Sediments and Geomorphology Academic Press, London, pp. 301-320.

CAEN - see de CAEN

CARLE,C.J. 1980: Forty Mile Bush: A tribute to the pioneers. North Wairarapa News 280 p.

CHERDYNTSEV,V.V.; I.V.KAZACHEVSKII, and E.A.KUZMINA 1965: Dating of Pleistocene carbonate formations by the Thorium and Uranium isotopes. Geochem. Internat. 2:794-801.

CHINN,T.J.H. 1983: New Zealand glacial record, 10 to 15 000 B.P.. In CHAPPELL,J.M.A. and A.GRINDROD (ed.) Proceedings of the 1st CLIMANX Conference. Australian Acadamy of Science, A.N.U., Canberra. pp. 71-72.

CHORLEY,R.J.; S.A.SCHUMM, and D.E.SUGDEN 1984: Geomorphology Methuem, London, 606 p.

CLARIDGE,G.G.C. 1975: Element accessions in rainwater, Catchment 4, Taita experimental station. 1969-1974. New Zealand Soil Bureau Science Report No.24 56 p.

COLE,J.W. 1984: Taupo-Rotorua Depression: an ensialic marginal basin basin of North Island New Zealand. In KOKELAAR,B.P. and M.F.HAWELLS (ed.) Marginal Basin Geology: Volcanic and associated sedimentary and tectonic processes in modern and ancient margin basins. Geological Society Special Publication No.16 pp 109-120.

COLE,J.W. and K.B.LEWIS 1981: Evolution of the Taupo-Hikurangi Subduction System. Tectonphysics 72:1-21.

COLENSO,W. 1884: Account of visits to, and crossings over the Ruahine Mountain Range, Hawke's Bay, Hew Zealand. Daily Telegraph, Napier.

COLLCUTT,S.N. 1979: The analysis of Quaternary cave sediments. World Archaeology 10(3):290-303.

CORBEL,J. 1959: Erosion en terrain calcarire. Annls. Geogr. 68:97-120.

COTTON,C.A. 1948: Landscape. Whitcombe and Tombs Ltd, Christchurch.

COULTER,J.D. 1969: Notes on the Climate of Wairarapa. New Zealand Metrological Service Technical Information Circular No.133 8 p.

CRAMER,H. 1941: Die systematik der karstdolinen. Neues Jb. Miner. Geol. Palaoat. 85:293-382.

CRAWFORD,J.C. 1870: On the Geology of the Provence of Wellington. Transactions of the New Zealand Institute 2:343-360.

CUMINGS,E.R. 1906: On the weathering of the sub-Carboniferous limestone of southern Indiana. Proceedings of the Indiana Academy of Science 1905:85-100.

CVIJIC,J. 1893: The Doline. ("Das karstphanomen") Translatered by Mary Fargher. In SWEETING,M.M. (ed.) 1981 Karst Geomorphology. Benchmark papers in Geology No.59 pp. 23-41.

CVIJIC,J. 1924: The evolution of lapiés - a study in karst physiography. Geographical Review 14:26-49.

DAVEY,F.J.; M.HAMPTON; J.CHILDS; M.A.FISHER; K.LEWIS and J.R.PETTINGA 1986: Structure of a growing accretionary prism,

Hikurangi margin, New Zealand. Geology 14:663-666.

DAVIS,W.M. 1899: The drainage of cuestas. Proceedings of the Geological Association, London 16:75-93.

DAY,M.J. 1978a: The morphology of tropical humid karst with particular reference to the Caribbean and central America. D.Phil Thesis, University of Oxford.

DAY,M.J. 1978b: Morphology and distribution of residual limestone hills (mogotes) in the karst of northern Puerto Rico. Geological Society of America Bulletin 89:426-32.

DAY,M.J. 1980: Rock hardness: Field assessement and geomorphic importance. The Professional Geographer 32:72-81.

DAY,M.J. 1981: Short communications: Rock hardness and landform development in the Gunung Mulu National Park, Sarawak, East Malaysia. Earth Surface Processes and Landforms 6:165-172.

DAY,M.J. 1982: The influence of some material properties on the development of tropical karst terrain. Cave Science - Transactions of the British Cave Research Association 9(1):27-37.

DAY,M.J. and A.S.GOUDIE 1977: Field asesssment of rock hardness using the Schmidt Test Hammer. British Geomorphological Research Group Technical Bulletin No.18.

de CAEN,R.F.B. and J.H.DARLEY 1969: An examimation of Wanganui carbonates of the Dannevirke area. Technical note No.39. New Zealand Geological Survey unpublished open-file Petroleum Report No.384.

De SITTER,L.U. 1959: Structural Geology. (1st edn.) McGraw-Hill, New York. 104 p.

DOUGLAS,I. 1968: Some hydrologic factors in the denudation of limestone

terrains. Zeitschift fur Geomorphology 12:241-255.

DOWLING,R.K. 1974: Solutional processes in the karst of the Riwaka Basin, Northwest Nelson. M.Sc. Thesis, University of Auckland.

DRAKE,J. and D.C.FORD 1972: The analysis of growth patterns of two generation populations; The example of karst sink holes. Canadian Geographer 16:381-384.

DRAKE,J. and D.C.FORD 1976: Solutional erosion in the southern Canadian Rockies. Canadian Geographer 20(2):158-170.

DUNKERLEY,D.L. 1983: Lithology and micro-topography in the Chillagoe karst, Queensland, Australia. Zeitschrift fur Geomorphology N.F. 27(2):191-204.

EMBLETON,C. and C.A.M.KING 1975: Periglacial Geomorphology. Edward Arnold. 203 p.

FAEGRI,K. and J.IVERSON 1964: Textbook of Pollen Analysis. N.Y.C. Hafner, 237 p.

FITTON,W.H. 1836: Observations on some of the strata - between the chalk and the Oxford Oolite in the south-east of England. Transactions of the Geological Society Series 2 iv:103.

FORD,D.C. 1964: Origin of closed depressions in the central Mendip hills. 20th International Geomorphological Congress abstracts:105-106.

FORD,D.C. 1982: Karst groundwater activity and landform gensis in modern permafrost regions of Canada. In La FLEUR,R.G. (ed.) Groundwater as a Geomorphic Agent. Allen and Unwin. Boston pp. 340-350.

FORD,D.C.; P.THOMPSON and H.P.SCHWARCZ 1972: Dating cave calcite deposits by the uranium disequilibrium method: Some preliminary results from Crows Nest Pass, Alberta. In

YATSU,E. and A.FALCONER (ed.) Research Methods in Pleistocene Geomorphology Guelph (Ontario), Univ. Guelph pp. 247-256.

FORD,D.C.; H.P.SCHWARCZ; J.J.DRAKE; M.GASCOYNE; R.S.HARMON and A.G.LATHAM 1981: Estimates of the age of the existing relief within the Southern Rocky Mountains of Canada. Arctic and Alpine Research 13(1):1-10.

FORDER,S.P. 1978: A review of the hydrocarbon potential of the PPL 38055 area, Hawke's Bay, New Zealand. New Zealand Geological Survey unpublished open-file petroleum report No.734.

FORNACA-RINALDI,G. 1968: Il Methado TH^{230}/U^{238} per la Datazione di Stalatti e Stalagmiti. Boll Geophis. teorica Appicata 10:3-14.

FRANK,R.M. 1965: Petrologic study of sediments from selected central Texas caves. M.A. Thesis, Univ. Texas.

GASCOYNE,M.; H.P.SCHWARCH and D.C.FORD 1978: Uranium series dating and stable isotope studies of speleothems. Part 1: Theory and techniques. Transactions of the British Cave Research Association 5:91-111.

GASCOYNE,M.; A.G.LATHEM; R.S.HARMON and D.C.FORD 1983: The antiquity of Castleguard Cave, Columbia icefields, Alberta, Canada. Arctic and Alpine Research 15(4):463-70.

GHANI,M.A. 1978: Late Cenozoic vertical crustal movements in the southern North Island, New Zealand. New Zealand Journal of Geology and Geophysics 21:117-25.

GIBBS,H.S. 1980: New Zealand Soils: an introduction. Oxford University Press, Oxford. 115 p.

GOBBY,L.I. 1979: Karren morphology in two areas of New Zealand. M.A. Thesis, University of Auckland. 115 p.

GOLDIE,H.S. 1973: The limestone pavements of Craven. Transactions of the Cave Research Group, Great Britain 15(3):175-190.

GOLDIE,H.S. 1981: Morphology of the limestone pavements of Farleton Knott, (Cumbria, England). Transactions of the British Cave Research Association 8(4):207-224.

GREGORY,K.J. 1966: Dry valleys and the composition of the drainage net. Journal of Hydrology 4:327-40.

GREGORY,K.J. and D.E.WALLING 1973: Drainage Basin Form and Process - a geomorphological approach. Edward Arnold, London, 458 p.

GROOM,G.E. and V.H.WILLIAMS 1965: The solution of limestone in South Wales. Geographical Journal 131(1):37-41.

GRUND,A. 1903: Die karsthydrographic - studien aus westbosnien. Penck's Geogr. Abhandl. 7:1-200

GUNN,J. 1978: Karst hydrology and solution in the Waitomo district, New Zealand. Ph.D. Thesis, University of Auckland.

GUNN,J. 1981: Hydrological processes in karst depressions. Zeitschift fur Geomorphology N.F. 25(3):313-31.

HALLIDAY,S.L. and A.GUDEX 1984: Report on a survey of caves in the Puketoi and Waewaepa Ranges. Unpublished Manawatu Museum Fieldwork Report No.2 17 p.

HARMON,R.S. 1980: Paleoclimatic information from isotopic studies of speleothems : a review. In MAHANEY,W.C. (ed.) Quaternary Paleoclimates Geo Abstracts pp. 299-318.

HARMON,R.S.; P.THOMPSON; H.P.SCHWARCZ and D.C.FORD 1975: Uranium-series dating of speleothems. NSS Bulletin 37(2):21-33.

HARMSEN,F.J. 1984a: Stratigraphy, depositional history, and digenesis of the Te Aute Group, a Pliocene temperate

carbonate-bearing sequence in southern Hawke's Bay, New Zealand. Ph.D. Thesis, Victoria University of Wellington.

HARMSEN,F.J. 1984b: Stratigraphic sections of the Pliocene Te Aute Group in central and southern Hawke's Bay, N.Z.. Publication of Geology Department, Victoria University of Wellington. No 29.

HARMSEN,F.J. 1985: Lithostratigraphy of Pliocene strata, central and southern Hawke's Bay, N.Z.. New Zealand Journal of Geology and Geophysics 28:413-433.

HEALY,J. 1962: Structure and volcanism in the Taupo Volcanic Zone, New Zealand. In: Crust of the Pacific Basin American Geophysical Union Monograph No.6 151-157.

HECTOR,J. 1877: Progress Report 1874-1876. New Zealand Geological Survey reports of geological explorations 1874-1877 (9):iii-xiii.

HEIM,A. 1878: Uber die karrenfelder. Jahrb. Schweiz. Alpenclubs 13:421-433.

HENDERSON,J. 1915: Notes on the geology of the Weber District. New Zealand Geological Survey 9th annual report No.103.

HENDY,C.H. and A.T.WILSON 1968: Palaeoclimatic data from speleothems. Nature 219:48-51.

HILL,R.T. 1896: Descriptive topographic terms of Spanish America. National Geographic Magazine 7:291-302.

HOCHSTETTER,F.von. 1864: Reise der Novara Geol. Th. 1 Bd.

HOCHSTETTER,F.von. 1867: New Zealand: Its physical geography, geology, and natural history. Stuttgart.

HOLLINGWORTH,S.E.; J.H.TAYLOR and G.A.KELLAWAY 1944: Large-scale

superficial structures in the Northampton Ironstone Field. The Quarterly Journal of the Geological Society of London 100:1-44.

HORTON,R.E 1932: Drainage basin characteristics. Transactions of the American Geophysical Union 13:350-61.

HJULSTRÖM,F.L. 1935: Studies on the morphological activities of rivers. Bulletin of the Geological Institute of Uppsala 25:221-227.

IRELAND,P. 1979: Geomorphological variations of "case-hardening" in Puerto Rico. Zeitschrift fur Geomorphology Supplementband 32:9-20.

IVANOVICH,M. and P.IRELAND 1984: Measurement of Uranium series disequilibrium in the case-hardened Aymamon Limestone of Puerto Rico. Zeitschrift fur Geomorphology N.F. 28(3):305-19.

JUDSON,S. 1947: Large-scale superficial structures - a discussion. Journal of Geology 55:168-175.

JENNINGS,J.N. 1971: Karst. Australian National University Press, Canberra.

JENNINGS,J.N. 1975: Doline morphometry as a morphogenetic tool : New Zealand examples. New Zealand Geographer 31:6-28.

JENNINGS,J.N. 1982: Quaternary complications in fluviokarst at Cooleman Plain, N.S.W. Australian Geographical Studies 15:137-147.

JENNINGS,J.N. 1985: Karst Geomorphology (2nd edn.) Basil Blackwell, Oxford 293 p.

JENNINGS,J.N. and M.M.SWEETING 1963: The limestone ranges of the Fitzroy Basin, Western Australia: A tropical semi-arid karst. Bonner Geogr. Abhand. 32:1-10.

KAMP,P.J.J. 1982: Landforms of Hawke's Bay and their origin : a plate tectonic interpretation. In SOON,J.M. and M.J.SELBY (ed.) Landforms of New Zealand. Longman Paul, Auckland, pp. 233-254.

KAMP,J.J. and C.G.VUCETICH 1982: Landforms of Wairarapa in a geological context. In SOONS,J.M. and M.J.SELBY (ed.) Landforms of New Zealand. Longman Paul, Auckland pp. 255-268.

KATZ,H.R. 1974: Ariel bank off Gisborne - an offshore late Cenozoic structure, and the problem of acoustic basement on the East Coast, North Island, New Zealand. New Zealand Journal of Geology and Geophysics 18:19-108.

KELLAWAY,G.A. and J.H.TAYLOR 1952: Early stages in the physiographic evolution of a portion of the East Midlands. Quarterly Journal of the Geological Society of London 108(4):343-366.

KEMMERLY,P.R. 1982: Spatial analysis of a karst depression population : clues to genesis. Geological Society of America Bulletin 93:1078-86.

KINGMA,J.T. 1962: Sheet 11 Dannevirke (1st edn.) Geological map of New Zealand 1:250 000. D.S.I.R. Wellington, New Zealand.

KINGMA,J.T. 1967: Sheet 12 Wellington (1st edn.) Geological map of New Zealand 1:250 000. D.S.I.R. Wellington, New Zealand.

KINGMA,J.T. 1971: Geology of the Te Aute Subdivision. New Zealand Geological Survey Bulletin No.70, 173 p.

KITT,W. 1962: Survey of limestone analysis 1917-1961. Dominion Laboratory Report No.D.C. 2060, DSIR Lower Hutt N.Z.

KNIGHTON,A.D. 1975: Form adjustment in a limestone dry valley at Castleton, Derbyshire. East Midland Geographer 6(3):130-35.

KUKLA,J. and V.LOZEK 1958: On the problem of investigations of cave deposits Czechoslovensky Karas 11:19-83.

LAING,A.C.M. 1963: The geology of the Waipatiki area (N150/5) M.Sc. Thesis, Victoria University of Wellington.

LATHAM,A.G.; H.P.SCHWARCZ; D.C.FORD and G.W.PEARCE 1979: Palaeomagnetism of stalagmite deposits. Nature 280:383-385.

LATHAM,A.G.; H.P.SCHWARCZ; D.C.FORD and G.W.PEARCE 1982: The paleomagnetism and U-Th dating of three Canadian speleothems : evidence for the westward drift, 5.4-2.1 ka B.P. Canadian Journal of Earth Science 19:1985-1995.

LATTMAN,L.H. and W.H.OLIVE 1955: Solution-widened joints in Trans-Pecos, Texas. Bulletin of the American Assocation of Petroleum Geologists 39(10):2084-2087.

LEHMANN,H. 1936: Morphologische studien auf Java. Stuttgart.

LEHMANN,O. 1927: Das tote gebirge als hochkarst. Mitt. Geogr. Ges. Wien. 70:201-242.

LESLIE,W.C. and R.J.S.HOLLONGSWORTH 1972: Exploration in the East Coast Basin, New Zealand. The APEA Journal 12:39-44.

LEWIS,K.B. 1971: Growth rates of folds using tilted wave-planed surfaces: coast and continental shelf, Hawke's Bay, New Zealand. In COLLINS,B.W. and R.FRASER Recent Crustal Movements Bulletin of the Royal Society of New Zealand No.9 pp. 225-231.

LEWIS,K.B. 1973: Erosion and deposition on a tilting continental shelf during Quaternary oscillations of sea level. New Zealand Journal of Geology and Geophysics 16:281-301.

LEWIS,K.B. 1974: Upper Tertiary rocks from the continental shelf and slope of southern Hawke's Bay New Zealand Journal of

Marine and Freshwater Research. 8:663-70.

LEWIS,K.B. 1976: Turnagain Bathymetry N.Z. Ocean. Inst. Chart. Coastal Series 1:200 000 (2nd edn.).

LEWIS,K.B. 1980: Quaternary sedimentation on the Hikurangi oblique-subduction and transform margin, New Zealand. Special Publication Inst. Ass. Sediment. 4:171-189.

LILLIE,A.R. 1953: The Geology of the Dannevirke Subdivision. New Zealand Geological Survey Bulletin No.46, 156 p.

LINK,A.G. 1966: Textral classification of sediment. Sedimentology 7:249-54.

LUNDBERG,J. 1971: The Geomorphology of Chillagoe Limestone: Variations in lithology. M.SC. Thesis, A.N.U..

LYONS,R.G. 1983: A study of palaeomagnetism in New Zealand cave deposits. M.Sc. Thesis, University of Auckland.

LYONS,R.G. 1984: Palaeomagnetic observations : Nettlebed Cave. New Zealand Speleological Society Bulletin 7(132):361-62.

McGLONE,M.S. 1983: New Zealand vegetation and climate since the last glaciation: 32+/-KA, 25-20KA, 18+/-2KA, 15-10KA, 7+/-2KA. In CHAPPELL,J.M.A. and A.GRINDROD (ed.) Proceedings of the 1st CLIMANZ Conference. Australian Acadamy of Science, A.N.U. Canberra pp.16-17, 38-39, 63-66, 81-82, 102-103.

McKAY,A. 1877a: Report on country between Masterton and Napier. New Zealand Geological Survey reports of geological exploration 1876-1877(10):67-94.

McKAY,A. 1877b: Report on country between Cape Kidnappers and Cape Turnagain. New Zealand Survey reports of geological exploration 1874-1876(9):43-53.

McCONNELL,H. and J.M.HORN 1972: Probabilities of surface karst. In CHORLEY,R.J. (ed.) Spatial Analysis in Geomorphology Harper and Row, New York pp. 111-133.

MAF ADVISORY SERVICES DIVISION, DANNEVIRKE 1979: Southern Hawke's Bay - Northern Wairarapa Agriculture; features and significance. Aglink NZA 47

MILOJEVIC,S.M. 1936: Les brachyclasas et leur role dans les relations hydraphiques et le relief du karst. Posebna izdanja Srp.kralj. Akad. 21 Dec.

MONROE,W.H. 1964: Large retrogressive landslides in north-central Puerto Rico. U.S. Geological Survey Professional Paper 501-B:B123-B125.

MONROE,W.H. 1966: Formation of tropical karst topography by limestone solution and reprecipitation. In SWEETING,M.M. (ed.) 1981 Karst Geomorphology. Benckmark papers in Geology No.59 pp. 266-272.

MONROE,W.H. 1976: The karst landforms of Puerto Rico. U.S. Geological Survey Professional Paper 899.

MONROE,W.H 1980: Some tropical landforms of Puerto Rico. U.S. Geological Survey Professional Paper 1159.

MOORE,P.R. and S.E.BELLISS 1979: The limestone resources of Southern Hawke's Bay and Northern Wairarapa. New Zealand Geological Survey Report N.Z.G.S. No.87 32 p.

MORGAN,P.G. 1919: The limestone and phosphate resources of New Zealand. Part 1 - Limestone. New Zealand Geological Survey Bulletin No.22 316 p.

MOSLEY,M.P. 1977: Southern Ruahine investigation; report on erosion and sedimentation. Manawatu Catchment Board and Regional Water Board, Palmerston North (N.Z.). 796 p.

MURRAY,J.W. and A.B.HAWKINS 1973: Geology and physical environment. In HADFIELD,C. and A.M.HADFIELD (ed.) The Cotswolds - a new study. 322 p.

MUSKETT,P.J. 1971: Periglacial gulls in the Upper Witham Valley. Transactions of the Lincshire Naturalistics Union 17:210-216.

NEEF,G. 1967: The geology of Eketahuna (N.Z.M.S. 1 N. 153) Ph.D. Thesis, Victoria University of Wellington.

NEEF,G. 1974: Sheet N153 Eketahuna (1st edn.) Geological map of New Zealand 1:63 360 D.S.I.R., Wellington, New Zealand.

NEEF,G. 1984: Late Cenozoic and Early Quaternaty stratigraphy of the Eketahuna district (N153) New Zealand Geological Survey Bulletin No.96 101 p.

New Zealand Meteorological Service 1983: Summaries of climatological Observations to 1980. New Zealand Metrological Service Misc. Pub. No.177 172 p.

National Water and Soil Conservation Authority 1978: New Zealand Land Resource Inventory Worsheets N/150, 151, 152. 1:63 360.

NOBLE,K.E. 1985: Land use capability classification of the southern Hawke's Bay - northern Wairarapa Region : a bulletin to accompany New Zealand Land Resource Inventory Worksheets. Water and Soil Miscellaneous Publication No.74, 128p.

ODELL,B. 1985: Karst landforms in Thailand 2. The Bogaz-caves in Po Hin Long Gla. Grotten 20(1):27-31.

OLLIER,C.D. 1981: Tectonics and landforms edited by K.M.CLAYTON Geomorphology Texts No.6. Longman, London and New York. 324 p.

ONGLEY,M. 1935: Eketahuna Subdivision New Zealand geological survey 29th Annual Report 1934-1936:1-6.

PALMQUIST,R.C. 1977: Distribution and density of dolines in areas in mantled karst. In DILAMARTER,R.R. and S.C.CSALLANY Hydrologic Problems in Karst Regions. Western Kentucky Universtiy.

PALMQUIST,R. 1979: Geologic controls on doline characteristics in mantled karst. Zeitschrift fur Geomorphology Supplementband 32:90-106.

PANOS,V. and O.STELCL 1968: Physiographic and geologic control in development of Cuban Mogotes. Zeitschrift fur Geomorphology 12(2):117-165.

PANTIN,H.M. 1963: Submarine morphology east of the North Island, New Zealand. Bulletin of the New Zealand D.S.I.R. 149 44p.

PECK,S.B. 1979: Stalactites and helictites of marcasite, galene and sphalerite in Illinois and Wisconsin. NSS Bulletin 41:27-30.

PENGELLY,W. 1864: The introduction of cavern accumulations. Report of the Transactions of the Devonshire Association 3:31-41.

PENMAN,H.L. 1948: Natural evaporation from open water, bare soil and grass. Proceedings of the Royal Society (London) 193: 120 p.

PETERSON,G.M. 1976: Pollen analysis and the origin of cave sediments in the Central Kentucky Karst. NSS Bulletin 38(3):53-58.

PICKETT,R.G.; L.G.BRAY and R.D.STENNER 1976: The chemistry of cave watera. In FORD,T.D. and C.H.D.CULLINGFORD (ed.) The Science of Speleology Academic Press, London, pp. 213-266.

PITTY,A.F. 1966: An approach to the study of karst waters: Illustrated by results from Poole's Cavern, Buxton. Hull University Occasional Papers in Geography No.5 70 p.

PITTY,A.F.; R.A.HALLIWELL and H.S.GOLDIE 1985: Karst landforms and processes. In PITTY,A.F. (ed.) Themes in Geomorphology. Croom Helm, London. pp. 158-178.

PURSER,B.H. 1952: The Geology of the Waikato Heads M.Sc. Thesis, University of Auckland.

RIDD,M.F. 1964: The geology of the northern Wairarapa, North Island, New Zealand. B.P. Shell and Todd Petroleum Development Report. Report No.28. New Zealand Geological Survey unpublished open-file petroelum report No.201.

ROQUES,H. 1956: Sur l'existence d'un gradient karstique des pressions partielles de i'acide carbonique. C.R. Acad. Sci 242:3100-3102.

ROGLIC,J. 1964: Karst valleys in the Dinaric karst (Symposium, Karst Commission of the I.G.U. Stuttgart 1963) Erdkunde 18(2):113-116.

SALOMONS,W.;GOUDIE,A. and W.G.MOOK 1978: Isotopic composition of calcite deposits from Europe, Africa and India. Earth Surface Processes 3:43-57.

SALINGER,M.J. 1984: New Zealand climate : the last 5 million years. In VOGEL,J.C. (ed.) Late Cainozoic Palaeoclimates of the Southern Hemisphere. SASQUA International Symposium/Swaziland/29 August-2 September 1983. pp. 131-150.

SAWICKI,L.R. 1909: Ein beitray zum geographischen zykles im karst. Geogr. Zeit. 15:185-204.

SCHMIDT,V.A. 1982: Magnetostratigraphy of sediments in Mammoth Cave, Kentucky. Science 217:827-829.

SCHMIDT,V.A.; J.N.JENNINGS and H.BOA 1984: Dating cave sediments at Wee Jasper N.S.W. by magnetostratigraphy. Australian Journal of Earth Science 31:361-70.

SCHOELLER,H. 1950: Les variations de la teneur en gas carbonique des eaux, souterraines en function de l'altitude. C.R. Acad. Sci. 230:560-561.

SCHUMM,S.A. and R.J.CHORLEY 1966: Talus weathering and scarp recession in the Colorado Plateaus. Zeitschrift fur Geomorphology 10(1):11-36.

SCHROEDER,S. and D.C.FORD 1983: Clastic sediments in Castleguard cave, Columbia Icefields, Alberta, Canada. Arctic and Alpine Research 15(4):451-461.

SELBY,M.J. 1980: A rock mass strength classification for geomorphic purposes : with tests from Antartica and New Zealand. Zeitschrift fur Geomorphology N.F. 24(1):31-51.

SHALER,N.S. 1890: The origin and nature of soils. U.S. Geological Survey 12th annual report. Part 1 - geology.

SIMONETT,D.S. 1968: Cuesta. In FAIRBRIDGE,R.W. (ed.) The encyclopedia of Geomorphology Reinheld Book Co, pp. 233.

SINGH,L.J. 1971: Uplift and tilting of the Oterei coast, Wairarapa New Zealand, during the last ten thousand years. Royal Society of New Zealand Bulletin 9:217-219.

SMART,P.C.; P.A.BULL; J.ROSE; M.LAVERTY; H.FRIEDERICH and M.NOEL 1985: Surface and underground fluvial activity in the Gunung Mulu National Park, Sarawak. In DOUGLAS,I. and T.SPENCER (ed.) Environmental Change and Tropical Geomorphology. British Geomorphological Research Group. George Allen and Unwin pp. 123-149.

SMITH,D.I. 1975: The problem of limestone dry valleys - implications of recent work in limestone hydrology. In PEEL,R.; M.CHRISTOLM and P.HAGGETT (ed.) Processes in Physical and Human Geography. Heinemann Educational Books pp. 130-147.

SMITH,D.I. and T.C.ATKINSON 1976: Process, landform and climate in limestone regions. In DERBYSHIRE,E. (ed.) Geomorphology and Climate. Wiley, London, pp. 367-409.

SMITH,D.I. and M.P.NEWSON 1974: The dynamics of solutional and mechanical erosion in limestone catchments on the Mendip Hills, Somerset. In GREGORY,K.J. and D.E.WALLING (ed.) Fluvial Processes in Instrumental Watersheds. Institute of British Geographers Special Publication No.6:155-167.

SMITH,K.G. 1950: Standards for grading textures of erosional topography. American Journal of Science 248:655-68.

STRAHLER,A.N. 1957: Quantitative analysis of watershed geomorphology. Transactions of the American Geophysical Union 38:913-920.

STRAW,A. 1966: Periglacial mass movements on the Niagara Escarpment near Meaford, Grey County, Ontario. Geographical Bulletin 8(4):369-376.

SWEETING,M.M. 1972: Karst Landforms. Macmillian, London, 362 p.

SWEETING,M.M. 1978: Some observations on New Zealand limestone areas. In DAVIES,J.L. and M.A.J.WILLIAMS (ed.) Landform Evolution in Australasia. A.N.U. Press, Canberra, pp. 250-258.

SWEETING,M.M. 1980: Karst and climate - a reviev. Zeitschrift fur Geomorphology N.F. Suppleband 36:203-216.

SWEETING,M.M. and G.S.SWEETING 1969: Some aspects of the Carboniferous limestone in relation to its landforms. Méditerranee 7:201-209.

THOMPSON,A.S. 1854: Description of two caves in the North Island of New Zealand containing bones of Moas. Edinbourgh New Philosophical Journal 56:268-295.

THOMPSON,P.; H.P.SCHWAECZ and D.C.FORD 1974: Continental Pleistocene climatic variation from speleothem age and isotopic data. Science 184:893-895.

THURBER,D.C.; W.S.BROECKER,R.L. and H.A.POTRATZ 1965: Uranium series ages of coral from Pacific atolls. Science 149:55-58.

TRICART,J. 1968: Periglacial landforms. In FAIRBRIDGE,R.W. (ed.) Encyclopedia of Geomorphology Reinheld Book Co, pp. 829-833.

TRICART,J. 1970: Geomorphology of Cold Environments. Macmillian 320 p.

TROMBE,F. 1952: Traité de spéléologie Paget, Paris.

TRUGILL,S. 1985: Limestone Geomorpholohy Edited by CLAYTON,K.M. Geomorphological Texts No.8. Lonngman, London, 196 p.

VALLE,P.La 1968: Karst depression morphology in south central Kentucky. Geografiska Annaler 50A:94-108.

VELLA,P. 1962: Biostratigraphy and paleoecology of Mauriceville District, New Zealand. Transactions of the Royal Society of New Zealand, Geology 1(12):183-199.

VELLA,P. 1965: Sedimentary cycles, correlation and stratigraphic classification. Transactions of the Royal Society of New Zealand, Geology 3:1-9.

WALCOTT,R.I. 1978: Present tectonic and late Cenozoic evolution of New Zealand. Geophys. J. R. Astr. Soc. 52:137-164.

WELLMAN,H.W. 1967: Report on studies relating to Quaternary daistrophism in New Zealand. Minutes of the working group meeting for the Neotectonic study of the Pacific Region, Appendix 5. Quaternary Research (Jpn) 6:34-36.

WEYL,R. 1953: Die Sierra de Bahoruces von Santa Domingo und ihre

Stellung im Antillenbogen. N. Jb. Geol. u. Palaontol. Abh. 98:1-27.

WHITE,W.B. 1964: Sedimentation in caves - a reveiw. Bull. NSS 26(2):77-8.

WHITE,W.B. 1976: Cave minerals and speleothems. In FORD,T.D. and C.H.D.CULLINGFORD (ed.) Studies in Speleology Academic Press, New York pp. 267-327.

WILFORD,G. and J.WALL 1965: Karst topography in Sarawak. Journal of Tropical Geography 21:44-70.

WILLETT,R.W. 1950: The New Zealand Pleistocene snow line, climatic conditions, and suggested biological effects. New Zealand Journal of Science and Technology 32(1):18-48.

WILLETT,R.W. 1965: Limestone and marbles. In WILLIAMS,G.J. (ed.) Economic Geology of New Zealand 4:271-278.

WILLIAMS,P.W. 1964: Aspects of the limestone physiography of parts of counties Clare and Galway, west Ireland. Ph.D. Thesis, Cambridge University.

WILLIAMS,P.W. 1966: Limestone pavements with special reference to western Ireland. Transactions of the Institute of British Geographers 40:155-172.

WILLIAMS,P.W. 1968: An evalution of the role and distribution of limestone solution and deposition in the river Fergus basin, western Ireland. In WILLIAMS,P.W. and J.N.JENNINGS Contributions to the Study of Karst. A.N.U. Dept. Geogr. Pub. G/5 pp. 1-40.

WILLIAMS,P.W. 1972a: Morphometric analysis of polygonal karst in New Guinea. Geological Society of America Bulletin 83:761-796.

WILLIAMS P.W. 1972b: The analysis of spatial characteristics of karst

terrain. In CHORLY,R.J. (ed.) Spatial Analysis in Geomorphology. Harper and Row, New York pp. 135-161.

WILLIAMS,P.W. 1978 Interpretations of Australisian Karsts. In DAVIES,J.L. and M.A.J.WILLIAMS Landform Evolution in Australisia A.N.U. Press, Canberra, pp. 259-286.

WILLIAMS,P.W. 1982a: Karst in New Zealand. In SOONS,J.M. and M.J.SELBY (ed.) Landforms of New Zealand. Longman Paul, Auckland, pp. 105-126.

WILLIAMS,P.W. 1982b: Speleothem dates, Quaternary terraces and uplift rates in New Zealand. Nature 298: 257-60.

WILLIAMS,P.W. 1983: The role of the subcutaneous zone in karst hydrology. Journal of Hydrology 61:45-67.

WILLIAMS,P.W. and R.K.DOWLING 1979: Solution of marble in the karst of the Pikikiruna Range, Northwest Nelson, New Zealand. Earth Surface Processes 4:15-36.

WILSON,E.M. 1974: Engineering Hydrology (2nd edn.) Macmillian 232 p.

WILSON,J.G. (and others) 1976: History of Hawke's Bay Capper Press, Christchurch, 468 p.

WOLFE,T.E. 1972a: A classification of cave sediments. In ADAMS,W.P. and F.M.HELLEINER (ed.) International Geography 1972 part 2. University of Toronto Press pp.1334-1335.

WOLFE,T.E 1972b: Fluvial cave sediments: A description and interpretation. In ADAMS,W.P. and f.m.helleiner (ed.) International Geography 1972 part 2. University of Toronto Press pp.74-76.

WORTHY,T. 1982: Subfossil remains from the Fred Catchment, Waitomo. NZSS Bulletin 7(122):46-48.

WORTHY,T. 1984: An extensive subfossil deposit in Gardner's Gut Cave,

Waitomo. NZSS Bulletin 7(130):257-262.

ZOTOV,V.D. 1941: Potholing of limestone by the development of solutional cups. Journal of Geomorphology 4:71-73.

GEOLOGICAL MAP OF THE PUKETOI RANGE

TOPOGRAPHIC LEGEND

ROADS
- Two lanes (sealed and metalled)
- Single lane (metalled)
- Bridge, one lane

WATER FEATURES
- Lake and/or Swamp
- Stream or River (permanent)
- Stream (intermittent) or Dry Valley

RELIEF FEATURES
- Trig Station beaconed, unbeaconed
- Elevation in metres (534)

GRID NORTH, G–M Angle, MAG NORTH

INDEX OF MAP SHEETS

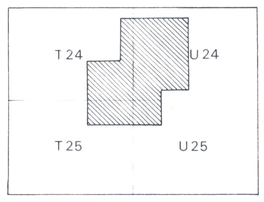

SCALE 1:50000

1 2 3 4 5 Kilometres

Geological survey of central and northern sections of the Puketoi Range by Halliday 1987, as part of a MSc. thesis Massey University. Survey of the southern section is from Neef (1967, 1974, 1984). Additional information is from Lillie (1953), Kingma (1962), Laing (1963), Ride (1964), de Caen and Darley (1969), and Harmsen (1984a, 1984b, 1985).

Drawn by Stuart Halliday

GEOLOGICAL LEGEND

MEMBER / FORMATION (Lithology) / GROUP STAGE SERIES

- Qf FLUVIAL DEPOSITS
- Qd DUNE SAND
- Qt TERRACE GRAVEL
- Ql LANDSLIP
- Kú KUMEROA (Limestone & mudstone) — limestone bed — HAWERA — HOLOCENE PLEISTOCENE — QUATERNARY
- Tō TE ONEPU (Limestone) — mudstone lens — NUKUMARUAN MANGANUIAN WAIPIPIAN OPOITIAN KAPITIAN — WANGANUI — PLIOCENE — TERTIARY
- Tr RAUKAWA (Mudstone) — TE AUTE ? — TARANAKI — UPPER MIOCENE
- Ta AWAPAWA (Limestone)
- Tm MANGATORO (Mudstone)
- Regional Unconformity
- Wa WAEWAEPA (Greywacke) — TAITAI ? — CRETACEOUS

GEOLOGICAL SYMBOLS

Contact

Faults — downthrown and upthrown — Established — Inferred

Bedding — 23 (from Neef 1974) — 23 (from Lillie 1953) — 23 (from Halliday 1987)

Fold Axis — Anticlinal — Synclinal

CROSS SECTIONS